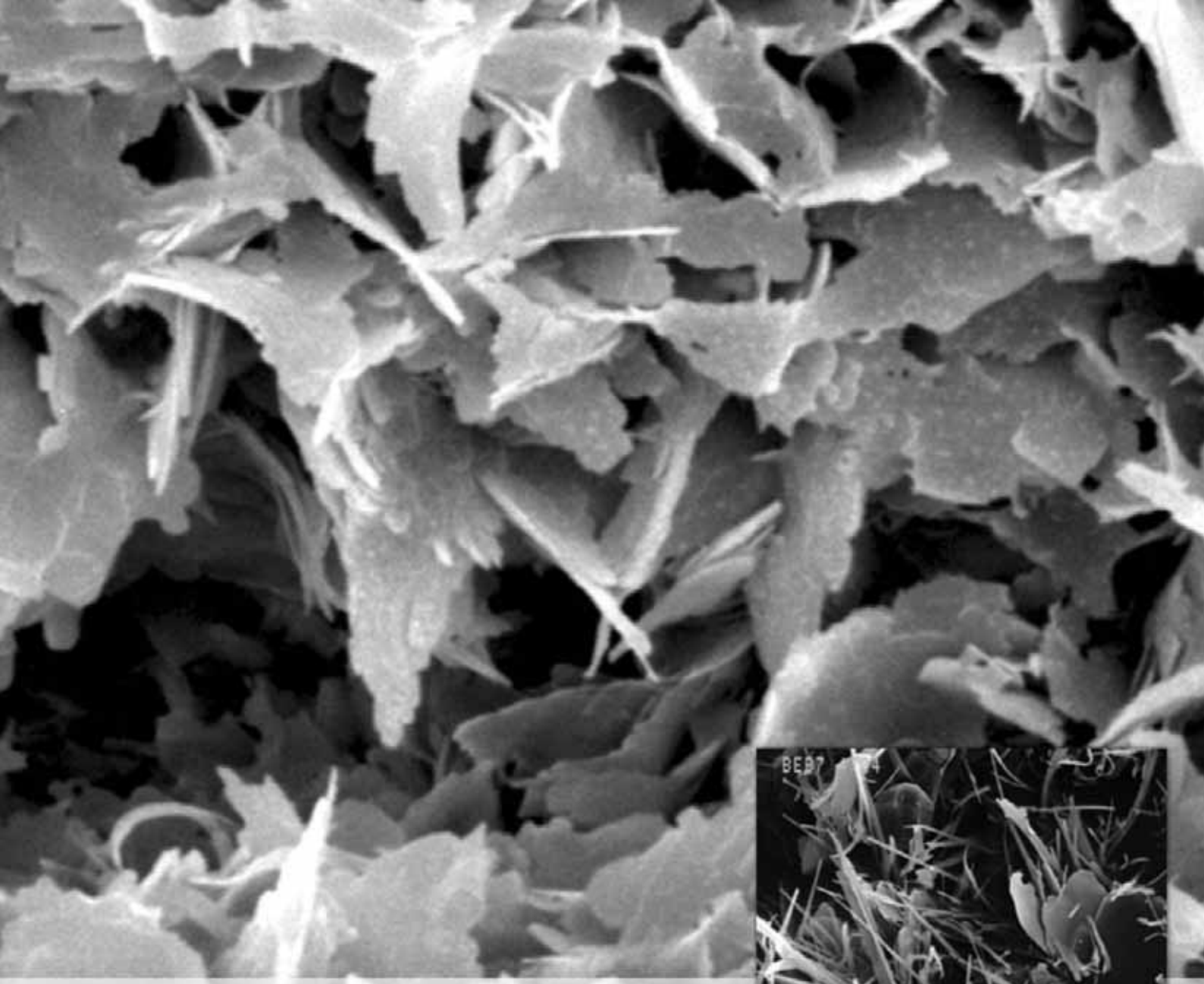

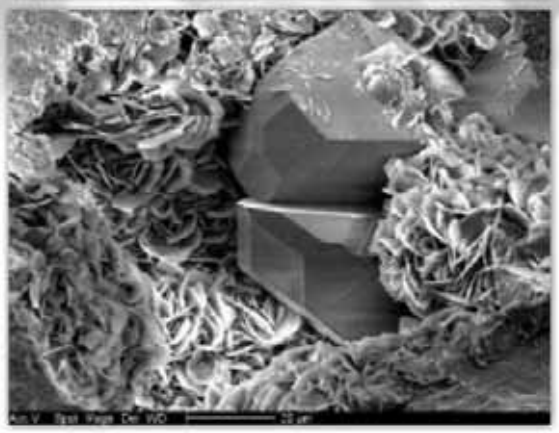

CLOGGING ISSUES ASSOCIATED WITH MANAGED AQUIFER RECHARGE METHODS

Edited by: Russell Martin

This work has been undertaken as part of the IAH Commission on Managing Aquifer Recharge. IAH-MAR has its roots in the Working Group on Artificial Recharge, founded in 1998 by Ivan Johnson of AIJ Consultants in Denver and formerly of USGS, an activist for more than 30 years in artificial recharge research and practice, and leader of the ASCE/EWRI Standards Committee for Artificial Recharge. The group had its first meeting in November 2000 at Cape Town (IAH XXX). The change in name from 'Artificial Recharge' to 'Management of Aquifer Recharge' reflects the reality that water banking and bank filtration harness natural processes to manage and enhance aquifer recharge, a vital tool in the sustainable management of the world's groundwater resources.

First published October 2013

ISBN 978-0-646-90852-6

Citation for Clogging Monograph:

Martin, R., (ed.) (2013) Clogging issues associated with managed aquifer recharge methods. IAH Commission on Managing Aquifer Recharge, Australia.

Citation for Chapter in Monograph (example) :

Rinck-Pfeiffer, S., Dillon, P., Ragusa, S., Hutson, J., Fallowfield, H., de Marsily, G., and Pavelic, P., (20130) Reclaimed Water for Aquifer Storage and Recovery: A Column Study of Well Clogging. In: Martin R (ed.) Clogging issues associated with managed aquifer recharge methods. IAH Commission on Managing Aquifer Recharge, Australia, 26–33.

Contacts

Specific enquires about the material contained in this publication should be directed to the respective lead authors. Contact details are listed at the back of this publication. Anyone wishing to contribute additional papers should contact the editor Russell Martin via e-mail rmartin@agwt.com.au

Production Assistance

Editing by Russell Martin, General Manager at Australian Groundwater Technologies. Layout and design by Gayle Bruggemann Graphics and GIS Specialist at Australian Groundwater Technologies.

FOREWORD

Significant advances in the areas of geochemistry, microbiology and aquifer hydraulics regarding the science of recharge of water to aquifers has been made over the past decade. With the increased uptake of managed aquifer recharge as water resources management practice that can augment traditional water supplies, or address a variety of legacy issues associated with overuse, a greater appreciation of how complex the problems associated with aquifer recharge, and in particular clogging, is becoming apparent.

This monograph presents a collection of papers that highlight the work being carried out within this area. It is intended to raise the awareness of practitioners and operators alike of how clogging may impact a managed aquifer recharge scheme, but with the appropriate level of investigation, can be effectively managed.

A MAR scheme will invariably experience clogging of some type, and to some degree, during its operational life. To recognise the potential for clogging and employ the appropriate mitigation or remediation measures, either through engineering design or through operational management practices, requires specialist knowledge and skills. It should also be noted that remediation methods to address clogging are very site specific and what works in one hydrogeological setting may not always be successful in another location. Indeed remediation approaches may differ between injection bores across the same scheme. Effective management and remediation of clogging can only come through the effective dissemination of information and learning from practitioners that have considerable operational experience.

Clogging should not be used as a justification as to why an MAR scheme was unsuccessful in a particular hydrogeological setting. With the appropriate level of investigation, inclusive of detailed characterisation of the target aquifer, source water quality, receiving water quality and the implementation of effective operational practices, clogging can be managed. Where clogging does occur it can also be effectively mitigated using a variety of techniques.

This monograph is not complete and addresses only some of the clogging issues associated with both surface infiltration basins and injection via bores. It does not address potential clogging issues associated with the various other methods of MAR such as bank filtration. This monograph is available online and has been structured so that it can be easily added to. The intent is to continually build on our operating knowledge of clogging and remediation methods and I would encourage all hydrogeologists practicing in this specialist field to share their experiences regarding clogging by submitting a paper to myself for review and inclusion within future revisions of this monograph.

Russell R Martin
Editor: Clogging Issues Associated with Managed Aquifer Recharge Methods
rmartin@agwt.com.au

ACKNOWLEDGEMENTS

My thanks to the authors of the various papers contained in this monograph and without their dedication and considerable time taken to compile their information this publication would not be possible. Special thanks also to Gayle for her invaluable assistance in preparing the layout and presentation of the monograph. The aim of the monograph is to share with other practitioners the collective knowledge that has been developed to date in an effort to advance the science in this highly specialised area of hydrogeology. I trust readers will find some of the information contained in the papers of value and would encourage others working in this field to contribute their experiences and knowledge to build this into a practical reference text. The purpose of providing this as a web based document presents the opportunity to continually add relevant text easily. Anyone wishing to contribute can send their paper to me for review at the e-mail address given in the foreword.

INTRODUCTION

R. Martin

General Manager, Australian Groundwater Technologies

Managed Aquifer Recharge (MAR) is a collection of water resource management practices employed to actively store water underground for recovery when needed. The approach used to recharge the water to the underlying aquifers is typically governed by the local hydrogeological conditions. Intentional aquifer storage, with the goal of recovering the water at a later date, has been used for hundreds of years, but is being further developed and refined as demand for fresh water threatens to exceed supply in many parts of the world. One of the challenges for the sustainable operation of MAR schemes is the management of clogging. Clogging leads to lost performance and can result in costly workovers or recompletions of bores and infiltration basins, or expensive stimulation jobs, such as acidisation. In extreame cases clogging may lead to uncontrolled fracturing of the aquifer formation or overlying confining beds as a result of the induced high bottom hole pressures.

Physical scarcity of water in many of the arid regions across the globe and the lack of clean drinking water is a significant and growing problem. Today, about one third of the world's population lives with moderate to high water stress. By 2025, largely because of population growth, two out of three of the world's people will live under these conditions (Mazur, 2012). Margaret Catley-Carlson, vice-chair of the World Economic Forum Global Agenda Council on water security wrote *If "business as usual" water management practices continue for another two decades, large parts of the world will face a serious and structural threat to economic growth, human well-being, and national security* (2011).

Water resources must be managed and used more efficiently and wisely if we are to sustain the needs of a growing world population (Pyne, 2005).

MAR, in its various forms, and related water management practices are evolving rapidly in response to declining groundwater levels, increased vulnerability of surface water supplies to contamination, increasing concerns regarding climate variability, and numerous other reasons. There is huge potential for MAR, used in conjunction with other water management techniques, to make more efficient use of existing water resources and capitalise on opportunities, previously overlooked, to augment traditional water supply sources.

While MAR is maturing as a recognised water management approach one of the most significant challenges for the sustainable operation of any MAR scheme is the potential for clogging (sometimes referred to as plugging). Physical, biological, and chemical clogging of infiltrating surfaces and injection bores with the resulting reduction in infiltration rates is perhaps the most obvious problem encountered in any MAR scheme. A MAR scheme will invariably experience clogging and where the selected MAR method involves an injection and recovery bore (aquifer storage and recovery) the risk of clogging is potentially greater.

Two of the most common methods employed for aquifer recharge include surface infiltration systems and injection bores and the clogging associated with these two methods of MAR is the primary focus of this monograph. The papers prepared by various authors contained within this monograph present aspects of clogging observed during column experiments, experience gained from infiltration basins and the use of recharge bores. The information is by no means exhaustive and there are still a number of knowledge gaps and issues not discussed within this monograph.

Clogging Processes

Clogging causes impaired injectivity restricting the volume of water that can infiltrate or be injected into the target aquifer. In recharge bores under a constant injection rate clogging may lead to excessive pressure heads that result in the failure of either the aquifer

formation or the overlying confining beds. More typically maximum injection heads are preset and the result is a reduced rate of injection.

Although spreading basins are less prone to serious clogging than injection bores, recharge water should be of an adequate quality to avoid clogging the infiltrating surface. Typically clogging of infiltration basins or trenches can be caused by precipitation of minerals on and in the soil, entrapment of gases in the soil, formation of biofilms and biomass on and in the soil, and by deposition and accumulation of suspended algae and sediment. Pre-treatment of the water can greatly reduce suspended solids and nutrients, but the infiltrating surfaces usually require periodic cleaning to maintain infiltration rates.

In recharge bores clogging generally occurs at the bore / aquifer interface that is, in the gravel pack (if present), the wall of the bore and in the target formation immediately surrounding the bore.

Clogging can be divided into four principal types:

1. *Chemical* which includes precipitation of elements such as, iron or aluminium, aquifer matrix dissolution and temperature.
2. *Physical* which includes suspended solids, migration of interstitial fines (e.g. illite or smectite clays), unintentional fracturing of the aquifer, and formation damage during bore construction.
3. *Mechanical* such as entrained air/gas binding.
4. *Biological* which includes algae growth, iron or sulphate reducing bacteria.

Table 1 presents a summary of the four principal types of clogging and the processes that can be ascribed to each type.

Table 1: Summary of clogging types and processes

Clogging Type	Clogging Process
Chemical	• Geochemical reactions that result in the precipitation of minerals e.g. iron aluminium or calcium carbonate growth; • Aquifer matrix dissolution (can also work to increase hydraulic conductivity); • Ion exchange; • Ion adsorption; • Oxygen reduction. • Formation of insoluble scales. • Formation dissolution.
Physical clogging	• Accumulation / Injection of organic and inorganic suspended solids. • Velocity induced damage e.g. migration of interstitial fines such as illite or smectite. • Clay swelling (e.g. montmorillonite). • Clay deflocculation. • Invasion of drilling fluids (emulsifiers) deep into the formation. • Temperature.
Mechanical	• Entrained air/gas binding (includes nitrogen &/or methane from microbiological activity). • Hydraulic loading causing formation failure, aquitard failure or failure of casing around joints or seals.
Biological	• Algae growth and accumulation of biological flocs. • Microbiological production of polysaccharides. • Bacterial entrainment and growth.

Chemical clogging processes – Recharge of waters not in equilibrium with the groundwater or aquifer materials can cause chemical reactions. These lead to the production of insoluble precipitates that alter the permeability of the porous media.

Dissolved iron occurs naturally in groundwater and surface waters throughout Australia in concentrations of up to 50 milligrams per litre (mg/L). Iron salts become increasingly soluble as groundwater becomes more acidic. Iron is normally found dissolved in groundwater in the reduced ferrous form ($Fe2^{+}$) and oxidises to relatively insoluble ferric form ($Fe3^{+}$) when the water pH is raised and with exposure to oxygen. When oxygenated water is recharged into the groundwater, carbon dioxide and hydrogen sulphide ("rotten egg" gas) is frequently released. The pH rises and the iron precipitates as ferric hydroxide where it causes clogging of the screens, gravel pack or pore spaces/fractures within the aquifer matrix. Where the right conditions are present, that is, the ambient groundwater has low pH and is oversaturated with aluminium oxyhydroxide, significant diurnal temperature variation of the recharge water may be the trigger that causes the aluminium to precipitate.

Precipitation of iron oxides, iron hydroxides, and calcium carbonate are the predominant forms of geochemical clogging, but are not widely identified as the major clogging mechanism. This is because they often coincide with other forms of clogging, or may take long periods of time to develop.

Many geochemical reactions, especially redox reactions, are catalysed by bacteria; thus it is difficult to separate chemical and biological processes in many situations. If the aquifer contains iron-rich or manganese-rich minerals, then the presence of oxygen or nitrate in the recharge water can stimulate bacteria (e.g. *Gallionella*) to precipitate iron or manganese oxides, and hydroxides, leading to clogging.

Two major types of *scale formation* occur during water injection operations. These being carbonate (i.e. calcite, $CaCo_3$) and sulphide (i.e. gypsum, $CaSO_4$) based usually associated with changes in pressure temperature or pH of the injected fluid. In addition complex iron containing scales (i.e. ferrous hydroxide ($Fe(COH_2)$), magnetite (Fe_3O_4) , trollite (FeS) and marcasites (FeS_2) are usually associated with downhole corrosion problems. Carbonate scales, while damaging, are relatively acid soluble in contrast to sulphate based scales which are virtually insoluble in acid and difficult to remove by any conventional means other than mechanical penetration. (Bennion et al., 1998)

Other geochemical reactions, such as *dissolution*, may have an unclogging effect by increasing the hydraulic conductivity (e.g. in places where calcite cement dissolves). In pronounced cases, dissolution may lead to bore instability and the subsequent failure of the formation induces changes to the hydraulic conductivity which results in reduced injection capability.

Potential injection zones may have water soluble materials such as highly hydratable clays, anhydride, halite etc. Partial or complete dissolution may lead to the migration or the release of insoluble fines immobilised within previously occluded pores. These particulates are then carried deeper into the formation where they may cause further blockage and clogging.

Physical clogging processes – During MAR activities it is critical to remove or reduce the *suspended solids* to practical levels for a number of reasons, the main one being to minimise clogging. A secondary reason to reduce suspended solids is to prevent shadowing of pathogens when ultraviolet (UV) light treatment is used prior to recharge. Ideally UV treatment units work most efficiently when the turbidity (associated with suspended solids) is equal to or less than five Nephelometric Turbidity Units (NTU). Therefore an NTU of five or less is a practical target to achieve in order to manage clogging in MAR bores and maximise pathogen dieoff where UV treatment is used.

Suspended sediments collect on the screen gravel pack or wall of the bore and eventually build up to form a cake, which inhibits the rate of recharge. Clogging by suspended particles is characterised by a slow but steady increase in the hydraulic heads for a given rate of recharge. As the thickness of the accumulated sediment increases on the screen or walls of the bore the permeability is reduced and the observed hydraulic head for a given rate of recharge increases more rapidly. The increasing hydraulic head applied to maintain recharge rates eventually causes the cake to compress and the rate of recharge efficiency can reduce exponentially. Like clogging associated with chemical precipitation the observed hydraulic heads in any nearby observation

bores should begin to decrease if the maximum pressure head in the injection bore is held constant.

Many formations, particularly sandstones, can contain a high fraction of clay platelets such as illite, smectite, kaolinite and chlorite which typically line or fill pores within the rock or soil matrix. *Velocity induced* clogging occurs during recharge or infiltration if the critical interstitial velocity is exceeded and the clay platelets become mobile. These fines, once dislodged migrate in the direction of flow until they reach the narrower pore throat where they become trapped and eventually block the pathway causing a reduction in the injection capacity for a constant injection pressure. Under a constant injection rate the clogging manifests as an increased hydraulic head in the injection bore.

Clogging associated with fines migration is aggravated by the turbulence effects related to stopping and starting an injection cycle. When injection ceases the fines settle but on the subsequent injection restart the fines are remobilised as a large floc and can quickly block the pore throats.

Mica (muscovite and biotite) is more prevalent in the recently deposited clays and soils and is more likely to be the main cause of pore clogging associated with infiltration basins. The source water can cause the micas to flake like shedding skin and once mobilised migrate through the larger pores until being trapped in the opening to the smaller pore throats. Management of these interstitial clays can prove to be problematic and the signs of clogging are a gradual decline in recharge rates and a slow build-up of hydraulic heads where a constant injection rate is maintained.

Mobilisation of interstitial fines from *clay swelling* may be more prevalent where fresh water is recharged into brackish or saline groundwater systems. Bennion et al. (1998) describe this process where the negative charge imbalance in the clay structure is stabilised by the substitution of a positively charged cation (i.e. NA^{+}, K^{+}, Ca^{++}, Mg^{++}) into the gap between the individual clay platelets. If an insufficient concentration of these ions is present (such as the case where fresh water is injected into a brackish or saline aquifer containing a swelling clay rich zone) the water, due to its polar nature, can substitute itself into the gap. The size of the water molecule, in comparison to the normally stabilising cations such as Na^{+} or K^{+}, causes the physical expansion or swelling of the clay. Depending on the concentration of the clay and its location in the pore system, this expansion can cause severe reductions in hydraulic conductivity.

If the ambient groundwater is brackish to saline the clay platelets tend to lie flat. Introduction of low salinity (less than 200 mg/L) water is like a toxic shock to the clay platelets. Bennion et al. (1998) identify that the potential for *clay deflocculation* is a common oversight in many water injection schemes if the formation does not appear to contain a substantial concentration of the classical (smectite or mixed layer) swelling clays. Clay deflocculation can also be caused by abrupt contact with fresh water, sudden salinity changes (shocks) or rapid increases in fluid pH levels. Abrupt changes in water composition or salinity shocks tend to greatly magnify problems associated with deflocculation due to rapid ion exchange involving surface cations and protons in the water phase. More gradual transitions from ambient groundwater to injection water over a period of time have been shown to reduce or eliminate this problem. Management of pH or the addition of Ca^{+} or Mg^{++} can assist in alleviating this potential problem.

Drilling muds are typically used to assist in transporting cuttings to the surface and also prevent the formation water from uncontrollably entering the bore through the formation of a filter cake. However, in fulfilling this purpose they can also cause significant formation damage in sandstone aquifers that can result in a permanent reduction in the effective hydraulic conductivity of the aquifer in the immediate area around the bore. Additionally, other drilling fluids such as bentonite and cement can also cause considerable formation damage.

Most drilling muds are designed to deflocculate clays and other fine particles in the bore, which is opposite to what is desirable in the formation rock. Therefore, filtrate invasion is potentially very damaging to the rock in the near-bore area. Potentially damaging filtrates are also lost to the formation during bore completions. Damage associated with the invasion of drilling fluids into the target aquifer can frequently extend up to a metre into the formation (depending on the properties of the drilling fluid e.g. weight, viscosity etc., and the hydraulic properties of the aquifer) which makes it difficult to remedy.

The drilling fluids contain bentonite and also clays and sands from the upper geological layers that have been penetrated to reach the target aquifer. The pore openings are initially blocked by the larger particles and then ever increasing smaller particles in the drilling fluids to form the filter cake. However a certain percentage of drilling fluids migrate into the aquifer. Additives are used to break down the drilling fluids during redevelopment of the bore but these may not be entirely effective especially where the drilling fluids have been left in the bore for an extended (three or four days) period of time before final completion. Inexperienced practitioners may not fully appreciate the importance of redevelopment and in their haste to complete the bore, fail to recognise that there is still a significant volume of drilling mud within the formation. Once the bore has been screened and gravel packed then it is impossible to remove the drilling muds and they act to impede the hydraulic conductivity in the same manner as the mobilisation of interstitial fines.

Because infiltration rates vary inversely with water viscosity, *temperature* also affects infiltration rates. In areas with large differences between winter and summer temperatures, viscosity effects alone can cause winter infiltration rates to be as low as about half of that in summer. Thus if recharge systems need to be based on a certain capacity, they should be designed on the basis of winter conditions, when water is coldest and infiltration rates lowest (Bouwer et al., 2008).

Exchange of cations between the recharge water and the clays within the aquifer can lead to either swelling or dispersion. This tends to be most prevalent where reactive clays (e.g. montmorillonite) are present, and where there is a large decrease in the salinity of the recharge waters compared to the ambient groundwater.

Mechanical clogging processes – *Gas entrainment (or gas binding)* is problematic in both recharge bores and spreading basins. In spreading basins the air within the vadose zone may become trapped reducing infiltration and storage capacity. During recharge via a bore, air may become entrained where water is allowed to cascade freely into balancing storage tanks or into the recharge bore. This may occur in some situations due to poorly functioning surface equipment or leaks in surface suction lines. If the downward velocity exceeds 0.3 m/sec (1.0 feet/sec) then the entrained air can enter the formation where it lodges in the pore spaces. This increases the resistance to flow, resulting in higher water levels (Pyne, 2005).

A secondary consideration is that cavitations generated in pumps by air entrainment is also potentially damaging to the injection equipment, increasing both corrosion potential and potential injected solids content of the water.

Clogging associated with gas entrainment is characterised by a sudden rise in the water levels in the recharge bore immediately upon startup of the injection cycle.

If the shear strength of the rock matrix is not well understood or is perhaps weakened through dissolution *hydraulic loading* may induce failure of the matrix or aquitard. Primary clogging by physical, chemical or microbiological processes will result in increased aquifer pressures where a constant injection rate is maintained. As the clogging increases the injection pressure required to maintain the constant injection rate also increase and may exceed the shear strength of the aquifer matrix, especially where dissolution may be occurring simultaneously. Initial failure of the matrix may result in increased injection performance but this is likely to be shortlived as, unlike deliberate hydraulic fracturing, there is no propping agent available to keep the induced fractures open.

Permeability decline in hydraulically induced fractures where no propping agent is used may result from creep and pressure solution of minerals or migration of insitu fines from previously occluded pores. Van Poollen (1990) in his electrical-model study demonstrated the influence on production of various degrees of damage surrounding the bore and the fracture. His work identified that the natural aquifer permeability could be reduced by as much as one third in the immediate area surrounding the bore and fracture.

Biological clogging processes – Injection water, irrespective of its source, usually contains bacterial agents. Equally the ambient groundwater may host iron or sulphate reducing bacteria together with a host of numerous other microorganisms. Bacterial problems associated with injection can occur with the growth of both aerobic and anaerobic bacteria in surface equipment, pumps, tubing, down hole equipment and within the formation itself.

The degree of biological growth is directly related to the amount of carbon and nutrients present. Although the concentration of nutrients in the source water may be low, the process of concentrating the suspended particles due to filtration near the bore often provides the substrate needed to foster biological growth. (Pyne, 2005).

Most commonly it is the biofilm produced by the microorganisms that result in clogging problems. Bacteria are sensitive to shear and tend to isolate themselves from fluid shear by the formation of stable biofilms. The physical adsorption of the growing biofilm on the surface of the rock matrix can, over a period of time, result in partial or total occlusion of the pore throats and a resulting reduction in injectivity (Bennion et al.,1998).

Iron bacteria typically colonise areas of high velocity and it is not uncommon to see large concretions hanging from submersible pumps. Sulphate reducing bacteria produce slimes and release gases (H_2S or "rotten egg" gas) that results in reduced permeability.

The signs of microbiological clogging are an initial slow increase in the hydraulic head for a given recharge rate followed by a sudden exponential increase in head buildup. A corresponding decrease in the hydraulic heads in adjacent observation bores should also be observed.

Conclusions

Prevention is the best, and also the most cost effective, cure to manage clogging and it starts with the basic assumption that clogging will occur at some point during the operational life of the MAR scheme. Clogging should not be used as a justification as to why an MAR scheme was unsuccessful in a particular hydrogeological setting because there are various remediation and management techniques available to support the sustainable operation of these schemes.

Understanding the types of clogging that are likely to occur in a particular hydrogeological setting for the source water quality that is being recharged influences the bore design and virtually all other aspects of the scheme such as, pre-treatment and operational activities.

Controlling the source water quality such as removing suspended solids, managing the pH or stripping any dissolved oxygen are obvious measures to minimise the potential for clogging. Managing the source water quality addresses perhaps 50% of the potential causes of clogging but does not minimise the potential for:

- Clogging associated with unintentional fracturing;
- Clogging caused by mobilisation of interstitial fines;
- Clogging caused by microbiological activity;
- Clogging resulting from thermal changes;
- Clogging associated with drilling methods and bore completion.

When the recharge method is via a bore adequate characterisation of the aquifer groundwater and aquifer matrix is critical to the design of the injection bore. The design should provide sufficient flexibility to be able to employ a variety of remediation techniques once clogging occurs. However, practitioners and operators should be aware that, more often than not, multiple causes of clogging may be occurring simultaneously, for example, gas entrainment may induce precipitation of iron which in turn stimulates an increase in iron bacteria. What started out as a simple air entrainment problem has the potential to develop into a significant clogging problem driven by three different processes. Each potential clogging cause may now potentially require individual treatment.

Additionally, the remediation methods to address clogging are very site specific and what works in one hydrogeological setting may not always be successful in another location. Indeed remediation approaches may differ between injection bores across the same scheme.

Some of the symptoms of clogging are similar e.g. chemical precipitation or buildup of suspended solids produces a similar hydraulic response for a given injection rate. Monitoring the aquifer hydraulic response during recharge over time in the production and nearby observation bores can assist in identifying the onset and type of clogging.

References

Bennion, D.B., Bennion, D.W., Thomas, F.B., and Bietz, R.F., (1998) *Injection Water quality – a key factor to successful waterflooding.* Journal of Canadian Petroleum Technology Vol 37. No. 26

Mazur, L., (2012) Water and Population: Limits to Growth? http://www.newsecuritybeat.org/2012/02/water-and-population-limits-to-growth/#.UPCkUqzAqPg *Laurie*

Mazur is a consultant on population and the environment for the Wilson Center's Environmental Change and Security Program and director of the Population Justice Project.

Pyne, R.D.G., (2005) *Aquifer storage and recovery: A guide to groundwater recharge through wells* 2nd Edition. ISBN 0-9774337-090000

Van Poollen, H. K. Dr, (1990) *Production vs. permeability damage in hydraulically produced fractures*. Published in Formation Damage SPE Reprint series No 29 1990.

Waughray, D., (2011) ed. *Water Security: the water-food-energy-climate nexus*: the world Economic Forum water initiative.

CONTENTS

OVERVIEW OF CLOGGING PROCESSES DURING MANAGED AQUIFER RECHARGE

Clogging in Managed Aquifer Recharge: Flow, Geochemistry and Clay Colloids

D.C. Mays, P.E., Ph.D.

Abstract

This chapter describes research from the allied fields of water treatment, soil science, and petrology, each of which sheds light on the mechanisms by which flow and geochemistry influence clogging in managed aquifer recharge. The primary focus is clogging by suspended solids, especially clay colloids, which are ubiquitous in natural porous media. When colloids deposit in aquifers, they reduce the effective porosity and alter the pore space geometry, both of which can inhibit the flow of groundwater. Management of clogging is complicated by the complexity inherent in this system, in which flow, geochemistry, clay mineralogy, and colloidal effects each play a role. To address this complexity, this chapter will briefly review colloid filtration, mobilization, and clogging models, then proceed to highlight the key physical and chemical variables that control clogging. It will be argued that clogging in managed aquifer recharge is analogous to clogging in soils or hydrocarbon reservoirs, rather than to granular media filters in water treatment. Based on this analogy, the chapter will conclude with several provisional recommendations to prevent or manage clogging in managed aquifer recharge.

1 Introduction

Managed aquifer recharge (MAR) is the engineered process by which water is delivered into an aquifer for storage, transmission, or treatment—the latter because aquifers remove suspended solids, neutralize acids, and provide beneficial ion exchange. In contrast to surface reservoirs, MAR essentially prevents evaporation losses, which consume nearly as much water worldwide as all municipal use combined (Levine and Asano, 2004). As such, MAR is the crucial first step in the increasingly popular water resources technology known as aquifer storage and recovery (ASR).

Despite its apparent simplicity, MAR requires planning, design, construction, operation, and maintenance commensurate with other civil infrastructure. In contrast to other water systems, however, the reservoirs and conduits in MAR are not engineered structures, but rather geologic formations. As such, the full spectrum of natural processes associated with groundwater flow in aquifers is relevant in MAR, so the related disciplines of geology, soil science, and colloid science must be brought to bear for successful project implementation (U.S. National Research Council 2008, page 234). Recognizing that the reservoirs and conduits in MAR are geologic formations also provides a framework in which to understand perhaps the most significant technical challenge in MAR, namely clogging.

Clogging, the detrimental reduction of permeability in porous media is a major technical challenge in MAR. By way of illustration, the U.S. National Research Council's (2008) report entitled *Prospects for Managed Underground Storage of Recoverable Water* mentions clogging 101 times. In the context of MAR, clogging results from (1) deposition of suspended solids, (2) rearrangement of deposits, (3) geochemical reactions, (4) biofilm growth, and (5) air binding (American Society of Civil Engineers, 2001; § 10.7.2; Pyne, 1995; § 4.2). Because clogging by one or more of these mechanisms is expected during recharge through wells, it is routinely managed by periodically backwashing wells and disposing the wash water, by adding a chlorine residual to injection water (Pyne, 1995; § 4.2), or by removing essentially all suspended solids and organics from the

injection water (American Society of Civil Engineers, 2001; § 10.7.2)—where adding chlorine and removing organics help to prevent biofilm growth. The focus in this chapter is clogging by suspended solids, especially clay colloids, corresponding to mechanisms 1–3 above. Clogging by these mechanisms does not require a high concentration of total suspended solids (TSS): Concentrations as low as 2 mg/L have been shown to be sufficient for clogging (Pyne, 1995; § 5.4). Even without considering biofilm growth or air binding, clogging by clay colloids comprises a host of interrelated physical and chemical phenomena that render a complex linked system (American Society of Civil Engineers, 2001; Pyne, 1995; U.S. National Research Council, 2008).

To place these clogging mechanisms in context, this chapter begins with a brief overview of filtration theory, highlighting deposition and mobilization of colloids and models for the resulting clogging. Having established the relevant context, the chapter then proceeds to an overview of clogging phenomena, first from the literature on water treatment engineering, and then from the literature on soil science and petrology. These two groups of literature will present something of a paradox, where the same physical or chemical perturbation either alleviates or exacerbates clogging, depending on the context. To resolve this paradox, the chapter discusses two lines of ongoing research based on the general concept of deposit morphology. The chapter concludes with a brief explanation why clogging in MAR is analogous to soil science and petrology, and in that context, provides several provisional guidelines for avoiding or managing clogging in MAR.

2 Deposition, Mobilization, and Clogging

Colloidal phenomena are important for flow and transport in natural porous media—soils, aquifers, and fractured rocks. By convention, colloids are defined as solid particles in the size range of 1 nm to 10 μm, including clays, weathering and precipitation products, microbial pathogens, and nanoparticles—the latter of which are generally defined as solid particles with at least one dimension less than or equal to 100 nm. The coupling between deposition, mobilization, and permeability was emphasized in the historical filtration literature, for which the primary motivation was granular media filters for water treatment, and which was reviewed by McDowell-Boyer et al. (1986). Later reviews focus on deposition under clean bed conditions, before significant deposits have accumulated, with more emphasis on microbial pathogens and engineered nanoparticles, and less emphasis on clogging beyond clean bed conditions (Kretzschmar et al., 1999; Ryan and Elimelech, 1996; Tufenkji, 2007). A schematic diagram of a typical filtration experiment is shown in Figure 1.

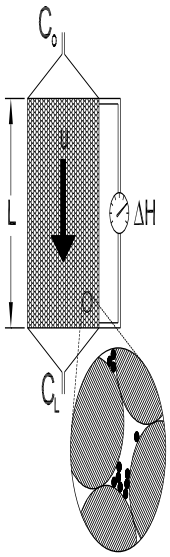

Figure 1: Schematic diagram of a typical filtration experiment with constant fluid velocity, u, and constant influent concentration, C_0. Inset shows colloid accumulation in the pore space

This section begins with the classical model for colloid filtration then proceeds to a discussion of empirical observations of colloid mobilization. Both processes are fundamental in the context of MAR: Filtration is the mechanism by which suspended solids in the recharge water accumulate within the pore space of the aquifer. Mobilization of previously deposited colloidal material is the first step in the process of sequential mobilization, transport, re-deposition, and additional clogging.

2.1 Deposition

Colloid filtration and mobilization in porous media are usually described by the advection-dispersion equation, a partial differential equation for colloid mass balance that

includes the effects of advection, dispersion (including molecular diffusion), deposition, and mobilization:

$$\varphi \frac{\partial C}{\partial t} = D \frac{\partial^2 C}{\partial x^2} - u \frac{\partial C}{\partial x} - k_d n C + k_m \rho_s \sigma \quad (1)$$

where x is position, t is time, φ is porosity, C is colloid concentration, D is a dispersion coefficient (here assumed to be homogeneous), $u = q/\varphi$ is the average pore water velocity, k_d is a first-order deposition rate constant, k_m is a first-order mobilization rate constant, ρ_s is solid density, and σ is the specific deposit, defined as the volume of deposited colloids divided by the total volume of porous media. Volumetric flux q is given by Darcy's law:

$$q = \frac{-k\rho g}{\mu}\left(\frac{\Delta H}{L}\right) \quad (2)$$

where k is permeability, ρ is fluid density, g is gravitational acceleration, μ is dynamic viscosity, ΔH is head loss, and L is flow distance.

The deposition rate constant k_d can be predicted theoretically from the DLVO model of Derjaguin, Landau, Verwey, and Overbeek (Yao et al., 1971), although empirical correlations are more accurate (Ma et al., 2009; Nelson and Ginn, 2011; Rajagopalan and Tien, 1976; Tufenkji and Elimelech, 2004). Equation (1) has also been modified to account for straining, in which colloids are retained by size exclusion rather than by physicochemical effects (Bradford et al. , 2002), although this approach has recently been called into question (Johnson et al., 2011). The mobilization rate constant k_m is typically fitted empirically, owing to the well-known limitations of filtration theory (e.g., Ryan and Elimelech, 1996). No widely accepted model is currently available to predict the mobilization rate constant k_m.

2.2 Mobilization

In principle, one might expect colloid mobilization to counteract the deposition described above. But in practice, colloid mobilization can contribute to additional clogging when previously deposited colloids are moved—sometimes en masse—to different locations within the pore space where they cause more clogging than before. For this reason, clogging has been attributed to colloid mobilization triggered by physical (Pavelic et al., 2011) or chemical (Zhou et al., 2009) perturbations.

Although no predictive model is currently available for colloid mobilization, it has long been recognized that physical and chemical perturbations can mobilize deposited colloids. A recent review of the filtration literature indicates that mobilization results from various changes in the fluid velocity, including velocity increases and on-off cycles (Manga et al., 2012, § 4.1.1). To generalize these observations, it is helpful to interpret conditions in terms of the hydrodynamic shear stress, τ, applied to the colloid deposits (Ives, 1970; Mays and Hunt, 2007):

$$\tau = \left(\frac{\mu\rho g q \Delta H}{\varphi L}\right)^{1/2} \quad (3)$$

Equation (3) can also be expressed using a characteristic pore length scale δ. This can be shown by solving Darcy's law (2) for the magnitude of head loss:

$$|\Delta H| = \frac{\mu L q}{k\rho g} \quad (4)$$

Substituting (4) into (3) gives

$$\tau = \left(\frac{\mu\rho g q\left[\frac{\mu L q}{k\rho g}\right]}{\varphi L}\right)^{1/2} = \left(\frac{\mu^2 q^2}{\varphi k}\right)^{1/2} = \frac{\mu q}{\sqrt{\varphi k}} \quad (5)$$

Equation (5) can also be expressed using fluid velocity $u = q/\varphi$, such that $q = \varphi u$:

$$\tau = \frac{\mu\varphi u}{\sqrt{\varphi k}} = \frac{\mu u}{\sqrt{k/\varphi}} = \frac{\mu u}{\delta} \quad (6)$$

which is equation (3) in Manga et al. , (2012), with characteristic pore length scale $\delta = \sqrt{k/\varphi}$. Using this framework, several investigators have reported results for clay deposits in terms of shear strength, that is, the shear above which mobilization is expected. As summarized by Manga et al. (2012, § 4.1.1), kaolinite deposited in porous media has a shear strength of τ = 2.7–4 dyn/cm^2 (Ives and Fitzpatrick, 1989); sodium-montmorillonite in a model fracture has a shear strength of τ = 1–8 dyn/cm^2

(Kessler, 1993); and sodium- and calcium-montmorillonite has a shear strength below $\tau = 7–14$ dyn/cm^2 (Mays and Hunt 2007). In any particular situation, the critical hydrodynamic shear would presumably depend on the details of the porous media, the colloids, the deposits, and the nature of the hydrodynamic loading. But as a general statement, laboratory experiments demonstrate that clay deposits have shear strengths in the range of 1–10 dyn/cm^2.

Chemical changes provide a second mechanism for deposit mobilization. Perhaps the most common example is clogging following pore fluid displacement by an invading fluid of lower ionic strength. In soil science, this scenario unfolds when low ionic strength water is used for irrigation (e.g. Quirk, 1994). In petrology, this scenario unfolds when fresh water is used to displace hydrocarbons in saline reservoirs, triggering formation damage (e.g. Tiab and Donaldson, 1996). In general, colloid mobilization occurs when the ionic strength, *I*, drops below the critical coagulation concentration (CCC), which depends on the colloid, the pH, and the sodium adsorption ratio (SAR). Thus, when *I*/CCC > 1, colloid flocculation is expected, corresponding to enhanced filtration and good soil structure with high permeability. Conversely, when *I*/CCC < 1, colloid dispersion is expected, corresponding to colloid mobilization and poor soil structure with low permeability, that is, clogging.

To help conceptualize the related effects of ionic strength, pH, and SAR on colloid deposition and mobilization, one can plot the CCC of the primary clay minerals as a function of SAR (Figure 2). Such a plot is called a Quirk-Schofield diagram (Mays, 2007; Quirk and Schofield, 1955; Sposito, 1989, Chapter 12). When (SAR, *I*) plots above the relevant CCC curve, colloid flocculation is expected, associated with high permeability. When (SAR, *I*) plots below the relevant CCC curve, colloid dispersion is expected, associated with colloid mobilization and clogging. Quirk-Schofield diagrams can also be extended to capture the effect of pH by plotting a family of CCC curves on the same (SAR, *I*) axes, with each curve corresponding to a given pH. In temperate environments where the pH exceeds the point of zero charge for the relevant clays, increasing pH tends to make the clay surface charge more negative, such that a larger ionic strength is required to overcome electrostatic repulsion, which corresponds to larger CCC. Under these conditions, therefore, the topmost CCC versus SAR curve corresponds to the largest value of pH (Mays, 2007).

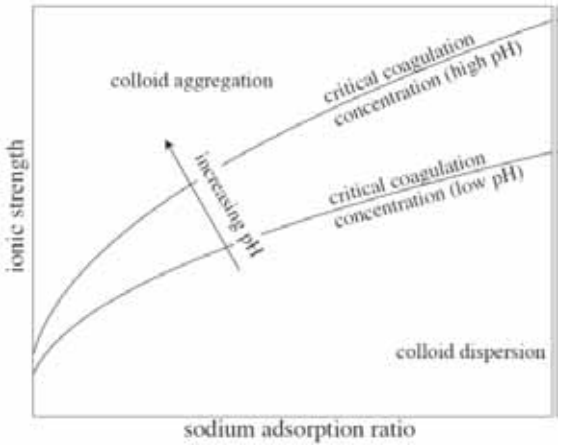

Figure 2: For a given colloid, the Quirk-Schofield diagram plots the critical coagulation concentration (CCC) versus sodium adsorption ratio (SAR). The effect of pH is captured by plotting a family of curves, one for each pH. When (SAR, I) plots above the relevant curve, then chemical conditions favor flocculation, which is associated with good soil structure. Conversely, when (SAR, I) plots below the relevant curve, then chemical conditions favor dispersion, which is associated with poor soil structure. Reproduced from Manga et al. (2012) with permission from the American Geophysical Union

2.3 Clogging

Although colloidal phenomena have a major effect on aquifer permeability, no model is currently available to predict permeability (Babadagli and Al-Salmi, 2004). In principle, complete knowledge of deposition and mobilization would allow one to exactly compute the specific deposit and therefore, by subtraction, the reduced porosity. But even in such an idealized scenario, knowing the reduced porosity would not allow one to predict the permeability. Why? Because clogging depends not only on the specific deposit by also—crucially—on deposit morphology (Mays, 2010; Wiesner, 1999). To shed light on the role of deposit morphology, this section provides a brief review of two contemporary clogging models that explicitly account for specific deposit and deposit morphology, with each model using a single empirical parameter.

Both clogging models are based on the Kozeny-Carman equation (Carman, 1937; Kozeny, 1927), which is valid for clean, monodisperse granular media, such as granular media filters for water treatment. The Kozeny-Carman equation is

$$k = \frac{\varphi^3}{(1-\varphi)^2}\left(\frac{{d_g}^2}{180}\right) \quad (7)$$

where φ is porosity and d_g is the porous media diameter. Lacking another standard porosity-permeability model, the Kozeny-Carman equation has been applied to all manner of porous media, from soils to filter cakes to settling colloidal aggregates. Despite its popularity, there is growing consensus that the Kozeny-Carmen equation is poorly suited for many natural porous media: Chen and Doolen (1998) noted that it works poorly for flow through networks; Selomulya et al., (2006) pointed out that it is inadequate because permeability depends on the connectivity of pores, not only on porosity and surface area; Zhou et al. (2009) concluded that the so-called Kozeny constant is not actually a constant; and Armstrong and Ajo-Franklin (2011) reported that the Kozeny-Carman equation was completely unable to quantify extreme clogging during biomineralization.

To address these shortcomings, two contemporary clogging models modify the Kozeny-Carman equation by including deposit morphology as an empirical parameter. In one approach, an empirical area factor γ is used to adjust the effective surface area of colloid deposits (O'Melia and Ali, 1978), which gives (Mays and Hunt, 2005):

$$\frac{k}{k_o} = (1+\gamma\sigma)^{-2} \quad (8)$$

where k_o is clean bed permeability. In an alternative approach, an empirical bulk factor b is used to adjust the effective volume of the colloid deposits (Ojha and Graham, 1992), giving (Krauss and Mays, 2013):

$$\frac{k}{k_o} = \left(\frac{\varphi_o - b\sigma}{\varphi_o}\right)^3\left(\frac{1-\varphi_o}{1-\varphi_o+b\sigma}\right)^2 \quad (9)$$

where φ_o is clean bed porosity. When fitted to available data, both γ and b display power law correlations with the fluid velocity u, or more generally with the Peclet number, N_{Pe}, which is the dimensionless ratio of advection to diffusion:

$$N_{Pe} = \frac{qd_g}{D_p} \quad (10)$$

where D_p is the particle diffusivity:

$$D_p = \frac{\kappa T}{3\pi\mu d_p} \quad (11)$$

where κ is Boltzmann's constant, T is absolute temperature, and d_p is the particle diameter. Specifically, $\gamma \sim N_{Pe}^{-0.55 \pm 0.09}$ (Mays and Hunt, 2007), and $b \sim N_{Pe}^{-n}$, where -2.0 n -0.15 (Krauss and Mays, 2013). Therefore, across multiple data sets, when the specific deposit is held constant, larger Peclet numbers are associated with smaller values of these empirical parameters, and therefore with reduced clogging compared to results with larger Peclet numbers. This appears to be a general pattern, but as discussed below, it is valid only for filtration experiments conducted in initially clean beds.

3 Observations from Allied Fields

Discussion of clogging is simplified by conceptualizing aquifers in two classes. In the first class are aquifers resembling clean beds, initially free of colloids, for which the relevant literature falls under the heading of water treatment. In the second class are aquifers containing a few percent colloids (by weight or volume), for which the relevant literature falls under the headings of soils science and petrology. The following sections discuss physical and chemical clogging phenomena in each of these two classes.

3.1 Water Treatment

In water treatment, granular media filters are used to remove suspended solids and microbial pathogens during the production of potable water. As these colloidal materials accumulate in the filter, permeability can drop by up to three orders of magnitude (Veerapaneni and Wiesner, 1997), which requires proportionally increased hydraulic head to maintain a constant production rate. Accordingly, granular media filters are backwashed every

1–4 days (MWH 2005, § 11–2), which entails pumping treated water upward through the filter at a rate sufficient to cause complete fluidization (i.e. liquefaction). Backwashing is usually augmented by simultaneous air injection, which assists with removal of deposited colloids, presumably because colloids sorb to air-water interfaces (Wan and Wilson 1994). Backwashed fluid, representing 1–5% of the treatment plant's production, is typically recycled to the plant intake (American Water Works Association, 1990, page 988). After backwashing, the granular media filter begins its next service cycle, starting as an essentially clean bed.

Review of data from water treatment plants and from laboratory columns reveals consistent relationships between clogging and physical and chemical variables. With regard to physical variables, as discussed in § 2.3, for a given specific deposit, clogging is more severe at lower fluid velocity, and less severe at higher fluid velocity (Krauss and Mays, 2013; Mays and Hunt, 2005). Equivalent results have also been observed in filtration experiments compared on the basis of equal pore volumes eluted, rather than on the basis of equal specific deposit. For example, Figure 3(a) shows more clogging from bentonite depositing in a granular media filter at slower velocity, manifested as a smaller normalized permeability k/k_o.

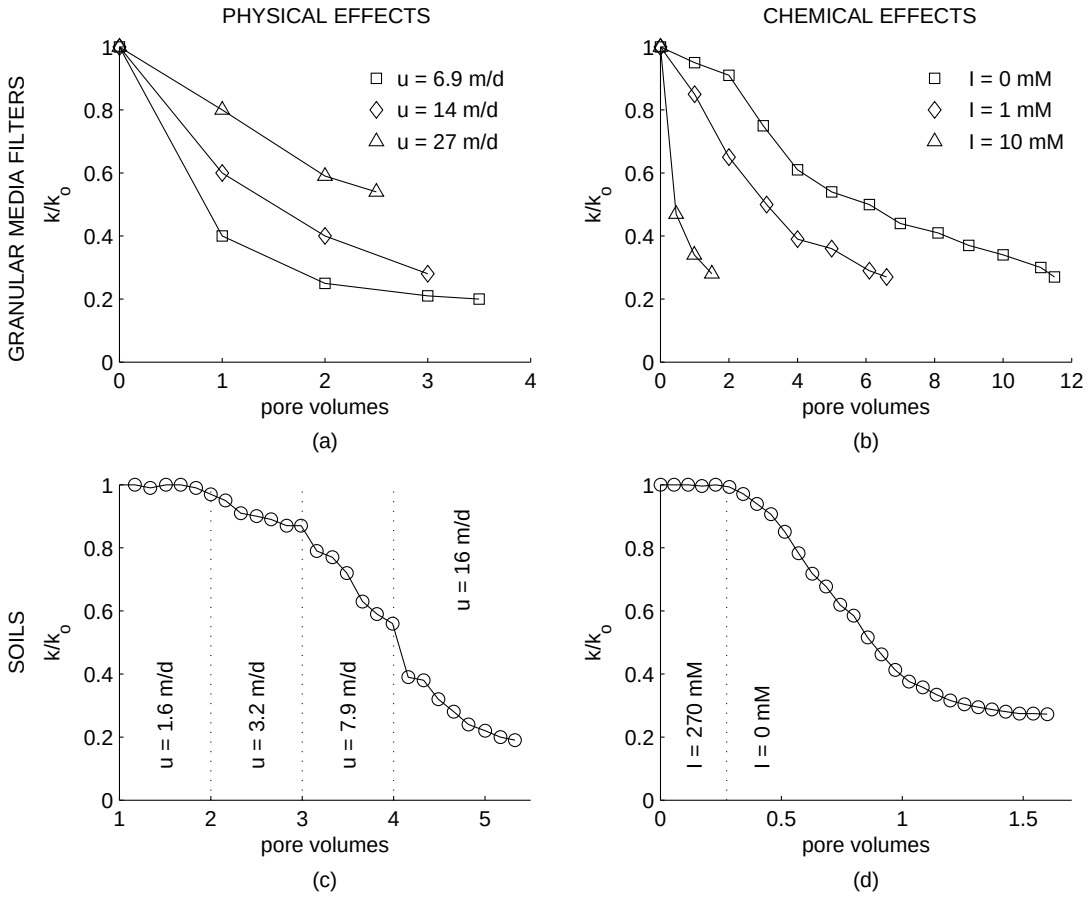

Figure 3: Comparing normalized permeability k/ko versus pore volumes eluted in various column experiments reveals that physical and chemical clogging effects are opposite in clean beds, resembling granular media filters versus porous media containing a few percent colloids, resembling soils. In granular media filters, clogging is associated with (a) lower fluid velocity, u, and with (b) higher ionic strength, I, reported by Rege and Fogler (1988) for filtration of bentonite in a granular media filter. In soils, clogging is associated with (c) higher fluid velocity and with (d) lower ionic strength, reported by Poesio and Ooms (2004) for flow through Berea sandstone. *Reproduced from Mays (2010) with permission from the American Society of Civil Engineers*

With regard to chemical variables, clogging is associated with chemical conditions favoring increased colloid retention. Because high ionic strength, low SAR, and low pH each contribute to additional colloid retention, they all tend to exacerbate clogging (Mays, 2007). As discussed in § 2.2, the effects of ionic strength, SAR, and pH can each be visualized using Quirk-Schofield diagrams (Figure 2). For example, Figure 3(b) shows more severe clogging at higher ionic strength, again for bentonite depositing in a granular media filter. Chemical effects can also play an important role in clogging even when comparing two experiments with similar ratios of I/CCC. For example, for matching specific deposits, sodium montmorillonite with I/CCC ≈ 13 causes approximately 20 times more clogging than calcium montmorillonite with I/CCC ≈ 17 (Mays and Hunt, 2007). In this case, the significant difference in clogging has been attributed to the qualitative morphological difference between sodium montmorillonite, which forms deposits of extremely high porosity (Borchardt, 1989), and calcium montmorillonite, which forms more compact quasi-crystals (Mohan and Fogler, 1997).

3.2 Soil Science and Petrology

In soil science, maintenance of soil structure is crucial for crops to prosper and for drainage to remove salts. In petrology, maintenance of adequate permeability is crucial for economic recovery of hydrocarbons. Most soils and hydrocarbon reservoirs include a few percent clays. For example, Berea sandstones—common in many hydrocarbon reservoirs—have 5–8% clay (Mohan et al., 1993), and their qualitative clogging behavior matches that of soils (Mays, 2010). Compared to granular media filters in water treatment, the preponderance of clays in soils and hydrocarbon reservoirs is not surprising considering that natural porous media accumulate clays from weathering reactions and from filtration of suspended solids, but never experience anything equivalent to the backwashing used in granular media filters for water treatment. Accordingly, clogging in soils and hydrocarbon reservoirs depends primarily on deposit morphology (Mays, 2010).

With regard to physical variables, clogging in soils and hydrocarbon reservoirs is associated with higher fluid velocity (Mays, 2010). Increasing clogging with increasing fluid velocity has been called "convective jamming" (Sen et al., 2002), and has been attributed to the formation of colloid bridges across critical pore throats (Panda and Lake, 1995; Ramachandran and Fogler, 1999; Valdes and Santamarina, 2006). For example, Figure 3(c) shows increasing clogging with increasing velocity, manifested as a smaller normalized permeability k/ko, for flow through Berea sandstone.

With regard to chemical variables, clogging in soils and hydrocarbon reservoirs is associated with chemical conditions favoring colloid dispersion. That is, in media already occupied by copious populations of clays, additional accumulation of clay is relatively unimportant, but rearrangement of existing clays is crucial. Chemical conditions favoring colloid dispersion include low ionic strength, high SAR, and low pH (Mays, 2007). For example, Figure 3(d) shows a distinct reduction in the permeability of Berea sandstone when water at I = 270 mM is displaced by distilled water.

Comparing the clogging phenomena discussed in § 3.1 for granular media filters in water treatment with the parallel phenomena discussed in this section reveals an apparent paradox, as the relationships between physical and chemical perturbations and clogging are generally opposite. To recapitulate: Faster flow causes less clogging in granular media filters, but more clogging in soils and hydrocarbon reservoirs. Colloid dispersion causes less clogging in granular media filters, but more clogging in soils and hydrocarbon reservoirs. To resolve this apparent paradox, research is underway to study clogging at a more fundamental level, using state-of-the-art laboratory techniques that provide quantitative measurements of deposit morphology.

3.3 Deposit Morphology

Two areas of current research are providing new insights into clogging by taking advantage of novel experimental techniques that can measure deposit morphology. These measurements, in turn, form the basis for innovative clogging models that—it is hoped—will account for the crucial role of deposit morphology in clogging.

The first approach is to record the full three-dimensional geometry of the pore space, including colloid deposits, using x-ray computed microtomography. Such measurements are typically performed on a high-energy

photon beamline, for example at Argonne National Laboratory (Gaillard et al., 2007) or Lawrence Berkeley National Laboratory (Armstrong and Ajo-Franklin, 2011). Flow through the 3D pore structure model is then simulated using techniques from computational fluid mechanics, most commonly lattice Boltzmann simulations (Armstrong and Ajo-Franklin, 2011; Gaillard et al., 2007). The flow simulation is then used to calculate a macroscopic permeability for the porous media. This approach has the advantage of capturing the full geometry of the pore space, but has limited ability to probe colloid deposits at resolutions less than several micrometers.

The second approach conceptualizes colloid deposits as fractals, based on the observation that colloid aggregates have fractal geometry (Elimelech et al., 1995), and on simulations of fractal colloid deposits (Veerapaneni and Wiesner, 1994). Fractals have non-integer fractal dimensions, Df, where the fractal dimension (formally defined here as a mass fractal dimension) is:

$$m \sim \lambda^{D_f} \tag{12}$$

where m is mass and λ is a characteristic length scale. The fractal dimension of colloid aggregates or deposits is measured optically, using a technique called static light scattering. This technique, originally developed to characterize suspensions of colloid aggregates, can be extended to characterize colloid deposits inside porous media either by re-suspending deposits into a traditional suspension (Veerapaneni and Wiesner, 1997), or within the pore space itself using refractive index matched (RIM) porous media (Mays et al., 2011). The RIM study recorded a fractal dimension of Df = 2.2 for deposits formed with a hydrodynamic shear stress of $\tau \approx 17$ dyn/cm^2. This fractal dimension indicates that the deposits were more densely packed than equivalent suspended aggregates, whose fractal dimension of Df = 1.8 resulted from hydrodynamic shear stress of $\tau \approx 0.3$ dyn/cm^2. The RIM study is currently being extended to simultaneously record clogging, specific deposit, and deposit fractal dimension in a flow column, with the goal of linking clogging to this quantitative measurement of deposit morphology.

4 Discussion and Conclusions

The literature reveals contradictory clogging behavior in the first class of porous media, resembling granular media filters in water treatment, and the second class of porous media, resembling soils or hydrocarbon reservoirs. Which set of phenomena is more likely relevant to MAR? The second class. Available data indicate that clogging in MAR is analogous to clogging in soils or hydrocarbon reservoirs, rather than granular media filters, at least when the primary clogging mechanism is filtration and mobilization of suspended solids, especially clay colloids. This analogy to soils and hydrocarbon reservoirs appears to be valid for both physical and chemical effects: With regard to physical effects, aquifer recharge using wells is "more vulnerable to clogging" than aquifer recharge using infiltration basins because the fluid velocity is generally higher with injection through wells (American Society of Civil Engineers 2001, § 10.7.2). Similarly, Pavelic et al. (2011) reported that recharge rates through infiltration basins were larger with 30 cm of ponding depth than with 10 cm, due to the increased head gradient, but that further increase of the ponding depth to 50 cm did not increase the recharge rate because clogging worsened. With regard to chemical effects, clogging in MAR results from water with low ionic strength (Pyne, 1995; § 5.4) and high SAR (American Society of Civil Engineers, 2001; § 10.7.2.2), both of which are associated with colloid dispersion (Figure 2). These results have been corroborated in the laboratory, where a column of sediments clogged after injecting low-ionic strength fluid (Zhou et al., 2009), analogous to the results in Figure 3(d).

In conclusion, the literature on water treatment, soil science, and petrology highlights several physical and chemical mechanisms that provide insight into clogging in MAR. These mechanisms may be summarized as follows:

- Available studies on hydrodynamic shear suggest a critical shear stress for colloid mobilization in the range of 1–10 dyn/cm^2. Colloid mobilization is associated with clogging in soils and hydrocarbon reservoirs.
- Colloids flocculate when I/CCC > 1 and disperse when I/CCC < 1. The transition from flocculated to

dispersed colloids triggers a qualitative change in permeability, in many cases from unclogged to clogged.

- Aquifers used for MAR are likely to manifest clogging phenomena analogous to soils or hydrocarbon reservoirs, rather than granular media filters in water treatment. Accordingly, during regular injection and extraction operations, the available data suggest the following provisional guidelines to prevent or manage clogging in MAR:
- Injection fluid should have TSS as low as readily achievable.
- Fluid velocity should be kept as low as possible, except during backwashing.
- Chemical conditions should favor colloid aggregation, where $I \geq Io$, $SAR \leq SARo$, and $pH \leq pHo$, where Io, SARo, and pHo refer to pre-MAR geochemical conditions in the target aquifer.

The results analyzed here pertain only to clogging resulting from filtration and mobilization of clays and other suspended colloids. These results should not be extrapolated to systems in which mineral precipitation or biofilm growth are the primary clogging mechanisms.

Acknowledgments and Disclaimer

Michael Manga graciously provided the graphic in Figure 2. This material is based, in part, on work supported by the U.S. Department of Energy under award DE-SC0006962. Neither the U.S. government nor any agency thereof, nor any of their employees, makes any warranty, express or implied, or assumes any legal liability or responsibility for the accuracy, completeness, or usefulness of any information, apparatus, product, or process disclosed, or represents that its use would not infringe privately owned rights. The views and opinions of the author do not necessarily state or reflect those of the U.S. government or any agency thereof.

References

American Society of Civil Engineers, (2001) Standard Guidelines for Artificial Recharge of Ground Water. EWRI/ASCE 34-01, American Society of Civil Engineers, Reston, VA.

American Water Works Association, (1990) Water Quality and Treatment: A Handbook of Community Water Supplies, 4 Ed., McGraw-Hill, Inc., New York.

Armstrong, R., and Ajo-Franklin, J., (2011) Investigating biomineralization using synchrotron based X-ray computed microtomography. Geophys. Res. Lett., 38, L08406, doi:10.1029/2011GL046916.

Babadagli, T., and Al-Salmi, S., (2004) A review of permeability-prediction methods for carbonate reservoirs using well-log data. SPE Reserv. Eval. Eng., 7(2), 75–88.

Borchardt, G., (1989) Smectites. In: Minerals in Soil Environments, J. B. Dixon and S. B. Weed, eds., Soil Science Society of America, Madison, WI.

Bradford, S.A., Yates, S.R., Bettahar, M., and Simunek, J., (2002) Physical factors affecting the transport and fate of colloids in saturated porous media. Water Resour. Res., 38(12), 1327, doi:10.1029/2002WR001340.

Carman, P. C., (1937) Fluid Flow through Granular Beds. Trans. Inst. Chem. Eng., 15, 150.

Chen, S., and Doolen, G.D., (1998) Lattice Boltzmann method for fluid flows. Annu. Rev. Fluid Mech., 30, 329–364.

Elimelech, M., Gregory, J., Jia, X., and Williams, R.A., (1995) Particle Deposition and Aggregation, Butterworth-Heinemann, Boston.

Gaillard, J.F., Chen, C., Stonedahl, S.H., Lau, B.L.T., Keane, D.T., and Packman, A.I., (2007) Imaging of colloidal deposits in granular porous media by X-ray difference micro-tomography. Geophys. Res. Lett., 34(18), L18404, doi:10.1029/2007GL030514.

Ives, K., (1970) Rapid filtration. Water Res., 4, 201–223.

Ives, K.J., and Fitzpatrick, C.S.B., (1989) Detachment of Deposits from Sand Grains. Colloid. Surface., 39 (1–3), 239–253.

Johnson, W.P., Ma, H.L., and Pazmino, E., (2011) Straining Credibility: A General Comment Regarding Common Arguments Used to Infer Straining As the Mechanism of Colloid Retention in Porous Media. Environ. Sci. Technol., 45(9), 3831–3832.

Kessler, J., (1993) Transport and channeling effects in a fracture partially clogged with colloidal material, Ph.D. dissertation, University of California Berkeley, Berkeley, CA.

Kozeny, J., (1927) Über Kapillare Leitung des Wassers im Boden. Sitzungsber Akad. Wiss., Wien, 136(2a), 271–306.

Krauss, E. D., and Mays, D.C., (2013) "Modification of the Kozeny-Carman Equation to Quantify Formation Damage by Fines in Clean Unconsolidated Porous Media." In: International Conference and Exhibition on European Formation Damage, SPE-165148, Society of Petroleum Engineers, Noordwijk, Netherlands.

Kretzschmar, R., Borkovec, M., Grolimund, D., and Elimelech, M. (1999) Mobile subsurface colloids and their role in contaminant transport. Adv. Agron., 66, 121–193.

Levine, A.D., and Asano, T., (2004) Recovering sustainable water from wastewater. Environ. Sci. Technol., 38(11), 201a–208a.

Ma, H.L., Pedel, J., Fife, P., and Johnson, W.P., (2009) Hemispheres-in-Cell Geometry to Predict Colloid Deposition in Porous Media. Environ. Sci. Technol., 43(22), 8573–8579.

Manga, M., Beresnev, I., Brodsky, E.E., Elkhoury, J.E., Elsworth, D., Ingebritsen, S.E., Mays, D.C., and Wang, C.Y., (2012) Changes in Permeability Caused by Transient Stresses: Field Observations, Experiments, and Mechanisms. Rev. Geophys., 50, RG2004, doi:10.1029/2011RG000382.

Mays, D.C., (2007) Using the Quirk-Schofield diagram to explain environmental colloid dispersion phenomena. J. Nat. Resour. Life Sci. Ed., 36, 45–52.

Mays, D.C. (2010) Contrasting clogging in granular media filters, soils, and dead-end membranes. J. Environ. Eng., 136(5), 475–480.

Mays, D.C., Cannon, O.T., Kanold, A.W., Harris, K.J., Lei, T.C., and Gilbert, B., (2011) Static light scattering resolves colloid structures in index-matched porous media. J. Colloid Interf. Sci., 363, 418–424.

Mays, D.C., and Hunt, J.R., (2005) Hydrodynamic aspects of particle clogging in porous media. Environ. Sci. Technol., 39(2), 577–584.

Mays, D.C., and Hunt, J. R., (2007) Hydrodynamic and chemical factors in clogging by montmorillonite in porous media. Environ. Sci. Technol., 41(16), 5666–5671.

McDowell-Boyer, L.M., Hunt, J.R., and Sitar, N., (1986) Particle transport through porous media. Water Resour. Res., 22(13), 1901–1921.

Mohan, K.K., and Fogler, H.S. (1997) Effect of pH and layer charge on formation damage in porous media containing swelling clays. Langmuir, 13(10), 2863–2872.

Mohan, K.K., Vaidya, R.N., Reed, M.G., and Fogler, H.S., (1993) Water Sensitivity of Sandstones Containing Swelling and Non-Swelling Clays. Colloid. Surface. A, 73, 237–254.

MWH., (2005) Water Treatment: Principles and Design, 2 Ed., John Wiley and Sons, Inc., Hoboken, NJ.

Nelson, K.E., and Ginn, T.R., (2011) New collector efficiency equation for colloid filtration in both natural and engineered flow conditions. Water Resour. Res., 47, W05543, doi:10.1029/2010WR009587.

O'Melia, C.R., and Ali, W., (1978) The role of retained particles in deep bed filtration. Prog. Water Res., 10(5/6), 167–182.

Ojha, C.S.P., and Graham, N.J.D., (1992) Appropriate use of deep-bed filtration models. J. Environ. Eng., 118(6), 964–980.

Panda, M.N., and Lake, L.W., (1995) A Physical Model of Cementation and Its Effects on Single-Phase Permeability. AAPG Bull., 79(3), 431–443.

Pavelic, P., Dillon, P.J., Mucha, M., Nakai, T., Barry, K.E., and Bestland, E., (2011) Laboratory assessment of factors affecting soil clogging of soil aquifer treatment systems. Water Res., 45(10), 3153–3163.

Poesio, P., and Ooms, G., (2004) Formation and ultrasonic removal of fouling particle structures in a natural porous material. J. Petrol. Sci. Eng., 45(3–4), 159–178.

Pyne, R.D.G., (1995) Groundwater Recharge and Wells: A Guide to Aquifer Storage Recovery, Lewis Publishers, Boca Raton, FL.

Quirk, J.P., (1994) Interparticle forces: A basis for the interpretation of soil physical behavior. Adv. Agron., 53, 121–183.

Quirk, J.P., and Schofield, R.K., (1955) The effect of electrolyte concentration on soil permeability. J. Soil Sci., 6(2), 163–178.

Rajagopalan, R., and Tien, C. (1976) Trajectory Analysis of Deep-Bed Filtration with Sphere-in-Cell Porous-Media Model. AIChE J., 22(3), 523–533.

Ramachandran, V., and Fogler, H.S., (1999) Plugging by hydrodynamic bridging during flow of stable colloidal particles within cylindrical pores. J. Fluid Mech., 385, 129–156.

Rege, S.D., and Fogler, H.S., (1988) A Network Model for Deep Bed Filtration of Solid Particles and Emulsion Drops. AIChE J., 34(11), 1761–1772.

Ryan, J.N., and Elimelech, M., (1996) Colloid mobilization and transport in groundwater. Colloid. Surface. A, 107, 1–56.

Selomulya, C., Tran, T.M., Jia, X., and Williams, R.A., (2006) An integrated methodology to evaluate permeability from measured microstructures. AIChE J., 52(10), 3394–3400.

Sen, T.K., Mahajan, S.P., and Khilar, K.C., (2002) Colloid-associated contaminant transport in porous media: 1. Experimental studies. AIChE J., 48(10), 2366–2374.

Sposito, G., (1989) The Chemistry of Soils, Oxford University Press, New York.

Tiab, D., and Donaldson, E., (1996) Petrophysics. Gulf Publishing Company, Houston, TX.

Tufenkji, N., (2007) Modeling microbial transport in porous media: Traditional approaches and recent developments. Adv. Water Resources., 30, 1455–1469.

Tufenkji, N., and Elimelech, M., (2004) Correlation equation for predicting single-collector efficiency in physicochemical filtration in saturated porous media. Environ. Sci. Technol., 38(2), 529–536.

U.S. National Research Council, (2008) Prospects for Managed Underground Storage of Recoverable Water. National Academies Press, Washington, DC.

Valdes, J.R., and Santamarina, J.C., (2006) Particle clogging in radial flow: Microscale mechanisms. SPE J., 11(2), 193–198.

Veerapaneni, S., and Wiesner, M.R., (1994) Particle Deposition on an Infinitely Permeable Surface - Dependence of Deposit Morphology on Particle-Size. J. Colloid Interf. Sci., 162(1), 110–122.

Veerapaneni, S., and Wiesner, M.R., (1997) Deposit morphology and head loss development in porous media. Environ. Sci. Technol., 31(10), 2738–2744.

Wan, J.M., and Wilson, J.L., (1994) Visualization of the Role of the Gas-Water Interface on the Fate and Transport of Colloids in Porous-Media. Water Resour. Res., 30(1), 11–23.

Wiesner, M.R., (1999) Morphology of particle deposits. J. Environ. Eng., 125(12), 1124–1132.

Yao, K.-M., Habibian, M.T., and O'Melia, C.R., (1971) Water and waste water filtration: Concepts and applications. Environ. Sci. Technol., 5(11), 1105–1112.

Zhou, J., Zheng, X.L., Flury, M., and Lin, G.Q., (2009) Permeability changes during remediation of an aquifer affected by sea-water intrusion: A laboratory column study. J. Hydrol., 376(3–4), 557–566.

Contact Details

David C. Mays, P.E., Ph.D.
University of Colorado Denver
Department of Civil Engineering
Campus Box 113
PO Box 173364
Denver, CO 80217-3364
United States of America
Phone: +1-303-352-3933
Fax: +1-303-556-2368
david.mays@ucdenver.edu
http://carbon.ucdenver.edu/~dmays

CLOGGING STUDIES LABORATORY COLUMN EXPERIMENTS

Reclaimed Water for Aquifer Storage and Recovery: A Column Study of Well Clogging

S. Rinck-Pfeiffer[1], P. Dillon[2], S. Ragusa[3], J. Hutson and H. Fallowfield[4], G. de Marsily[5], and P. Pavelic[2]

[1] *Vivendi-Water Deutschland, Berlin, Germany*

[2] *CSIRO Land & Water, Glen Osmond, South Australia*

[3] *E.M. Biotechnology, Sydney, Australia*

[4] *Flinders University of SA*

[5] *Université Pierre et Marie Curie, Paris VI, France*

Abstract

The injection of reclaimed water derived from a municipal sewage treatment plant into a brackish aquifer for recovery and reuse in irrigation is currently being evaluated at Bolivar, South Australia. A primary concern before the trial was the potential for clogging of the injection well, so laboratory column experiments were performed to understand and predict bore clogging, and allow the development of management strategies. This paper describes the methods and results obtained from a series of three laboratory column studies each run over three weeks, when samples of different qualities of reclaimed water were passed through columns of repacked limestone aquifer material, and the extent of clogging was observed. Reclaimed water samples with and without suspended solids and micro-organisms were used. Hydraulic conductivities decreased in all columns, stabilised, and recovered slightly. The results suggest that physical clogging is the main cause of clogging in these cases followed by biological clogging which manifests itself at a slower rate as bacterial biomass and associated polysaccharides accumulate. The extent of clogging was relieved during all column experiments due to calcite dissolution and the resulting porosity change of the aquifer matrix. A numerical model was used to scale-up the clogging effects to infer the likely hydraulic impact to be encountered at the injection well in a field trial.

1 Introduction

As the conventional use of water resources in arid parts of the world approaches the limits of sustainable use, the need to address water reclamation and appropriate reuse is becoming critical. Aquifer Storage and Recovery (ASR) is one of the ways excess surface water can be stored and treated for future use. This involves injecting water into an aquifer where it is stored until it is extracted from the same well for reuse (Pyne, 1995). Since 1993 in South Australia the practice of storing urban and rural stormwater runoff over winter in brackish aquifers has been successful in generating summer landscape and agricultural irrigation supplies (Dillon et al., 1997). Water quality improvements were observed and guidelines written on the quality of stormwater and treated wastewater for injection into aquifers for storage and reuse (Dillon and Pavelic, 1996). That work gave evidence that sustainable water quality improvements in the subsurface were possible when injecting waters of impaired quality into aquifers that were otherwise not fit for drinking or irrigation water supply. The quantity of stormwater injected into aquifers in arid areas is limited by the infrequency of rainfall events and the need for some form of surface storage, such as artificial urban wetlands, in order to allow time for injection at a much slower rate than the rate at which water runs off a catchment.

Consequently, the Bolivar Reclaimed Water ASR Research Project was launched, to harvest water from a wastewater reclamation plant built adjacent to the largest sewage treatment plant of the city of Adelaide. The reclamation

plant serves an extensive horticultural area with more than 20 Gigalitres of irrigation water from a low-pressure pipeline. However in winter, demand is less than the supply and water is discharged into the sea. The research project aims at determining the technical feasibility, environmental sustainability and economic viability of ASR using reclaimed water (Dillon et al., 1999). If successful up to 10 GL of reclaimed water could be stored in depleted confined aquifers beneath the irrigation area, and enable expansion of crops, alleviate over-exploitation and consequent salinisation of groundwater supplies and reduce discharge of nutrients into the sensitive coastal environment of the Gulf of St. Vincent.

Clogging is often perceived as a significant barrier to artificial recharge by well injection, and was monitored at a research site for stormwater ASR (Pavelic et al., 1998) and found to be controllable. For nutrient-rich waters, the constraint was considered to be more severe due to the enhanced potential for biofilm to grow in the well and aquifer, so more stringent management practices would be required to sustain injection rates in the long term. Hence before conducting the field trial for the Bolivar Reclaimed Water ASR Research Project, it was decided to undertake column tests to determine the potential for clogging.

2 Previous Studies

Clogging has frequently been observed in well-injection studies, and therefore has been extensively studied. Suspended solids (SS) in injectant have commonly been a key determinant in injection well performance, despite advances in injection well technology (Hauser and Lotspeich, 1967; Harpaz, 1971; Vecchioli, 1972; Olsthoorn, 1982). Previous experimental results (Okubo and Matsumoto, 1983) have shown that recharge water used for ASR should have levels of SS < 2mg/L to avoid major clogging problems, although levels in excess of 150 mg/L have not caused irreversible clogging in a calcareous aquifer at a stormwater ASR site in South Australia (Pavelic et al., 1998). The second most important factor causing injection well clogging is biological clogging (Oberdorfer and Peterson, 1985).

Several methods have been used to predict the potential clogging rates for a given recharge water. These include the modified fouling index (MFI) (Hutchinson, 1997) the assimilable and biodegradable dissolved organic carbon content (AOC, bDOC) of the recharged water (Schippers et al., 1995), and mathematical, empirical and analytical models (Taylor et al., 1990; Okubo & Matsumoto, 1979; Vandevivere et al., 1995). The main disadvantage of these predictive clogging tools is that they focus on a single clogging process by assessing either biological, physical, chemical or mechanical clogging. However, all these processes are interrelated and there is a need for improved understanding of these interactions. Column infiltration studies using treated effluent have previously been used to study biological clogging (Rebhun and Schwarz, 1968; Vecchioli, 1970; Ehrlich et al., 1973; Okubo and Matsumoto, 1983).

Column studies involving the continuous injection of treated reclaimed water rather than artificial effluent and using aquifer material from the target aquifer to study clogging processes have not been performed widely and no conclusive results have been obtained to date to the authors' knowledge. Considering the lack of research in the field of clogging and the relevance of clogging in ASR systems, it is evident that research on prediction and minimisation of clogging is warranted.

3 Methods

Column experiments were performed to investigate the effect of continuously injecting recycled water with and without suspended material and/or microorganisms, into columns packed with aquifer material. This study provided a comparison of aquifer clogging by physical and biological processes both separately and in combination.

3.1 Packing of laboratory columns

Cores of a sandy limestone aquifer (aquifer T2, known as the Port Willunga Limestone) were taken during construction of the ASR well at Bolivar on the Northern Adelaide Plains, South Australia. The recovered core was packed in PVC tubes, flushed with nitrogen gas on-site and stored at 4° C. The core was partly sectioned and analysed for mineralogy and hydraulic properties. X-ray diffraction showed that the core material was predominantly quartz and calcite in approximately equal proportions.

The core material was sub-sampled in an anaerobic chamber flushed with argon. The edges of the core material were removed and the inner piece of the core

was submerged in groundwater collected at the field site. The material was crushed, sieved through a 1mm sieve, and packed into columns (2.5 cm diameter and 16 cm long), all within the anaerobic chamber. Although intact samples were considered, it was decided to homogenise samples to enable replication, and to focus on changes in permeability as a result of physical, chemical and biological processes. This avoided confounding due to random differences in microstructure and permeability. Microfractures had a significant effect on the permeability of confined aquifer cores at effective stresses lower than those within in-situ aquifer material (Dillon et al., 2001), so homogenisation was an important consideration.

Breakthrough curves were obtained using a bromide tracer in native groundwater, to check that no preferential flow occurred, prior to the inoculation of the columns with additional groundwater. The effective porosity was found to range from 0.37 to 0.40, similar to that measured in the field. The columns were shaded from light by using aluminium foil, and the room temperature was kept at 20 ±2° C (the temperature of the groundwater at the depth of the core), during the experiments. The columns were flushed with groundwater from the field site to facilitate inoculation of the columns, and stabilisation and acclimatisation of native micro-organisms before introducing reclaimed water. The columns used for experiment 3 (i.e. physical clogging only) were sterilised in an autoclave twice before the injection of disinfected recycled water.

3.2 Column experiments

Three column experiments were performed separately but in the same manner by pumping reclaimed water through the packed columns at a rate of 5 L/day/column (Darcian velocity of 10.2 m/d) using a peristaltic pump. The velocity of recycled water (influent) pumped through the columns corresponded to that expected at the ASR site in the vicinity of the injection well.

The development of clogging and the resulting decrease in hydraulic conductivity was monitored by logging pressure sensors located in the intake and outflow and along the column. Daily measurements of flow were recorded and the permeability calculated. Water quality of column influent and effluent was monitored daily and other observations such as bacterial biomass and polysaccharide production were related to changes in hydraulic conductivity.

Column experiment 1 (where physical and biological clogging were possible) involved the use of the water intended to be injected at the Bolivar ASR site, namely secondary treated municipal effluent post-treated by dissolved air flotation/filtration (DAF/F) and containing suspended solids, nutrients (i.e. organic carbon, N and P) and microorganisms (see Table 1). Column experiment 2 (where only biological clogging was possible) used micro-filtered water from a membrane activated sludge process (Biosep®) which contained nutrients (i.e. organic carbon, N and P) and microorganisms (due to post-filtration contamination and bacterial regrowth) but no suspended solids. Column experiment 3 (where physical clogging was possible) used DAF/F water treated with formaldehyde. This water contained suspended solids and nutrients, but the packed columns had been sterilised to insure that no microbial growth was possible. Triplicate columns were run concurrently for each experiment.

3.3 Numerical modelling

Modelling of flow around the injection well in 2D axi-symmetric mode was simulated using the finite-element model FEFLOW (Diersch, 1996). A most important aspect of the model was that it could handle the time-varying material properties that occur through clogging. Injection takes place into a confined aquifer, which is assumed to be homogeneous and isotropic, at a constant rate of 25 Ls^{-1} (2160 m^3d^{-1}) for a period of 7 days. This period represents only the beginning of the injection cycle. A full-cycle simulation would also need to incorporate the effect of well redevelopment and the effect of calcite dissolution, which are not taken into account in the model. The volume of the aquifer around the well affected by clogging is assumed to extend a radial distance of 1.0 metre and is uniform. Only the DAF/F treated water scenario has been considered, as the data shows that the clogging experienced with this water type would be most severe. For comparison, a simulation was performed where there was no clogging.

4 Results and Discussion

4.1 Changes in hydraulic conductivity

The changes in hydraulic conductivity (K) along the columns were calculated from the average of each triplicate, and the part of the column where most clogging occurred was within 3 cm of the inlet (Figure 1).

Table 1: Typical reclaimed water quality used in each laboratory column experiment

Experiment	1. Physical and Biological Clogging	2. Biological Clogging only	3. Physical Clogging only
Water treatment	DAF/F treated water	Microfiltration (Biosep® treated water)	DAF/F and formaldehyde treated water
Parameter (mg/L unless otherwise specified)			
Total bacterial count (cells/mL)	10^4	10^4	0
Suspended Solids (SS)	4	0	4
pH	7.3	7.3	7.0
EC (mS/cm)	2.48	1.35	2
Alkalinity (as CaCO3)	130–140	120–130	140–160
Total Organic Carbon (TOC)	15–20	8–10	10–15
Biological Oxygen Demand (BOD)	2–3	2–3	2–3
Phosphorus (as P)	0.2–0.3	6–8	0.4
Ammonium-N	0.2–0.3	0.5–1.0	0.1
Nitrate + Nitrite (as N)	6–10	8–10	4

In all columns there was an initial decline in permeability lasting between 10 and 19 days, stabilisation and subsequently an increase. The most pronounced clogging effect was observed for experiment 1 with DAF/F water containing both suspended solids and nutrients permitting physical and biological clogging. K decreased from 0.8 metres/day to 0.04 metres/day after about 10 days of injection, stabilised until day 16, and then increased gradually up until the end of the experiment on day 22 when K reached 0.25 m/day.

The lowest clogging rate was obtained with the micro-filtered (Biosep* treated) water containing nutrients but no SS, whereby K decreased gradually from 0.9 metres/day to 0.24 metres/day in 19 days before a slight increase in K on days 21 and 22. The water with only SS and no microbial growth (i.e. DAF/F + formaldehyde) caused a clogging rate which was intermediate between the other two experiments. In Table 2, the results for initial permeability decline are presented as a percentage of the initial permeability (K0). These results demonstrate that the rate of K reduction is higher for physical and biological clogging combined (column experiment 1), followed by physical clogging alone (2) and biological clogging alone (3).

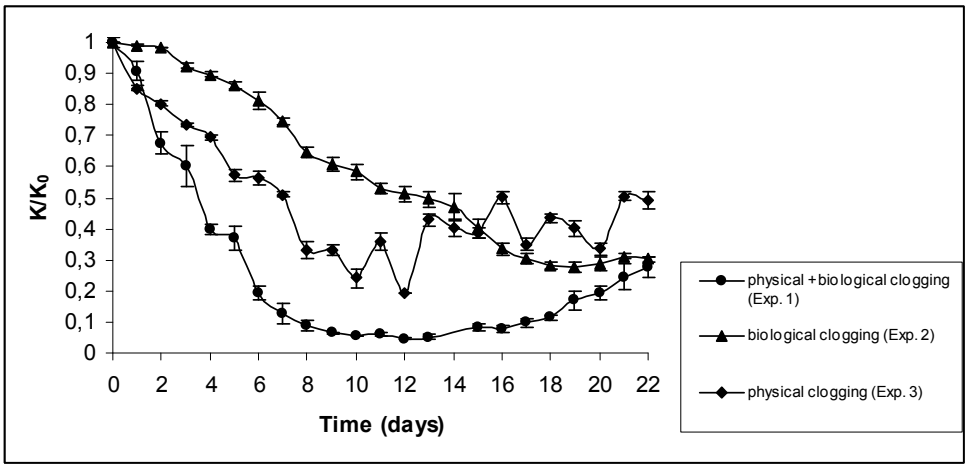

Figure 1: Decrease in hydraulic conductivity (K) at the inlet end of the column (0–3cm) during passage of reclaimed waters with and without suspended solids and micro-organisms for a period of 22 days. (Physical + Biological Clogging: Column Experiment 1, Biological Clogging: Column Experiment 2, Physical Clogging: Column Experiment 3)

Table 2: Comparison of initial reduction in hydraulic conductivity in column experiments

Experiment and Type of Clogging	Minimum K achieved K/K_0 (%)	Time to reach minimum K (days)	Initial Rate of K reduction (% per day)
1. Physical+ Biological	6	10	13
3. Physical	19	12	7
2. Biological	24	19	4

Filtration of suspended solids starts as soon as an experiment commences so physical clogging manifests itself earlier than biological clogging which is caused by the production of biomass and polysaccharide by microorganisms. This is not instantaneous, and is expected to depend on the levels of nutrients and organic carbon present in the injectant and on the initial population of microorganisms. Biological clogging was fastest in column experiment 1 because of the high level of organic suspended solid concentration that was present in the injected water. In column experiment 2, the organic carbon present in the injected water did not come from the suspended material as none was present but was in soluble form and was found to be partly recalcitrant. Biofilm growth is likely also to be responsible for enhanced entrapment of particulate matter. Hence we see that the rate of clogging for combined physical and biological clogging is greater than the sum of the clogging rates for separate physical and biological clogging.

The increase in hydraulic conductivity observed at later stages of all column experiments is attributable to the dissolution of calcite from the aquifer matrix. Calcite dissolution was observed in all the column experiments, as explained later.

In column experiment 1 the minimum value of hydraulic conductivity stayed constant at about 0.04 m/day between days 7 and 16. During this period calcite dissolution compensated for reducing permeability of the filter cake composed of suspended solids and biofilm. Permeability increased after day 16 due to porosity changes in the aquifer matrix and resulting fissure formation throughout the columns that disturbed the compacted filter cake near the column inlet.

Biomass assays have indicated that cell mass accumulation and resulting polysaccharide production from certain bacteria (e.g. Pseudomonas) have contributed significantly to the observed decrease in hydraulic conductivity in column experiments 1 and 2. This would also be expected for non-calcareous aquifers where biological clogging may be as important as physical clogging, depending on the nutrient and organic carbon concentrations of the injected water.

4.2 Calcite dissolution

Calcite dissolution started as soon as the reclaimed water was introduced into the columns, which had been flushed with the ambient groundwater that was in geochemical equilibrium with the matrix. This process is clearly evident from the increase in calcium levels in column effluent for experiment 1 (Figure 2) and occurred in all experiments. There was a high percentage of carbonate minerals (49%) present in the aquifer material contained in the columns. By the end of experiment 1, approximately 10% of the calcium initially present at the inlet end of the columns had been dissolved (Rinck-Pfeiffer et al., 2000). Concurrent increases in pH, alkalinity and a slight increase in EC were also observed and are additional indicators of calcite dissolution. Some of the dissolved calcium was re-precipitated towards the outlet end of the column. Towards the end of the experiment, respiration of carbon dioxide by biomass produced carbonic acid, which was buffered by dissolution of calcite.

As a result of calcite dissolution, fissures were observable at the inlet end of all three columns halfway through experiment 1. Fissures appeared to form earlier (from about 5 days) in the columns receiving water without micro-organisms (experiment 3), probably as the pH was lower. For the micro-filtered reclaimed water the increase in permeability was small and occurred near the end of the experiment, indicating that the rate of calcium dissolution was lower for this experiment. This may be due to higher phosphorus concentrations in influent reacting with calcite to precipitate an apatite coating.

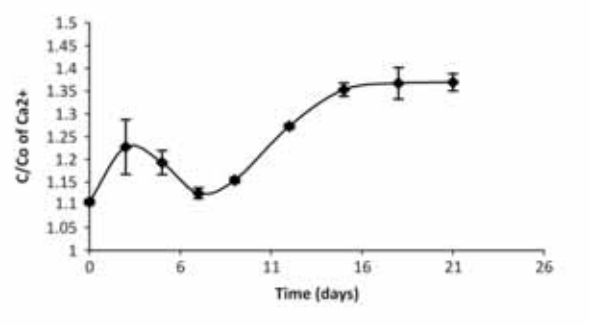

Figure 2: Ratio of calcium concentrations in column effluent to influent in the columns (mean and standard deviation of 3 replicates) for experiment 1 (DAF/F water)

4.3 Modelling results

A numerical model was applied making use of the experimental data, to simulate the effect of clogging on injection rate decline over time around the well. The predicted increase in piezometric head at the injection well over seven days is shown in Figure 3 in the case where the rate of K reduction is 0.10 m/day per day, analogous to the injection of DAF/F treated water. The figure shows that the piezometric head increase is most severe in the latter half of the simulation, when K is lowest, with the total piezometric head increase of 112 m, with ~90 m of buildup due to clogging after seven days. This predicted clogging would be intolerable in practice as pumping costs would be high. The success of redevelopment would also be impaired if the magnitude of the reversed hydraulic gradient during recovery did not exceed that during injection, so that retrieval of particulates from aquifer pores could be incomplete.

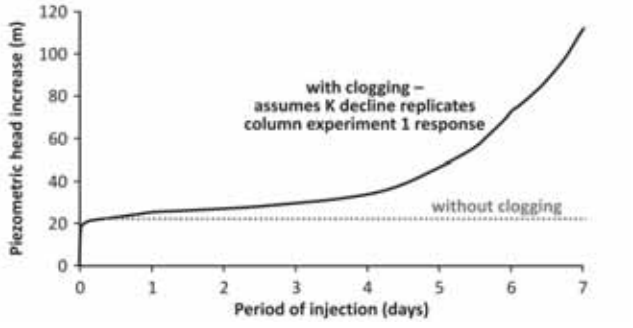

Figure 3: Predicted increase in piezometric head at the injection well during 7 days of continuous injection with and without clogging.

In a field situation, the specification of an upper limit for piezometric head increase is common. For instance, if a total head increase of 40 m was allowed, then redevelopment to restore the K in the clogging zone would be required within 4.6 days. Pumping costs are higher and the success of redevelopment measures could be reduced if the clogging zone penetrates further into the aquifer. Given that the rates of permeability reduction for other tested water types were lower, in these cases longer periods between redevelopment would be acceptable. This simulation represents a worst case scenario for clogging as the effects of calcite dissolution have been neglected.

5 Conclusions

The highest clogging rate of the three column experiments was obtained with undisinfected reclaimed water that contained 4 mg/L of suspended solids. The abiotic reclaimed water containing the same suspended solids concentration had an intermediate clogging rate. Columns receiving micro-filtered reclaimed water (no suspended solids) had the lowest clogging rate. The combination of micro-organisms and suspended sediments produced a rate of clogging, which exceeded the sum of clogging rates of water containing suspended sediments alone and micro-organisms alone.

Column studies allowed prediction of head increases due to clogging in an injection well, to give a preliminary indication of the required frequency of redevelopment.

Calcite dissolution is likely to be a significant geochemical process occurring in the vicinity of an injection well in a carbonate aquifer, as dissolution can counteract the formation of filter cake during injection. Dissolution is initiated primarily by oxidation reactions, including respiration by micro-organisms, and the resulting formation of carbon dioxide leading to an acid-base reaction with buffering of carbonic acid by limestone.

6 References

Dillon, P.J., and Pavelic, P., (1996) Guidelines on the quality of stormwater and treated wastewater for injection into aquifers for storage and reuse. Urban Water Research Assoc. of Aust. Research Report No 109. (Centre for Groundwater Studies Report No 63A)

Dillon, P., Pavelic, P., Sibenaler, X., Gerges, N., and Clark, R., (1997) Aquifer storage and recovery of stormwater runoff. AWWA J. Water 24 (4) 7–11.

Dillon, P., Pavelic, P. Toze, S. Ragusa, S., Wright, M., Peter, P. Martin, R., Gerges, N., and Rinck-Pfeiffer, S., (1999) Storing recycled water in an aquifer: benefits and risks. AWWA J. Water 26(5) 21–29.

Dillon, P., Pavelic, P., Wright, M., Peter P. and Nefiodovas, A., (2001) Small-scale heterogeneity and anisotropy of a confined carbonate aquifer from triaxial tests on core samples. submitted to Proc IAH XXXI Congress, 'New Approaches to Characterising Groundwater Flow', Munich, Sept 2001.

Diersch, H.J., (1996) Feflow: Interactive, graphics-based finite-element simulation system for modelling groundwater flow, contaminant mass and heat transport processes. Feflow User's Manual Version 4.5. WASY, institute for Water resources Planning and System Research Ltd, Berlin, Germany.

Ehrlich, G.G., Ehlke, T.A., and Vecchioli, J., (1973) Microbiological aspects of ground water recharge injection of purified unchlorinated sewage effluent at Bay Park, Long Island, New York. J. Res. U.S. Geol. Surv. 1, 341–344.

Harpaz, Y., (1971) Artificial Groundwater Recharge by means of wells in Israel. Journ. Hydraul. Div. pp 1947–1964.

Hauser, V.L., and Lotspeich, F.B.,(1967) Artificial ground water recharge through wells. Journal of Soil and Water Conservation, Jan–Feb 1967, pp 11–15.

Hutchinson, A.S., (1997) Estimation and quantification of injection well of injection well clogging. Tucson, AZ. MS Thesis, University of Arizona.

Oberdorfer, J.A., and Peterson, F.L., (1985) Waste-water injection : geochemical and biogeochemical clogging processes. Ground Water 23(6), 753–761.

Okubo, T., and Matsumoto, J., (1979) Effect of infiltration rate on biological clogging and water quality changes during artificial recharge. Wat. Resour. Res. 15, 1536–1542.

Okubo, T., and Matsumoto, J., (1983) Biological clogging of sand and changes of organic constituents during artificial recharge. Water Research 17 (7), 813–821.

Olsthoorn, T.N., (1982) The clogging of recharge wells, main subject. KIWA Communications-72, The Netherlands Testing and Research Institute, Rijswijk, Netherlands.

Pavelic, P., Dillon, P., Barry, K., Herczeg, A., Rattray, K., Hekmeijer, P, and Gerges, N., (1998) Well clogging effects determined from mass balances and hydraulic response at a stormwater ASR site in Proc 3rd Intl. Symp. Artificial Recharge, Amsterdam, Sept 1998 (Ed. J.H. Peters), Balkema, Rotterdam, pp 61–66.

Pyne, R.D.G., (1995) Groundwater Recharge and Wells: A Guide to Aquifer Storage Recovery. Lewis Publishers, CRC Press, 376p.

Rebhun, M., and Schwarz, J., (1968) Clogging and contamination processes in recharge wells. Wat. Res. 4, 1207–1217.

Rinck-Pfeiffer, S., Ragusa, S., Sztajnbok, P., and Vandevelde, T., (2000) Interrelationships between biological, chemical, and physical processes as an analog to clogging in Aquifer Storage & Recovery (ASR) wells. Water Research, 34(7): pp 2110–2118.

Schippers, J.C., Verdouw, J., and Zweere, G.J., (1995) Predicting the clogging rate of artificial recharge wells. J.Wat. SRT-Aqua. 44, 18–28.

Taylor, S.W., Milly, P.C.D., and Jaffe, P.R., (1990) Biofilm growth and the related changes in the physical properties of a porous medium. II. Permeability, Wat. Resour. Res. 26, 2161–2169.

Vandevivere, P., Baveye, P., Sanchez De Lozada, D., and DeLeo, P., (1995) Microbial clogging of saturated soils and aquifer materials: Evaluation of mathematical models. Water Resour. Res. 31(9): 2173–2180.

Vecchioli, J., (1970) A note on bacterial growth around a recharge well at Bay Park, Long Island, New York. Wat. Res. 6, 1415–1419.

Vecchioli, J., (1972) Experimental injection of tertiary treated sewage in a deep well at Bay Park, Long Island, NY. New England Water Works Association 86, 87–103.

7 Acknowledgments

The authors gratefully acknowledge support for this study by the Bolivar Reclaimed Water ASR Research Project, composed of Department of Water Resources South

Australia (DWR), South Australian Water Corporation, United Water International Pty Ltd (UWI), CSIRO Land and Water and S.A. Department of Administrative and Information Services. We are also grateful to the "Association Nationale de la Recherche Technique" (ANRT), Paris, France, for supporting this work through the grant of a "Convention Industrielle de Formation par la Recherche" (CIFRE) bursary. We thank DWR staff, notably Russell Martin, project manager, for collection and storage of cores. The work was undertaken in the CSIRO Land & Water Laboratories at Urrbrae, SA and most chemical analyses were performed at the Australian Water Quality Centre (AWQC). Chris Bosher (UWI) is acknowledged for his help in the design and set up of a small post-secondary treatment pilot plant at the Bolivar Sewage Treatment Plant. The technical staff at the School of Physical Chemical and Earth Sciences at the Flinders University, and Karen Barry of CSIRO Land & Water are acknowledged for their assistance.

Contact Details

Dr. Stéphanie Rinck-Pfeiffer
Vivendi-Water Deutschland, Unter den Linden 21, 10117 Berlin, Germany
Ph: + 49 30 536 53 808, Fax: + 49 30 536 53 888
Email: stephanie.rinck-pfeiffer@generale-des-eaux.net

Dr. Peter James Dillon
(FIEAust.) CSIRO Land & Water and Centre for Groundwater Studies, PMB2, Glen Osmond, SA 5064, Australia
Ph: +61 8 8303 8714, Fax: +61 8 8303 8750
Email: Peter.Dillon@adl.clw.csiro.au

Dr. Santo Rosario Ragusa
Environmental and Mining Biotechnology,
20 Peter Crescent, Greenacre, NSW 2190, Sydney, Australia
Ph: +61 2 9758 7864, Fax: +61 2 9758 7854
Email: embiotec@rivernet.com.au

Dr. John Hutson
School of Chemical, Physical and Earth Sciences, Flinders University of SA, GPO Box 2100, Adelaide 5001, Australia
Ph: +61 8 8201 2616, Fax: +61 8 8201 2676
Email: john.hutson@flinders.edu.au

Associate Professor Howard Fallowfield
Department of Environmental Health, Flinders University of SA, GPO Box 2100, Adelaide 5001, Australia
Ph: +61 8 8204 5730, Fax: +61 8 8204 5226
Email: howard.fallowfield@flinders.edu.au

Professor Ghislain de Marsily
Université Pierre et Marie Curie, Paris VI,
4 place Jussieu, F-75252 Paris Cedex 05, France
Ph: 01 44 27 43 07, Fax: 01 44 27 49 65
Email: GDemarsily@aol.com

Mr. Paul Pavelic
CSIRO Land & Water and Centre for Groundwater Studies, PMB2, Glen Osmond, SA 5064, Australia
Ph: +61 8 8303 8772, Fax: +61 8 8303 8750
Email: Paul.Pavelic@adl.clw.csiro.au

Potential for Injection Well Clogging in an Anoxic Sandstone Aquifer Receiving Fresh, Deoxygenated but Chlorinated Injectant

J. Vanderzalm,[1] C. Smitt,[2,4] K. Barry,[1] P. Dillon,[1] S. Davidge,[3] D. Gornall,[3] H. Seear,[4] and D. Ife[5]

[1] *CSIRO Land and Water, Water for a Healthy Country Research Flagship*

[2] *EHS Support*

[3] *Santos Ltd*

[4] *URS Australia Pty Ltd*

[5] *URS Australia Pty Ltd*

Introduction

The coal seam gas (CSG) industry has been rapidly developing within Australia over the past decade (Geoscience Australia, 2008). CSG has developed to such an extent that Australia is now the second largest producing country after the USA (Freij-Ayoub, 2012).

Santos Ltd is developing their CSG operations in the Surat and Bowen geological basins of Queensland, within the Santos GLNG Project. CSG extraction typically results in the co-production of water to reduce pressure in the coal bed and allow desorption of hydrocarbon gas, predominantly methane, from the coal surface (Rice et al., 2000). Management of produced water is a challenge for the CSG industry (Rice et al., 2000; Orem et al., 2007; Bately and Kookana, 2012; Freij-Ayoub, 2012) and managed aquifer recharge (MAR) has been nominated by the Queensland Government as one of a suite of acceptable management options for this produced water. During the Santos GLNG project, extending from 2010 to around 2033, it has been estimated by Santos GLNG that a total of about 340 GL of associated water could be produced from Santos' gas extraction bores in the Roma, Fairview and Arcadia CSG fields (Santos-Petronas, 2009), of this about 150 GL would be produced from the Roma field, which is the focus of this study. Santos GLNG, supported by URS and CSIRO, is evaluating the feasibility of using MAR to recycle water, produced from the Walloon Coal Measures in Roma, for treatment and re-injection into the Gubberamunda Sandstone aquifer. This aquifer system is currently used for drinking water supply in the town of Roma. Over the last 100 years groundwater pressures in the Gubberamunda Sandstone aquifer have declined more than 80 m, due to urban, industrial and stock water use, and groundwater demand for the town water supply now exceeds 5 ML/day (GHD, 2004). This demand for water supply and the storage capacity within the Gubberamunda Sandstone aquifer (URS, 2009), provide an impetus for the beneficial use of treated CSG water via MAR.

The aim of this paper is to evaluate the potential for injection well clogging, a key operational hazard in MAR (NRMMC-EPHC-NHMRC, 2009); which impacts on aquifer pressures, injection flow rates and energy considerations in response to injection of treated CSG water into the Gubberamunda Sandstone aquifer. The clogging mechanisms assessed are iron precipitation, clay dispersion and swelling, which could be induced following injection of a source water treated by reverse osmosis, disinfection and deoxygenation. This paper covers batch and column studies for laboratory evaluation of clogging potential, in conjunction with subsequent results of an injection and recovery trial.

Methodology

Study area and Hermitage Dam MAR trial

Oil and gas exploration commenced in the Surat Basin in the 1960s (Cadman and Pain, 1998). Recent developments include the Roma lease area in south-east Queensland, in excess of 3,000 km^2 (Figure 1), predominantly used for cattle grazing or cultivation farming. The Hermitage Dam MAR trial site location was adjacent to an existing dam for collection of associated water, Hermitage Dam, approximately 40 km northeast of the town of Roma. It was established as an Aquifer Storage and Recovery (ASR) trial with a well-field comprising an injection and recovery well (HIG1), and observation wells in the Gubberamunda Sandstone aquifer (HOG1; ~40 m N of HIG1) and in the overlying Orallo Formation (HOO1; ~10 m S of HIG1) (Table 1).

A seven day pumping test within the injection bore was conducted in October 2010 and gave an aquifer transmissivity value of approximately 43 m^2/d and a storage coefficient of 3 x 10^{-5}. An injection and recovery trial was conducted from August 2012 til November 2012, to trial the injection of treated water associated with CSG production into the Gubberamunda Sandstone aquifer (Table 2).

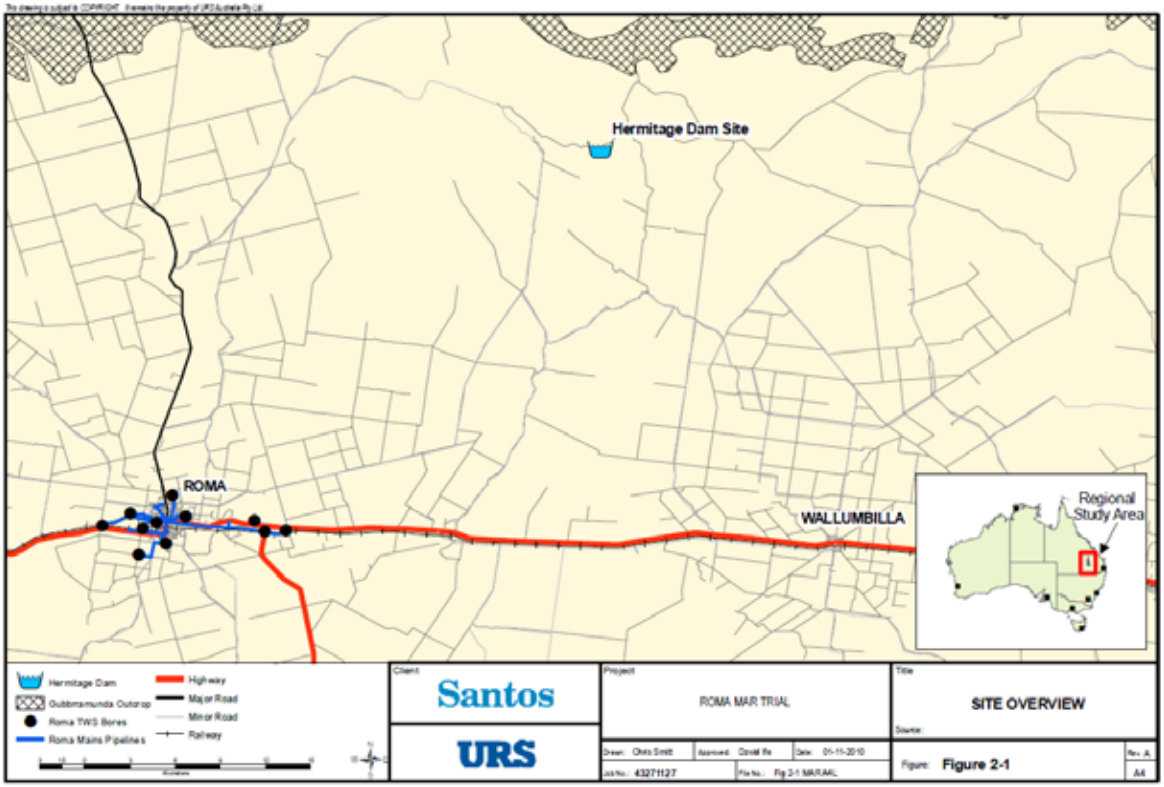

Figure 1: Roma study area showing the location of the Hermitage Dam MAR trial site and the town of Roma

Table 1: Hermitage Dam MAR trial site bore construction details (after Smitt et al., 2010)

Bore ID	Date constructed	Casing diameter (mm)	Casing material	Terminal depth (m)	Screen interval (m)	Screen size	Formation screened
HIG1	7/10/10	206	Mild Steel	225.0	198.0–219.0	Stainless steel, 2 mm aperture	Gubberamunda Sandstone
HOG1	28/8/10	100	Class 18 PVC	230.2	202.0–223.0	Stainless Steel, 1 mm aperture	Gubberamunda Sandstone
HOO1	31/7/10	50	Class 18 PVC	169.5	144.9–165.9	PVC, 0.4 mm aperture	Orallo Formation

Table 2: Event schedule for Hermitage Dam MAR trial

Phase	Interval	Days	Volume (m^3)	Average flow rate (L/s)	Comments
Injection	20/8/12–12/9/12	23	4,400	2.5	Intermittent injection due to equipment failure and injection rate decline
Storage	13/9/12–4/11/12	52	–	–	
Recovery	5/11/12–20/11/12	15	5,100	4	

CSG water from a storage dam (Hermitage Dam) was treated prior to use as the source water for the MAR trial, by the following steps (Le et al., 2012; Santos, 2012):

- Microfiltration
- Disinfection using chloramination to mitigate RO membrane bio-fouling
- Reverse osmosis (RO), reducing EC to <400 µS/cm
- De-oxygenation by vacuum degassing followed by nitrogen sparging/storage to maintain DO <0.5 mg/L.
- During the injection phase of the MAR trial, the impact of the source water sodium adsorption ratio (SAR) on injection rates was examined. Amendment with liquid calcium chloride (CaCl2), via dosing in the blend tank prior to injection, was added between 10/9/12 and 12/9/12 to alter the SAR of the source water.

Aquifer and source water characterisation

An aquifer core sample was collected from borehole HOO1 in July 2010 between 0 and 234 m using diamond core drilling (HQ 63.5 mm diameter). The recovered core was photographed, wrapped in cling wrap, placed in PVC tubes, purged with nitrogen gas and sealed soon after sampling to prevent any geochemical reactions caused by exposure to the atmosphere. Selected core lengths were sent to CSIRO Waite Laboratories and refrigerated until analysed.

Selected lengths of aquifer material were sub-sampled in a nitrogen filled anaerobic chamber, again to prevent exposure to the atmosphere and used for aquifer characterisation and laboratory studies. Eleven aquifer core samples from the Gubberamunda Sandstone aquifer were prepared by oven drying at 45° C for 72 hours, grinding and sieving to less than 2 mm, for the following analyses:

- Mineralogy (X-ray Diffraction (XRD))
- Major elemental composition (X-ray Fluorescence (XRF))
- Physio-chemistry (electrical conductivity EC 1:5 soil:water, Cl 1:5 soil:water, pH 1:5 soil:water and 0.01M $CaCl_2$, organic carbon, carbonate content, cation exchange capacity (CEC), exchangeable cations)
- Minor/trace elemental composition (XRF, acid digestible metals ICP-ES)
- Particle size
- Water content
- Dry bulk density.

Water quality data for the ambient groundwater in the Gubberamunda Sandstone aquifer and the MAR source water (untreated and treated) were provided by URS and Santos with analysis undertaken by ALS Laboratory Group. Field parameters, temperature, pH, electrical conductivity (EC), dissolved oxygen (DO) and oxidation reduction potential (ORP), were measured in situ at the time of sampling using an Aquaprobe AP-2000 multiparameter probe (Aquaread, 2012).

The PHREEQC modelling software (Parkhurst and Appelo, 1999) was used to examine potential geochemical reactions upon injection of treated CSG water into the Gubberamunda Sandstone aquifer, based on data from the Hermitage Dam MAR trial. Chloride values were set to achieve charge balance in all PHREEQC simulations.

Measured ORP values were converted to *Eh* (mV SHE) by addition of the appropriate correction value for the temperature of the sample, ranging from +203 mV @ 30° C to +214 mV @ 15° C (Aquaread, 2012). *Eh* was converted to pe for PHREEQC simulations according to the following equation, Eh = 0.059 x pe at 25° C (Appelo and Postma, 1999).

Laboratory tests of clogging potential

Batch and column studies were undertaken at the CSIRO Waite Laboratories to examine the potential for different source waters to cause aquifer clogging. Aquifer material for the laboratory tests was taken from an aggregate of core material from the Gubberamunda Sandstone between 215.8–216.8 and 220.8–221.7 metres below ground surface (m bgs), homogenised and sieved to <2 mm. This material consisted of friable medium sand with a median particle size of 398 µm.

Manipulation of sampled material in packed columns may alter the reactivity of the sediment through exposure of surfaces not previously in contact with water, through loss of fine grained material or changes in the bulk aquifer characteristic properties. However, column studies are a useful tool for comparing the relative clogging rates of various source waters and/or sediment types prior to progressing to a full-scale trial or operation (NRMMC-EPHC-NHMRC, 2009).

Ten source waters of varying salinity concentrations and SAR were tested in the laboratory studies of clogging potential (Table 3), with all applied in the batch study and four applied in the column study. Source waters A, G (S1) and H (S2) in Table 3 were sampled during the Hermitage Dam MAR trial in August and September 2012. The remaining seven source water solutions were prepared by adding varying amounts of NaCl and CaCl2 to RO treated water (sampled in August 2012, Smitt, 2012).

Batch study

The batch study examined the potential for dispersion of clay minerals in the matrix, using a method based on the principles of the 'Emerson' method (McKenzie et al., 2002). The approach characterises dispersion using combinations of aquifer materials and source waters by measuring the increase in the turbidity of the supernatant, relative to that of the water alone.

A 100 mL sub-sample of each source water was added to beakers containing a 0.6 g sub-sample of aquifer material. The aquifer material used in the batch study was sieved to <300 µm to increase the portion of fine-grained reactive minerals. Three replicate beakers were prepared for each aquifer material-water combination and the source water without sediment was a control solution. Turbidity of each solution was measured after a period of 48 hours to allow equilibrium conditions to establish. There was no opportunity for loss of fine material during the batch test.

Column study

Four laboratory columns were used within the column study to evaluate the impact of water-rock interactions on aquifer clogging, and were operated as two sets of duplicates (C1 and C2; C3 and C4). The columns used were manufactured from polycarbonate tubes and were 160 mm long with an internal diameter of 20 mm. A filter disc (0.16 x 0.1 mm mesh size) was in place at each column inlet and outlet. For column packing the previously prepared aquifer material was mixed with groundwater until 'moist' (~10% water). Groundwater was pumped through the columns for 24 hours prior to connecting the source water reservoirs. The source water reservoirs consisted of two 20 L containers connected in tandem for each pair of columns. A multi-channel peristaltic pump was used to maintain a constant flow rate of ~3 mL/min (4.3 L/day) through each column. For the duration of the experiment, columns were kept at a temperature of 19 ±1° C and light penetration was minimised by wrapping the columns in aluminium foil.

Pressure was measured at 0 cm (inlet) using a pressure sensor and at 3 cm, 8 cm, 13 cm and 16 cm (outlet) along the column using 4 mm (internal diameter) tube manometers. One column in each set of duplicates was connected to a tipping bucket gauge for continuous flow measurement. Manual flow readings were taken twice daily on all four columns.

Tracer tests were run to determine the pore volume of each column, using KCl solution, with a starting EC of 2,230 ±10 µS/cm, as the tracer. Application of a monovalent cation with a reasonably small salinity contrast between the groundwater (~1,600 µS/cm) and the tracer was employed to minimise salinity impacts on clay minerals within the aquifer column material. Pore volumes were calculated based on the volume of salt solution pumped through the column when 50% breakthrough of the salt solution was observed and revealed a pore volume of 19.6–22.9 mL and porosity of 0.39–0.46.

Four different source waters (S1–4) were used to represent two different salinity concentrations and SAR (Table 3). Low or moderate salinity refers to TDS <150 mg/L or 150–400 mg/L, respectively, while low or

high SAR is judged relative to the groundwater SAR value of ~5–6.

Initially, in test 1, the duplicate columns (columns 3 and 4 (C3, C4), columns 1 and 2 (C1, C2)) were run with low SAR source waters S1 and S2, respectively. Later, in test 2, the source water was changed to S3 and S4 with high SAR (Table 3). Column shutdown intervals were incorporated within each test to simulate unplanned power outages during the Hermitage Dam MAR trial, which were reported to coincide with considerable reductions in injection rates.

Table 2: Typical source water quality used in laboratory batch and column studies

Source water		EC (µs/cm)	~TDS* (mg/L)	Na (mg/L)	K (mg/L)	Ca (mg/L)	Mg (mg/L)	SAR	SAR ranking†
Batch	Column study								
A		36	20	5.27	<0.1	0.14	<0.1	3.9	low
B		78	55	5.41	<0.1	6.05	<0.1	0.6	low
C		320	170	51.0	0.1	3.14	<0.1	7.9	high
D		330	200	33.9	<0.1	16.6	<0.1	2.3	low
E		630	380	90.5	0.13	12.4	<0.1	7.1	high
F		610	370	64.5	0.13	30.9	<0.1	3.2	low
G	S1 – Columns 3 and 4	345	200	50.3	0.67	5.32	0.31	5.7	low
H	S2 – Columns 1 and 2	55	30	7.15	<0.1	0.43	0.10	2.6	low
I	S3 – Columns 3 and 4	366	220	64.8	<0.1	0.64	<0.1	16	high
J	S4 – Columns 1and 2	162	98	27.1	<0.1	0.25	<0.1	9.1	high

*TDS (mg/L) ~ 0.6 x EC (µS/cm); †high or low SAR is judged relative to groundwater SAR value of ~5–6

Results and Discussion

Aquifer and source water characterisation

The aquifer core obtained from HOO1 (core collected from 94.94–234.45 m bgs) revealed the Gubberamunda Sandstone consisted of fine to medium grained quartz rich sandstone (Table 4), dominated by quartz (86 ± 4%), with traces (<5%) of albite, orthoclase, kaolin, chlorite, mica, smectite (montmorillonite) and siderite (Smitt et al., 2010) (Table 5).

Of these, montmorillonite was expected to be the most reactive phase present. It has the greatest capacity for cation exchange (CEC 80–120 meq/100 g, Appelo and Postma, 1999) and may be affected by clay swelling and dispersion thus leading to a reduction in aquifer permeability. The average cation exchange capacity of the core samples was low at 1.9 meq/100 g and is consistent with up to 2% contribution from montmorillonite, given the organic carbon content was generally <0.1%.

Smectite (montmorillonite) was not quantified in the aggregate of Gubberamunda Sandstone sample material used in the laboratory studies (Table 5). However, trace amounts (<5%) were reported in the <200 µm fraction, increasing to a minor amount (5–20%) in the bulk clay fraction (<2 µm). Kaolin was the dominant mineral phase (>60%) in the clay fraction (<2 µm).

Ambient groundwater for the Gubberamunda Sandstone aquifer, sampled from HIG1 soon after well completion and a further seven samples from HOG1 prior to the Hermitage Dam MAR trial, had an average sodium concentration of 205 mg/L, calcium of 88 mg/L, magnesium of 27 mg/L, potassium of 6 mg/L, resulting in a SAR of 4.9 (Table 6). Based on the conversion from electrical conductivity, total dissolved solids (TDS) (mg/L) ~0.6 x EC µS/cm (APHA, 2005), TDS of the ambient groundwater was approximately 960 mg/L.

MAR source water from the Hermitage RO plant was sampled on six occasions, once prior to the start of the injection trial and five occasions during the injection trial. TDS varied from <10 to 199 mg/L and was dominated by sodium, chloride and bicarbonate (Na-Cl-HCO_3 water

type), (Figure 2), without the contribution from calcium that was evident in the ambient groundwater (Na-Ca-Cl-HCO_3 type). Calcium in injected water was <1 mg/L, until the latter stages of injection when it increased to 7 mg/L following amendment with $CaCl_2$ to reduce the SAR of the source water. To calculate SAR when calcium and magnesium were reported at concentrations below the analytical detection limit (<1 mg/L), calcium and magnesium concentrations were predicted, assuming the same rejection rate by reverse osmosis treatment as that of sodium (1–6%, calculated from median untreated associated water reported in Vanderzalm et al., 2010). Calculated SAR ranged from 8 to 22 prior to amendment with calcium, after amendment the SAR value was ~6 which is in the same range as the ambient groundwater (~5–6).

Disinfection within the source water treatment train resulted in a total chlorine residual (0.25 to 0.66 mg/L) and may explain the elevated redox potential of the source water (pe ~6) given that the concentration of other oxidants, such as oxygen and nitrate, was extremely low.

Table 4: Stratigraphical and lithological information obtained after drilling HOO1 (after Smitt et al., 2010)

Formation	Depth interval (m)	Lithology
Mooga Sandstone	0–20	Outcropping weathered sandstone with minor agglomerate at base.
Orallo Formation	20–182	Siltstone and mudstone, fine interbedded sand lenses, some bentonite and minor coal.
Gubberamunda Sandstone	182–220	Fine to medium grained quartz rich sandstone. Grain size increased with depth.
Westbourne Formation	220–235	Siltstone and mudstone.

Table 5: Mineralogical composition of HOO1 core material determined by XRD

Sample		Quartz	Albite/ Andesine	Orthoclase	Kaolin	Chlorite	Mica	Smectite	Siderite	Berthierine	Calcite/ Dolomite
core 183.5 m bgs		D	T	T	T	T	T	T			
core 190.3 m bgs		D	T	T	T	T	T	T			
core 193.5 m bgs		D	T	T	T	T					
core 196.6 m bgs		D	T	T	T	T					
core 200.0 m bgs		D	T	T	T	T	T	T			
core 204.2 m bgs		D	T	T	T	T	T	T			
core 212.5 m bgs		D	T	T	T	T	T				
core 215.4 m bgs		D	T	T	T	T	T	T	T		
core 215.9 m bgs		D	T	T	T	T	T	T	T		
core 221.1 m bgs		D	T	T	T	T					
core 222.4 m bgs		D	T	T	T	T	T				
laboratory aggregate†	bulk	D	T	T	T				T	T	
	<200 µm	D	M	M	M			T	M	M	T
	<2 µm	T	T	T	CD			M	T	CD	

D – Dominant (>60%), CD – Co-dominant (sum of components >60%), SD – Sub-dominant (20–60%), M – Minor (5–20%), T– Trace (<5%); † from 215.8–216.8 and 220.8–221.7 m bgs

Table 6: Hydrochemistry of ambient groundwater from the Gubberamunda Sandstone in comparison to source water for MAR at the Hermitage Dam MAR trial site

	Unit	Ambient groundwater (n=9)	Source water (n=6)
		Average ± stdev	Average ± stdev
pH	pH units	7.5 ± 0.6 (5)	7.0 ± 1
Temperature	°C	28 ± 1 (3)	19 ± 2
Electrical Conductivity (EC)	µS/cm	1,580 ± 60 (3)	220 ± 130 (5)
Dissolved Oxygen	mg/L	<0.1	<0.1
Total Dissolved Solids #	mg/L	960 ± 40 (6)	150 ± 50 (5)
Suspended Solids	mg/L	7 ± 6 (3)	<5
Turbidity	NTU	1.5 ± 0.7 (3)	2 ± 3
Calcium	mg/L	88 ± 6	2 ± 3
Magnesium	mg/L	27 ± 2	<1
Sodium	mg/L	205 ± 13	42 ± 18
Potassium	mg/L	6 ± 3	<1
Chloride	mg/L	317 ± 16 (8)	50 ± 25
Sulfate	mg/L	75 ± 8	4 (4)
Bicarbonate Alkalinity as $CaCO_3$	mg/L	370 ± 140 (6)	24 ± 12 (4)
SAR		4.9 ± 0.2	23 ± 19
Ammonia as N	mg/L	0.22 ± 0.08	0.23 ± 0.02 (4)
Nitrate as N	mg/L	0.02 ± 0.03	0.02 ± 0.01
Total Phosphorus as P	mg/L	0.4 ± 0.1 (3)	0.04 ± 0.04
Total Organic Carbon	mg/L	5 ± 2 (5)	<1
Silica	mg/L	47 ± 2	0.7 ± 0.3
Aluminium – filtered	mg/L	<0.01	0.01 ± 0.005
Iron - filtered	mg/L	0.4 ± 0.2 (6)	<0.05
Manganese – filtered	mg/L	0.18 ± 0.01 (7)	<0.001

(n)=number of samples; nd=not determined; # TDS ~ 0.6 x EC (µS/cm)

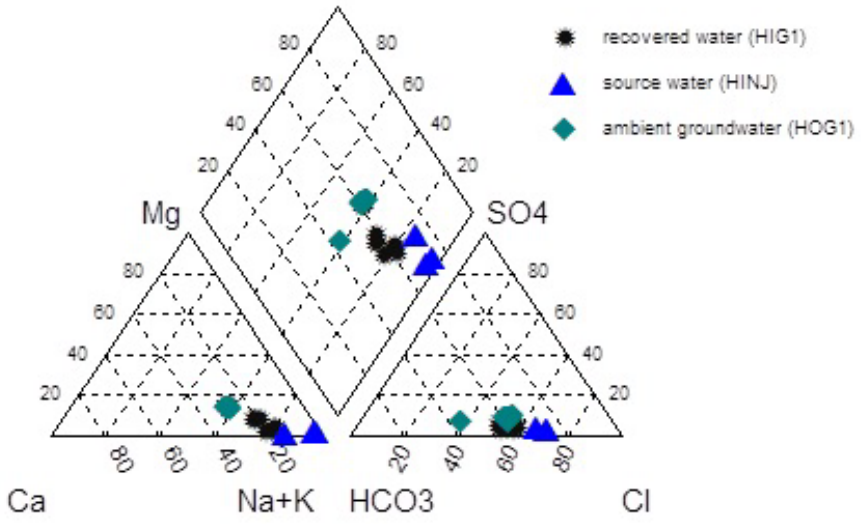

Figure 2: Piper diagram illustrating the major ion composition of the ambient groundwater (HOG1), the source water (HINJ) and the recovered water (HIG1) during the Hermitage Dam MAR trial

Batch study

The greatest increase in turbidity of 8.1 NTU (Table 7) was evident for the source water with initial EC 320 µs/cm (moderate salinity; source water C) and a SAR of 7.9. This is comparable to previous testing using the fine fraction of the Gubberamunda Sandstone aquifer sediment, which reported a turbidity increase of 10.6 ± 4.3 NTU for laboratory reverse osmosis (RO) water with an EC of 320 µs/cm and high SAR of 30, compared to a smaller increase of 2.0 ± 0.8 NTU for source water with EC of 540 µs/cm and a SAR of 2 (Vanderzalm et al., 2010).

Addition of calcium lowered the SAR value to <4 and was effective in reducing the final turbidity. This result is indicative of reduced dispersion in the samples with an EC value of 330 µs/cm and 610 µs/cm source waters (source water D and F).

The lowest salinity source water, A, did not lead to the greatest dispersion and in this case the addition of calcium (B) increased the final turbidity. The low salinity water in the batch test had a SAR lower than that of the ambient groundwater.

Table 7: Turbidity and major ion composition results of dispersion testing; salinity and SAR of Hermitage Dam MAR trial source water and ambient groundwater included for comparison

Source water	Test ID	Control		Dispersion test results					Na	K	Ca	Mg	SAR
		EC (µs/cm)	Turbidity (NTU)	Turbidity		Δ Turbidity		EC (µs/cm)	(mg/L)				
				mean	SD	mean	SD						
1	A	36	1.7	3.2	3.3	1.5	3.3	50	6.56	1.92	0.42	<0.1	2.8
2	B	78	1.6	5.7	3.8	4.1	3.8	90	6.80	0.41	5.37	0.23	0.8
3	C	320	0.5	8.6	4.1	8.1	4.1	340	50.1	0.42	3.09	0.24	7.4
4	D	330	0.8	3.7	2.5	2.9	2.5	330	34.6	0.30	15.7	0.24	2.4
5	E	630	2.0	6.0	2.2	4.1	2.2	640	91.0	0.59	12.1	0.23	7.1
6	F	610	1.3	2.3	0.7	1.1	0.7	620	64.4	0.44	29.7	0.31	3.2
7	G	345	0.4	2.5	1.5	2.2	1.5	325	50.3	0.67	5.32	0.31	5.7
8	H	55	0.5	2.0	0.6	1.4	0.6	52	7.15	<0.1	0.43	0.10	2.6
9	I	349	0.3	2.1	0.4	1.8	0.4	359	63.8	<0.1	0.93	0.16	16
10	J	175	0.3	1.2	0.5	0.9	0.5	173	26.7	<0.1	0.47	0.11	9.1
Hermitage Dam MAR trial								EC (µs/cm)	Na	K	Ca	Mg	SAR
									(mg/L)				
Low salinity source water (20/8/12)								23	7	<1	<1	<1	6[#]
Moderate salinity source water (6/9/12)								296	55	<1	<1	<1	47[#]
HOG1 ambient groundwater (17/5/012)								1,500	205	5	88	28	5

[#]0.1 mg/L Ca and 0.0 mg/L Mg used for SAR calculation

Column study

Figure 3 illustrates the hydraulic heads of the four columns during the two test intervals. As these tests were conducted with constant flow rate, an increase in head gradient through the column (i.e. an increase in head at P1), suggests reduction in hydraulic conductivity. Conversely a decline in head at P1 suggests hydraulic conductivity in the column is increasing.

Considering the variation in the source water quality, there was relatively little difference between the changes in hydraulic conductivity of the columns for all experiments. Replicates also performed similarly giving confidence that the observed changes are reliable. The laboratory columns were not impacted by clogging.

It was anticipated that high SAR source water (S3 and S4) would result in higher rates of clogging than low SAR source water (S1 and S2). However S3 and S4 showed stable hydraulic conductivity and S1 and S2 showed a marginal increase near the start of test 1 that was sustained for S2, but gradually diminished for S1. The observed changes in hydraulic conductivity in the first test interval was consistent with some loss of fine material from the column during the initial stages of column

operation, which contained the reactive clay minerals expected to cause clogging. Loss of fine material and column conditioning during the first test interval may have reduced the sensitivity of the column material to high SAR source water prior to the second test interval. The column study reflects the sensitivity of clay dispersion and swelling processes to the amount of clay minerals present.

The composition of the aquifer column material within the 0–4 cm and 4–16 cm intervals of each of the four columns at the end of the column study (test 2) confirmed the loss of fine material from the columns (Vanderzalm et al., 2013). The contribution from the silt fraction at the inlet (0–4 cm) of each of the four columns (0.4–3.3% silt) was lower than in the 4–16 cm internal (3.3–5.0%) or the initial column material (4.2% silt). Corresponding with this reduction in fine material was a reduction in the concentration of many elements, including iron (Vanderzalm et al., 2013). Iron accumulation, which can contribute to aquifer clogging, was not evident during the column study.

MAR trial

Injection phase

The injection phase of the MAR trial was planned to continue for 30 days, but was truncated to 23 days due to declining injection rates and operational issues. Figure 4 illustrates a rapid reduction in the injection rate which is coincident with very low source water EC (20–30 µS/cm). Some recovery in injection rate was achieved with a ten-fold increase in source water EC (~300 µS/cm). While the RO plant was capable of removing TDS to <20 mg/L, such low salinity was not favourable for the injection trial and resulted in a rapid reduction in injection rate.

Calcium and magnesium concentrations remained <1 mg/L in the low salinity source water. Applying the same rejection rate by reverse osmosis treatment for calcium and magnesium as for sodium, the calculated SAR of the low salinity source water was ~8, while the moderate salinity source water was ~20. Amendment with calcium to reduce the source water SAR toward the end of the injection phase to ~6 also resulted in a minimal improvement to the injection rate. Ideally, the calcium amendment could have been increased slightly to ensure a SAR less than that of the ambient groundwater. In addition, injection stoppages resulted in more significant reductions in permeability when the lowest salinity source water was injected (21–25/8/2013, Figure 4), than for stoppages when source water EC was >200 µS/cm (5–6/9/2013, Figure 4). The importance of SAR was also shown in the batch study where the lowest salinity source water, with low SAR, was not identified as posing a clay mobilisation risk.

Aquifer clogging due to interaction between low salinity source water and clay minerals, namely montmorillonite and kaolinite, within the Gubberamunda Sandstone aquifer may have contributed to the loss in injection rate. Swelling and non-swelling clays can be responsible for permeability loss in sandstone aquifers (Mohan et al., 1993; Mohan and Fogler, 1997). The mechanisms for permeability reduction or clogging include detachment from the solid surface and migration through porous media where they can clog pore spaces (applicable to non-swelling clays such as kaolinites and illites); swelling and reduction in pore space (applicable to swelling clays such as montmorillonite); and release of fines as a result of swelling which can also migrate and clog pore spaces (Figure 5) (Mohan et al., 1993). Swelling can be crystalline (swelling clays such as smectite) and osmotic (Figure 6). Crystalline swelling is caused by hydration of the interlayer cation, while osmotic swelling is due to expansion of the double layer, both of which are effects of a decrease in electrolyte concentration (Mohan et al., 1993).

Formation damage due to water sensitivity, or loss of permeability due to the composition of the flowing aqueous fluid, has received attention within the literature from the petroleum industry (e.g. Mohan et al., 1993; Mohan and Fogler, 1997), but less in relation to MAR (e.g. Konikow et al., 2001). Previous laboratory investigations used intact core material saturated with a single cation and examined permeability change when a lower salinity solution was passed through the porous media (Mohan et al., 1993; Mohan and Fogler, 1997). Passing deionised water through Na-saturated cores resulted in the greatest permeability reduction as sodium montorillonite can swell more than potassium or calcium montmorillonite (Mohan et al., 1993).

Given, that there was some recovery in injection rate with an increase in the source water salinity, it is likely that swelling of smectitic clays (Figure 5 mechanism b), and possibly swelling-induced migration (Figure 5 mechanism c) may have contributed to the permeability reduction during the injection trial. Clay swelling is a chemically

reversible process, whereas swelling-induced migration is not. The reduction in permeability after an injection stoppage may also be indicative that migration has occurred. The stagnant period allows for migration to occur due to greater opportunity for osmotic swelling, or allowed previously detached colloidal particles to flocculate and form larger agglomerates, both of which can lead to pore clogging upon recommencement of injection. It is hypothesised that the addition of calcium to the injectant will minimise detachment.

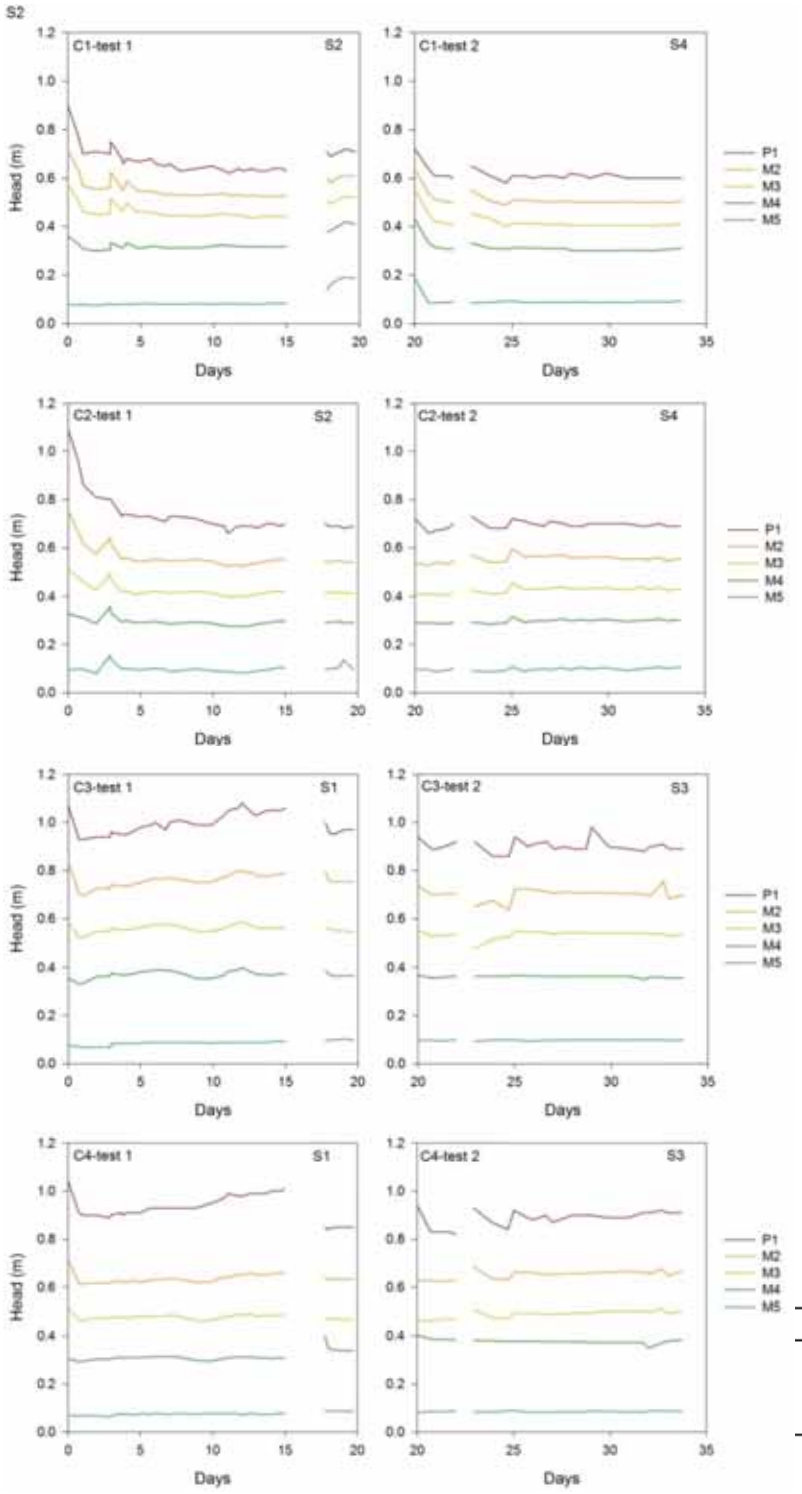

	SAR	
EC (µs/cm)	Low	High
Low	S2	S4
Moderate	S1	S3

Figure 3: Hydraulic head of columns during two test intervals; P1=from pressure sensor, M2–5=from manometers

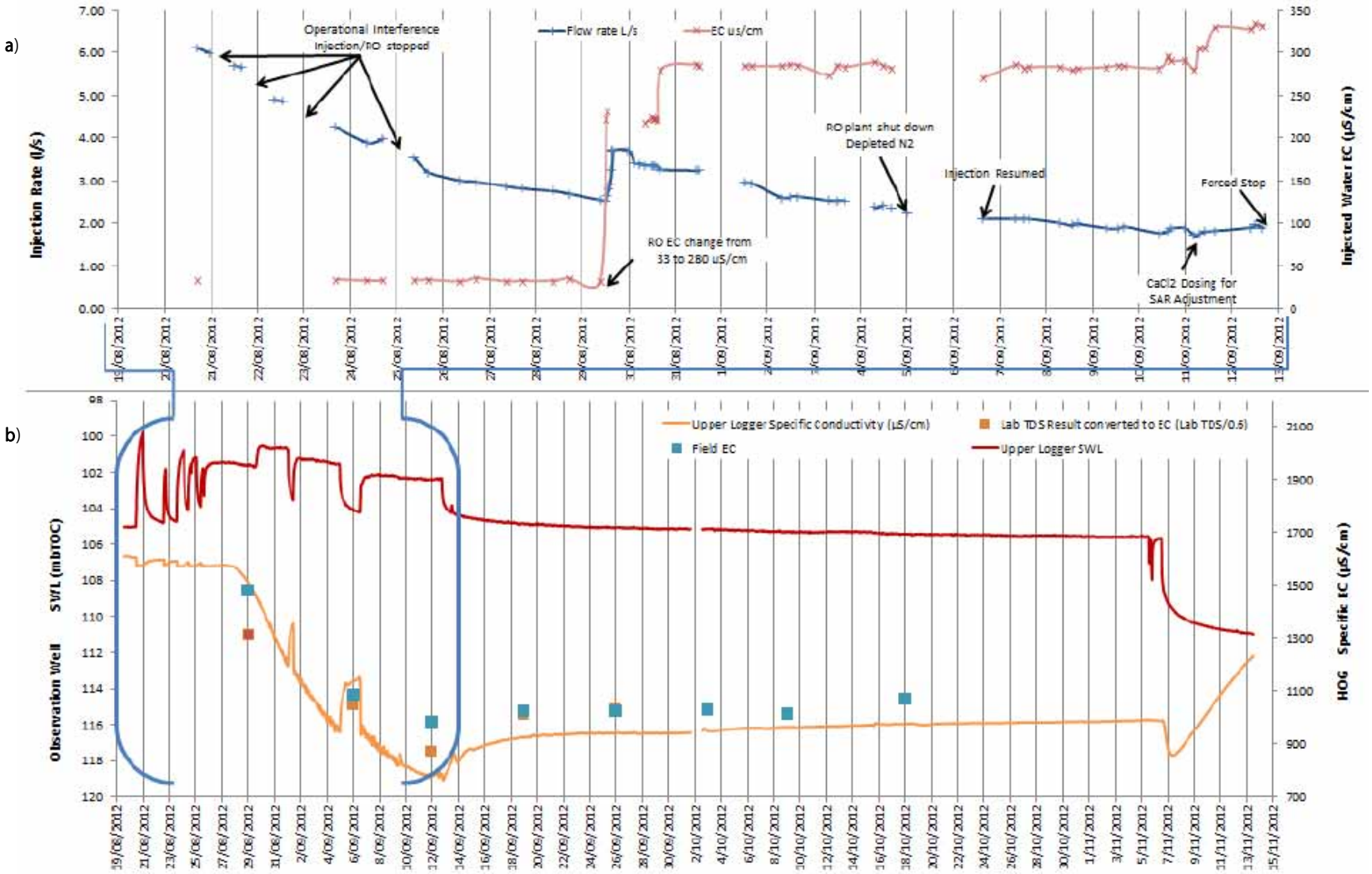

Figure 4: Summary of injection trial results. a) Injection rate in HIG1 and EC of source water. b) Standing water level and EC in HOG1 (Smitt, 2012)

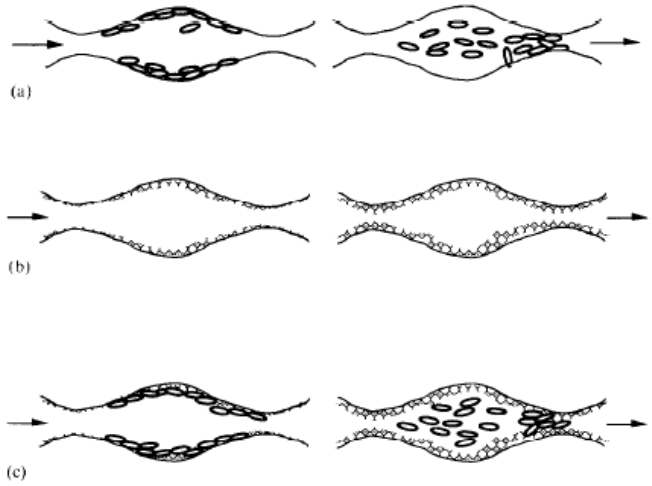

Figure 5: Mechanisms of permeability reduction by clays in porous media. a) Migration: release of clays from pore walls. b) Swelling: reduced cross-sectional area for flow. c) Swelling-induced migration: swelling dislodges fines from pore walls (from Mohan et al., 1993)

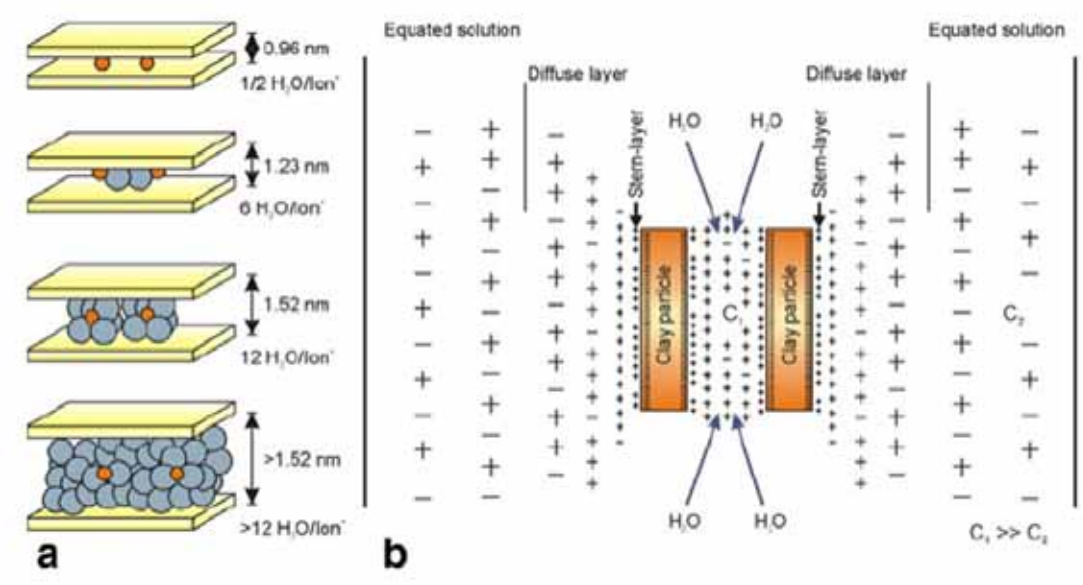

Figure 6: a) Crystalline swelling due to hydration of interlayer cations. b) Osmotic swelling due to double layer expansion (from Ruedrich et al., 2011)

Recovery phase

The initial water quality recovered from HIG1 during the recovery phase of the MAR trial was high in suspended solids, turbidity and ferric iron, likely to be within iron oxide/oxyhydroxides. This is consistent with an accumulation of particulate matter around the injection well during the injection phase, which may have contributed to the decline in injection rate. Given the high level of source water treatment undertaken it is unlikely this particulate matter originated in the treated source water. With subsequent recovery, iron was predominantly as dissolved ferrous iron, expected to originate from interaction between the source water and iron-bearing minerals in the aquifer or mixing with groundwater.

It is possible that some of this accumulated particulate matter may have been produced from biogeochemical reactions, such as precipitation of iron oxide/oxyhydroxide or clay mobilisation. PHREEQC

simulations representing 1:1 mixing between the source water and ambient groundwater solution chemistry at pe=0, representing the ambient condition in the aquifer, did not result in super-saturation of any mineral phases, which could then result in chemical clogging. However, mixing at an elevated pe of 6, typical of the source water at the point of injection, resulted in super-saturation with respect to amorphous iron hydroxide. This suggests that iron oxide/oxyhydroxide precipitation could contribute to chemical clogging at the well face, but clogging due to iron mineral precipitation would be unlikely within the majority of the Gubberamunda Sandstone aquifer assuming the storage zone remains sub-oxic. This potential clogging mechanisms was not evident in the column study, conversely sediment iron concentrations reduced over the duration of the study. The elevated redox potential of the source water may be reduced through revision of the disinfection requirements.

In USA there has been a reliance on trickle chlorination, including during periods of no injection, for prevention of biofouling in injection wells (Bouwer, 2008), whereas in Europe chlorine is not used and pre-treatments focus on reducing labile organic carbon to control bacterial activity. The reverse osmosis treatment at this site is expected to be effective in removing labile organic carbon.

From observations of iron-rich material flaking from the bore casing (C. Smitt, 2012 pers. comm. Figure 7) it is possible that a considerable amount of particulate matter was added through corrosion of the mild steel bore casing (Anderson et al., 2010), in the period between well construction and development in 2010 and the MAR trial in 2012. This corrosion would not occur within an operational MAR scheme where stainless steel or fibre reinforced plastic casing would be used. Iron concentrations in groundwater at the observation bore HOG1 were slightly elevated at the start of the injection phase, reaching 0.9 mg/L of total iron, but remained below 0.3 mg/L for the bulk of the storage interval and during recovery.

Conclusion

Laboratory and field–based investigations deemed the use of treated CSG water in MAR can proceed to full-scale operation, with preventative measures to manage the operational risk from clogging (Smitt et al., 2010; Smitt, 2012).

Figure 7 a) Accumulation of iron-containing matter on geophysical probe in HIG1. b) Iron-staining upon discharge of iron-rich groundwater from injection trial (photographs courtesy of C. Smitt)

Advanced pre-treatment of the source water involved reverse osmosis, disinfection via chloramination and deoxygenation treatment steps.

While oxygen was removed to minimise chemical clogging due to redox reactions, the presence of free chlorine still provided some oxidative capacity and could interact with the aquifer substrate. Additionally, the contrast in salinity and SAR between the source water and groundwater was sufficient to lead to clay mobilisation and swelling. This paper reports a number of studies to evaluate the potential for treated CSG water to lead to well clogging during injection, which were undertaken to inform the design and management strategies of an operational scheme.

Laboratory batch tests confirmed that a source water with high SAR could result in clay dispersion. However, the laboratory column study showed no clogging, which is

positive for future MAR operation in the Gubberamunda Sandstone aquifer. There was no sign of a reduction in aquifer permeability in the column study, despite the application of four different qualities of source waters which encompassed a range of salinity and SAR values. The aggregated material used in the column study was lower in smectite content than some of the individual samples of aquifer material and the reactivity of the packed columns may have been further reduced by loss of fine material containing clay minerals. It is also likely that the degree of clogging observed in the trial was exacerbated by a number of clogging mechanisms, not just clay swelling and dispersion considered in the laboratory studies, including artefacts of injection bore construction.

Within the MAR trial it was possible that swelling of smectitic clays and possibly swelling-induced migration contributed to the permeability reduction during the injection trial. The low clay content and cation exchange capacity of the Gubberamunda Sandstone sediment suggests clay swelling and mobilisation will not have a significant impact on the MAR operation. However, to minimise any injection rate impacts, it is recommended that source water EC should be continuously monitored and remain above 300 µS/cm (up to ~1,000 µS/cm or aesthetic ADWG value) with calcium amendment to ensure the SAR is comparable to that of the ambient groundwater (~5–6).

Geochemical modelling suggested that mixing between the source water and the ambient groundwater at an elevated pe of 6, typical of the source water with residual chlorine (disinfectant) and possible at the point of injection, could result in iron oxide/oxyhydroxide mineral precipitation, which could in turn contribute to chemical clogging at the well face. The elevated redox potential of the source water may be reduced through revision of the disinfection requirements, thereby mitigating the potential for precipitation of iron minerals at the point of injection.

This work highlights the importance of understanding near well physical, geochemical and microbial processes. Information derived from laboratory experiments in which there was a close relationship to aquifer *in situ* conditions was valuable in developing criteria for injectant water quality, but also revealed the sensitivity of results to aquifer material selection. The use of an existing mild steel well for even a short term injection trial proved a significant impediment to injection rates due to the faster than expected oxidation of iron, even in deoxygenated water, by a small chlorine residual. Inert casing materials were already intended for the operational project and now will be used for all trials.

Acknowledgements

The authors gratefully acknowledge the efforts of URS Australia Pty Ltd and Santos Ltd personnel in providing the information and samples necessary to undertake this study. Analysis was provided by CSIRO Land and Water Analytical Services and Mineralogical Services. The authors would also like to thank Russell Martin and Gideon Steyl for their peer review of this manuscript.

References

American Public Health Association (APHA) (2005) Standard methods for the examination of water and wastewater. Washington D.C., American Public Health Association, American Water Works Association and Water Environment Federation, Washington.

Anderson, T., Cauchi, T., Ibrahimi, F., Llewellyn, B. and Ray, E., (2010) Groundwater bore deterioration: schemes to alleviate rehabilitation costs. Waterlines Report Series No 32, October 2010, National Water commission, Canberra. http://archive.nwc.gov.au/__data/assets/pdf_file/0018/10962/32_Groundwater.pdf

Appelo, C.A.J., and Postma, D., (1999) Groundwater, geochemistry and pollution. A. A. Balkema, Netherlands.

Aquaread, (2012) Instruction manual for the Aquaprobe AP-2000. http://www.aquaread.co.uk/downloads/manuals/Aquaread-AP2000-Aquaprobe-Manual.pdf

Batley, G.E., and Kookana, R.S., (2012) Environmental issues associated with coal seam gas recovery: managing the fracking boom. Environmental Chemistry 9: 425–428.

Bouwer, H., (2008) Artificial recharge of groundwater: hydrogeology and engineering. Hydrogeology Journal 10: 121–142.

Cadman, S.J. and Pain, L., (1998) Bowen and Surat Basins, Clarence-Moreton Basin, Gunnedah Basin and other minor onshore basins, Queensland, NSW and NT. Australia Petroleum Accumulations Report 11, Bureau of Resource Sciences, Canberra.

Freij-Ayoub, R., (2012) Opportunities and challenges to coal bed methane production in Australia. Journal of Petroleum Science and Engineering, 88-89: 1–4.

Geoscience Australia, (2008) Australia's Identified Mineral Resources 2008. Geoscience Australia, Canberra.

GHD, (2004) Roma water supply system planning study for Roma Town Council. GHD, Brisbane.

Konikow, L.F., August, L.L. and Voss, C.I., (2001) Effects of clay dispersion on aquifer storage and recovery in coastal aquifers, Transport in Porous Media 43: 45–64.

McKenzie, N., Coughlan, K., and Cresswell, H., (2002) Soil physical measurement and interpretation for land evaluation, CSIRO, 390pp.

Le, H., Samadi, Y., Innell, W., and Hochman, P., (2012) Relocatable RO plant treats coal seam gas water. AWA Journal Water, March: 56–59.

Mohan, K.K., and Fogler, H.S., (1997) Colloidally induced smectitic fines migration: existence of microquakes, Fluid Mechanics and Transport Phenomena 43(3): 565–578.

Mohan, K.K., Vaidya, N., Reed, M.G., and Fogler, H.S., (1993) Water sensitivity of sandstones containing swelling and non-swelling clays, Colloids and Surfaces A: Physiochemical and Engineering Aspects 73: 237–254.

NRMMC-EPHC-NHMRC, (2009) Australian Guidelines for Water Recycling: Managed Aquifer Recharge, National Resource Management Ministerial Council, Environment Protection and Heritage Council and National Health and Medical Research Council, Canberra. http://www.ephc.gov.au/sites/default/files/WQ_AGWR_GL__Managed_Aquifer_Recharge_Final_200907.pdf.

NHMRC–NRMMC, (2011) Australian Drinking Water Guidelines, National Health and Medical Research Council and National Resource Management Ministerial Council, Canberra. http://www.nhmrc.gov.au/_files_nhmrc/publications/attachments/eh52_aust_drinking_water_guidelines_update_120710_0.pdf.

Orem, W.H., Tatu, C.A., Lerch, H.E., Rice, C.A., Bartos, T.T., Bates, A.L., Tewalt, S., and Corum, M.D., (2007) Organic compounds in produced waters from coalbed natural gas wells in the Powder River Basin, Wyoming, USA. Applied Geochemistry 22: 2240–2256.

Parkhurst, D.L., and Appelo, C.A.J., (1999) User's guide to PHREEQC (version 2) A computer program for speciation, reaction path, advective transport, and inverse geochemical calculations. Report 99-4259, USGS Water Resources Investigation.

Rice, C.A., Ellis, M.S., and Bullock, J.H., Jr. (2000) Water co-produced with coalbed methane in the Powder River Basin, Wyoming: preliminary compositional data. USGS Open-File Report 00-372, USGS, Denver, Colorado.

Ruedrich, J., Bartelsen, T., Dohrmann, R., and Siegesmund, S., (2011) Moisture expansion as a deterioration factor for sandstone used in buildings, Environmental Earth Science 63: 1545–1564.

Santos, (2012) Santos GLNG project Hermitage Dam MAR trial injection management plan, document no 020-GLNG-4-1.3-0141, Santos, Brisbane.

Santos-Petronas, (2009) GLNG associated water management plan, Santos-Petronas, document no. 3301-GLNG-3-1.3-0056-DOC.

Smitt, C., (2012) Roma MAR Project Update Report,commercial-in-confidence report prepared for Santos GLNG. URS, Melbourne.

Smitt, C.M., Vanderzalm, J.L., Dillon, P.J., Barry, K., Page, D.W., and Ife, D., (2010) Santos GLNG – Roma MAR study: Report and pre-trial risk assessment, commercial-in-confidence report prepared for Santos GLNG. URS, Melbourne.

URS, (2009) Santos GLNG – Associated water injection study, report prepared for Santos. URS, Melbourne.

Vanderzalm, J.L., Barry, K.E., and Levett, K.J., (2010) Santos GLNG – Roma MAR study phase 1–4 deliverables: Background data review, core analysis, laboratory batch studies and risk assessment, commercial-in-confidence report to URS. CSIRO: Water for a Healthy Country National Research Flagship, Australia.

Vanderzalm, J.L., Barry, K.E. and Dillon, P.J., (2013) Santos GLNG – Roma MAR study geochemical evaluation and pre-commissioning residual risk assessment: Phase 4c-6 deliverables, commercial-in-confidence report to URS. CSIRO: Water for a Healthy Country National Research Flagship, Australia.

Contact Details

J. Vanderzalm, K. Barry and P. Dillon
CSIRO Land and Water
Water for a Healthy Country Research Flagship,
Private Bag No 2, Glen Osmond, SA, 5064, Australia

C. Smitt
EHS Support
907/57 Bay St, Port Melbourne, VIC, 3207, Australia,
previously URS Australia Pty Ltd, VIC.
URS Australia Pty Ltd
Level 17, 240 Queen Street, Brisbane, QLD, 4000, Australia

S. Davidge
Santos Ltd
GPO Box 1010, Brisbane, QLD, 4001, Australia

H. Seear
URS Australia Pty Ltd
Level 17, 240 Queen Street, Brisbane, QLD, 4000, Australia

D. Ife
URS Australia Pty Ltd
Level 6, 1 Southbank Boulevard, Southbank, VIC, 3006,
Australia

Porous Media Filter Test in Order to Prevent Well Clogging during Groundwater Reinjection due to Ferrous and Ferric Mineral Precipitation

R.U. Ruemenapp, C. Hartwig, S.M. Akhtar and M. Nishigaki
Okayama University Department of Environmental and Civil Design, Okayama, Okayama-Ken, Japan

Abstract

Groundwater that is directly used for geothermal heat transport in an open system will be re-injected after its usage into the aquifer it was taken from. Aqueous mineral species can precipitate in the well or aquifer when mixed with oxygen during the injection. Cheap and commonly available filter materials can improve the feasibility of an open geothermal heat exchanger by adsorbing the aqueous bi- and tri-valent iron and manganese ions under anaerobic conditions. Often used Ferrolite sand filled filter are effective, but expensive.

In order to prevent mineral precipitation in the heat exchanger system as well as in the injection well and aquifer, three different filter materials were analysed for their adsorption potential of aqueous bi- and tri-valent iron ions in laboratory experiments. Columns (V= 2.4 (dm^3)) were filled each with wooden charcoal (n= 0.59–0.85, k= 0.103 (cm s^{-1})), Yamasuna sand (n= 0.38–0.40, k= 1.0–0.01 (cm s^{-1})), or volcanic ash (n= 0.907, k= 4.99 * 10^{-2} (cm s^{-1})). The filter were supplied under constant pressure head with ambient groundwater from a nearby well with a background concentration of dissolved iron of C_{Fe2+}= 7.9 (mg L^{-1}) (± 0.61 (mg L^{-1}). Water samples were taken every 48 hours, in order to analysis aqueous bi- and tri-valent iron ion concentration in the solution by atomic absorption spectro-photometry (AAS). Additionally electrical conductivity was measured at each sampling port, inlet and outlet of the columns and at the well. Furthermore, pH, temperature, and dissolved oxygen concentration were monitored. In order to estimate the influence of the fluid velocity, wooden charcoal filter were analysed for their dissolved iron adsorption capacity under various constant fluid velocities (1.02 (cm min^{-1}), 0.504 (cm min^{-1}), 0.252 (cm min^{-1})). In an additional field test, with wooden charcoal and layers of gravel, middle and fine sand at the inlet and the outlet, filled pilot filter (V= 150.9 (dm^3)) was tested under realistic operational conditions with an average flow rate of 10 (L min^{-1}). The treated water was then used to lower the temperature in a room of 18.9 (m^2) (H= 2.55 (m)) and was re-injected into the aquifer.

All three filter materials were capable to adsorb aqueous ferric and ferrous iron ion below the detection limit of 0.1 (mg L^{-1}) with an adsorption capacity of 3.5 (g (kg charcoal)$^{-1}$). The break-through curves for each test column and material, as well as temperature, pH, electrical conductivity, changes in hydraulic conductivity, and dissolved oxygen levels are presented. The field test focused on the practicability of the wooden charcoal filter as adsorbent. Suggestions are made for installation and maintenance of the filter under field conditions.

1 Introduction

This work was accomplished as part of a national project, in order to estimate the potential of groundwater to be used as heating and cooling medium for domestic usage in Japan. In comparison to a closed water cycle system, that is cooled or heated from the surrounding groundwater in the well, an open-loop system uses

groundwater directly from a pumping well as heat medium in the applied facility before it is re-injected into the aquifer.

One challenge of using an open-loop system is the physical and hence chemical change of used groundwater. Pressure and temperature fluctuations will lead to changes in the chemical composition of the groundwater due to fumigation or precipitation of mineral phases (Pourbaix, 1966; Näseretal, 1990). The reactions can lead to corrosion of the pipe material, or precipitation of mineral phases at the inner pipe wall, which lowers the heat conductivity of the material drastically and therefore, reduces the efficiency of the system. Furthermore, when this groundwater is re-injected into an aquifer, mixing with atmospheric oxygen is difficult to avoid, which often causes oxidation of dissolved mineral ions and results in precipitation of mineral phases in the aquifer porous media. Consequently, the aquifer clogs and becomes unusable after an operation period (Bouwer, 2002).

Besides spacious facilities for the physical removal of dissolved iron and manganese due to oxidation, such as sedimentation tanks, or slow sand filter for the treatment of groundwater before usage, expensive alternatives are available for domestic purification of groundwater, such as activated carbon filtration, or chemical precipitation by introducing flocculation agents to the water (Mutschmann and Stimmelmayr, 1991).

This study aims to investigate the adsorption ability for dissolved iron ions of three cheap and easily available materials in Japan: wooden charcoal, Yamasuna sand (Igarashi and Saito, 2005), and volcanic ash (Oba et al., 1967). Especially the used wooden charcoal (2.76 (Yen kg^{-1})) is compared to activated carbon particles (1.65–9.90 (US$ kg^{-1}) (Marsh and Rodrìguez-Reinoso, 2006)) about 50 to 320 times cheaper and may serve, due to its large surface area and various functional groups (as it can be seen in Figure 1) as appropriate and efficient adsorbent for the removal of dissolved iron from groundwater. However, functional groups change their charge according to the pH of the groundwater, and hence the adsorption of dissolved iron will vary depending on the pH, initial concentration of dissolved iron, adsorbent mass loading, temperature, porosity, surface area, fluid velocity, and concentration of other ions and dissolved species (Näser et al., 1990; Worch, 2012). The advantage in using wooden charcoal to other incombustible solid filter materials lays in its possible usage as fertilizer after incineration or decomposition of the material. Less research has been done on the usage of wooden charcoal as filter material. Ahmad and Jawed (2011) used coarse charcoal as filter material under anaerobic conditions and successfully reduced the dissolved iron concentration of groundwater from initially 1–10 (mg L^{-1}) in Assam region.

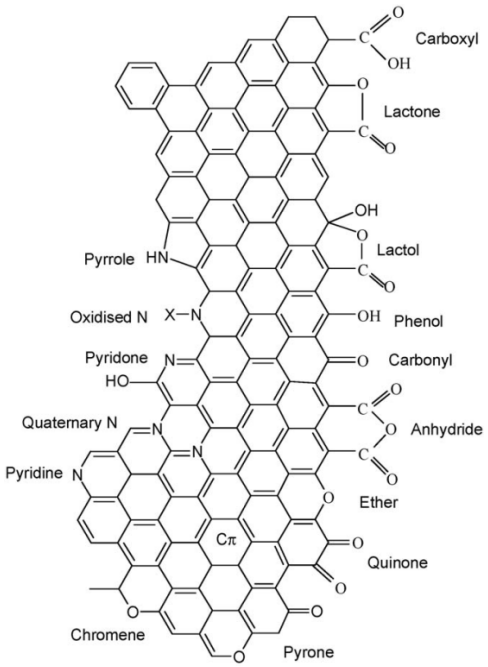

Figure 1: Functional groups of activated charcoal (from Figueiredo and Pereida, 2010)

In this study the adsorption capacity for dissolved iron on fine wooden charcoal (JFE, 2009), fine sand (Yamasuna), and volcanic fly ash (Oba et al., 1967) were investigated in column experiments, using site groundwater with an initial dissolved iron concentration of 7.9 (mg L^{-1}) (± 0.61 (mg L^{-1})) [1].

Dissolved oxygen concentration, temperature and pH were monitored along with the concentration profiles of dissolved iron ions in the column. A larger wooden charcoal filled filter was used in a field test, in order to filter a vast amount of groundwater and test the feasibility of the adsorbent on-site.

[1] *Five percent confidence interval (n= 24) (Storm, 1969). Used for all intervals in this article.*

2 METHOD

2.1 Column Experiments

In order to estimate the adsorption capacity of the JFE wooden charcoal, Yamasuna sand, and volcanic fly ash, laboratory column filter experiments were conducted. The break-through curves of dissolved iron concentration were monitored at each of the six sampling ports of the column, as it is shown in Figure 2.

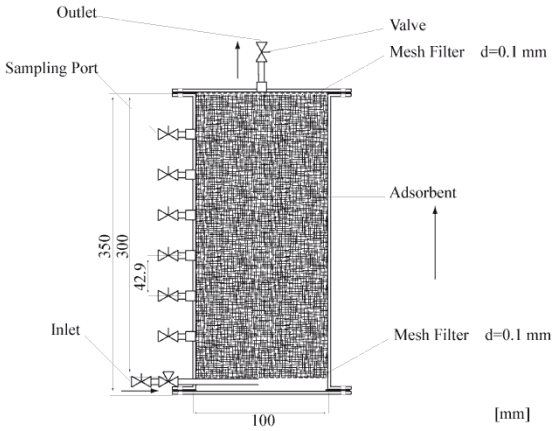

Figure 2: Setup and size of adsorbent filled small column with six sampling ports

PH, dissolved oxygen, conductivity and temperature were documented as well. The adsorbed amount of dissolved iron onto the material surface was later analytically estimated for every five cm layer of adsorbent material for each column.

The design of the experiment is shown in Figure 3. Pump 1 delivered groundwater to a nitrogen gas filled tank that was placed indoor at a constant height (const. level). The tank pressure was controlled over valve 5 (V_5) and kept constant at the pressure of the surrounding air, measured by a manometer. Overflow water from the tank discharged over V_8 (Syphon) into a drain. Over Valve 7 the laboratory columns were fed with water from the tank. The columns outlet water level head was changed accordingly to the requirements of the experiment, in order to control the flow within the columns. Samples were taken at the well (Q_R), the inlet of the columns Q_N, and at the six sampling port of the columns, including the outlet of the columns. The aim of each columns operation was to keep a constant retention time (velocity) in the porous medium ($C_{1\text{-}3}$, $S_{1\text{-}2}$) or a constant hydraulic pressure head (C_0, S_0, V_0), as shown in Table 1.

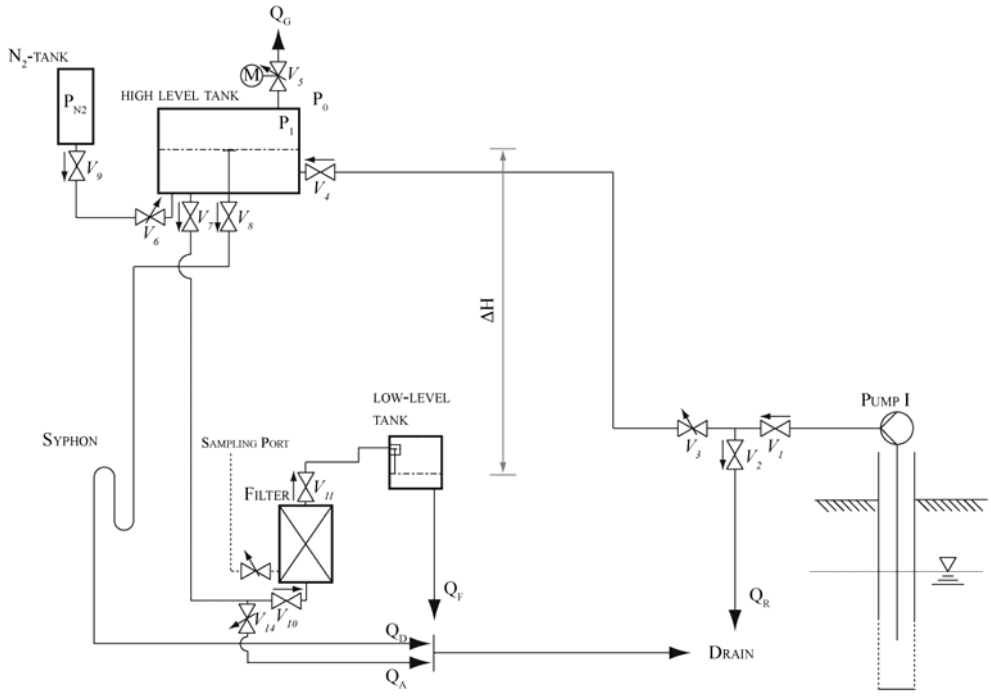

Figure 3: Assembly of the laboratory column experiment. Pump 1 delivered groundwater to a nitrogen gas filled tank that was placed indoor at a constant height (const. level). Pressure in the tank was controlled over valve 5 (V5). Overflow water from the tank discharged over V8 (Syphon) into the drain. Over Valve 7 the columns were fed with water from the tank. The column outlet water level head was changed accordingly to the requirements of the experiment, in order to control the flow within the column. Samples were taken at the well (QR), the inlet of the column QN, and at the six sampling ports along the column, including the outlet of the columns

Table 1: Physical and operation parameter of used columns, with SA and SB referring to the sand filled columns, V_0 to the volcanic ash filled column, and C_A to C_C to wooden charcoal filled columns under different operational conditions

Material		Yamasuna Sand			Volcanic Ash	Wooden Charcoal			
Parameter	Unit	S_0	S_A	S_B	V_0	C_0	C_A	C_B	C_C
Dry mass	g		3586.7	4293.8		1080.1	813.9	532.1	532.1
Porosity	%	0.39	37.6	40.1		67	61	59.1	84.6
Retention time	min	23.4–488	15	15	42	4.7–890	15	30	45
Darcy velocity (U)	cm s^{-1}	$8.3x10^{-3}$-$4.3x10^{-4}$	$1.8x10^{-2}$ (± 7%)	$1.6x10^{-2}$ (± 20%)	0.71 (± 9.8%)	$5.6x10^{-4}$ – 0.11	$1.7x10^{-2}$ (± 9.8%)	$8.4x10^{-3}$ (± 10%)	$4.2x10^{-3}$ (± 10%)
Note		const. head		washed	const. head	const. head			

At each port 40 (ml) sample were taken, filtered through 5–10 (µm) filter paper (ADVANTEC©) and mixed with 1 (ml) 0.1 molar HNO_3, in order to reduce the samples pH below 2 to prevent dissolved iron ions to oxidize even though they were stored under aerobic condition. The sample bottles were then kept in a freezer until final analysis.

2.2 Washing of Material

In order to avoid the transport of fine wooden charcoal material from the filter into the Aquifer, the required flushing time of the charcoal, previous of its usage, was estimated in a washing experiment for various velocities.

From a constant head tank water flowed under gravity into the column. In a time interval of 5, 15, 30, 60, 120, 240, and 480 seconds, 10 (ml) glass vials were filled with water samples from the outlet of the columns. The samples were later shaken and analyzed in a P2100 Turbidimeter from HACH. The instrument was calibrated previous to the experiment.

2.3 Field Filter

In order to test the applicability of the adsorbent under field conditions, a JFE wooden charcoal and a ferrolite sand filter were separately used to adsorb dissolved iron from groundwater under anaerobic conditions before it was used in a test room for cooling in winter time and heating in summer time. The water from the Ferrolite sand filter was re-injected into the aquifer after its usage, in order to estimate the impact of dissolved iron on clogging.

2.3.1 Wooden Charcoal Filter

A with 25.27 (kg) dry wooden charcoal filled filter was installed onsite. The filter was made from 10 (mm) thick acryl with three sample ports. From the sampling ports a stainless steel pipe of 5 (mm) diameter lead to the center of the filter, in order to take samples from the middle of the adsorbent material body. At the bottom of the filter a perforated acryl plate was used to distribute the inflow evenly through the filter cross-area, as shown in Figure 4. From the inlet a layer of 8 (cm) gravel, middle sand and fine sand were given each into the filter, followed by a layer of 68 (cm) wooden charcoal. Finally, a 4 (cm) layer of gravel prevented the transport of charcoal from of the filter. The filter casing was insulated with a 1.0 (cm) thick porous foam blanket with outer aluminum insulation, in order minimize the effect of solar insulation on the water temperature. Groundwater was pumped from a recovery well to the filter and entered the filter from the bottom. The pressure in the filter was controlled with a manometer and the flow was adjusted accordingly, in order to not exceed a pressure of 200 (kPa) to avoid damage at the filter casing. The flow was regulated by a MAEZAWA© 13 (mm) flow meter. The filtered water was then re-injected into a heat exchanger, in order to heat (winter time) or cool (summer time) a room of 5.25 (m) length, 3.6 (m) width, and a height of 2.55 (m). The groundwater that was filtered by the wooden charcoal filter was not re-injected back into the aquifer, but rather disposed in the drain. This was done to prevent damage to the aquifer due to clogging as long as the practicability of the adsorbent was unconfirmed.

2.3.2 Ferrolite Filter

To estimate whether clogging may occur in the aquifer due to inner-aquifer particle movement rather than precipitation of ferric or ferrous mineral phases, a Ferrolite TOHKEMY© MCC granulate filled filter was used, in order to remove dissolved iron and manganese from groundwater. The price for the Ferrolite granulate is 380 (Yen L^{-1}) (= 4.12 (US$ L^{-1})).The cylindrical stainless steel filter casing had a height of 2.5 (m), and diameter of 0.8 (m). The filter was filled from the bottom to the top with four layer, each of 10 (cm) thickness, of 12–20 (mm), 6–12 (mm), 3–6 (mm), and 2–4 (mm) sand, followed by a 1.55 (m) layer of FERROLITE MCC material (ø = 0.3–0.65 (mm)) and a final layer of 15 (cm) Anthracite sand. The flow from the top to the bottom was adjusted in order to not exceed a water pressure of more than 0.22 (MPa), resulting in an average flow rate of 25 (L min^{-1}).

2.4 Sample Analysis

The quantity of dissolved iron in liquid samples was analyzed with an Atomic Absorption Spectrophotometer (Hitachi©, Z-6100 polarized Zeeman) after calibrating the instrument with standards of known concentrations.

In order to estimate the adsorbed amount of dissolved iron on the adsorbent material, the extraction method after Ryan et al. (2001) was used.

3 Material and Site description

3.1 Adsorbent Material

As adsorbent Yamasuna sand and JFE wooden charcoal were chosen, since both materials showed a possible adsorption capacity for the removal of dissolved iron in field tests (Ahamad and Jawed, 2011). JFE charcoal is finer than the previous used wooden coal and Yamasuna sand (Igarashi and Saitou, 2005) was chosen, as it is commonly available and is a standard sand for laboratory experiments in Japan. Volcanic fly ash (Oda et al., 1967) from the area of Kagoshima/Japan was additionally tested, since the fine particles and similar chemical composition to quartz sand promised a high adsorption capacity of dissolved iron after the first screening test of Yamasuna sand. The physical properties of these three adsorbent materials are summarized in Table 2.

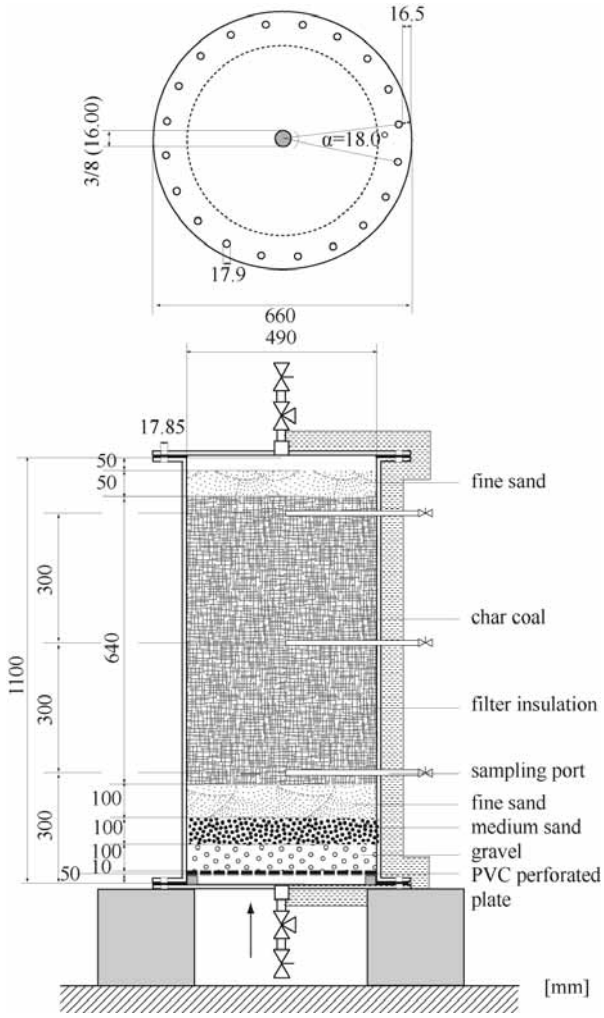

Figure 4: Assembly of JFE wooden charcoal on-site filter

Table 2: Physical properties of JFE wooden charcoal, Yamasuna sand (Igarashi and Saitou, 2005) and volcanic ash (Oba et al., 1967), used in the Experiments

Property	Unit	Coal	Sand	Volcanic
Spec. surface area	$m^2 g^{-1}$	139– 154		
Hydraulic Conductivity	cm s^{-1}	$1.03x10^{-1}$	$4.7x10^{-2}$	$4.9x10^{-2}$
Porosity	–	0.67	0.39	0.90
Density	g cm^{-3}	1.45	2.74	2.29
D_{10}	mm	0.12	0.14	0.114
D_{60}	mm	0.7	0.7	0.38

Sieve curves for all three adsorbent materials are shown in Figure 5. It can be seen that the maximum particle diameter for Yamasuna sand and Charcoal is 2 (mm), whereas volcanic ash has about 20 (%-mass) in the range of 2–30 (mm) particle diameter. Yamasuna and wooden charcoal diameter differ slightly in their fine corn content. Yamasuna has almost no fine particles below 0.1 (mm) diameter, while Charcoal has a mass fraction of 10 (%-mass) for particles with a diameter smaller than 0.1 (mm). Results of washing experiment from the charcoal producer showed that BTEX, PAH or other harmful substances that are created during the carbonization process, are not dissolved from the wooden charcoal.

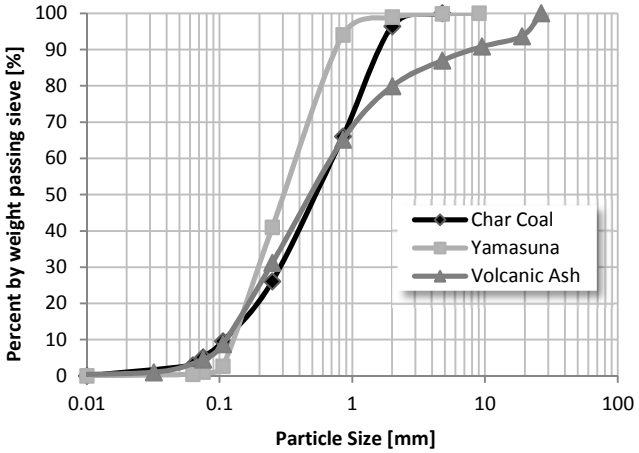

Figure 5: Sieve curves for JFE Charcoal, Yamasuna sand, and volcanic fly ash

3.2 Aquifer and Groundwater

For the recovery of groundwater and re-injection of filtered water two wells were installed, 48 meter apart from each other in north-south direction. The site is located in the city of Okayama, Japan, in the north part of the city, on the campus of the University of Okayama, as shown in Figure 6. The Aquifer consists of unconsolidated sediments of gravel, sand, and clay at a former flood land area (Nlid, 2011). Figure 7 shows the bore profile for well #1 (north well – groundwater recovery) and well #2 (south well – injection well). Additionally, four observation wells were established. The test site consist out of two aquifer: (1) Aquifer 1 is a shallow clay-sand aquifer (0–6 m below ground surface), and (2) Aquifer 2 is a confined aquifer starting 6 (m) below the surface area. The second Aquifer consists of gravel-sand with a high hydraulic conductivity of 0.16 (cm s^{-1}). Therefore, Aquifer 2 was chosen for the recovery of groundwater and re-injection.

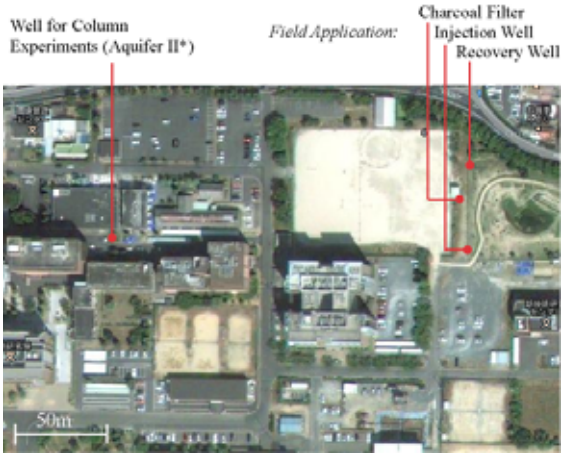

Figure 6: Location of the recovery well for groundwater used in the column experiments (Aquifer II*) as well as the location of the wooden char coal filter, injection and recovery well for groundwater (Aquifer II) for the field experiment at the Tsushima Campus in Okayama, Japan (N 34° 41.28, E 133° 55.18) (Google Inc.)

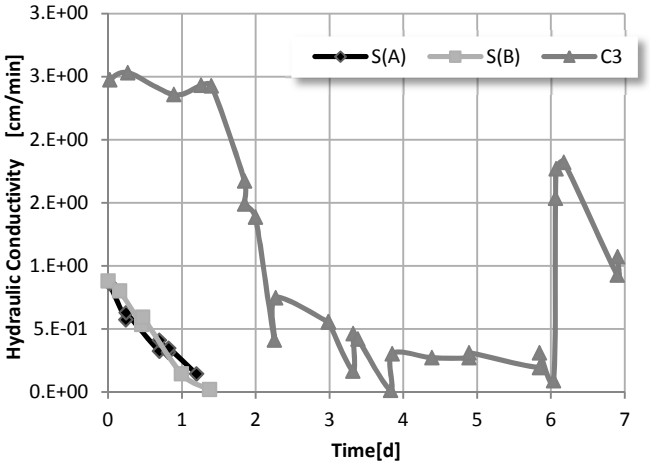

Figure 7: Change over time in hydraulic conductivity of column S_A, S_B (Yamasuna Sand), and C_C (Wooden Charcoal). After six days the hydraulic conductivity of wooden charcoal could be recovered through back flushing

The groundwater that was used for the laboratory column experiments was also delivered from Aquifer 2, 200 (m) in west direction from the site. The chemical and physical parameter of the used groundwater of both experiments is summarized in Table 3. It can be seen that both groundwater differ in their concentration of dissolved iron, which results in a higher electric conductivity for the water used in the column experiments. Groundwater for the field experiment was delivered from Aquifer 2 from well #1 (Recovery well). The well was sealed with an

inflatable packer MD-3.4 BASK I, in order to prevent air mixing with groundwater.

Table 3: Physical and chemical parameters for Aquifer II* (column experiment) and Aquifer II (field experiment), with average temperature (T), initial dissolved iron and manganese ion concentration, pH, electric conductivity, dissolved oxygen level and hydraulic conductivity

Parameter	Unit	Aquifer II*	Aquifer II
T	° C	19.02 ±0.18	17.6
($Fe^{2+/3+}$)	mg L^{-1}	7.9 ±0.61	3.71 ±0.09
(Mn^{2+})	mg L^{-1}	2.18 ±0.08	2.98 ±0.11
pH	–	6.77 ±0.05	6.8
EC	mS cm^{-1}	0.37 ±0.03	0.22
DO	mg L^{-1}	0.8 ±0.09	0.5
k	cm s^{-1}	–	0.16
E(h)	mV	-47	

3.3 Analytic Instruments

In order to measure the turbidity in the washing experiment a P2100 TURBIDIMETER HACH© was used. The instrument was calibrated with standard solutions prior to the experiments.

Conductivity was measured with a Horiba©, CONDUCTIVITY METER B-173 TWIN COND. The instruments calibration was controlled with a 1.41 (mS cm^{-1}) standard solution from Horiba Ltd. Japan©.

The pH in all experiments was measured with a GST-2729C pH probe and a WM-32EP pH meter from TOA DI©. The probe was calibrated with a pH 4.01 and pH 6.86 standard solutions.

Dissolved oxygen and temperature were measured with a 17SD pH/ORP, DO, CD/TDS, Salt Meter from SATO SHOUJI INC©. The DO probe was one-point calibrated with air. The DO was automatically adjusted to the samples temperature, due to a temperature sensitive DO probe.

Dissolved iron concentration was analyzed with an Atomic Absorption Spectrophotometer (Hitachi©, Z-6100 POLARIZED ZEEMAN).

4 Results

4.1 Small Filter Experiments

4.1.1 Hydraulic Conductivity Change

In order to keep a constant filter velocity, the hydraulic head difference of the constant pressure tank and the column outlet (see Figure 3) was adjusted accordingly to the changes in the flow rate. These changes were on one hand caused by adsorbent particle movement within the column material and on the other hand originated from external accumulated particles at the inlet of the column, which decreased the hydraulic conductivity of the system. These particles consisted mainly of brown colored iron-oxides and could easily be removed by back flushing.

However, changes in the hydraulic conductivity could not completely be recovered for the adsorbent Yamasuna sand, as displayed in Figure 8. The hydraulic conductivity of the volcanic ash filled column range about 2.94 (cm min^{-1}), whereas Yamasuna sand ranged from 2.82 (cm min^{-1}) (S_0), 0.86 (cm min^{-1}) (S_A), and 0.88 (cm min^{-1}) (S_B).

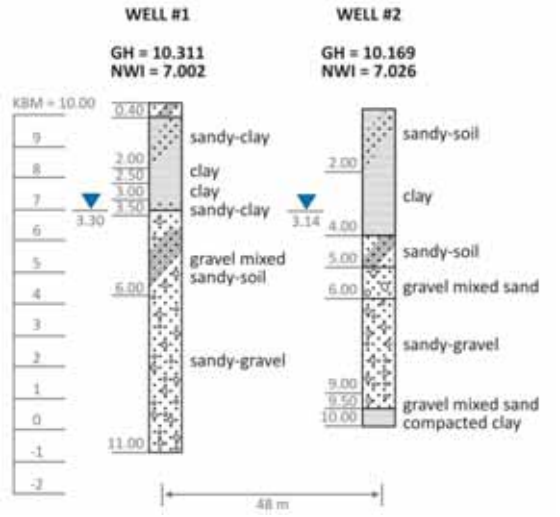

Figure 8: Structure of Aquifer I and II at the two bore holes for the pumping well (#1) and injection well (#2) with the water table of the confined Aquifer II at the installation time

The hydraulic conductivity of wooden charcoal adsorbent ranged from 0.034–6.6 (cm min^{-1}) (C_0), 1.02 (cm min^{-1}) (C_A), 0.504 (cm min^{-1}) (C_B), and 0.252 (cm min^{-1}) (C_C). Figure 8 shows that S_A hydraulic conductivity reduced from 0.86 (cm min^{-1}) to 0.14 (cm min^{-1}) within 1.2 days, and S_B hydraulic conductivity reduced from 0.88 (cm min^{-1}) to

0.019 (cm min^{-1}) within 1.4 days. Both were not recoverable due to back flushing, in contrast to all wooden charcoal filters. However, it was assumed that silt and clay particles from the sand may cause clogging within the filter. Filter SB was therefore installed with washed Yamasuna sand, in order to reduce the quantity of these particles, but the material still remained unrecoverable in terms of its hydraulic conductivity.

Do to the low and not recoverable hydraulic conductivity of Yamasuna sand even after washing, Yamasuna sand was excluded from further column studies regarding the removal of dissolved iron.

4.1.2 Iron Removal

Yamasuna Sand Column

In the first constant-head experiment, Yamasuna sand showed a strong decrease in its hydraulic conductivity; however, it was also able to reduce the dissolved iron concentration below 0.2 (mg L^{-1}) as shown in Figure 9.

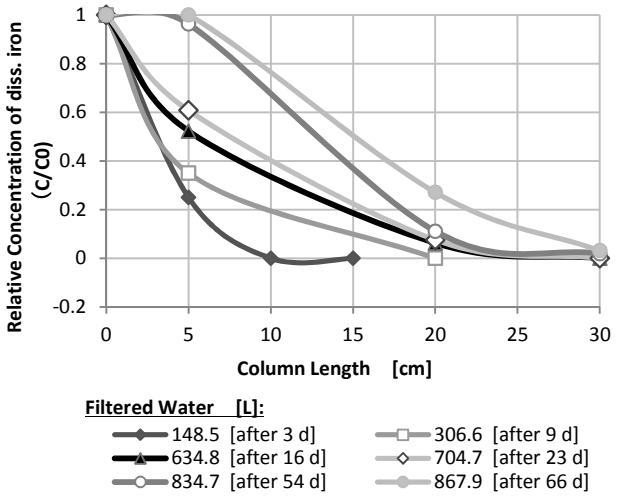

Figure 9: S_0 (constant head) column relative dissolved iron concentration (-), after filtering 148; 307; 635; 705; 835 and 868 (L) of groundwater

The material was able to filter effectively 868 (L) of groundwater before a break-through of dissolved iron occurred at the outlet of the column with 0.2 (mg L^{-1}). The weighted average Inlet concentration was 4.8 (mg L^{-1}). The speed of the break-through curve through the column seem to increase after 307 (L) of groundwater were filtered, even though the flow rate decreased from initially 39.3 (mL min^{-1}) to 1.9 (mL min^{-1}). During the experiment a total of 3.04–3.16 (g) dissolved iron has been removed from groundwater.

These results show that Yamasuna sand was in principle capable of reducing the amount of dissolved iron, even though the hydraulic conductivity of the material decreased and hence also the velocity. In order to maintain a constant velocity, the water head difference of the experimental system was changed in a second experiment, accordingly.

The other two sand columns, under constant velocity, were highly reduced in hydraulic conductivity after one and a half day, as it can be seen in Figure 8. As the columns velocity (hydraulic conductivity) could not be recovered through back flushing, Yamasuna sand was abandon as adsorbent for practical reason.

Volcanic Ash

Volcanic ash was refused as adsorbent material, as its performance, regarding the adsorption of dissolved iron, was lower than Yamasuna sand or wooden charcoal.

Figure 10 shows the relative dissolved iron concentration profile at sampling port I (4.3 cm), II (8.6 cm), III (12.9 cm), IV (17.2 cm), and the outlet (30 cm) of the column after 174, 343, and 458 (L) of groundwater were filtered. After 458 (L), a dissolved iron concentration of 15.3% of the initial inlet concentration was detectable at the outlet, even though the concentration at Port I was still with 36.7% relatively low compared to Yamasuna sand (100%) or wooden charcoal (95.8%), after break-through. The long tailing of the concentration profile would require a longer column and more filter material to be equally effective in removing dissolved iron from groundwater compared to wooden charcoal or Yamasuna sand. In total the volcanic ash filter was able to remove 2.9–3.9 (g) dissolved iron from groundwater until break-through.

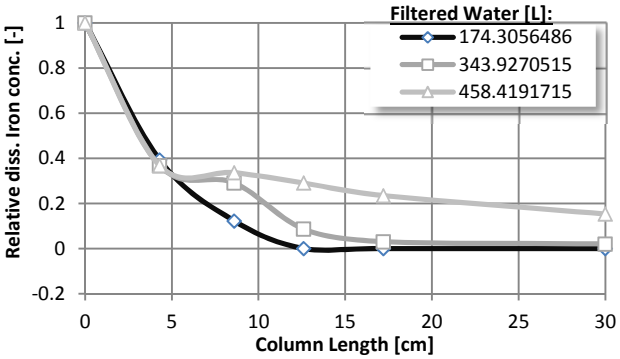

Figure 10: V_0 (constant head) column relative dissolved iron concentration (-), after filtering 174; 343; and 458 (L) of groundwater

Wooden Charcoal

Initially a filled wooden charcoal column (C_0) was set up and operated under constant pressure head (Δh), in order to estimate the behavior of clogging and hence velocity change, as an applied system will be under constant pressure.

In this experiment wooden charcoal was able to filter 2016.4 (L) of groundwater before a break-through of dissolved iron was detectable at the outlet of the column. However, due to minor precipitations of ferric and ferrous mineral phases in the constant head pressure tank, the weighted average inlet concentration of dissolved iron was 5.27 (mg L^{-1}). Hence, the wooden charcoal filter removed a total of 9.7–10.6 (g) dissolved iron from the groundwater until break-through.

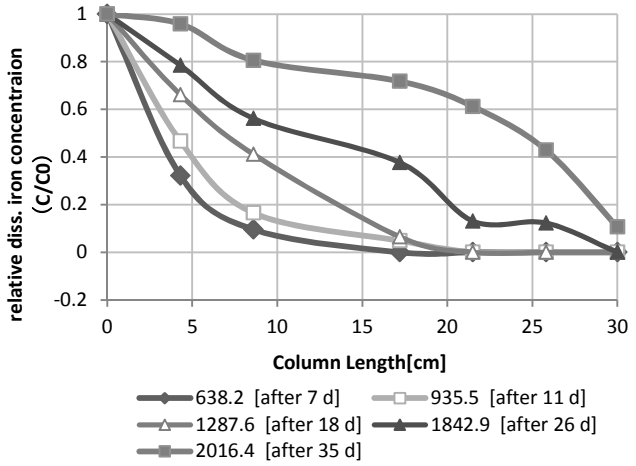

Figure 11: C_0 (constant head) column relative dissolved iron concentration (-), after filtering 638; 936; 1,288; 1,843 and 2,016 (L) of groundwater

Column C_A was filled with 813.9 (g dry coal) and was operated at a retention time of 15 minutes, resulting in a filter velocity of 0.017 (cm s^{-1}) (± 9.8%). Figure 12 shows the movement of the relative concentration profile of dissolved iron through Column C_A for four sampling days.

Break-through of dissolved iron at the outlet occurred after 676 to 891 (L) of groundwater were filtered. The decrease of dissolved iron concentration at Port I between the 2nd and 3rd sampling period may have been caused by minor fluctuations of the flow rate, resulting in a decrease of velocity in the pores. During this time a total amount of 5.43 (g)–7.16 (g) dissolved iron were adsorbed from the groundwater with a weighted inlet concentration of 8.03 (mg L^{-1}).

Column C_B was filled with 532.1 (g dry coal) and operated at a retention time of 30 minutes, resulting in a filter velocity of 0.084 (mm s-1) (± 10%). Figure 13 shows the movement of the relative concentration profile of dissolved iron through Column C_B for three sampling days. Break-through of dissolved iron at the outlet occurred after 191 to 541 (L) of groundwater were filtered.

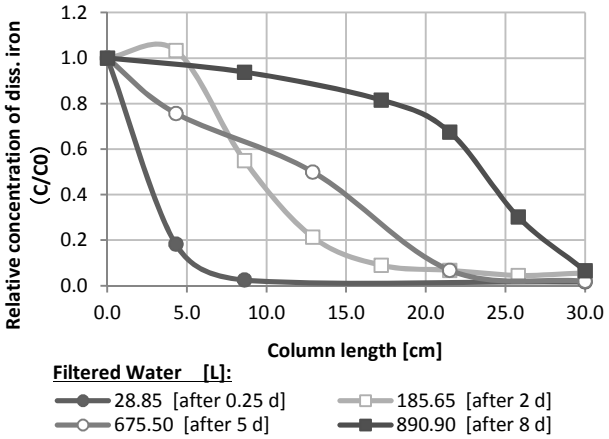

Figure 12: C_A (constant velocity: 1.02 (cm min^{-1}) (±9.8%)) column relative dissolved iron concentration (-), after filtering 29; 186; 676 and 891 (L) of groundwater

The break-through occurred more rapidly as initially expected based on the results from Column C_A. However, as the mass of dry coal differed from Column C_A to C_B of Δm= -34.6% a decrease in the total amount of adsorbed iron was expected. During this time a total amount of 2.3 (g)–6.4 (g) dissolved iron were adsorbed with a weighted inlet concentration of 11.8 (mg L^{-1}).

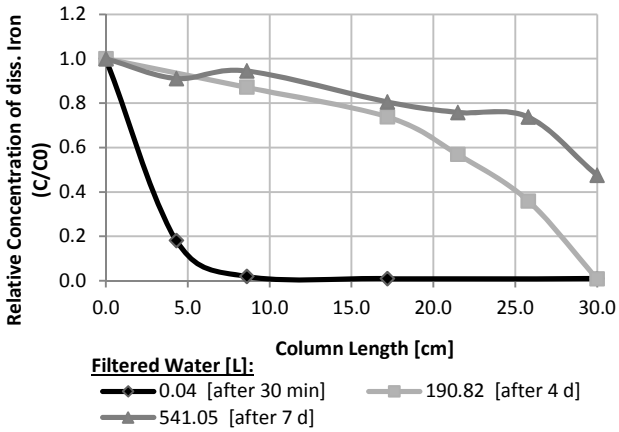

Figure 13: CB (constant velocity: 0.504 (cm min^{-1}) (±10%)) column relative dissolved iron concentration (-), after filtering 0.04, 191, and 541 (L) of groundwater

Column C_C was filled with 766.6 (g dry coal) and was operated at a retention time of 45 minutes, resulting in a filter velocity of 0.042 (mm s^{-1}) (±10%). Figure 14 shows the movement of the relative concentration profile of dissolved iron through Column C_C for seven sampling days. Besides minor fluctuation of the dissolved iron concentration at Port I and III between the profile for the concentration profile after 882 (L) were filtered, the profile moves through the column from the inlet to the outlet, and changes its concave form after 656 (L) to a convex curve shape. Break-through of dissolved iron at the outlet occurred after 882 to 1,007 (L) of groundwater were filtered. During this time a total amount of 10.8 (g) – 12.1 (g) dissolved iron were adsorbed with a weighted inlet concentration of 12.2 (mg L^{-1}).

All profiles show the same curve shape change from concave to convex and increased tailing with proceeding time.

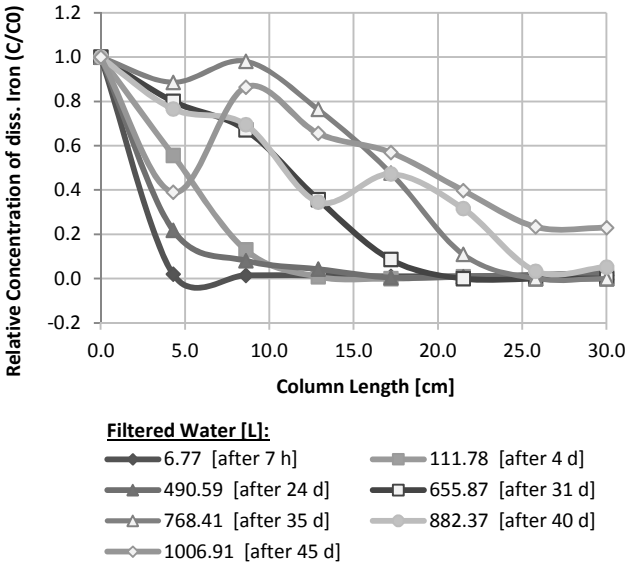

Figure 14: C_C (constant velocity: 0.252 (cm min^{-1}) (±10%)) column relative dissolved iron concentration (-), after filtering 7; 112; 491; 656; 768; 882; and 1,007 (L) of groundwater

4.1.3 Surface Adsorption on Wooden Charcoal

The adsorption capacity of wooden charcoal is summarized in Table 4. The maximum adsorption capacity (qeq) for dissolved iron was derived from the total content of iron per samples, with respect to the iron concentration of blank sample (n=9) of 1.29 ((g (kg coal)$^{-1}$)) (± 0.29 (g (kg coal)-1)) for the first 10 (cm) of each column, as the first 10–15 cm of each column showed constant values for the total iron concentration. The qeq for C_A to C_C lays within each other's error interval of about 3.5 (g (kg coal)-1). The different velocity of each column shows no effect on the total adsorption capacity. However, qeq for C_0 shows a lower adsorption capacity when compared to C_A to C_C. With a total adsorption load of qeq, C_0 = 1.01 ((± 0.38) (g (kg coal)-1) its adsorption capacity lays more than 70% lower than qeq, C_A–C_C.

It can be seen from Table 4 that the iron adsorption capacity estimated with the method after Ryan et al., (2012) showed no difference in the adsorption capacity for Column C_A–C_C regarding the 5%-confidence interval. However, the control adsorption capacity (qeq control), that is calculated from the inflow dissolved iron concentration, mass of used dry coal, and flow rate, showed significant differences in the adsorption capacity for each column. These differences will be discussed in Section 5.

Table 4: Summary of maximum dissolved iron adsorption capacity (qeq) of C_0, C_A, C_B, and C_C (g (kg coal)$^{-1}$). The mean iron content of a blank samples is 1.29 ((g (kg coal)$^{-1}$)) (± 0.29 (g (kg coal)$^{-1}$)). As well as total input of dry wooden charcoal (g), flow rate based calculated dissolved iron take-out (Fe2+ t.o. (g)) and derived adsorption capacity (control)

Para-meter	Unit	C_0	C_A	C_B	C_C
t.fe	(g (kg coal)$^{-1}$)	2.3± 0.09	4.7± 0.29	3.8±0.1	4.99± 0.22
q_{eq}	(g (kg coal)$^{-1}$)	1.01 ±0.38	3.41 ±0.58	3.94 ±0.63	3.7 ±0.51
$m_{c, dry}$	(g)	1,080.1	813.9	532.1	766.6
Fe^{2+} t.o.	(g)	9.7–10.6	5.4–7.2	2.3–6.4	10.8–12.3
q_{eq} control	(g (kg coal)$^{-1}$)	8.9–9.8	6.6–8.9	4.3–12.0	14.1–16.1

4.1.4 Washing of Wooden Charcoal

In order to estimate the time necessary to flush the filter (material) before re-injection, the wooden charcoal adsorbent was washed with supply water in column experiments for various filter velocities. The results are shown in Table 5 and Figure 15.

Average supply water turbidity was estimated (n=8) to range at 0.179 (NTU) (± 0.004 (NTU)). In all eight

experiments the initial turbidity value of the tab water could not be reached within eight minutes of flushing. However, for filter velocities (U) lower than 0.2 (cm s^{-1}) a turbidity of 2 (NTU) could be reached after at least one pore volume flushing ($V\varphi$,eq). For filter velocities from 0.2 to 0.3 (cm s^{-1}) at least two filter pore volumes were necessary. The result of the experiment with U=0.07 (cm s^{-1}) and a coal input dry mass of m0 = 600 (g) is outstanding, since 2.12 $V\varphi$,eq were necessary.

Table 5: Summary of eight wooden charcoal adsorbent filled filter flushing experiments under various filter velocities (U), initial dry coal mass (m0), turbidity after five seconds (T5), filtered water volume until a turbidity of 2 (NTU) was reached (Vw,2), and equivalent filter pore volume until 2 (NTU) are reached ($V\varphi$,eq)

U (cm s^{-1})	m_0 (g)	T_5 (NTU)	$V_{w,2}$ (mL)	$V_{\varphi,eq}$ (-)
0.04	510.7	30.9	400–816	0.30–0.61
0.05	527.6	36.8	221	0.15
0.07	503.4	54.2	664–1,329	0.50–1.01
0.07	600.0	104.7	2,749	2.12
0.18	601.9	56.73	432–864	0.29–0.57
0.23	588.9	36.4	2,147	1.52
0.24	481.8	90.3	2,306	1.80
0.28	584.2	72.6	1,299–2,598	0.85–1.70

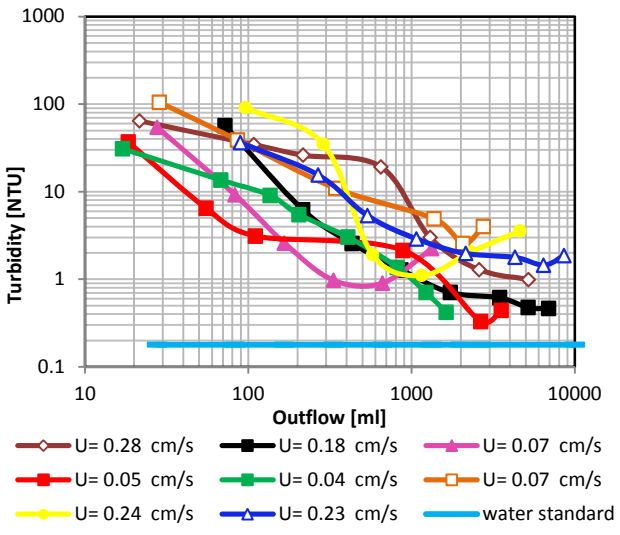

Figure 15: Results of the wooden charcoal adsorbent washing experiment for various filter velocities (U) from 0.04 (cm s^{-1}) to 0.28 (cm s^{-1}). Further results and initial conditions are given in Table 5

4.2 Pilot Wooden Charcoal Filter

The wooden charcoal filled pilot filter (Figure 4) was on-site tested from 22nd of August 2012 to 12th of September 2012. During this time 44.6 (m^3) groundwater were filtered with a weighted average flow rate of 5.52 (L min^{-1}) (U = 2.93 (cm min^{-1})), but not re-injected into the aquifer, as it could initially not be ensured that dissolved iron adsorption takes place. However, during this time no dissolved iron break-through was detectable neither at the outlet of the filter nor at the middle of the filter length (Port II). Based on the maximum adsorption capacity (qeq ≈ 3.5 (g (kg dry coal)$^{-1}$)) of the wooden charcoal from the laboratory column experiments, the 25.27 (kg) dry wooden charcoal would have been able to adsorb 88.4 (g) of dissolved iron, with a groundwater dissolved iron concentration of 3.71 (mg L^{-1}) (± 0.09 (mg L^{-1})) resulting in a total of 23.8 (m^3) filtered groundwater. This difference in the adsorption capacity results between the column studies and the on-site filter will be discussed in Section 5.

4.3 Used Groundwater Re-injection

For the estimation of the potential usage of ambient groundwater heat (17.6 (° C)) to cool and heat a facility on-site, groundwater was previously filtered through a Ferrolite filter and re-injected back into the aquifer after utilization. The groundwater table (interval: 30 (min)) and temperature (interval: 30 (s)) were continuously observed during the re-injection period of 55 (d) (from 15th of November 2012 to 8th of January 2013) in the injection well and an observation well one meter in north direction from the injection well.

The different in hydraulic head between the observation and the injection well during the injection is shown in Figure 16. While the Ferrolite filter removed dissolved iron (C_0 = 3.71 (mg L^{-1}) (± 0.09 (mg L^{-1}))) from the groundwater for the initial 36 days the head difference was stable between 0.2–0.7 (cm). The dissolved oxygen level of the injected water was 0.7 (mg L^{-1}), respectively. However, as soon as the groundwater was injected into the well it got in contact with oxygen through mixing with air. At the time the dissolved iron broke through, after 1,296 (m^3) filtered groundwater had been injected into the Aquifer, the head difference decreased rapidly until the shutdown of the pump after 55 days of continues operation. At the moment of shutdown a total of 1,899 (m^3) groundwater had been re-injected into the

Aquifer and the absolute head difference between the observation well and the injection well was 24.4 (cm).

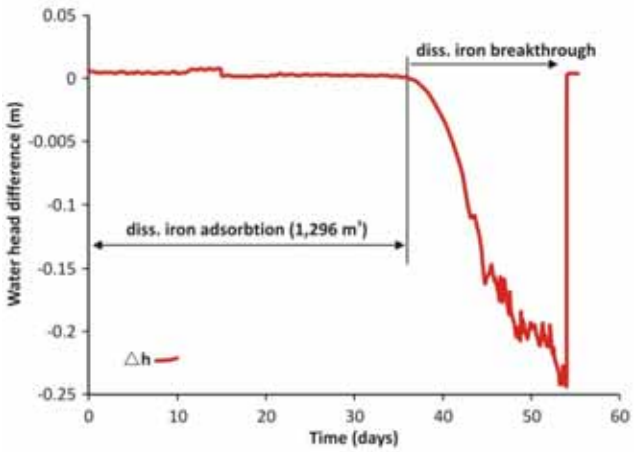

Figure 16: Water head difference between the observation well (one meter north of injection well) and the injection well. Breakthrough of dissolved iron occurred 36 days after the start of the injection and caused an immediate increase in head difference due to clogging

The general groundwater fluctuation during the re-injection period can be seen from the bottom graph of Figure 17. The groundwater head of observation well #4 (OW#4), which is located between the recovery and injection well, was assumed to has not been influenced by drawn down or up-coning effects of these wells. It can be seen, that the groundwater table highly fluctuated from 6.4 (m) above mean sea level (AMSL) to 7.1 (m) AMSL. If compared to precipitation data (JMA, 2012) of that period, a general trend of increasing groundwater level after a precipitation event becomes obvious. This indicates a high influence of surface water on the second Aquifer.

The head difference between the observation well one meter south of the RW (OW#1) and OW#4 shows a constant decrease in head from initially -0.29 (m) to 0.421 (m) before shutting down the pump. The average difference between both wells was +0.033 (m), when the groundwater is not influence by pumping or injecting. An influence of the groundwater fluctuations is not visible. However, it has to be noted, that the recovery well was operating discontinuously over one year prior to the experiment, but has been operated continuously with the highest amount of recovered groundwater in the re-injection period described above. Consequently, the gradient of the decrease in head difference of OW#1 compared to OW#4 is 0.131 (m) in total, or -5.46×10^{-3} (m m^{-1}), if the space between both well is considered. It is assumed that this decrease has been caused by aquifer material movement, resulting in a slightly increased clogging during the 55 days pumping and re-injecting period. On the other hand, the increase in head difference at the Injection well is assumed to be caused by clogging due to precipitation of ferric and ferrous mineral phases, which formed when dissolved iron got in contact with atmospheric oxygen. The increase in head difference of 0.245 (m), or 0.245 (m m^{-1}) in only 20 days occurs about 120 times faster in space and time than the clogging at the recovery well.

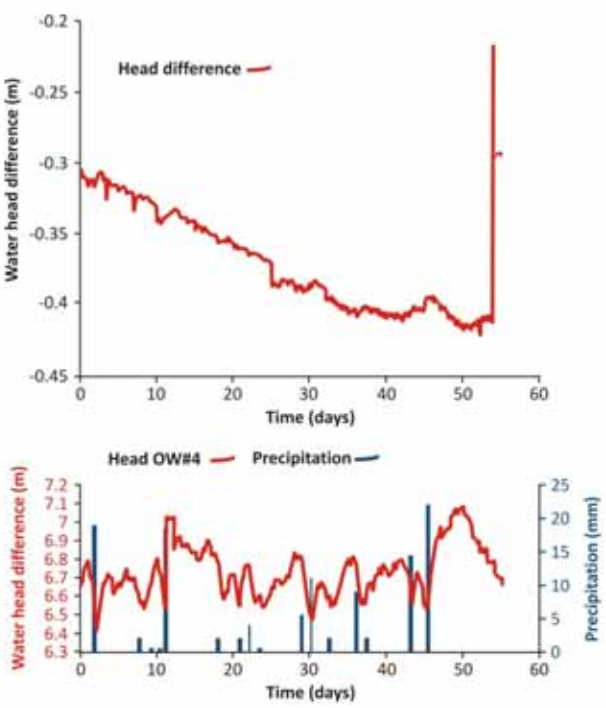

Figure 17: Water table in observation well #4 (OW#4) (25 m south of recovery well (RW) and 25 m north of IW) with precipitation data (mm) (JMA) (BOTTOM). Head difference between OW#1 (one meter south of RW) and OW#4 during the Injection period (TOP)

5 Discussion

The results show that the used JFE wooden charcoal is capable of adsorbing and removing dissolved iron from groundwater under anoxic condition. Additionally laboratory scale column experiments with Yamasuna sand and volcanic ash as adsorbent, showed that these two materials are also able to adsorb dissolved iron.

However, the adsorption time of volcanic ash was longer, compared to wooden charcoal and Yamasuna sand, which lead to a wider tailing of the concentration profile and an earlier break-through of dissolved iron. This made volcanic ash as adsorbent inapplicable. Even though Yamasuna sand reduced the concentration of dissolved iron in groundwater as well, the hydraulic conductivity of the material was already reduced by power one to two after 1.4 days of operation and was not recoverable due to back flushing. This indicates that clogging happened within the filter material and not exclusively at the inlet of the column due to iron hydroxide or ferric-oxide precipitation. Wooden charcoal showed the highest adsorption capacity for dissolved iron with an average q_{eq} 3.5 (g (kg charcoal)$^{-1}$) with respect to the confidence interval of each measurement. This value may represent a minimum adsorption value, as the control value for column C_A to C_C was 1.9–2.6 (C_A), 1.0–3.0 (C_B), and 3.8–4.3 (C_C) times higher than the adsorption capacity found by the analytical method proposed by Ryan et al. (2001). A possible source for this difference in results was published 2012 by Braunschweig et al. The method by Ryan et al. (2001) is using a two molar HCL solution to dissolve ferric oxides and iron hydroxides, which got created during the incineration process over 24 hours at 500° C. The contact time with the acid is 20 minutes, which may be to low in order to dissolve all ferric oxides, especially goethite and magnetite. Braunschweig et al., (2012) proposed that at least 6 molar HCL should be used with a contact time of 24 hours. Whether the method of Ryan et al. (2001) is source of the difference in adsorption capacity, is currently under research.

If the performance of the on-site wooden charcoal filter with an initial mass of dry coal of 25.27 (kg) is compared to the laboratory column filter experiment results, the adsorption capacity of this filter was at least double or three times higher. This difference could be taken as evidence that the method explained above leads to an analytical mistake.

However, it has to be noticed that the adsorption capacity is highly depended on the initial concentration of ions, the pH of the used groundwater, which will change the charge of active groups on the charcoal surface, and the existence of other ions or affinitive molecules, such as organic substances (Worch, 2012).

In comparison to the Ferrolite filter, which was able to adsorb dissolved iron from 1,890 (m^3) of groundwater and the wooden charcoal on-site filter, the Ferrolite filter showed a adsorption capacity of 6.17 (g (L material)$^{-1}$), whereas the wooden charcoal (based on q_{eq} = 3.5 (g (kg coal)$^{-1}$)) reaches a adsorption capacity of 1.11 (g (L material)$^{-1}$), and hence, is about 6 times less effective, than Ferrolite granulate. However, if the higher performance of the on-site wooden charcoal filter is taken into account, an adsorption capacity of 2.2–3.3 (g (L material)$^{-1}$) is possible, which means a 36%–53% efficiency of the Ferrolite filter. Since the wooden charcoal was almost not capable of removing dissolved manganese from the groundwater, the Ferrolite filter has the advantage that it removes both ions effectively. Nonetheless, as the price for the JFE wooden charcoal material is lower than the Ferrolite granulate, it could be used for groundwater with low manganese concentration and moderate flow rate. Such an application example is shown in Table 6.

Assuming that the average domestic water demand is 320 (L d^{-1} person^{-1}) in Japan, three examples for a filter design that operates half a year, are given in Table 6. They are based on the experimental design and results for column C_A–C_C, for a four person household, with a water usage of 16 hours and under the assumption that 25% of the water demand is used together, for an initial dissolved iron concentration of 10 (mg L^{-1}). 30% of dry coal mass was additionally included as safety factor, in order to consider the length of the tailing of the dissolved iron concentration. For such a household a filter based on the design of column C_C is less spacious, if seven tubes of 75.5 (cm) diameter are used and are arranged in a box shape of 1 (m) height, and 2.40 (m) width and length. Other designs of box shape filter units are also possible. The example shows that a filter, designed with the minimum adsorption capacity estimated from the column laboratory experiments, leads to a practical filter design. However, as mentioned before is a detailed investigation of the used groundwater and adsorption capacity of the charcoal under realistic conditions necessary.

It is necessary prior to the operation of the filter, that the adsorbent material is flushed with a volume of one to two filter pore volumes, as found in the washing experiment (4.1.4).

Table 6: Application of the wooden charcoal filter material in n tubes (N) of the diameter dFilter, with height (H), assembled in a box shape of the length (L). The design is based on the filter velocity and adsorption capacity of each column, assumed to operate 0.5 (a), for a flow of 960 (L d^{-1}) in 16 (h). Initial dissolved iron concentration: 10 (mg L^{-1})

	Unit	C_A	C_B	C_C
m_{Coal}	(kg)	770.7	667.0	710.3
+30%	(kg)	1,001.9	867.1	923.4
$V_{coal(+30\%)}$	(m^3)	2.90	3.45	2.84
d_{Filter}	(m)	0.353	0.50	0.757
(N) H x L^2	(m)	(30) 1 x 3.56	(18) 1 x 3.26	(7) 1 x 2.40

During the laboratory column experiments brownish sediments accumulated in the nitrogen gas filled constant head tank. These precipitates were assumed to be iron hydroxides. As the groundwater is put under pressure change when pumped up and slightly mixed with air in the well, the physical and chemical composition may change. For instance may CO_2 fumigate which changes the pH of the groundwater. The highest impact is caused by even a slight mixing with air, as the redox-potential of the groundwater will change immediately. This effect can be seen from the Pourbaix (1996) diagram in Figure 18. The diagram shows the state of iron at 25 (° C) for a pure iron solution when only solid iron and iron hydroxides are present. The blue lines mark the conditions for the groundwater of Aquifer II. It cannot necessarily be assumed that the groundwater is in a redox-equilibrium; however, even the estimation of state and stability of dissolved species is difficult due to the inaccuracy of the redox-potential measurement (Thorstenson, 1984). An increase in pH or E(h) can lead to the precipitation of iron hydroxides in the system due to changes in the redox-equilibrium, as observed in the constant head tank. These species can later further oxidize to ferric-oxides.

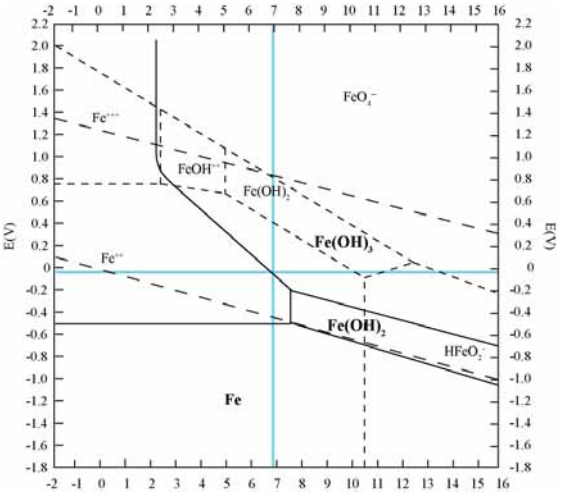

Figure 18: POURBAIX-Diagram for iron ions at 25° C in pure solution. Blue lines mark the range of used groundwaters pH and E(h), after (Pourbaix, 1966)

For prevention of accumulation of iron hydroxides, which may be inevitable be created during the pumping process, a simple filter, such as a textile filter, should be used, in order to prevent clogging of the filter material. Furthermore, an automatically back flush program is suggested for removing such accumulated material from the filter surface, restores the initial hydraulic conductivity, and ensures a stable flow rate under constant pressure.

This research was able to demonstrate the necessity of an anaerobic filter process for removing dissolved iron ions from groundwater that is used in geothermal heat system and is re-injected into the aquifer it was recovered from, in order to prevent clogging of the porous aquifer material. As adsorbent material Yamasuna sand, volcanic ash, JFE wooden charcoal, and Ferrolite granulate were evaluated. Only wooden charcoal and Ferrolite were capable to remove dissolved iron from the groundwater and maintain an operational porous matrix. Suggestions for a charcoal filter design and its system operation were given. Further research will have to proof the applicable of the filter under various groundwater conditions and the change in its adsorption capacity. Finally a long-term, on-site charcoal filter test will be conducted to evaluate the suitability of the filter under more practical conditions.

References

Ahamad, K.U., and Jawed, M., (2011) Breakthrough Column Studies for Iron(II) Removal from Water by Wooden Charcoal and Sand: a low cost approach, Int. J. Environ. Res., *5*(1): 127–138.

Bouwer, H., (2002) Artificial Recharge of Groundwater: Hydrogeology and Engineering, Hydrogeology Journal, 10: 121–142.

Braunschweig, J., Bosch, J., Heister, K., Kuebeck, C., Meckenstock, R.U.,(2012) Reevaluation of Colorimetric Iron Determination Methods commonly used in Geomicrobiology, Journal of Microbiological Methods, 89: 4 – 48.

Google Inc., (2013) Map of Tsushima Campus, Okayama, Japan retrieved from Google Maps: https://maps.google.de/maps?q=japan&hl=en&ll=34.689982,133.925014&spn=0.002488,0.005284&sll=51.151786,10.415039&sspn=7.776562,21.643066&t=h&hnear=Japan&z=18

Igarashi, M., and Saito, K. Estimation of Impervious Hydraulic Gradient for used Yamasuna Sand, Japanese Society of Civil Engineering (JSCE), 2005(3): 153 – 154.

JFE Recycling Management Japan Inc., http://www.jfe-rmj.co.jp/, 2009.

JMA Japan Meteorology Agenca, http://www.jma.go.jp , 2012.

Marsh, H., and Rodríguez-Reinoso, F., (2006) Activated Carbon, 1st ed., ElSevier, Oxford, UK.

Mutschmann, J., and Stimmelmayr, F., (1991) Taschenbuch der Wasserversorgung, 10th ed., Franckh-Kosmos, Stuttgart, Germany.

Näser, K.-H., Lempe, D., and Regen, O., (1990) Physikalische Chemie für Techniker und Ingenieure, (in German), 19th ed., VEB Deutscher Verlag für Grundstoffindustrie Leipzig, Leipzig, Germany.

NLID – National Land and Information Division, National and Regional Policy Bureau, Tokyo, 2011: National Land Agency, Okayama Prefecture, Map (Internet): http://nrb-www.mlit.go.jp/kokjo/tochimizu/F3/ZOOMA/3304/index.html

Oba, N., Tsuyuki, T., and Ebihara, H., (1967) Mineral and Chemical Composition, and Genesis of the Yamasuna (in Japanese), Gansekikoubutsukoushougakkukaishi, 58(3): 81–97.

Pourbaix, M., (1966) Atlas of Electrochemical Equilibria of Aqueous Solutions: Chapter IV, Pergamon Press, Cebelcor, Brussels.

Ryan, J., Estefan, G., and Rashid, A., (2001) Soil and Plant Analysis Laboratory Manual, 2nd Ed., Aleppo, Syria.

Storm, R., (1969) Wahrscheinlichkeitsrechnung, mathematische Statistik und statistische Qualitätskontrolle, (in German), 3rd ed., VEB Fachbuchverlag Leipzig, Leipzig, Germany.

Thorstenson, D.C., (1984) The Concept of Electron Activity and its Relation to Redox Potentials in Aqueous Geochemical Systems, U.S. Geological Survey, Report 84 – 072.

Worch, E., (2012) Adsorption Technology in Water Treatment, 1st ed., Walter de Gruyter, Bonn/Bosten, Germany/USA.

Contact Details

Email: n_makoto@cc.okayama-u.ac.jp

Laboratory Experiments in Porous Media in Order to Predict Particle Remobilization

C. Hartwig[1], M. Nishigaki[1], T. Takuya[2] and R.U. Ruemenapp[1]

[1] *Geo-environmental Evaluation Laboratory, Department of Environmental Design and Civil Engineering, Graduate School of Environmental Science, Okayama University, Japan*

[2] *Tokyu Construction Corporation, General Administration of Civil Engineers, Civil Engineering Department, Ground-Foundation Group, Tokyo, Japan*

Abstract

In several countries pumping of groundwater results in overexploitation, saltwater intrusion, or land subsidence which can be mitigated by artificial groundwater recharge is a countermeasure for these problems and/or flooding. Well injection is one of the best method for artificial recharge but also accompanied with difficulties, such as clogging. In this research, investigation on physical clogging regarding to particle mobilization was done. A one and two-dimensional laboratory experiment were carried out, in order to determine the critical hydraulic gradient. The one-dimensional horizontal-flow column experiments showed that not only fine content of the soil can be mobilized, but also particle sizes between 0.25 and 2 mm moved by velocity forces. An axisymmetric confined aquifer model (2-dimensional) was constructed to simulate radial groundwater flow away from an injection well. For the experiment, two types of soils with different distribution curves were used in order to investigate the problem of fine particle movement and determine the critical water level rise in the injection well. From the results of the axisymmetric experiment, it is plausible to conclude that at a critical hydraulic gradient (i) of 0.3, for a content of fine particles in the aquifer below 0.104 mm, was determined for injection in the field, which indicates that clogging does not occur.

1 Introduction

Groundwater is used by more than half of the world's population, especially in semi-arid areas where water resources are rare. But unlimited pumping of groundwater results in overexploitation, saltwater intrusion, or land subsidence. In order to maintain sustainable groundwater management artificial recharge is a practicable technique.

Furthermore, artificial groundwater recharge can be applied in order to store exceed storm water in the subsurface or for energy storage such as groundwater (open-loop) heat pump systems.

However, regarding injection of water into an aquifer, clogging does often occur which alters the artificial recharge system in its efficiency. Among the three clogging types, physical clogging is still an unsolved problem especially according particle mobilization of soil particles initially present in the aquifer.

Due to water injection into an aquifer, the hydraulic gradient decreases with radial distance from the injection well. When soil particles near the well are moving, permeability decreases with moving distance resulting in accumulation of the soil particles and clogging occurs (Figure 1). Thus, determination of the critical hydraulic gradient and also the critical velocity are of great importance.

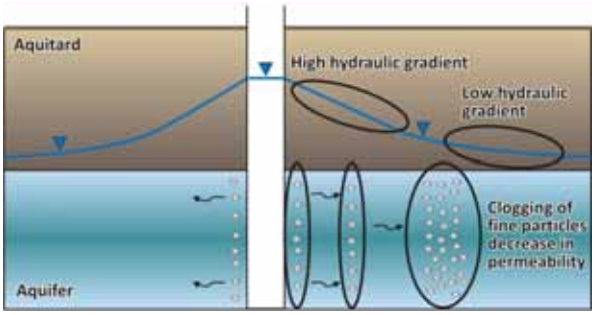

Figure 1: Clogging because of fine particle movement in the aquifer

1.1 Literature Review regarding physical clogging

In almost every case the authors agreed that physical clogging leads to about 70% in permeability reduction (Bichara, 1988; Reddi, 2000; Holländer et al., 2005). Obviously, the major factors affecting the particle deposition are suspended solids concentrations of the recharging water, soil size and distribution, and porosity.

In order to develop mathematical models, efforts were made to describe the movement of suspended particles in the aquifer (Vigneswaran and Thiyagaram, 1984; Vigneswaran et al., 1985; Ahfir et al., 2009). But these mathematical models all include constants which definitions vary from author to author, thus the models in these studies could be verified with the experimental data from the respective study site, but are not applicable for different recharge areas with different conditions.

Since 1940, infiltration of surface water into an aquifer is successfully utilized in the Netherlands. In order to avoid clogging, periodic backwashing is used. They are also using three main clogging parameters (Bouwer, 2002). The Membrane Filtration Index (MFI) is determined by membrane filtrations and shows the slope of inverse filtered flow versus cumulative filtered volume. In some literature, the MFI is also termed as the Modified Fouling Index (Olsthoorn, 1982; Pérez, 2000). The Assimilable Organic Carbon Content (AOC) investigates a water sample for growth of bacteria. The third parameter is the Parallel Filter Index (PFI). This parameter is determined via laboratory experiments, passing recharge water through columns filled with aquifer material. It is assumed, that clogging in the columns occurs faster than in the field and thus an early warning factor can be defined.

But previous studies showed that the parameters are not valid for predicting clogging because the influences of well construction and aquifer characteristics cannot be considered in laboratory scale studies. (Hijnen and van der Koou, 1992; Dillon et al., 2001; Bouwer, 2002).

Up to present day, most research are done on suspended solids contained in the injection water (McDowell-Boyer et al., 1986; Herzig et al., 1970; Moghadasi, 2004; Ahfir, 2009; Ye, 2010). Moghadasi (2004) investigated the movement of fine particles in the aquifer. They applied a porous bed made of glass beads filled with alumina particles. The experiment showed that during injection the pressure drop increases rapidly after some time, thus the pores become plugged because of particle mobilization. After some time plugs and bridges present in the water flow path break and wider path becomes available for water flow. The pressure drop decreases and the cycle starts from the beginning again.

In order to overcome a solution for physical clogging because of particle mobilization, characterization of a critical hydraulic gradient or rather to say a critical velocity should be carried out.

1.2 Literature Review regarding critical hydraulic gradient and critical velocity

Studies on critical hydraulic gradient or critical velocity have already been done regarding the piping effect of earth fill dams, whose are summarized in Table 2.

One of the first author was Terzaghi (1922) who proposed a critical hydraulic gradient, where the effective stress in a test specimen where water flows through, approaches to near zero, then, the flow pressure ($i \cdot \gamma_w$) is quite the same as the submerged (buoyant) unit weight of the soil.

1924 Justin carried out an equation for critical velocity depending on the effective particle size of the regarding soil. Because to determine the effective size of a soil sample is known to be difficult, Justin recommended, applying a safety factor of 4 to the theoretical critical velocity value for practical utilization.

Kubota (Japanese Geotechnical Society, 1965) published critical velocities regarding to particle sizes of a narrow range, which he concluded from experiments. Unfortunately, either experimental method neither calculation method was explained.

Ohno et al., (1984) obtained an equation for critical velocity out of experimental data with uniform particle sizes and shapes. In case of a wide range of particle sizes, they found out that the movement particles under 25–32 mm are to be considered for piping, thus D_{25} should be used as for determining the critical velocity.

Nakashima et al., 1985 carried out experimental data by observing the movement with x-ray radiography. The results showed that the data are nearly approaching those obtained from Ohno et al.

These are just examples, especially in the Japanese literature there can be much more papers found which are referring to critical velocity or critical hydraulic gradient with experimental data results. One point comes clear in each of these studies, the theoretical critical hydraulic gradient introduced by Justin, is greater than the value obtained from experimental data. Another question comes up, to which extend the study on piping can be applied to clogging phenomena, since piping describes an expansion of the flow path way, whereas clogging has the opposite meaning. The equations shown in Table 1 are including a mean grain diameter (d), here, the problem of the determination of the mean grain diameter of an existing soil is known to be difficult.

Table 1: Experimental characteristics of test specimen

Author	Year	Equation	Parameter
Terzaghi	1922	$i_c=\frac{\gamma'}{\gamma_w}=\frac{G_s-1}{1+e}$	i_c: critical hydraulic gradient (-) γ': submerged unit weight of the soil (N cm^{-3}) γ_w: unit weight of water (N cm^{-3}) G_s: specific gravity of the soil (g cm^{-3}) e: void ratio (-)
Justin	1924	$v_c=\sqrt{\frac{2}{3}g(G_s-1)d}$	v_c: critical velocity (cm s^{-1}) g: acceleration of gravity (m s^{-2}) d: particle size with main impact on permeability (mm) G_s: specific gravity of the soil (g cm^{-3})
Ohno et al.	1984	$V_p=2.25d^{1.94}$	V_p: critical velocity (cm s^{-1}) d: particle size (mm)

1.3 Content and Purpose of this study

A number of studies in clogging have been proposed before, but almost every study considers suspended particles included in the recharge water. But according to physical clogging, fine particles initially present in the aquifer have to be considered. During the recharge process these particles will be mobilized, due to injection velocity, and plug flow path ways. This laboratory study was carried out in order to make step forward in understanding the physical processes occurring during injection. The aim of this study is to get some idea of injection guidance to avoid particle mobilization; investigation in critical hydraulic gradient was done.

2 One Dimensional Groundwater Model

When fine particles move because of velocity forces, voids are getting clogged and thus permeability decreases with time. For water injection methods, it is important to operate with a flow rate where clogging doesn`t occur for a preferably long time.

2.1 Materials and Method

In the laboratory a cylindrical column of 100 cm length, and 10 cm diameter were used in order to analyze the particle movement in every 10 cm soil layer. The columns were densely packed with Masa soil, which is a weathered granite soil and typical for the Okayama Prefecture

(western Japan). Before the soil was packed into the column, every 10 cm layer was sieved in order to compare the sieve curves before and after the experiment. The experiments were performed with different hydraulic gradients (i) of 0.2 and 0.3 by the use of a constant pressure head difference Δh, considering darcy flow.

$$Q=-K\frac{\Delta h}{\Delta l}A \quad (1)$$

In order to observe the permeability during the experiment, the outflow was recorded by a balance and a manometer was installed on the column to observe water head changes along the column.

Table 2: Experimental characteristics of test specimen

Test #	Hydraulic gradient i (-)	Saturated permeability coefficient k_s (cm s^{-1})	Void ratio e (-)	Specific gravity G_s (g cm^{-3})
A	0.2	2.8×10^{-3}	0.265	2.46
B	0.3	2.8×10^{-3}	0.273	2.46

Experimental results and discussion

When fine particles move because of velocity forces, voids are getting clogged and thus permeability decreases with time. The experiments were operated until such a permeability decrease could be observed. When almost no flow could be observed, the experiment was stopped and the soil was taken out and separated into the same 10 cm layers as were taken in.

After drying the soil in the oven by 105° C for 24 hours, each soil layer was sieved again in order to compare the sieve curves to the original ones. For test A the particle movement and a clearly difference in the particle distribution curves could be observed within the first 50 cm of the column length. Compared to that, test B showed the most differences up to 30 cm column length. Examples of the particle distribution curves are shown in Figures 3–6. Thus, with increasing hydraulic gradient, clogging occurs more and more near the injection point.

If we look to the hydraulic head changes (Figure 7), after half of the time, the heads show a serious decrease in each manometer up to 50 cm column length. The biggest decrease could be observed at the point of 20 cm, which leads to the statement, that the flow path ways got blocked. However, the decrease doesn't continue, which shows, that the settled particles in that zone got mobilized again.

If Terzaghi's equation for the critical hydraulic gradient (i_c) is applied, for test A and B a gradient of 1.15 results. A comparison of this value to the experimental results for i=0.2 and i=0.3, an assumption that Terzaghi's value seems to be a high estimation. Comparing our results with the critical velocity studies before, it is difficult to evaluate, because the velocity decreased with time, so it cannot be said which particle moved at which time, thus with which velocity.

Regarding to the particle sizes which moved during the experiment, following results could be obtained:

- Masa soil includes a high amount of particles between 0.85 mm and 4.75 mm.
- 10–20 cm (i=0.2): particle sizes between 0.106 mm and 0.25 mm deposited, and between 0.25 mm and

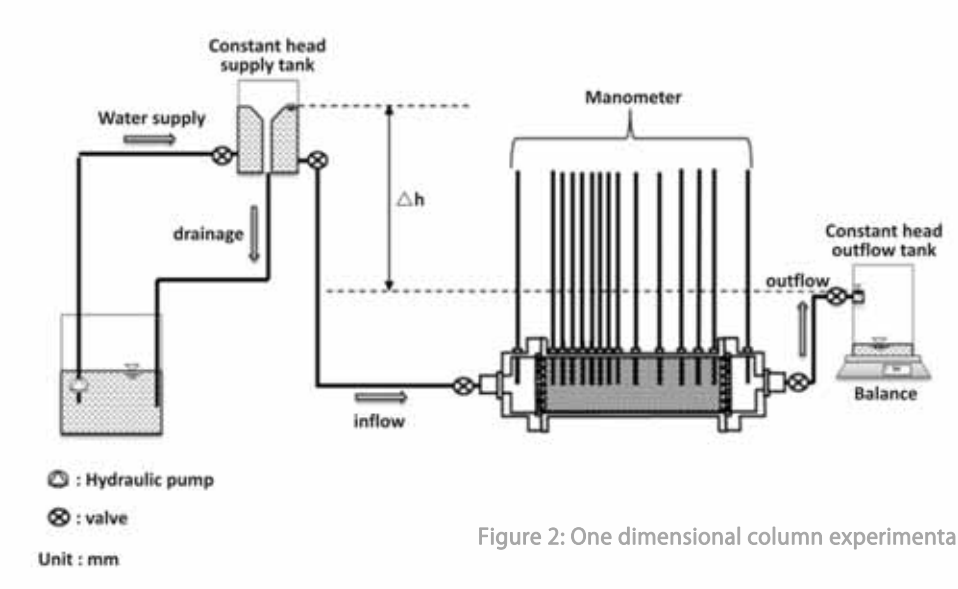

Figure 2: One dimensional column experimental setup

0.85 mm moved forward.

- 30–40 cm (i=0.2): particles below 0.85 mm settled down, particles below 0.106 mm doubled.
- 50–80 cm (i=0.2): deposition of particles below 0.25 mm
- 80–100 cm (i=0.2): almost no observable change in the particle distribution.
- 0–30 cm (i=0.3): movement of particle between 0.85 mm and 2 mm.
- 40–50 cm (i=0.3): particle between 0.25 and 0.85 moved into the next layer.

As for test A and also for test B it can be said that particle between 0.25 mm and 2 mm, against all expectations, are showing the highest moving capacity.

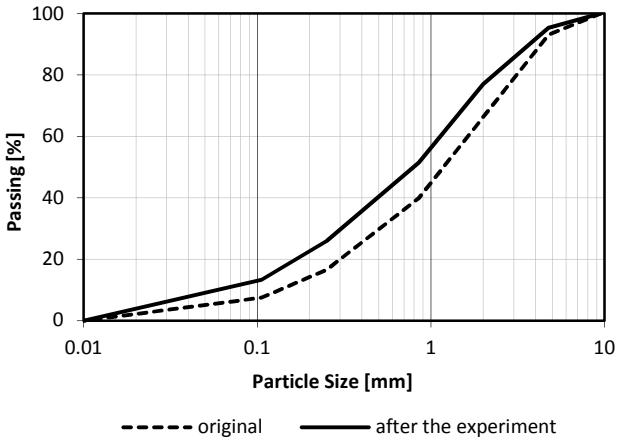

Figure 3: Comparison of soil distribution curves for i=0.2 (3,040 cm)

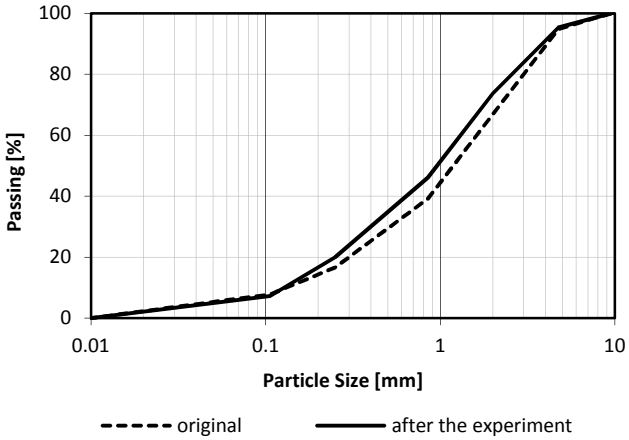

Figure 4: Comparison of soil distribution curves for i=0.2 (50—60 cm)

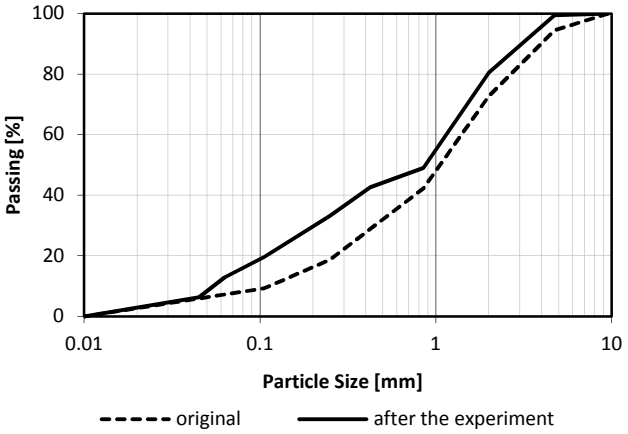

Figure 5: Comparison of soil distribution curves for i=0.3 (10—20 cm)

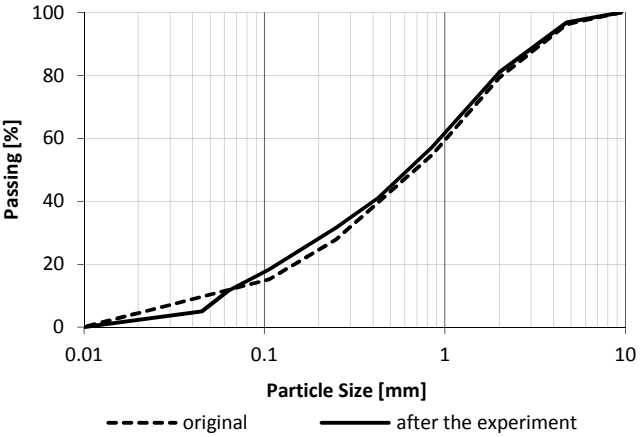

Figure 6: Comparison of soil distribution curves for i=0.3 (60—70 cm)

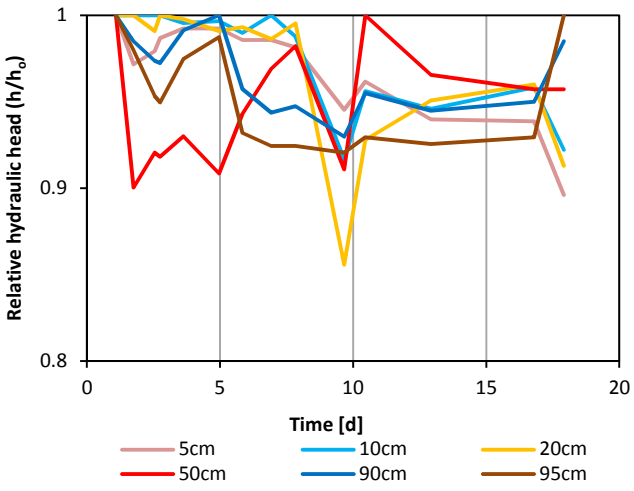

Figure 7: Change of the pressure heads over time at different points of the column length, measured by manometer for i=0.2

3 Axisymmetric Model

One dimensional groundwater models only can give information about flow in x-direction. An axisymmetric aquifer model gives information in radial flow direction, thus it gives more realistic results. An axisymmetric model was constructed to simulate radial groundwater flow away from an injection well.

3.1 Experimental setup and procedure

In order to evaluate the relationship between grain distribution curve and injection flow rate due to clogging, an axisymmetric confined groundwater model was applied. The purpose of this study is to investigate the problem of fine particle movement and determine critical water level rise in the injection well.

The experimental setup is shown in Figure 8. Riversand and Narita- sand (from the Narita region in Tokyo) were used as aquifer material, and as for the aquitard, Masa-soil was utilized. The physical properties of the sands are shown in Table 3. The grain size distribution curves for the aquifer material were changed as shown in Figure 9 and 10. Figure 11 shows the distribution curve for the Masa-soil.

The water level in the injection well- tank was gradually increased until 72 cm (Japanese Geotechnical Society, 2000). This water level was kept constant using a mariotte tank. In order to control the injection flow rate, a mariotte syphon was applied. The experiment was operated with a flow rate of 0.025 cm s^{-1}.

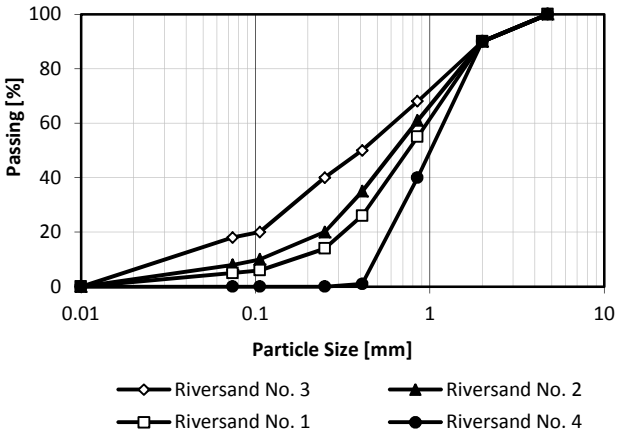

Figure 9: Riversand grain size distribution curves

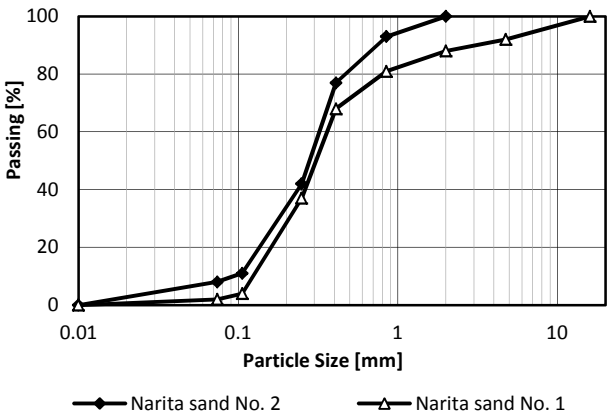

Figure 10: Narita-sand grain size distribution curves

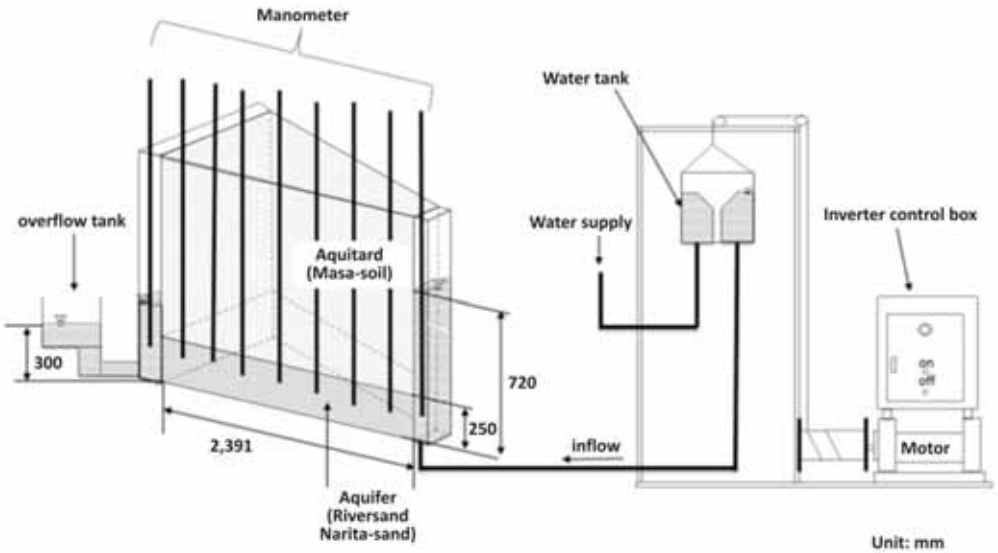

Figure 8: Experimental Setup of the axisymmetric confined groundwater model

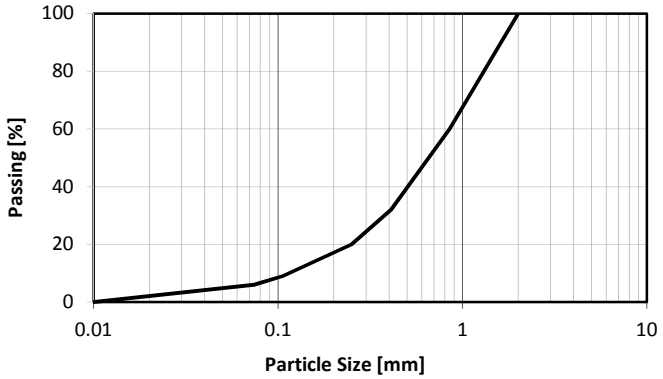

Figure 11: Masa soil grain size distribution curve

Table 3: Physical properties of each soil type used for the experiment

Soil type		Specific gravity (g/cm3)	Porosity (-)	Permeability (cm/s)
Riversand	No.1	2.69	0.5	7.46×10^{-2}
	No.2	2.69	0.5	4.50×10^{-2}
	No.3	2.69	0.5	3.08×10^{-2}
	No.4	2.69	0.5	4.50×10^{-1}
Narita-sand	No.1	2.72	0.7	2.25×10^{-2}
	No.2	2.72	0.7	3.02×10^{-2}
Masa-soil		2.65	0.42	4.83×10^{-6}

3.2 Permeability and hydrological gradient calculation

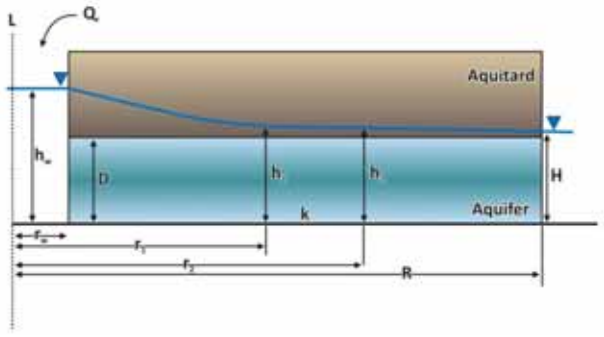

Figure 12: Axisymmteric confined aquifer model

The fundamental Equation of groundwater movement in a confined aquifer can be expressed as (Figure 12):

$$Q_r=-2\pi rDk\left(\frac{\partial h}{\partial r}\right) \quad (2)$$

With Q_r as the injection flow rate (L^3/T), D is the aquifer thickness (L), k as permeability coefficient of the aquifer material (L/T), h as the total head (L) and r as the range of influence in radial direction (L).

Regarding to flow between two points (Figure 5)

($r_1 \leqq r \leqq r_2$) , Equation 1 can be written as

$$\ln\left(\frac{r_2}{r_1}\right)=-\frac{2\pi Dk}{Qr}\left(h_2-h_1\right) \quad (3)$$

Solving Equation 2 for permeability (k) follows in

$$k=\frac{-Qr}{2\pi D}\frac{\ln\left(\frac{r_2}{r_1}\right)}{\left(h_2-h_1\right)} \quad (4)$$

or solving for flow rate (Q_r)

$$Q_r=\frac{-2\pi Dk\left(h_2-h_1\right)}{\ln\left(\frac{r_2}{r_1}\right)} \quad (5\}$$

Substituting Equation 4 in Equation 1, it follows

$$i=\left(\frac{\partial h}{\partial r}\right)=\frac{-\left(h_2-h_1\right)}{\ln\left(\frac{r_2}{r_1}\right)}\left(\frac{1}{r}\right) \quad (6)$$

3.3 Experimental results and discussion

During the experiment the flow decreased about 17%, when the material included fine particles below 0.42 mm (Riversand No.4). This result states that no clogging occurs. If the material includes 20% of fine particles below 0.104 mm (Riversand No.3), the injection flow decreased about 80%. With regard to Narita-sand, it was observed that if the amount of fine particles increases, the rate of diminution of flow rate also increases.

Regarding the area where permeability reduction took place, the relations between hydraulic gradient and permeability are shown in Figure 13–16 for Riversand and Figures 17 and 18 for Narita-sand. The shaded parts in the graphs indicate the above mentioned relation between hydraulic gradient and permeability in the area of flow rate reduction. The unshaded areas in the graphs represent the relation between hydraulic gradient and permeability, outside the area of permeability reduction at the end of the experiment.

From the graphs, a relation between hydraulic gradient (i) and permeability (k) can be obtained (Mulqueen, 2005).

$$k=ai^{-b} \quad (7)$$

with a and b as constants.

Values and the coefficients a, b from Equation 6 of each sample, correlation coefficients between the measured values (R^2), and the smallest hydraulic gradient (i_{min}) at the starting point of permeability reduction (Figure 13–18) are summarized in Table 4. From Table 4 it can be confirmed, that a minimum hydraulic gradient exists at the starting point of permeability reduction.

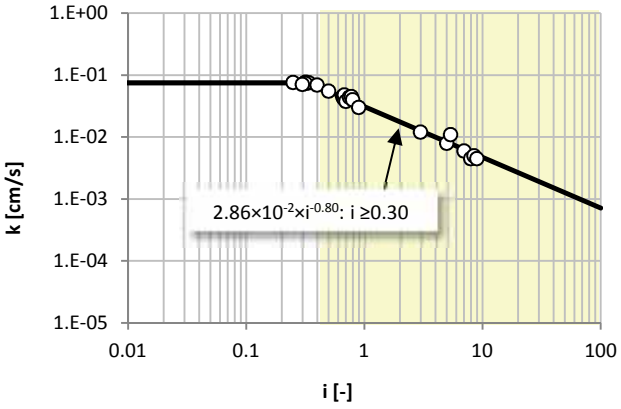

Figure 13: Relation between permeability (k) and hydraulic gradient (i) for Riversand No. 1

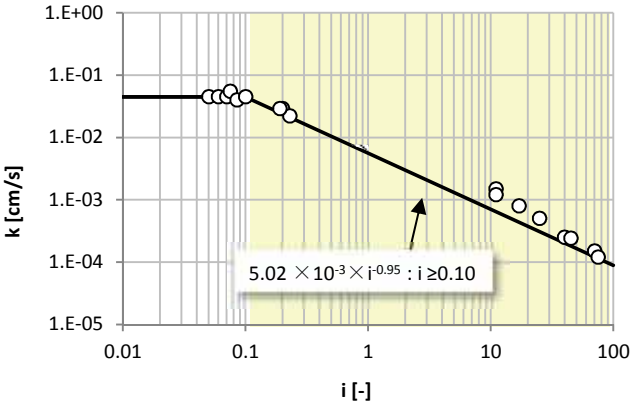

Figure 14: Relation between permeability (k) and hydraulic gradient (i) for Riversand No. 1

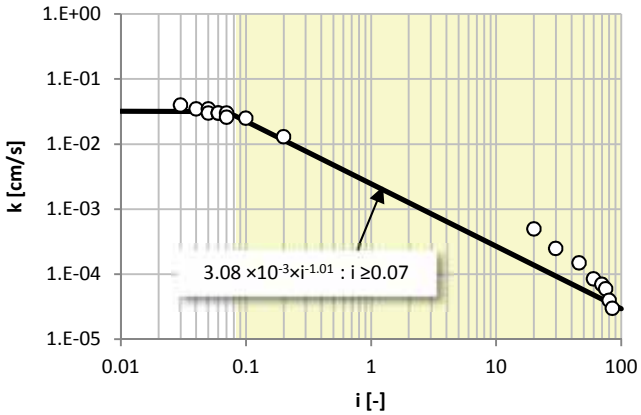

Figure 15: Relation between permeability (k) and hydraulic gradient (i) for Riversand No. 3

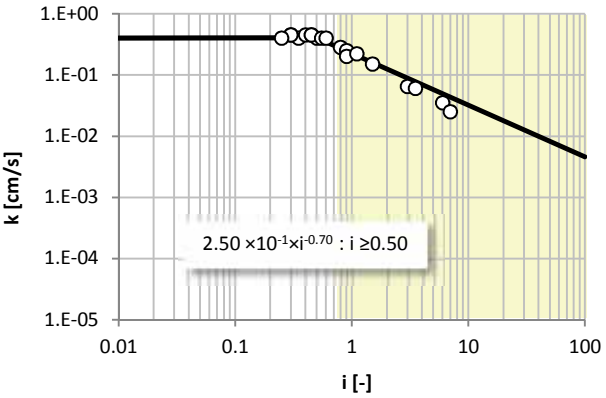

Figure 16: Relation between permeability (k) and hydraulic gradient (i) for Riversand No. 4

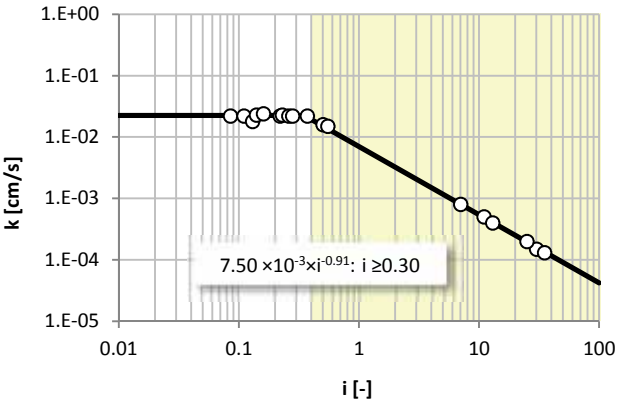

Figure 17: Relation between permeability (k) and hydraulic gradient (i) for Narita-sand No. 1

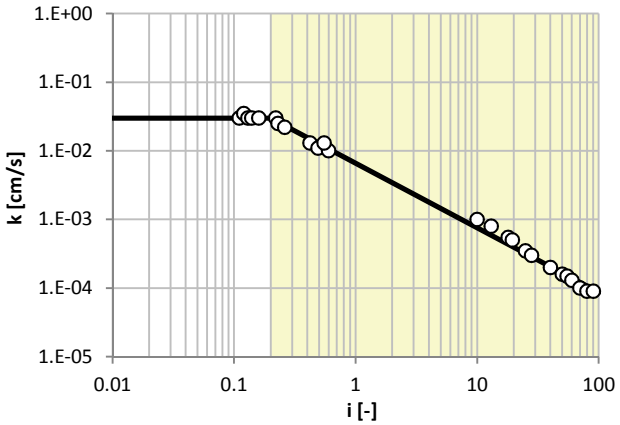

Figure 18: Relation between permeability (k) and hydraulic gradient (i) for Narita-sand No. 2

Table 4: Experimental results and determined values of Equation 7

Soil type	a (cm s^{-1})	b	R^2	k_0 (cm s^{-1})	i_{min}
Riversand					
No.1	2.86×10^{-2}	0.8	0.97	7.46×10^{-2}	0.3
No.2	5.02×10^{-3}	0.95	0.98	4.50×10^{-2}	0.10
No.3	3.08×10^{-3}	1.01	0.87	3.08×10^{-2}	0.07
No.4	2.50×10^{-1}	0.7	0.96	4.50×10^{-1}	0.50
Narita- sand					
No.1	7.50×10^{-3}	0.91	0.99	2.25×10^{-2}	0.30
No.2	6.59×10^{-3}	0.94	0.99	3.02×10^{-2}	0.20

Figure 19 shows the relation between hydraulic gradient and the materials which include grain sizes below 0.104 mm. From this graph it can be concluded, that clogging because of fine particle movement occurs when the hydraulic gradient is below 0.3.

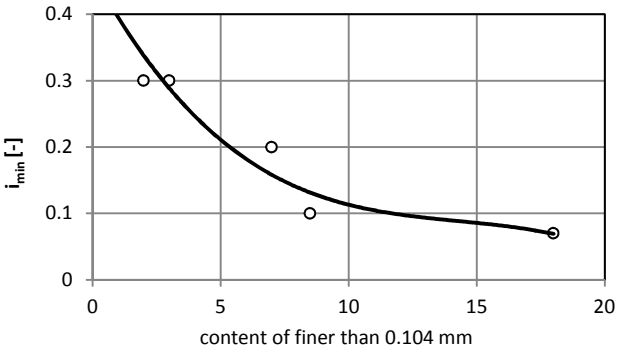

Figure 19: Relation between minimal hydraulic gradient and soil content finer than 0.104 mm

4 Conclusion

In this study a one dimensional and an axisymmetric aquifer model were used in order to define the critical hydraulic gradient during injection of water. First of all, the study showed, that also mobilization of fine particles initially present in the aquifer take into account for physical clogging. Furthermore, the mobilization velocity or critical hydraulic gradient can be a used as guidance for reverse pumping in order to unclog the aquifer. In the one-dimensional experiments, the results showed, that not only fine particles are (≦0.106 mm) are mobilized during injection, but also particles between 0.25–2 mm showed a movement. Especially for the higher hydraulic gradient (i=0.3) bigger particle sizes were mobilized. Furthermore, after Darcy`s law (Equation 1), with increasing hydraulic gradient, the velocity of injected water will increase. Thus, when the hydraulic gradient will be too high then the following high velocity causes a fast movement of particles what finally results in an accumulation of particles near the injection point. This was also observed in present experiments. In the axisymmetric experiment a critical hydraulic gradient could be determined to be 0.3 if the soil includes particle sizes below 0.104 mm. If Terzaghi's law will be applied, then the critical hydraulic gradient will be as for the Masa-soil 1.15, Narita-sand 1.01 and for the Riversand 1.13. These values lead to the statement that for clogging problems Terzaghi's equation gives a too high critical hydraulic gradient. A comparison of the critical hydraulic velocity between the axisymmetric experiment and previous studies is shown in Figure 20.

From Figure 20 it can be seen, that the experimental results show a good fit with other studies except Justin's equation. Thus, Justin's equation leads to an overestimation of the critical velocity, even when the safety factor of 4 will be applied. In contrast to that Ohno's equation seems to be more applicable even for physical clogging problems.

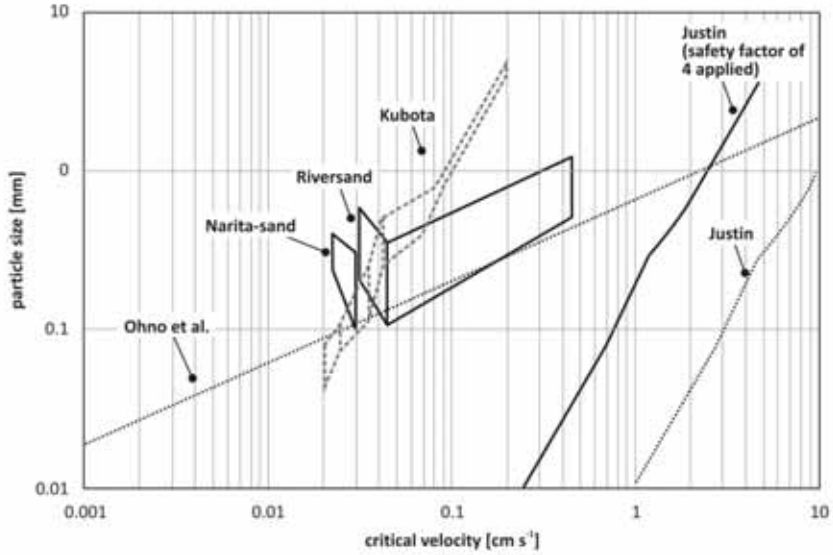

Figure 20: Comparison of experimental results and previous studies on critical velocity regarding to particle size

For further research it has to be considered, that not only physical problems leads to clogging, also biological and chemical causes have to be included as well as suspended materials in the injection water. In order to apply a critical hydraulic gradient for field application in artificial recharge, a field test method for critical hydraulic gradient determination is necessary. Artificial recharge should be made more practicable with cheap and easy methods to maintain for applying also in developing countries.

References

Ahfir, N.D., Benamar, A., Alem, A., and Wang, H.Q., (2009) Influence of Internal Structure and Medium Length on Transport and Deposition of Suspended Particles A Laboratory Study. Transport in Porous Media, Springer Netherlands 76(2): 289–307.

Bichara, A.F., (1986) Clogging of recharge wells by suspended solids. J. of Irrigation and Drainage Eng, 112(3): 210–224.

Bichara, A.F., (1988) Redevelopment of clogged recharge wells. J. of Irrigation and Drainage Eng,. 114(2): 343–350.

Bouwer, H., (2002) Artificial recharge of groundwater: Hydrogeology and engineering. Hydrogeol., J. , 10 (1): 121–142.

Dillon, P., Pavelic, P., Massmann, G., Barry, K., and Correll, R., (2001) Enhancement of the Membrane Filtration Index (MFI) Method for Determining the Clogging Potential of Turbid Urban Stormwater and Reclaimed Water Used for Aquifer Storage and Recovery. Desalination 140 (2): 153–165.

Herzig, J.P., Leclerc, D.M., and Le Goff, P., (1970) Flow of suspensions through porous media. Application to deep filtration. Industrial and Eng. Chemistry, 62(5): 8–35.

Hijnen, W.A.M., and Van der Koou, D., (1992) The Effect of Low Concentrations of Assimilable Organic Carbon (AOC) in Water on Biological Clogging of Sand Beds. Water. Research 26 (7): 963–972.

Holländer, H.M., Boochs, P. W., Billib, M., and Panda, S.N., (2005) Laboratory experiments to investigate clogging effects in aquifers. Grundwasser, vol. 10, issue 4: 205–215. (in German)

Japanese Geotechnical Society, (1965) Handbook of soil mechanics and foundation engineering, Tokyo, Japanese Geotechnical Society: 93. (in Japanese)

Japanese Geotechnical Society, (1982) Handbook of soil mechanics and foundation engineering, Tokyo, Japanese Geotechnical Society: 1222–1223. (in Japanese)

Japanese Geotechnical Society, (2000) Geotechnical methods and explanations: 342.

Justin, J.D., (1924) The Design of Earth Dams. Transactions of the American Society of Civil Engineers, Vol. LXXXVIII, No. 1: 1–61.

McDowell-Boyer, L.M., Hunt, J.R. and Sitar, N., (1986) Particle Transport through Porous Media. Water Resources Research 22 (13): 1901–1921. doi:10.1029/WR022i013p01901.

Moghadasi, J., Müller-Steinhagen, H., Jamialahmadi, M., and Sharif, A., (2004) Theoretical and experimental study of particle movement and deposition in porous media during water injection. J. Petrol. Sci. Eng. 43: 163–181.

Ohno, M., Yamazaki, H., and Tran Duc, P.O., (1984) Experimental Study of piping property of sand, Report of HAZAMA: 33-40. (in Japanese)

Olsthoorn, T.N., (1982) The Clogging of Recharge Wells, Main Subjects. Keuringsinstituut voor Waterleiding Artikelen, KIWA.

Pérez-Paricio, A., (2000) Integrated modeling of clogging processes in artificial groundwater recharge. Ph.D. Thesis Department of Geotechnical Engineering & Geosciences, Technical University of Catalonia (UPC).

Reddi, L.N., Ming, X., Hajra, M.G., and Leel, M., (2000) Permeability reduction of soil filters due to physical clogging. J. Geotech. Geoenviron. Eng., 126(3): 236–246.

Terzaghi, K., (1922) Der Grundbruch an Stauwerken und seineVerhütung. Die Wasserkraft, Vol. 17, No. 24: 445–449. (in German) (Includes English translation : Piping in Dams and Its Prevention;)

Terzaghi, K., Peck, R.B., and Mesri, G., (1996) Soil Mechanics in Engineering Practice, 3rd ed., McGraw Hill, New York, NY, USA. p. 85–87.

Characklis, W.G., Trulear, M.G., Bryers, J.D., and Zelver, N., (1982) Dynamics of biofilm processes: methods. Water Research 16: 1207–1216.

Vigneswaran, S., and Thiyagaram, M., (1984) Application of Filtration Theories to. Ground Water Recharge Problems, Journal of Air and Soil Pollution, U.S.A., Vol. 22: 417–428.

Vigneswaran, S., Jeyaseelan, S., and Das Gupta, S., (1985) A Pilot-Scale Investigation of Particle Retention During Artificial Recharge , Water, Air, and Soil Pollution, 25: 1–13.

Ye, X., Du, X., Li, S., and Yang, Y., (2010) Study on Clogging Mechanism and Control Methods of Artificial Recharge. In 2010 International Conference on Challenges in Environmental Science and Computer Engineering (CESCE), 2:29–32.

Contact Details

Email: claudia_hartwig@gmx.net

CLOGGING ASSOCIATED WITH INFILTRATION BASINS

Soil Clogging Phenomena in Vertical Flow

A. Benamar
LOMC UMR 6294 CNRS-Université du Havre, Franc

Abstract

Particle movement and deposition are known to be serious problems for filtration systems. Dramatic reductions in filter permeability are observed in such cases as consequence of deposition of fine particles transported by fluid in the porous media. Accumulation and deposition of suspended solids in porous media can ultimately lead to clogging. The main purpose of this paper is to assess some relations governing filtration behaviour. Packed sand columns were used to investigate soil clogging, focusing on the questions of identification and the description of porosity damage. Some laboratory filtration tests were carried out using various granular sizes of filters and changes in soil water retention, pore size distribution, and saturated hydraulic conductivity due particle deposition were investigated. The results obtained show that filtration and likely clogging depend on particle concentration and flow conditions. The research results clearly show under what conditions soil clogging occurs and how to mitigate this problem. This potential for clogging has been expressed in terms of soil-type parameters used in soil physics, such as a pore damage index, which gives engineers and geo-hydrologists a tool to assess the potential for clogging in a specific soil condition. Maximum clogging occurs mainly in the upper lay of the bed and is dependent on the suspension concentration, pore structure and flow rate.

1 Introduction

Permeability reduction caused by particle deposition (physical clogging) in porous media is important in filter beds. Soil filters, which are commonly used to provide stability and drainage in dams and dykes, are prone to long-term accumulation of fine micron-sized particles. This causes reduction in the permeability, which in turn may lead to intolerable decreases in their drainage capacity and uplift pressures in the core. Soil bed layers operating as filters are also prone to clogging since the flow involves suspended particles. The operation of deep-bed filters for water treatment is constrained by the available head loss. In natural aquifers, controlling permeability is essential for the operation of injection or extraction wells and in quantifying contaminant mobility (Kretzschmar et al., 1999). Clogging is relevant to enhanced bioremediation, since microbial growth alters flow and transport. The flow of suspended particles through a filter is a complex phenomenon owing to define two mechanisms in deep filtration: a mechanical filtration for large particles and a physicochemical filtration for small particles (Herzig et al., 1970). When flowing through porous medium, the particles are brought in contact with retention sites; they stop there or are carried away by the stream. The deep filtration is therefore the result of several mechanisms: the contacting of particles with the retention sites, the fixing of particles on sites, and eventually the breaking away of previously retained particles.

During the flow of suspended particles through a porous medium, particle transport and retention derived from several forces and mechanisms depending on particle size, pore distribution and flow rate (Ahfir et al., 2009), (Benamar et al., 2007), (Silliman et al., 1995). The particle retention may reduce the permeability of the porous medium as observed during the artificial recharge of aquifers or the exploitation of oil wells (Moghadasi et al., 2004). The flow results obtained by Khilar et al. (1987) elucidate the interaction of colloid chemistry and hydrodynamics in entrapment and release of fine particles. They do not distinguish between size distributions of particles in suspension, and assume that

particle trapping does not occur until the concentration of clay particles in suspension reaches a certain threshold value. The release occurs below a critical salt concentration and above a critical flow velocity. The capture of fines at the pore constrictions is partly due to direct interception and partly due to size exclusion. Several studies have noted that, for a given mass of deposited material, experiments conducted at greater fluid velocity show greater permeability (Mays et al., 2005). Previous researchers have recognized the importance of deposit morphology during long-term particle retention in saturated porous media. The different mechanisms leading to permeability damages due to particle deposition were analysed under various situations by Chauveteau et al. (1998). They noted the influence of hydrodynamic forces and the effects of the location where the particles are deposited on permeability. Recent researches indicate that the rate of particle straining within saturated porous media is sensitive to the ratio of particle diameter (dp) to sand-grain diameter (dg), the shape of surface roughness of the solid matrix, particle size non uniformity, pore-scale hydrodynamics and pore water chemistry (Bradford et al., 2007), (Xu et al., 2006), (Xu et al., 2009), (Porubcan et al., 2011). The flow of suspended particles through a filter is a process owing to define two mechanisms in deep filtration: a mechanical filtration for large particles and a physicochemical filtration for small particles. When flowing through porous medium, the particles are brought in contact with retention sites; they stop there or are carried away by the stream. The deep filtration is therefore the result of several mechanisms: the contacting of particles with the retention sites, the fixing of particles on sites, and eventually the breaking away of previously retained particles. The capture of fines at the pore constrictions is partly due to direct interception and partly due to size exclusion (Benamar et al., 2007). Previous researchers have recognized the importance of deposit morphology during long-term particle retention in saturated porous media. The physicochemical filtration of colloidal particles in saturated porous media was studied by Tufenkji et al. (2004) and a new equation for predicting the single-collector contact efficiency is presented. The correlation equation is developed using the sum of the contributions of the transport mechanisms.

This work identifies the main phenomena that control the transport and deposition of clay particles in a sand core and likely clogging. The reduction in the vertical permeability as a result of clogging has been analysed. Under constant flow conditions, clogging is observed through a head loss and the amount of deposited particles. An experimental investigation was undertaken to look into the possible causes of permeability damage and clogging. Sand and glass beds were used to study the general behaviour of fine particles movement and deposition in porous media. The experiments were firstly conducted with constant flow rate and secondly with fixed head condition. An investigation was used to quantify the amount of particles retained in the medium.

2 Description of filtration test

In general, the experiments performed in order to investigate the soil filtration mainly fall in two categories: those using slurry of fine soil forced against the filter by high pressure water, or those having the fine soil compacted against the filter and often simulating the formation of a crack by a pinhole through the base soil.

The results reported here are dealing with the first category of laboratory experiments (Figure 1). Fine particles (kaolinite clay) and several filter grain sizes are used. Laboratory flow tests were performed in a vertical column under constant flow conditions in the first part and under constant head conditions in the second part. The column is 400 mm length and 40 mm diameter and packed in 5 cm increment by pouring the material (sand) into the pre-filled column with fresh water. Six piezometers are installed along the column in order to carry out the permeability reduction during the filtration tests. The column is fed by two reservoirs containing degassed water (pH of 6.8) and suspended particles, using a peristaltic pump (for tests under constant flow rate). As the porous medium is saturated the flow toward the column is switched to particle suspension. Figure 1 shows the configuration of the experimental device under constant flow conditions. The detection system consists of a Fisher Instrument turbidity meter which determines the turbidity level by measuring the amount of light scattered at 90° by the suspended particles. The particle concentrations in the effluent were determined with the help of correlations made a priori between suspended

particles concentrations in water and turbidity. Various size distributions of silica sand and glass beads are used as porous media, whose average diameter D50 ranges from 0.23 to 2.7 mm. The porosity obtained is close to 36%, except the coarser sand which presents a porosity of 40%. Suspended particles used are kaolinite clay whose 90 % of particles are finer than 10 µm and D50 close to 1.2 µm. These clay particles are used because of their small size and their less-dispersive properties and low electrochemical activity. Different concentrations of suspended particles are used and particle retention is determined through the concentration reduction at the outlet of the column. After each test, the soil sample is extracted carefully from the column in slices and analysed to determine the mass particle retained during filtration at a given location from the top of the column. In further experiment using a prismatic cell made of aluminium and equipped with ultrasonic sensors (Tran et al., 2012), the distribution of particles (silt) retained along the cell was also addressed. During these experiments, the main operating parameters, i.e. particle concentration, flow rate (either water head) and soil filter were systematically varied.

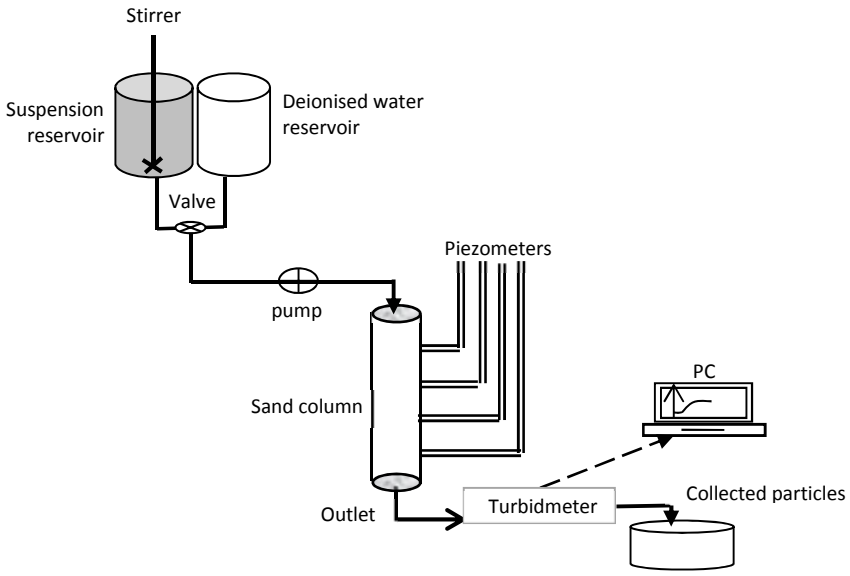

Figure 1: Drawing of experimental set-up

3 Results and modification of pore structure

3.1 Induced permeability reduction

The filter permeability reduction caused by the in-depth retention of small particles is analysed. This analysis leads to the definition of deposition kinetics in the soil filter, which depends on both the flow rate and the mechanism determining permeability damage. As a consequence of deep-bed filtration process, fluid pressure (measured through water head) increases when flow rate is taken constant. Pressure increase concerns the top part of the filter (first 4 cm), and hydraulic gradient increases strongly in this first part, reaching a value of 10 times the initial value after a flowing time more than 5 hours. The pressure evolution along the filter shows that the major clogging occurs at the front of the filter and even at high particle concentration the filter reminds operating without large increase of pressure. Maximum clogging occurs only in the upper lay of the bed and is dependent on the suspension concentration, pore structure and flow rate (or water head). During filtration tests at constant head, the uplift pressure measured is higher than those obtained from constant flow rate tests, particularly at the

front filter. The reduction of permeability of the filters is shown on Figure 2 and data indicate exponential depth dependence of particle accumulation.

The flow rate has a considerable influence on the permeability reduction in the first layer of the soil filter. Figure 2 shows the variation of the relative permeability in the upstream part of the filter with a several decrease during the first step (until 10 pore volumes of injected suspension), particularly for the lowest flow velocity. As flow rate decreases, permeability reduction increases, showing the effect of particle velocity in the filtration process. For the lowest flow rate, important particles deposition occurs at the front column, and a drastic permeability reduction operates early and then the filter remain clogged. For higher flow rate the permeability reduction operates progressively. This reduction, inversely proportional to the flow rate, is nonlinear, describing an exponential permeability reduction. The dependence of clogging process on flow rate suggests that fluid velocity controls mainly deposit morphology, rather than the depth of particle penetration. From permeability reduction and the relative concentration measured at the outlet, the clogging occurs when C/C0 > 0.2 and k/k0 <0.3.

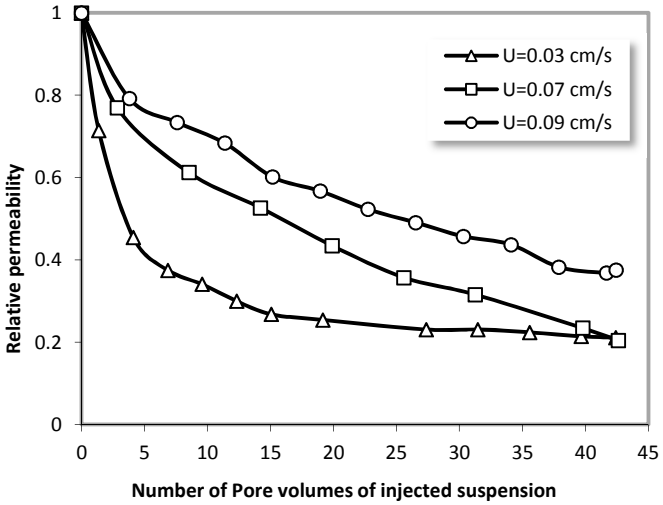

Figure 2: Influence of flow velocity on local permeability reduction of fine sand (El Kawafi, 2010)

3.2 Deposit distribution in clogging filters: depth dependent filtration.

Filtration theory predicts an exponential distribution of particles only in the initial phase of deposition, but an exponential deposit is more realistic than a uniform deposit. All the available data indicate no uniform particle distribution, even for low particle concentration. After each test, the soil sample is extracted carefully from the column in layers and analysed to determine the mass particle retained during filtration at a given location from the top of the column. The variation of filter porosity is then deduced layer by layer. Figure 3 shows the measured porosity distribution using grain size distribution of collected soil layers after the test accomplished. The porosity reduction in the soil filter along the column is dependent on the concentration of the injected suspension. Particle deposit distribution seems to be exponential and the porosity reduction operates mainly in the upstream part (first 10 cm) of the soil filter, leading to the drastic permeability reduction (Figure 2) and thus clogging. The decrease is mainly observed at the entrance of the column and the downward part is not affected by particle deposition. The stronger decrease of porosity reaches more than 10% when using a concentration of 5g/l. The depth of particle penetration is important because clogging is non-linear with mass deposit. Other things being equal, a filter with a double mass deposit in the top half and zero in the bottom half will be less permeable (and ultimately clogged) than a filter with a simple mass deposit throughout. If comparing between results obtained with two different materials (sand with angular shape and glass beads with rounded shape), for the inlet concentration of 2g/l, the maximum reduction of porosity was respectively 10% and 6%, indicating that sand is more favourable to clogging than glass beads. This result leads to an extended conclusion that grains of angular shape provide more likelihood clogging than grains of rounded shape. This result was already provided (Benamar et al., 2007) as attachment occurrence of suspended particles within two different porous media (sand and glass beads). Indeed, the effect of packing was causing lower porosity in sand and so lower permeability. The weak connectivity between pores was then leading to more occurrence of particle trapping. During transport of suspended particles in a porous medium with angular shape of grains, the narrow pores created by column

packing contribute to more particles trapping and then influence clogging. The deposition rate is larger in gravel because of the wide range pore distribution in this medium where many retention sites participate in particle trapping. It is known that the distinction in terms of conductance and storage in the respective pore domain are characterized by the fact that: macro-pores are primary flow paths where both dispersion and advection are prevalent; meso-pores are intermediate flow paths where advection becomes dominant; micro-pores are supplemental flow paths and mass storage spaces where only diffusive flow is manifested.

The correlation between porosity and permeability was achieved by using Kozeny-Carman equation. The permeability values along the sample were then derived from the results of Figure 3 and the permeability reduction is presented on Figure 4. A drastic reduction of permeability was occurred in the front of the filter and the maximum permeability reduction (80 % to 90%) is close to that encountered with other materials. Note that in the experiment using ultrasonic characterization no measured permeability was available. So, correlation between porosity reduction and permeability reduction was achieved using Kozeny-Carman relation.

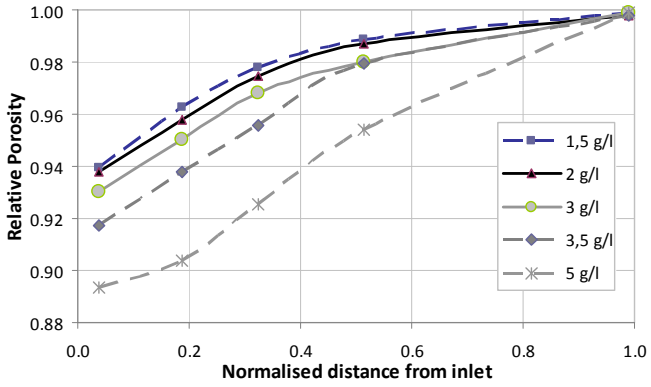

Figure 3: Porosity reduction from particle deposit along the soil filter (Tan et al., 2012)

3.3 Size selection of clogging particles

After each test, the soil sample is extracted carefully from the column in slices and analysed to determine the mass particle retained during filtration, and the size distribution of filtered particles. Figure 5 below shows the granular distribution of particles retained within each slice. The examination of such curves through Figure 5 suggests that coarser particles are retained within the first slice (filter front), and the mean size of trapped particles decreases along the filter. This result corroborates the particle size selection deduced from the outlet analysis. This process of "self-filtering" is known for fine soils. Some erosion occurs from the base soil into the filter thereby modifying the grading of the filter which prevents any further movement from the base soil.

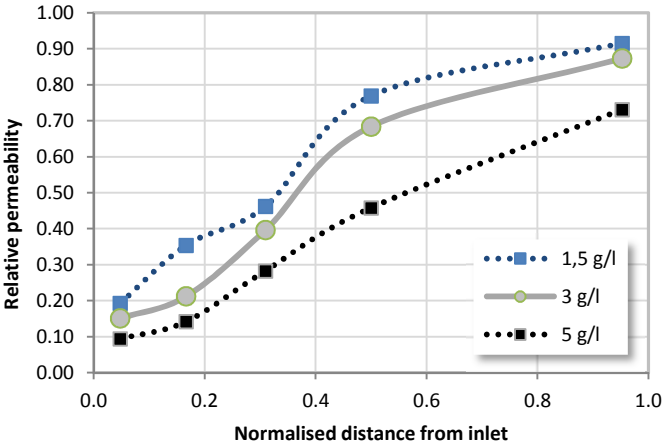

Figure 4: Permeability reduction along the filter (glass beads) using Kozeny-Carman correlation

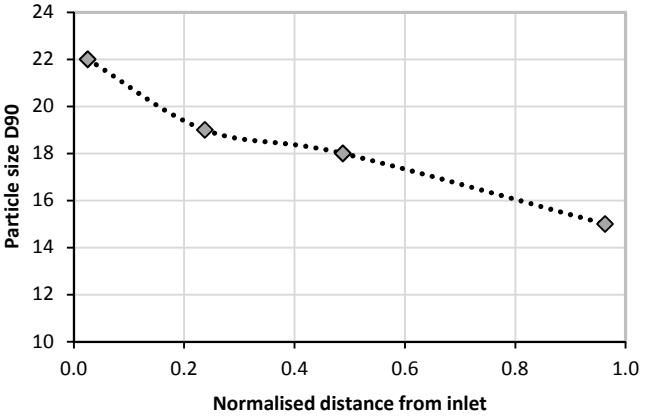

Figure 5: Variation of trapped particles size along the column (Inlet particle size: 22 µm)

These results indicate that the largest particles are trapped within the front (first two centimetres) of the filter and then particles of same size are retained over the following sections. This process, called self-filtration, contributes to the development of clogging by formation of a "cake" in the front of the filter sample. The kinetics of clogging occurrence depend on the ratio of size (D90) flowing particles and filter opening (suggested being D15

by dams designers), the flow conditions (constant head water favours clogging) and the particle concentration.

It was known from literature (Bradford et al., 2007; Porubcan et al., 2011; Xu et al., 2006; 2009) that the rate of particle straining within saturated porous media is sensitive to the ratio of particle diameter dp to sand-grain diameter dg, and usual filtration criteria involve this ratio. Several models were also developed to predict the mechanical blockage (straining) of the particles flowing through a porous medium. (Bradford et al., 2006) showed that the straining rate coefficient was related to the ratio of particle diameter and the median sand grain size through a power function. (Xu et al., 2006) suggested that the mechanical blockage may be important when the ratio of the mass-averaged diameter dg50 (50% of mass finer than grain diameter) of the porous medium and the particle diameter dp is lower than 120.5 when using particles of same size, while (Bradford et al., 2004) proposed the value 200 for the ratio dg50/dp. Size non uniformity can have also a significant impact on straining kinetics: the straining of smaller particles was enhanced by the presence of larger particles due to the blockage of pore opening by the larger particles while the straining of larger particles was reduced by the smaller particles primarily due to the faster depletion of straining capacities (Xu et al., 2006).

It is usual in soil filter design to express the filter criteria through the opening filter size and the maximum particle size. In order to address the suitability of such criterion of mechanical straining, the ratio dg50/dp(50) and dg50/dp(90) of the finest filter were derived. The values are respectively 25.5 and 10.5. If considering the ratio of 120 (obtained in laboratory as being the lower one below which mechanical straining occurs) as a limit value, the mechanical straining so operates widely.

4 Conclusions

The filtration results obtained show that filtration and clogging depend on concentration and flow conditions. Experiments conducted with a constant hydraulic head show more occurrence of clogging than experiments carried out with a constant flow rate. For a given mass of deposited particles, experiments conducted at greater fluid velocity or water head show greater permeability. Experimental data indicate exponential depth dependence of particle accumulation, which is in agreement with literature. The usual filter design criteria used for the soil filters tested show that fine filters can fail according to the geometric considerations. The results obtained show that filtration and clogging depend on concentration and flow rate. For a given mass of deposited particles, experiments conducted at greater fluid velocity show greater permeability. The investigation of clogging magnitude in the porous medium indicates that maximum clogging occurs only in the upstream layer of the bed and is dependent on the suspension concentration, pore structure and flow rate. The use of ultrasonic sensors to derive the clogging distribution along the test column shows a good achievement of such process. The grain size analysis of retained particles within the filter indicates that the largest particles are trapped within the front (first few centimetres) of the filter and then particles of same size are retained over the following sections. This process, called self-filtration, contributes to the development of clogging by formation of a "cake" in the front of the filter sample.

References

Ahfir, N.D., Benamar, A., Alem, A., Wang, H.Q., (2009) Influence of Internal Structure and Medium Length on Transport and Deposition of Suspended Particles: A Laboratory Study, Transp. in Porous Media 76, 289–307

Benamar, A., Ahfir, N., Wang, H.Q., and Alem, A., (2007) Particle transport in a saturated porous medium: pore structure effects, C.R.Géosciences 339, 674–681.

Bradford, S.A., Bettahar, M., Simunek, J., van Genuchten, M.Th., (2004) Straining and attachment of colloids in physically heterogeneous porous media. Vadose Zone Journal 3:384–394.

Bradford, S.A., and Bettahar, M., (2006) Concentration dependent transport of colloids in saturated porous media. Journal of Contaminant Hydrology, 82, 99– 117

Bradford, S.A, Torkzaban, S., and Walter, S.L., (2007) Coupling of physical and chemical mechanisms of colloid straining in saturated porous media, Water res. 41, 3012–3024

Chauveteau, G., Nabzar, L., and Coste, P-J., (1998) Physics and modeling of permeability damage induced by

particle deposition. Society of Petroleum Engineers, SPE 39463, 409–419.

El Kawafi, A., (2010) Colmatage d'un milieu poreux saturé soumis à un écoulement chargé de particules. Thèse de Doctorat, université du Havre

Khilar, K.C.,and Fogler H.S., (1987) Colloidally induced fines in porous media, Review in chemical engineering, vol. 4 N° 1& 2

Kretzschmar, R., and Borkovec, M., (1999) Grolimund, D.; Elimelech, M. Mobile subsurface colloids and their role in contaminant transport. Adv. Agron., 66, 121–193.

Mays, D.C., and Hunt, J.R., (2005) Hydrodynamic aspects of particle clogging in porous media, Environ. Sci. Technol., N° 39, pp. 577–584.

Moghadasi, J., Jamialahmadi, M., and Sharif, A., (2004) «Theoretical and experimental study of particle movement and deposition in porous media during water injection», Journal of Petroleum Science and Engineering, vol. 43, 2004, 163–181.

Nabzar, L., and Chauveteau, G., (1997) Permeability damage by deposition of colloidal particles. Society of Petroleum Engineers, SPE 38160. 161–171.

Porubcan, Alexis A., and Xu, S.P., (2011) Colloid straining within saturated heterogeneous porous media, water Research 45 (2011) 1796–1806

Silliman, S.E., (1995) Particle transport through two-dimensional, saturated porous media: influence of physical structure of the medium, Hydrology J., Vol. 167, pp 79–98.

Tran, D.H., Derible, S., Franklin, H., Benamar, A., and Wang, H., (2012) Ultrasonic measurements of particle retention by a porous medium, Ultrasonics 52, pp. 62-68.

Tufenkji, N.G.F., Miller, J.N., Ryan, R.W., Hervey, M., and Elimelech, (2004) Transport of Cryptosporidium Oocysts in porous media: Role of straining and physicochemical filtration. Environ. Sci. Technol. 38: 5932–5938

Xu, S.P., Gao, B., and Saiers, J.E., (2006) Straining of colloidal particles in saturated in porous media; Water Resources Research, VOL.42, doi:10.1029/2006 WR004948,2006

Xu, S.P., and Saiers, J.E., (2009) Colloid straining within water-saturated porous media : effect of colloid size nonuniformity, Water Resources Res. 45, W05501, doi:10.1029/2008WR007258

Contact Details

Email: benamar@univ-lehavre.fr

Evaluation of Potential Gas Clogging Associated with Managed Aquifer Recharge from a Spreading Basin, Southwestern Utah, USA

V.M. Heilweil and T.M. Marston
U.S. Geological Survey, 2329 Orton Circle, Salt Lake City, Utah 84119

Summary

Sand Hollow Reservoir in southwestern Utah, USA, is operated for both surface-water storage and managed aquifer recharge via infiltration from surface basin spreading to the underlying Navajo Sandstone. The total volume of estimated recharge from 2002 through 2011 was 131 Mm^3, resulting in groundwater levels rising as much as 40 m. Hydraulic and hydrochemical data from the reservoir and various monitoring wells in Sand Hollow were used to evaluate the timing and location of reservoir recharge moving through the aquifer, along with potential clogging from trapped gases in pore throats, siltation, or algal mats.

Several hydrochemical tracers indicated this recharge had arrived at four monitoring wells located within about 300 m of the reservoir by 2012. At these wells, peak total dissolved-gas pressures exceeded two atmospheres (>1,500 mm mercury) and dissolved oxygen approached three times atmospherically equilibrated concentrations (>25 mg/L). These field parameters indicate that large amounts of gas trapped in pore spaces beneath the water table have dissolved. Lesser but notable increases in these dissolved-gas parameters (without increases in other indicators such as chloride-to-bromide ratios) at monitoring wells farther away (>300 m) indicate moderate amounts of in-situ air entrapment and dissolution caused by the rise in regional groundwater levels. This is confirmed by hydrochemical differences between these sites and wells closer to the reservoir where recharge had already arrived.

As the reservoir was being filled in 2002, managed aquifer recharge rates were initially very high (1.5×10^{-4} cm/s) with the vadose zone becoming saturated beneath and surrounding the reservoir. These rates declined to less than 3.5×10^{-6} cm/s during 2008. The 2002–08 decrease was likely associated with a declining regional hydraulic gradient and clogging. Increasing recharge rates during mid-2009 through 2010 may have been partly caused by dissolution of air bubbles initially entrapped in the aquifer matrix. Theoretical gas dissolution rates, coupled with field evidence of a decline in total dissolved-gas pressure and dissolved oxygen from nearby monitoring wells, support the timing of this gas dissipation.

Introduction

Sand Hollow basin is a 50 km^2 basin located in the southwestern part of Utah, USA, about 20 km northeast of St. George (Figure 1). It is part of the Virgin River drainage of the Lower Colorado River Basin and the upper Mohave Desert ecosystem. Altitudes range from 900 to 1,500 m.

Sand Hollow is underlain primarily by Navajo Sandstone that is either exposed at the surface or covered by a veneer of soil (Hurlow, 1998). The Navajo is part of the Dakota-Glen Canyon aquifer system, consisting of permeable sedimentary formations ranging in age from

Lower Jurassic to Upper Cretaceous, and is the principal source of groundwater in the Colorado Plateau region (Robson and Banta, 1995). This aquifer system covers an area of more than 190,000 km^2 in Utah, Arizona, Colorado, and New Mexico. Many municipalities in this region, including most cities and towns in Washington County, Utah, derive the majority of their municipal water from the Navajo Sandstone.

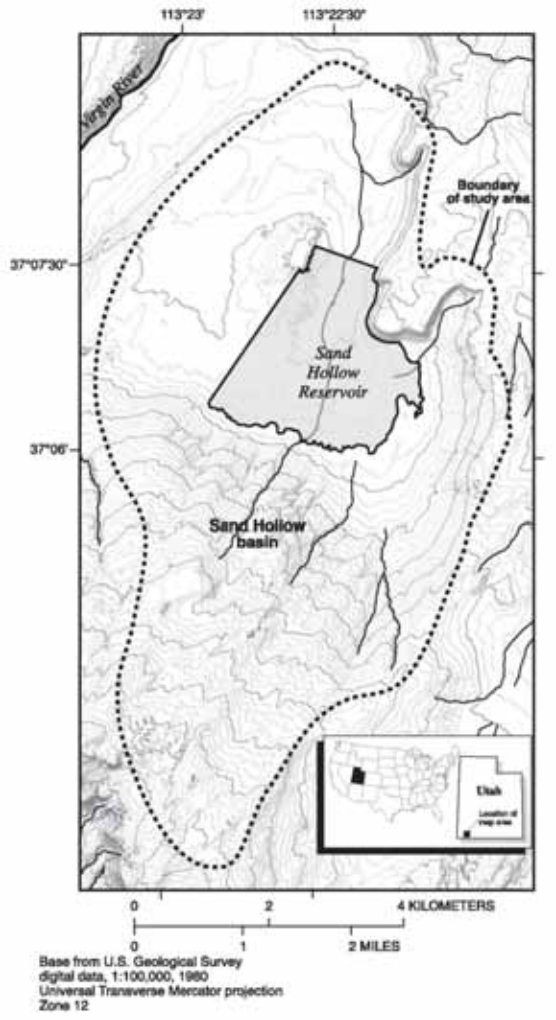

Figure 1: Location of Sand Hollow basin, south-western Utah, USA

The average stratigraphic thickness of the Navajo Sandstone in Sand Hollow basin is around 250 m, but ranges from about 100 to 370 m. The Navajo Sandstone is characterized as a fine-grained quartzose sandstone cemented with calcite (Cordova, 1978). Predominant cross-bedding features reflect its eolian depositional environment (Hurlow, 1998). Because the Navajo Sandstone at Sand Hollow is only loosely cemented and well sorted, it has a relatively high porosity and permeability. Laboratory porosity and saturated hydraulic conductivity, as determined from core samples within the study area, range from 20 to 27 percent and 1.1 x 10^{-5} to 4.9 x 10^{-4} cm/s (0.03 to 1.38 ft/d), respectively (Heilweil et al., 2004). Laboratory porosity and hydraulic conductivity of the overlying unconsolidated soils range from 29 to 45 percent and 3.5 x 10^{-6} to 7.1 x 10^{-5} cm/s (0.01 to 0.2 ft/d). A multiple-well aquifer test in Sand Hollow yielded an anisotropic range in hydraulic conductivity of 2.8 x 10^{-4} to 7.8 x 10^{-4} cm/s (0.8 to 2.2 ft/d) associated with fracture orientation (Heilweil et al., 2000). Depth to the water table measured in monitoring wells installed in Sand Hollow prior to the completion of the reservoir ranged from about 15 to 45 m (50 to 150 ft) below land surface in the central and northern parts of the basin (Heilweil et al., 2005), providing a substantial volume of the vadose zone that could be available for conversion to groundwater storage. These properties make the Navajo Sandstone in Sand Hollow a good target for managed aquifer recharge (MAR) via spreading basin infiltration.

Evidence of Managed Aquifer Recharge at Sand Hollow

Sand Hollow Reservoir was constructed in 2002 to provide surface-water storage and MAR to the underlying Navajo Sandstone. The reservoir is an off-channel facility that receives water from the Virgin River, diverted near the town of Virgin, Utah. Although this river water is not treated prior to entering the reservoir, water with visibly high suspended sediments is not diverted to the reservoir (Washington County Water Conservancy District, written comm., 2004). From 2002 through 2011, total surface-water diversions (inflow) to Sand Hollow Reservoir were about 245 Mm^3 (199,000 acre-ft). Surface-water storage and reservoir stage increased from 0 Mm^3 and 910 m (2,990 ft) 2002 to a maximum of about 62 Mm^3 (51,000 acre-ft) and 930 m (3,060 ft), respectively, in early 2006 (Figure 2). From 2006 through 2011, storage varied between about 38 to 54 Mm3 (31,000 and 44,000 acre-ft) and reservoir stage fluctuated between 928 and 933 m (3,045 and 3,060 ft; Marston and Heilweil, 2013).

A water budget method accounting for inflow, evaporation, and surface-water storage was used to quantify MAR from Sand Hollow Reservoir to the underlying aquifer.

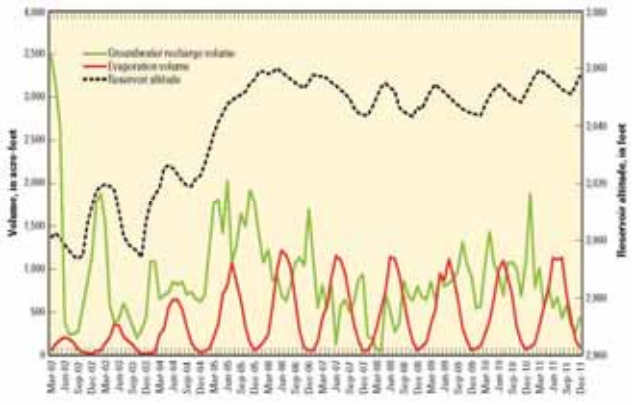

Figure 2: Monthly reservoir altitude, estimated evaporation, and calculated managed aquifer recharge, Sand Hollow Reservoir, Utah, 2002–2011

Inflow from the Virgin River during 2002 through 2011 ranged from 1 to 69 Mm^3/yr (800 to 56,000 acre-ft/yr), for a total of 245 Mm3. (199,000 acre-ft). Evaporation off the surface of the reservoir ranged from 1.4 to 8.3 Mm3/yr (1,100 to 6,700 acre-ft/yr), for a total of 62 Mm3 (50,000 acre-ft), based on the McGuinness and Bordne (1971) version of the Jensen-Haise method, which utilizes air temperature and solar radiation data. The resulting estimates of MAR to the Navajo Sandstone aquifer beneath Sand Hollow Reservoir during 2002-11 ranged from 6.7 to 22 Mm3/yr (5,400 to 18,2 00 acre-ft/yr) and totaled 131 Mm3 (106,000 acre-ft) (Marston and Heilweil, 2013). This recharge has resulted in a rise in the regional water table, with groundwater levels in monitoring wells rising by as much as 40 m (130 ft) from 2002 through 2011. The monthly change in volume of MAR (Figure 2) is more variable than changes in reservoir stage (altitude) and evaporation volumes.

Monthly recharge from March 2002 through December 2011 ranged from about 0.06 to 4.3 Mm3 (50 to 3,500 acre-ft), with two standard deviation (2σ) composite uncertainties ranging from about 6 to 14 percent of the estimate. Higher composite uncertainties in the summer reflect the large importance of evaporation losses during the warmer season, which have the highest uncertainty.

Major-ion chemistry, Cl:Br ratios, and tritium have all been effectively used to identify the arrival of recharge from Sand Hollow Reservoir at downgradient monitoring wells (Marston and Heilweil, 2013). Native groundwater and reservoir water each have distinctly different geochemical signatures, with MAR typically located at an intermediate location between these end members (Figure 3).

Figure 3: Chloride-to-bromide ratios of reservoir water and groundwater from selected monitoring wells in Sand Hollow, Utah

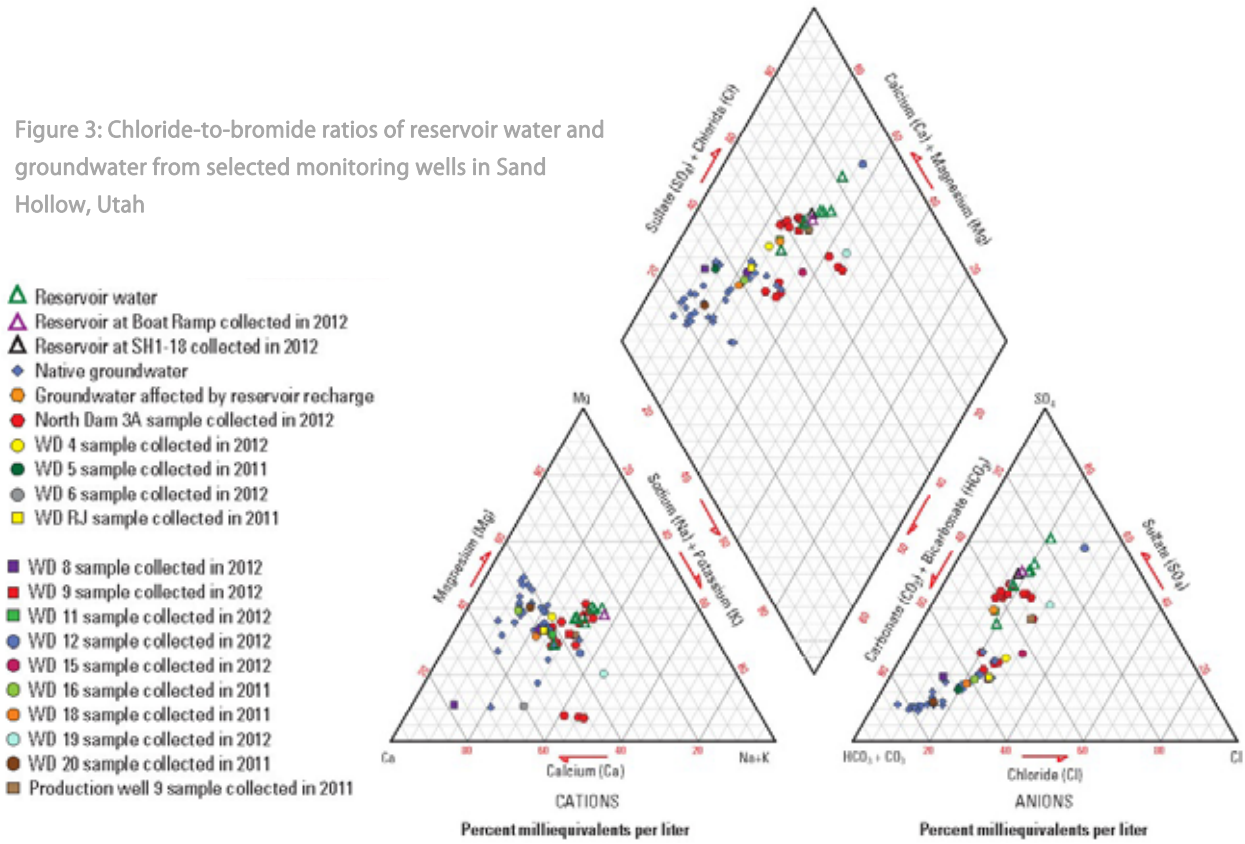

While fluctuating because of leaching of surficial salts (particularly while the reservoir was being initially filled), Cl:Br ratios of reservoir water are generally over 1,000; in contrast, Cl:Br ratios of native groundwater in Sand Hollow are generally less than 300 (Figure 4).

Tritium concentrations of about 3.5 tritium units (TU) in the reservoir are generally higher than naturally recharged groundwater, having concentrations of less than about 0.5 TU, except downgradient of areas with high natural recharge (Figure 5).

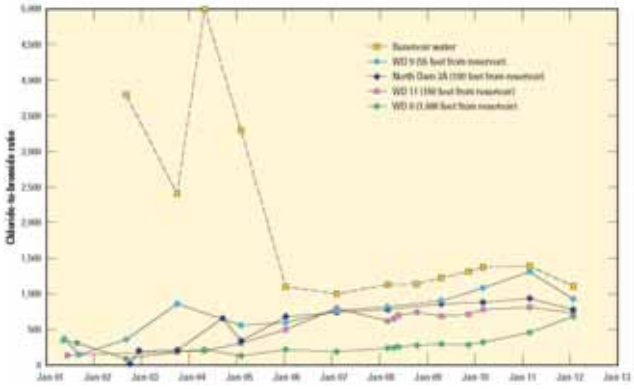

Figure 4: Major-ion chemistry from selected surface water and groundwater sites in Sand Hollow, Utah

All of these hydrochemical tracers indicate that MAR has travelled up to distances of about 300 m away from the reservoir during the 10-year period from 2002 through 2011. More detail regarding MAR tracer travel times is provided in Table 4 of Marston and Heilweil (2013).

Potential Clogging Processes at Sand Hollow

There are three primary clogging mechanisms from spreading basin MAR: (1) siltation (Rice, 1974; Bouwer, 1996); (2) algal mats (Katznelson, 1989; Baveye et al., 1998; Rinck-Pfeiffer et al., 2000); and (3) gas clogging (Christiansen, 1944; Constantz et al., 1988; Faybishenko, 1995; Heilweil et al., 2004; Heilweil et al., 2009). Siltation is assumed to cause a long-term decline in recharge rates at Sand Hollow because silts are continually building up along the bottom of the reservoir from suspended sediments of inflowing water and eolian dust deposition; treatments for permeability restoration of the reservoir bottom are not a practical option due to excessive reservoir water depths (up to 20 m).

Figure 5: Tritium concentrations of reservoir water and groundwater from selected monitoring wells in Sand Hollow, Utah, measured in February 2012

In contrast, algal (cyanobacterial) mats have been observed to develop only beneath the shallower parts of Sand Hollow

Reservoir during the summer, then dissipate during the winter, likely causing a bi-annual fluctuation in recharge rates at these locations (Heilweil et al., 2009). Entrapped gas bubbles likely were formed everywhere beneath the reservoir as the vadose zone became saturated as the regional water table connected with the reservoir. Entrapped gas, by definition, is no longer connected to the atmosphere and occurs in the form of small, immobilized disconnected bubbles (Faybishenko, 1995). Entrapped gas bubbles typically block the largest pore throats during saturation because wettability (the natural affinity for water to adhere to aquifer solids) causes trapped air to reside in the center of pores. This reduces permeability by restricting flow and increasing tortuosity (Figure 6). Laboratory experiments have documented entrapped air contents of 8 to 16 percent of otherwise saturated pore spaces (Marinas et al., 2013). Laboratory testing of sandstone cores from Sand Hollow showed that a 10 percent reduction in saturation resulted in an order-of-magnitude reduction in hydraulic conductivity (Beckwith and Baird, 2001; Heilweil et al., 2004). Two

potential sources of gas bubbles in the porous media beneath a spreading basin are (1) air entrapment during saturation as the water table rises in response to managed or natural aquifer recharge (Constantz et al., 1988; Holocher et al., 2003), and (2) biogenic gases (C02, CH4, and H2S) formed during plant respiration and decay of organic-rich sediments (Beckwith and Baird, 2001; Heilweil et al., 2009). The objective of this paper is to examine the variability and decline in recharge rates at Sand Hollow, with particular emphasis on using both hydraulic and geochemical data to evaluate potential gas clogging.

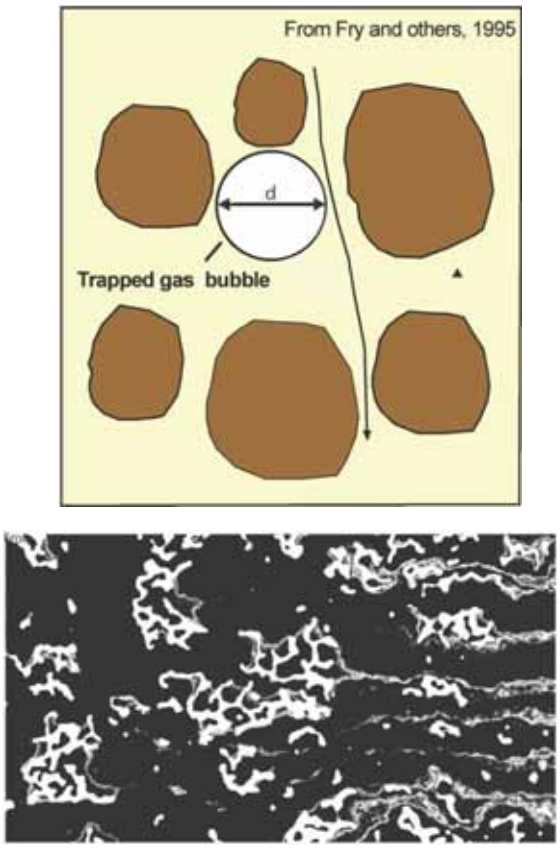

Figure 6: (A) Diagram showing gas clogging of pore throats in porous media; and (B) photograph of air entrapment in two-phase flow experiment (white area)

Approach and Methods

In order to examine temporal changes in MAR and potential clogging processes, volumetric recharge, Q (L3/T), was divided by the reservoir area, L2, to determine recharge rates, q (L/T), beneath Sand Hollow Reservoir. Reservoir area was calculated with reservoir stage data from a pressure transducer installed in the reservoir adjacent to the North Dam, and converted using stage-area relations for the reservoir (Washington County Water Conservancy District, written comm., 2004).

MAR from Sand Hollow Reservoir has an initial hydrochemical signature similar to the reservoir water, but evolves as it moves into the aquifer. Along its travel path, MAR initially encounters the organic-rich silt layer that has accumulated beneath the reservoir. This infiltration then moves through the pre-reservoir vadose (now saturated) zone where (1) solutes that had naturally accumulated beneath the root zone during the Holocene (Heilweil et al., 2006) are mobilized, and (2) air was entrapped in pore spaces (Heilweil et al., 2004) during filling of the reservoir. Such hydrochemical changes result in an overall MAR signature that is distinctly different than that of native groundwater. Water-quality data from Sand Hollow Reservoir and surrounding monitoring wells, therefore, can be used to assess the movement of MAR from the reservoir through the Navajo Sandstone aquifer. These include both field parameters and laboratory analysis of various chemical and dissolved-gas constituents.

Field water-quality parameters included total dissolved-gas (TDG) pressure and dissolved oxygen (DO). While specific conductance also has been used to differentiate between native groundwater (generally <500 μS/cm) and reservoir water (generally >800 μS/cm), this metric has been problematic because of the mobilization of salts that had previously accumulated in the vadose zone of Sand Hollow basin (Marston and Heilweil, 2013). TDG pressure is the combination of the partial pressures of all the dissolved gases in water (Manning et al., 2003). Assuming these gases are primarily of atmospheric origin, they will be predominantly nitrogen and oxygen, either from atmospheric equilibrium solubility or entrapped air, which likely formed in the previously partially saturated vadose zone as the wetting front beneath the reservoir connected with the underlying aquifer (Heilweil et al., 2005). As hydrostatic pressure increases with depth below the reservoir surface (stage), trapped gas in the porous media is gradually dissolved by the recharging water. In areas affected by plant respiration or microbial decay, biogenic gases (CO_2, CH_4, H_2S) may also form and dissolve, contributing to TDG pressure. Dissolved oxygen and TDG pressure may also decrease through microbially-mediated reducing conditions associated with bacterial

consumption of dissolved organic carbon in the organic-rich sediments beneath the reservoir. TDG pressure also has been analyzed since 2009 in the laboratory using advanced diffusion samplers (Gardner and Solomon, 2009) for selected monitoring wells with high TDG pressures. Unfortunately, this technique was not used prior to 2009, so measurements of 1,500 to 2,250 millimeters mercury (mm Hg) during 2003–08 have a higher but unknown amount of uncertainty and pressures greater than 2,250 mm Hg could not be measured.

Along with these field parameters, laboratory hydrochemical analyses of surface water and groundwater from Sand Hollow were used for evaluating potential gas clogging. This included chlorofluorocarbons (CFCs) and sulfur hexafluoride (SF6). Chlorofluorocarbons (CFC–11, CFC–12, and CFC–113) and SF6 are industrial gases found in trace amounts in the atmosphere, and thus are found in well-aerated surface-water bodies such as Sand Hollow Reservoir (as governed by their Henry's Law solubility). CFC–12 is considered the most stable of the three chlorofluorocarbons; both CFC–11 and CFC–113 are more likely to be affected by microbial decay. Dissolved CFC–12 concentrations in Sand Hollow Reservoir gradually increased from about 1.5 to 3.0 pmol/kg between 2008 and 2010 and then remained relatively stable during 2011–12 (Marston and Heilweil, 2013). The measured SF6 concentrations in the reservoir increased from about 1.5 to 1.9 fmol/kg in 2008-09 up to 2.9 fmol/kg in 2011–12. CFC-12 and SF6 concentrations in native groundwater are generally small (< about 1 pmol/kg and 1 fmol/kg, respectively) indicating natural recharge in Sand Hollow basin moves along slow (>50-year) pathways through the vadose zone to the water table. In addition to being used as tracers of MAR from Sand Hollow, CFCs and SF6 were also used to evaluate trapped gas processes. If large amounts of trapped air bubbles are dissolved into infiltrating MAR, this excess air will cause increases above atmospheric equilibrium of CFCs and SF6.

Data Collection Methods

Field parameters were measured with a multi-parameter sonde placed at the bottom of each 50-mm diameter (2-in) monitoring well within the screened interval, and in the reservoir at water depths of approximately 0.6 m (2 ft). Because the multi-parameter sonde was too large to enter the 25-mm (1-in) monitoring wells (North Dam 3A, WD 1, WD 4, WD 5, WD RJ, and WD 12), field measurements (except for TDG pressure) from these wells were made onsite with a flow-through chamber connected to the discharge line from either a Waterra hand pump or peristaltic pump.

The multi-parameter sonde used for TDG pressure measurements relies on a 5 psi transducer; measurements of less than 1,500 mm Hg have errors of less than 5 percent. The sonde could not measure pressures greater than 2,250 mm Hg and is not within its linear calibration range above about 1,500 mm Hg. Because of this non-linearity of in-situ measurements greater than 1,500 mm Hg, are only considered qualitative. Additional details regarding field parameter methods are given in Heilweil et al., 2005.

Hydrochemical samples were collected from 50-mm (2-in) monitoring wells using either a Grunfos or Bennett sample pump; 25-mm (1-in) wells were sampled with the Waterra pump; production wells were sampled utilizing installed turbine pumps. Prior to water chemistry sample collection, each monitoring well was purged until field parameters had stabilized and a minimum of three casing volumes were removed. Since 2009, a set of replicates for all constituents has been separately analyzed yearly at one randomly selected sampling site for quality assurance. CFC and SF6 samples were collected without head space in 250-ml and 1-L glass bottles, respectively, according to procedures described at http://water.usgs.gov/lab/ and were analyzed by the U.S. Geological Survey at the Chlorofluorocarbon Laboratory in Reston, Virginia.

Results

Variability in Managed Aquifer Recharge Rates

Estimated average monthly recharge rates beneath Sand Hollow Reservoir have generally declined from about 1.5 x 10^{-4} cm/s in March 2002 to about 3.5 x 10^{-6} cm/s in December 2011 (Figure 7). Three general periods can be observed, with Period 1 (March 2002 through mid-2003) beginning with very high initial rates that rapidly decrease as the vadose zone of the Navajo Sandstone becomes saturated and a hydraulic connection between the reservoir and aquifer is established (causing an abrupt

decrease in hydraulic gradient). This establishment of a saturated hydraulic connection is supported by measurements in monitoring wells closest to the reservoir, which had rapidly rising water levels beginning in late spring 2002 near the southern end of the reservoir.

Although consecutive monthly recharge rates occasionally fluctuate by more than 100 percent, Period 2 (mid-2003 through mid-2007) generally shows a gradual decline in recharge rates, while recharge rates are relatively steady during Period 3 (mid-2007 through 2011). During Period 3, recharge rates rebounded from mid-2008 through 2010. Recharge rates are generally higher during the winter months (particularly evident in 2003 through 2007), even though infiltrating water is cooler and more viscous during that time of year.

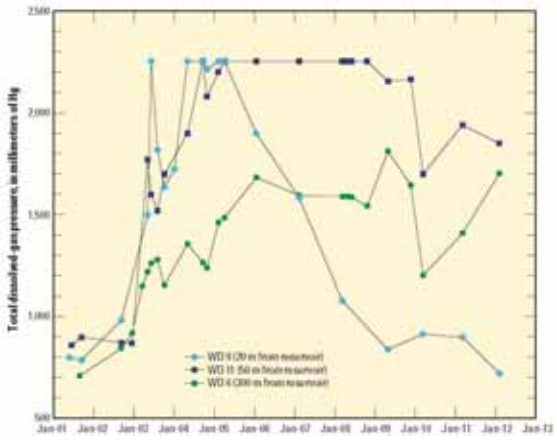

Figure 7: Monthly calculated recharge rates beneath Sand Hollow Reservoir, Utah, 2002 –2011

TDG pressures at monitoring wells within 500 m of the reservoir (WD 6, WD 8, WD 9, WD 11, WD 12) have exceeded 1,300 mm Hg. While field parameters at WD 8 and WD 12 have only recently been measured, longer time series from WD 6, WD 9, and WD 12 show the arrival and passage of peak values associated with reservoir recharge (Figure 8).

TDG pressures at these wells increased from background values of 700 to 850 mm Hg to values of 1,800 to more than 2,250 mm Hg (maximum value of sonde), or about two to three times atmospherically equilibrated concentrations. During 2011–12, TDG pressures remained elevated at WD 6, but have declined at wells closer to the reservoir (WD 9 and WD 11). TDG pressure at WD 9 exceeded 2,250 mm Hg during February and April 2005, indicating peak arrival occurred about 3 years after

Figure 8: Total dissolved-gas pressure in groundwater from selected monitoring wells in Sand Hollow, Utah

construction of the reservoir. TDG pressures at WD 9 have since declined to pre-reservoir conditions; the 2012 measurement of 720 mm Hg is only slightly higher than

the measured reservoir TDG and local barometric pressure of about 700 mm Hg. TDG pressures measured at WD 11 exceeded 2,250 mm Hg from 2005 through 2008, so an exact peak arrival date could not be determined; since 2010, TDG pressures declined slightly, fluctuating between about 1,700 and 1,900 mm Hg.

TDG pressures at WD 6 reached a peak of about 1,800 mm Hg in April 2009 and declined to 1,200 mm Hg in 2010, increasing back up to 1,700 mm Hg in 2012. These fluctuations are likely caused by changing hydraulic conditions associated with nearby pumping at Well 8. Of the other monitoring wells in Sand Hollow basin, TDG pressures > 1,300 mm Hg have only been measured at WD 15, located 730 m from the reservoir and screened shallower in the aquifer than the other wells (Marston and Heilweil, 2013, Table 2). Low Cl:Br ratios (<300) suggest that these elevated TDG pressures are likely caused by rising water levels and nearby entrapment of air bubbles rather than signifying the arrival of reservoir recharge.

DO concentrations at monitoring wells in Sand Hollow basin show patterns similar to the TDG pressures. DO increased from background groundwater values of 6.1 and 8.7 mg/L, reaching concentrations of 18 to 26 mg/L (about two to three times atmospheric equilibration) in monitoring wells near the reservoir (Figure 9).

DO at both WD 9 and WD 11 reached maximum values in April 2005; DO may have peaked at WD 6 in April 2009, although the recent variability is associated with nearby

pumping. In contrast to the TDG pressures (assumed to be controlled predominantly by the partial pressure of N2), DO has recently declined at WD 9 to <0.5 mg/L, much lower than concentrations in both background groundwater and reservoir water (9 to 11 mg/L). This may be due to either the higher solubility of oxygen (compared with N2) or an indication of the microbial oxidation of organic carbon in the shallow sediments beneath the reservoir.

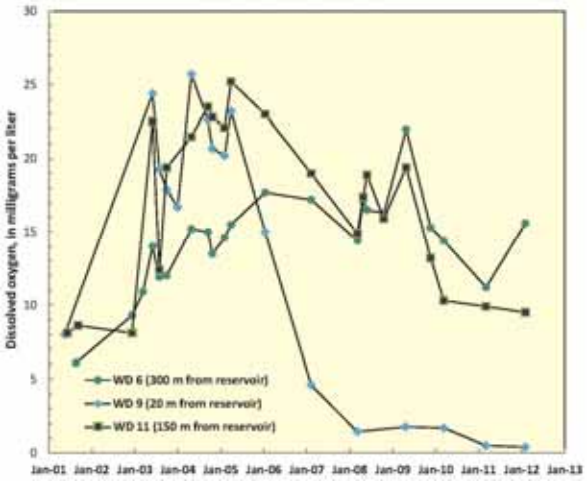

Figure 9: Dissolved oxygen in groundwater from selected monitoring wells in Sand Hollow, Utah

The latter is consistent with relatively high dissolved organic carbon concentrations at the nearby monitoring wells (1.6 to 1.8 mg/L), compared with background groundwater concentrations generally < 1 mg/L (Marston and Heilweil, 2013, Table 3).

Groundwater concentrations of the dissolved industrial gases SF6 and CFCs at WD 11 are even higher than the reservoir water concentrations, further evidence of large amounts of trapped gas and subsequent dissolution of excess air, which increases groundwater concentrations above atmospheric equilibrium solubility. SF6 concentrations of as much as 3.5 fmol/kg have been measured at WD 11, compared with reservoir values of only up to 2.9 fmol/kg. Groundwater SF6 and CFC-12 concentrations have also been elevated at both WD 15 and WD 19, located 750 and 1,500 m from the reservoir (Figure 10), but not at other distant monitoring wells. This contrasts with the low 3H concentrations and Cl:Br ratios at these two wells, indicating that MAR has not yet arrived at these distant locations. Each of these wells is the shallowest of nested pairs of monitoring wells and were drilled with air in 2008; it is likely that artificially large amounts of CFCs and SF6 were dissolved in the shallow aquifer adjacent to these two wells during the drilling process. In contrast, the deepest of each well pair (WD 16, WD 20) were not drilled with air and have much lower SF6 and CFC-12 concentrations.

Figure 10: CFC–12 concentrations of reservoir water and ground water from selected monitoring wells in Sand Hollow, Utah, measured in February 2012

Discussion and Conclusions

The overall decrease in monthly MAR rates from Sand Hollow Reservoir during 2002 through 2011 (Figure 7) is consistent with the effects of both a declining hydraulic gradient and clogging, as reported at other surface spreading basins used for MAR when actions are not taken to rejuvenate permeability through surface treatment (Bouwer, 2002). Numerical groundwater flow modeling confirmed that the decline in MAR rates at Sand Hollow cannot be entirely accommodated for by the decline in regional hydraulic gradient, but also required temporally decreasing permeability in the shallow subsurface beneath the reservoir (Marston and Heilweil, 2012). Because of the scale of this model and its inability to simulate multiphase flow (gas phase), it unfortunately

could not be used to differentiate between the potential causes of this clogging.

Superimposed on this overall trend are seasonal fluctuations in monthly recharge rates, particularly during Phase 2 (Figure 7). Recharge rates are generally higher during the winter months (particularly evident in 2003 through 2007), even though infiltrating water is cooler and more viscous during that time of year. Further studies are needed to evaluate if the variability is caused by (1) the seasonal die-off of the algal mat and a decrease in physical clogging, (2) a reduction of plant-respired gases and increased solubility of biogenic gas bubbles due to cooler water temperatures, and (or) (3) the dissolution of, or physical reduction in the size of, trapped gas bubbles due to cooler temperatures. Previous calculations using the ideal gas law have shown that a 25˚C reduction in reservoir water temperature from summer to winter would cause an 8 percent reduction in the volume of entrapped gas bubbles (Heilweil et al., 2004). Heilweil et al., 2009 found positive or near-zero excess TDG pressures calculated from measurements at four (of 11) shallow piezometers installed temporarily in the shallow sediments at various locations beneath Sand Hollow Reservoir. Such excess pressures typically indicate the presence of gas bubbles. These higher excess TDG pressures, in general, were found at piezometers located in shallow water (<3.5 m) during warmer periods (water temperatures from 13 to 20° C). Calculations based on measured noble-gas concentrations in these piezometers show that at 30ºC, all but the deepest piezometer (at 6-m water depth) would have had positive or near-zero excess TDG pressures, indicating gas exsolution and bubble formation. In contrast, calculations for the minimum water temperature of 5° C indicate no bubble formation during this cooler period. This suggests that gas clogging associated with algal decay and plant respiration only occurs beneath the shallower parts of the reservoir (water depths of less than 6 m) during the warmest months. Elevated concentrations of carbon dioxide and methane in water from these shallow piezometers support a biogenic source of these gas bubbles.

Another interesting anomaly is the increase in monthly recharge rates from mid-2008 through 2010, which may be explained by the dissolution of trapped gas bubbles in the matrix beneath and adjacent to Sand Hollow Reservoir. This increase is consistent with the doubling of intrinsic permeability observed during the Infiltration Pond experiment (conducted just north of Sand Hollow Reservoir), which was attributed to the dissolution of trapped gas (Heilweil et al., 2004). Theoretical calculations can be used to assess the timing of trapped-gas dissolution beneath Sand Hollow. For this calculation, a column having a volume of 30 m^3 (30 m tall by unit horizontal dimensions) is used to represent the average 30-m rise in the water table as the vadose zone beneath the reservoir becomes saturated. The following assumptions have been made: (1) a 20 percent Navajo Sandstone effective porosity, yielding a pore-space volume of 6 m^3, (2) 20 percent of this porosity is initially filled with trapped gas, resulting in a volume of 1.3 m^3 after wetting occurs, (3) the trapped gas is predominantly N2 (the primary constituent of air), (4) a median increase of 15 m of hydrostatic pressure, representing half the mean difference between the pre-reservoir groundwater table altitude and the nearly-full reservoir stage (after hydraulic connection was established between the regional water table and the reservoir water), (5) a mean water temperature of 17˚C, and (6) a time-averaged volume of 5.4 m^3 of pore water (the median value, assuming initial and final water-saturated pore volumes of 4.8 and 6.0 m^3, respectively). Using the increase in nitrogen solubility associated with the increase in hydrostatic pressure, it would require approximately 45 m^3, or eight pore volumes, of water passing by the trapped gas bubbles for complete dissolution. Assuming a long-term (2002–11) average infiltration rate of 0.013 m/d beneath Sand Hollow Reservoir, it would require about 10 years to dissolve all of the initially trapped air beneath the reservoir. This is consistent with both the rise in MAR rates from mid-2008 through 2010 and the decline in TDG pressure at the nearest monitoring well (WD 9). Because the time required to dissolve gases beneath a spreading basin is a function of infiltration rate, assuming similar hydrostatic pressure and water-temperature conditions as in Sand Hollow, it would take much less time for the dissipation of trapped gases in a higher permeability aquifer matrix. Dissolution of the same 1.2 m^3 volume of trapped gas per unit area would likely require only about one year in a medium sand aquifer (assuming an infiltration rate of 1 m/d) and one month in a gravel aquifer (assuming an infiltration rate of 14 m/d).

In summary, monthly water-balance calculations indicate that there has been a gradual decline in MAR beneath Sand Hollow Reservoir over the past decade. Superimposed on this trend are seasonal fluctuations that may be caused by algal mat development/dissipation and temperature-dependent trapped gas bubble contraction (winter) and expansion (summer). Very elevated TDG pressure and dissolved oxygen in monitoring wells near the reservoir indicate initially large amounts of trapped air were dissolved into the infiltrating MAR. Recent declines in these field parameters indicate that much of the trapped gas bubbles have dissolved, consistent with theoretical calculations. This gas dissolution may be responsible for the slight increase in infiltration rates during mid-2008 through 2010.

References

Baveye, P., Vandevivere, P., Hoyle, B.L., DeLeo, P.C., and Sanchez de Lozada, D., (1998) Environmental impact and mechanisms of the biological clogging of saturated soils and aquifer materials. Critical Reviews in Environmental Science and Technology, CRC Press 28(2):123–191.

Beckwith, C.W., and Baird, A.J., (2001) Effect of biogenic gas bubbles on water flow through poorly decomposed blanket peat. Water Resources Research 37(3): 551–558.

Bouwer, H., (2002) Artificial recharge of groundwater: Hydrogeology and engineering. Hydrogeology Journal 10: 121–142.

Christiansen, J.E., (1944) Effect of entrapped air upon the permeability of soils. Soil Science 58 (5): 355–365.

Clarke, W.B., Jenkins, W.J., and Top, Z., (1976) Determination of tritium by mass spectrometric measurements of 3He. International Journal of Applied Radiation Isotopes 27: 515–522.

Constantz, J., Herkelrath, W.N., and Murphy, F., (1988) Air encapsulation during infiltration. Soil Science Society of America Journal 52: 10–16.

Cordova, R.M., (1978) Ground-water conditions in the Navajo Sandstone in the central Virgin River basin, Utah. State of Utah Department of Natural Resources Technical Publication No. 61, 66 p.

Cordova, R.M., (1981) Ground-water conditions in the upper Virgin River and Kanab Creek basins area, Utah, with emphasis on the Navajo Sandstone. State of Utah Department of Natural Resources Technical Publication No. 70, 87 p.

Faybishenko, B.A., (1995) Hydraulic behavior of quasi-saturated soils in the presence of entrapped air: Laboratory experiments. Water Resources Research 31(10): 2421–2435.

Freeze, R.A., and Cherry, J.A., (1979) Groundwater. Prentice-Hall, Inc., Englewood Cliffs, New Jersey, 604 p.

Fry, V.A., Istok, J.D., Semprini, K.T., O'Reilly, K.T., and Buscheck, T.E., (1995) Retardation of dissolved oxygen due to a trapped gas phase in porous media. Ground- Water 32 (1): 391–398.

Gardner, P., and Solomon, D.K., (2009) An advanced passive diffusion sampler for the determination of dissolved gas concentrations. Water Resources Research, v. 45, issue 6, W06423 doi:10.1029/2008WR007399

Glass, R.J., and Nicholl, M.J., (1995) Quantitative visualization of entrapped phase dissolution within a horizontal flowing fracture. Geophysical Research Letters 22 (11): 1413–1416.

Heilweil, V.M., Freethey, G.W., Stolp, B.J., Wilkowske, C.D., and Wilberg, D.E., (2000) Geohydrology and numerical simulation of ground-water flow in the central Virgin River basin of Iron and Washington Counties, Utah. Utah Department of Natural Resources Technical Publication 116, 182 p.

Heilweil, V.M., and Marston, T.M., (2011) Assessment of managed aquifer recharge from Sand Hollow Reservoir, Washington County, updated to conditions in 2010. U.S. Geological Survey Scientific Investigations Report 2011–5142, 39 p.

Heilweil, V.M., and McKinney, T.S., (2007) Net-infiltration map of the Navajo Sandstone outcrop area in western Washington County, Utah. U.S. Geological Survey Scientific Investigations Map 2988.

Heilweil, V.M., McKinney, T.S., Zhdanov M.S., and Watt, D.E., (2007) Controls on the variability of net infiltration to desert sandstone. Water Resources Research, v. 43, W07431. DOI:10.1029/2006WR005113, 15 p.

Heilweil, V.M., and Solomon, D.K., (2004) Millimeter– to kilometer–scale variations in vadose-zone bedrock solutes: Implications for estimating recharge in arid settings, in Phillips, F., Scanlon, B., and Hogan, J., eds.,

Ground-water recharge in a desert environment: the southwestern United States, Water Science and Application 9. American Geophysical Union, Washington, D.C., p. 49–67.

Heilweil, V.M., Solomon, D.K., and Gardner, P.M., (2006) Borehole environmental tracers for evaluating net infiltration and recharge through desert bedrock. Vadose Zone Journal, v. 5, p. 98–120.

Heilweil, V.M., Solomon, D.K., and Ortiz, G., (2009) Silt and gas accumulation beneath an artificial recharge spreading basin, southwestern Utah, U.S.A. Boletin Geologico y Minero, v. 120 (2), p. 185–195.

Heilweil, V.M., Solomon, D.K., Perkins, K.S., and Ellett, K.M., (2004) Gas-partitioning tracer test to quantify trapped gas during recharge. Ground Water, v. 42, no. 4, p. 589–600.

Heilweil, V.M., Susong, D.D., Gardner, P.M., and Watt, D.E, (2005) Pre- and post-reservoir ground-water conditions and assessment of artificial recharge at Sand Hollow, Washington County, Utah, 1995–2005. U.S. Geological Survey Scientific Investigations Report 2005–5185, 74 p.

Heilweil, V.M., and Watt, D.E., (2011) Trench infiltration for managed aquifer recharge to permeable bedrock. Hydrological Processes 25, DOI: 10.1002/hyp.7833, p. 141–151.

Holocher, J., Peeters, F., Aeschbach-Hertig, W., Hofer, M., Brennwald, M., Kinzelbach, W., and Kipfer, R., (2002) Experimental investigations on the formation of excess air in quasi-saturated porous media. Geochemica et Cosmochimica Acta 66(23): 4103–4117.

Holocher, J., Peeters, F., Aeschbach-Hertig, W., Kinzelbach, W., and Kipfer, R., (2003) Kinetic model of gas bubble dissolution in groundwater and its implications for the dissolved gas composition. Environmental Science and Technology 37: 1337–1343.

Hurlow, H.A., (1998) The geology of the central Virgin River basin, southwestern Utah, and its relation to ground-water conditions. State of Utah Water Resources Bulletin 26, 53 p.

Manning, A.H., Solomon, D.K., and Sheldon, A.L.,(2003) Applications of a total dissolved gas pressure probe in groundwater studies. Ground Water 41 (4): 440–448.

Marinas, M., Roy, J.W., and Smith, J.E., (2013) Changes in entrapped gas content and hydraulic conductivity with pressure. Ground Water 51 (10: 41–50).

Marston, T.M., and Heilweil, V.M., (2012) Numerical simulation of groundwater movement and managed aquifer recharge from Sand Hollow Reservoir, Hurricane Bench area, Washington County, Utah. U.S. Geological Survey Scientific Investigations Report 2012–5236, 34 p.

Marston, T.M., and Heilweil, V.M., (2013) Assessment of managed aquifer recharge from Sand Hollow Reservoir, Washington County, updated to conditions in 2012. U.S. Geological Survey Scientific Investigations Report 2013–5057, 40 p.

McGuinness, J.L., and Bordne, E.F., (1971) A comparison of lysimeter-derived potential evapotranspiration with computed values. U.S. Department of Agriculture Technical Bulletin 1472, Agricultural Research Service, Washington, D.C., 71 p.

Robson, S.G., and Banta, E.R., (1995) Ground-water atlas of the United States, Segment 2: Arizona, Colorado, New Mexico, Utah. U.S. Geological Survey Hydrologic Investigations Atlas 730-C., 32 p.

Sheldon, A., (2002) Diffusion of radiogenic helium in shallow ground water: Implications for crustal degassing. Salt Lake City, Utah, University of Utah, Ph.D. Dissertation, 185 p.

Clogging Phenomena Related to Surface Water Recharge Facilities

A. Hutchison[1], M. Milczarek[2] and M. Banerjee[2]

[1] *Recharge Planning Manager Orange County Water District*

[2] *GeoSystems Analysis, Inc.*

1 Introduction

Dr. Herman Bouwer once wrote:

> *"Clogging of the infiltration surface and resulting reductions in infiltration rates are the bane of all artificial recharge systems." (added emphasis) (Bouwer, 2002).*

In many cases, clogging is what limits the capacity of managed aquifer recharge (MAR) facilities, whether they be injection wells, subsurface recharge galleries or surface spreading facilities. Needless to say, in order to maximize the capacity of MAR facilities, understanding clogging and developing successful mitigation strategies are critical. This section of the clogging monograph focuses on clogging of surface spreading facilities and is divided into two parts. Part I presents a summary of literature reviewed on this topic Part II presents surface spreading performance data for Orange County Water District (OCWD or District), located in southern California, USA. The purpose of Part I of the Clogging Monograph is to present a literature review of the mechanisms that control clogging.

2 Clogging of Surface Spreading Facilities

Over time, all surface water spreading facilities will clog (Baveye et al., 2001; Bouwer et al., 2001; Bouwer and Rice, 2001; Schubert, 2004). Surface waters used for recharge often contain significant quantities of suspended sediments and microorganisms, which lead to clogging (Bouwer and Rice, 1989; Behnke, 1969). It must be noted that the clogging seen in spreading basins is different than in rivers and stream channels due to the self-cleaning potential of rivers and stream channels (e.g., bed sediment transport), which can reduce clogging depending on the timing and magnitude of runoff events (Rehg, 2005; Schubert, 2004, Lacher, 1996).

Clogging can be caused by physical, biological and chemical processes. Each of these processes can work individually or collectively to reduce infiltration rates. Factors that influence the development and extent of a clogging layer include the effluent water quality, basin soil texture, ponding depth, hydraulic loading rate and cycle, and vegetation. Moreover, due to changes in water quality, water depth, and basin bottom conditions, these processes can be active at different times and in different locations (Becker et al., 2012; Racz et al., 2012). Thus obtaining a detailed understanding of how clogging affects infiltration rates is challenging because it involves multiple processes that are changing in importance in time and space.

Clogging of the infiltration surface has multiple effects, including:

1. Reducing infiltration rates (Duryea, 1996; Bouwer and Rice, 1989; Behnke, 1969; Allison, 1947);
2. Diminishing the effectiveness of soil aquifer treatment (Siegrist, 1987);
3. Necessitating regular maintenance (e.g., draining and scraping basin floors); and,
4. Potentially leading to site abandonment in extreme cases (Grischek, 2006).

The clogging layer is often thin (millimeters to 4 centimeters) and may consist of suspended solids,

algae, microbes, dust, and salts. As defined by Houston et al. (1999), the clogging layer is the zone of material over which a sharp drop in hydraulic head occurs as water infiltrates into a sedimentary profile. That is, the clogging layer reduces the hydraulic conductivity of the sediment such that the underlying material below the basin bottom will eventually become unsaturated. Hydraulic conductivity is a quantitative measure of sediment's ability to transmit water when subjected to a given hydraulic gradient. The effective hydraulic conductivity (Ke) is the overall hydraulic conductivity of an infiltrative zone that includes the clogging layer and the sediment below (Beach, 2005). Ke will be used in this paper to discuss the hydraulic conductivity of sediments except if specified otherwise.

Two distinct types of clogging layers typically exist:

1. Upper Layer – is an accumulation of particulate matter, algae, and/or microbes above the original sediment surface (outer blockage); and,
2. Lower Layer – the native sediment with organic and inorganic solids trapped in the pore space (inner blockage).

Consolidation from overburden pressure caused by the depth of ponding typically controls the conductivity of the upper layer (outer blockage). Loss of high conductivity pore space in the native soil controls the conductivity of the lower layer (inner blockage).

The water quality components that primarily influence the formation of a clogging layer are physical (accumulation of suspended solids) and biological (blockage by microorganisms and their byproducts). In addition, extended ponding periods enhance soil clogging, whereas wetting and drying cycles tend to destroy the clogging layer; under long-term ponding conditions, the hydraulics of an infiltration basin is often controlled by the clogging layer, regardless of the native soil media (Beach, 2005; Houston, 1999; Duryea, 1996).

2.1 Physical Clogging

Physical clogging is caused by the deposition and accumulation of organic and inorganic solids (such as clay and silt particles, algae cells, and microorganisms) at the water-sediment interface, leading to the formation of a filter cake (outer blockage). The rate of clogging is determined by the rate of suspended solids deposition, the size distribution of the suspended solids and the size distribution of the receiving sediments. Larger suspended solids will tend to accumulate on the sediment surface, but smaller suspended solids can potentially migrate into the pore space of the receiving sediment and cause inner blockage (Bouwer, 2002; McDowell-Boyer et al., 1986). If deep penetration of particles occurs, it can reduce the effectiveness of surface cleaning, thus potentially leading to irrecoverable losses in infiltration capacities (Rehg, 2005).

Additional suspended solids can be introduced to a spreading facility by erosion, wave action, and windborne dust. When suspended solids in the influent water are relatively high, the clogging caused by these additional factors is secondary to the clogging caused by the accumulation of solids in the influent water. When recharging water with low suspended solids, these factors dominate physical clogging processes. To address this, it is recommended to design recharge facilities to minimize the impact of erosion or wave action (Bouwer, 2002).

2.2 Biological Clogging

Microbial cells and their metabolic byproducts (gas entrapped in pores or exopolymers that clog pores) can alter a number of sediment properties such as pore size, pore volume, and flow path interconnectedness, which in turn affect the hydraulic conductivity of the media (Baveye et al., 1998). Water quality, in particular the nutrient load, is the most important factor that influences the development of the microbial component of the clogging layer (Winter and Goetz, 2003). Elevated concentrations of carbon and macro-nutrients (i.e. nitrogen and phosphorus), commonly found in treated sewage effluent, stimulate microbial growth such that biological clogging rates correlate to the biological oxygen demand. Clogging from algal blooms may also occur even in relatively low nutrient waters and may need to be actively managed via herbicides or algal feeders (fish). Nonetheless, biological clogging can be reversed, typically by allowing the facility to dry, which causes the extracellular polysaccharides and microbes that cause clogging to biodegrade (Houston et al., 1999; Magesan et al., 1999; Duryea, 1996).

2.3 Other Clogging Factors

Other factors that play a minor role in clogging include chemical precipitation and deposition in the pores (Bouwer, 2002; Platzer and Mauch, 1997), growth of plant-rhizomes and roots (Vymazal et al., 1998; Brix, 1994, 1997; McIntyre and Riha, 1991), formation and accumulation of humic substances (Siegrist et al., 1991), generation of gas (Langergraber et al., 2003), and compaction of the clogging layer (Houston et al., 1999; McDowell-Boyer et al., 1986). Chemical properties of soil particles and the infiltrating water, such as electrolyte concentration, pH, redox potential, and mineralogical composition of the sediment may influence the geometry of the pore space and may affect the shape and stability of the pores, which in turn determines the hydraulic conductivity of the media (Baveye et al., 1998).

3 Parameters that Influence Clogging

Achievable infiltration rates in surface spreading operations, or the bulk Ke, is controlled by four main factors (Beach, 2005):

1) Hydraulic conductivity of the infiltrative surface, including the clogging layer;
2) Height of ponding above the infiltrative surface;
3) Thickness of the clogging layer; and,
4) Moisture pressure potential (tension) of the subsurface sediments.

Nonetheless, many studies show that the bulk Ke, is generally controlled by the characteristics of the clogging layer (Phipps et al., 2007; Beach, 2005; Houston, 1999; Duryea, 1996). Moreover, total suspended solids and the nutrient load, typically characterized by Biological Oxygen Demand (BOD), appear to be the most important components that influence the formation of a clogging layer.

Physical clogging has been observed to depend on the total mass of suspended solids and particle size distribution of the porous media with reduction in basin recharge rates well described by an exponential decay function (Phipps et al., 2007). Microbial clogging has been observed to reduce hydraulic conductivity and eventually stabilize to a constant value (Taylor and Jaffe, 1990; Frankenberger et al., 1979). Clogging usually occurs on or near the surface except in two instances: when a soil has hydraulic properties similar to those of the clogging material or when fines migrate and accumulate in a soil at a depth significantly below the surface, thereby resulting in a deeper restricting zone (Duryea 1996).

The following parameters influence the extent of clogging:

1) Water quality. The reduction and/ or prevention of clogging, is largely dependent on the quality of the infiltrated water (e.g. Hollander et al., 2005; Bouwer, 2002). Bouwer (2002) and EWRI/ASCE (2001) recommend treating recharge water to "drinking water quality" to reduce or eliminate clogging. Attempts to develop guidelines on the quality of water suitable for aquifer recharge are often based on sparse data, and have not been reliably validated (Alvarez 2008; Pavelic 2007). To date, models to predict theoretical clogging time due to physical clogging have been limited in real-world application (e.g. Langergraber et al., 2003; Aaltomaa and Joy, 2002), or not fully tested at the field scale (e.g. Phipps et al., 2007). The extent of soil clogging is closely correlated to total suspended solids (TSS), biological oxygen demand (BOD), and carbon to nitrogen (C:N) ratio. Following are more detailed descriptions of water quality impacts on clogging.

a. Total suspended solids (TSS). Clogging resulting from the deposition of TSS is typically the key determinant in recharge performance (Hutchinson, 2007; Winter and Goetz, 2003; Siegrist and Boyle, 1987; Vecchioli, 1972; Harpaz, 1971; Hauser and Lotspeich, 1967). The direct relationship between TSS load and recharge performance, however, is typically site specific. TSS consisting of primarily fine-grained (clay) particles may result in greater recharge reduction than a coarser particle load. Recharge facilities in the Netherlands and Great Britain do not allow recharge water with turbidity of more than 2 to 5 NTU (Hollander, 2005); most recharge facilities appear to develop their own turbidity criteria. Although turbidity measures approximately the same water quality property as TSS, direct conversion between turbidity and TSS is typically not possible. Turbidity is caused by suspended matter or impurities that interfere with the clarity of the water; whereas larger light weight

particles (e.g. algae) can cause greater turbidity than smaller, heavier inorganic particles.

b. BOD and C:N ratio. Soil irrigated with water that has a high C:N ratio (i.e. 50:1) and/or high BOD exhibits significant increases in soil microbial biomass and extracellular carbon deposition, with a subsequent decrease in hydraulic conductivity (Aaltomaa and Joy, 2002; Jnad, 2001, Magesan et al., 1999; Vandeviere and Baveye, 1992a).

c. Other water quality parameters. Soil clogging layer development is loosely associated with total nitrogen and total phosphorous content, which also contribute to biological growth (Magesan et al., 1999). Bouwer (1988) also proposed the Sodium Adsorption Ratio (SAR) as a parameter for water quality assessment, due to the influence of sodium on the hydraulic property of clays.

2) Particle-size of sediment media. The importance of particle size on the extent of clogging varies. In the short term, clogging layer formation is accelerated in fine-grained sediments and reduction of infiltration rates occurs faster in these sediments than in coarse-grained sediments (Aaltomaa and Joy, 2002). However, there is potentially a greater relative reduction in Ke in coarse-grained sediments than in fine-grained soils. Where the Ke may be similar to that of the clogging material, the clogging layer may not govern the Ke of the soil profile, whereas, sandier sediments may experience reductions of 0.5 to 5 orders of magnitude in hydraulic conductivity (i.e. from 10^{-2} cm/sec up to 10^{-7} cm/sec, Duryea, 1996; Rinck-Pfeiffer, 2000; Beach, 2005; Taylor and Jaffe, 1990; Magesan, 2000; Jnad et al., 2001; Rodgers et al., 2004). Soil particle-size can impact the depth of the clogging layer with sandy sediments having shallower (up to a few cm) clogging layers, and gravels clogging deeper (more than 100 cm) (Blazejewski and Murat-Blazejewski, 1997).

3) Ponding depth. Depending on clogging conditions, ponding depth may increase, decrease, or not affect the infiltration rate and Ke (Houston et al., 1999; Duryea, 1996). Two opposing factors result from ponding water depth: an increased hydraulic gradient versus increased compaction of the clogging layer. Increasing the water ponding depth increases the infiltration rate if all other factors remain the same. However, increasing the water ponding depth causes the loose clogging layer to compact which can then cause a reduction in the infiltration rate (Bouwer and Rice, 1989). In general, field studies have found that infiltration rates decrease as clogging layer thickness and ponding depth increases (Houston et al., 1999).

4) Hydraulic loading rate. Loading rate, the rate at which water is applied to the soil surface, also affects the extent of clogging. Lower loading rates may reduce the formation of a clogging layer (Siegrist, 1987). However, in the long-term, for a given media and application method, the clogging layer may reach a maximum reduction in hydraulic conductivity independent of loading rate (Beach, 2005). In practice, a lower hydraulic loading rate is best achieved through loading cycles (see below).

5) Loading cycles. Techniques such as cycles of flooding and drying can restore hydraulic conductivity to higher levels by disturbing the clogging layer (Houston et al., 1999; Duryea, 1996). Many managed aquifer recharge operations use 1:1 on-off cycle ratios where basins are allowed to dry for 50 percent of the time.

6) Vegetation. Vegetation may contribute to a decrease in soil hydraulic conductivity in wetland environments (Winter and Goetz, 2003; Dahab and Surampalli, 2001; Blazejewski, 1997; Jiang, 1995; Brix, 1994; McIntyre and Riha, 1991). Production of root exudates by plants may cause soil clogging, resulting in a decrease in hydraulic conductivity (McIntyre and Riha, 1991). Leaf litter may also contribute to surface clogging (Batchelor and Loots, 1997) whereas certain plants (i.e. Phragmites australis) may reduce soil clogging via penetration by plant roots and rhizomes which loosens the soil and increases the hydraulic conductivity (Cooper et al., 2005). Dead roots and rhizomes may create large pores or channels for water movement (Brix, 1997).

Tables 1 and 2 present an overview of published data showing the influence of various parameters on extent of clogging. Table 1 gives actual Ke values with particular soil types and water quality. For studies where the actual Ke was not published, Table 2 shows the relative reductions in Ke due to clogging parameters. Table 3 provides water quality data from research where clogging was limited or absent.

Table 1: Effects of Soil Clogging on Effective Hydraulic Conductivity (Ke) with Various Soil Types and Influent Quality

Author	Study Conditions	Method	Soil Type, USCS/USDA Classification	Influent Quality* (mg/l)	Initial/ potential K_e (cm/sec, (ft/day))	Final Effective Hydraulic Conductivity K_e (cm/sec)	Reduction in K_e of surface soil (cm/sec)
Duryea (1996)	Column Study Using Soils and Wastewater from Tucson and Phoenix, Arizona	Falling head permeability test Final conductivity measurements were taken 18 months after first wetting Columns were subject to a series of wetting and drying cycles during the 18 months	Agua Fria Soil SP (sand)	DSE N: 2–9; P: 3–6; TSS: 3–7 TOC: 8–10	8.4×10^{-2} (23.8)	0–2 cm: 1.31×10^{-2}	< 0.5 order of magnitude reduction
						2–4 cm: 3.16×10^{-2}	
						4–6 cm: 2.38×10^{-2}	
						6–8 cm: 2.16×10^{-2}	
			North Pond Soil SM (fine or loamy sand)	SE N:15–27; P: 2–5; TSS: 20–30 TOC: 15–25	1.8×10^{-4} (0.5)	0–2 cm: 6.67×10^{-5}	≈ 0.5 order of magnitude reduction
						2–4 cm: 6.97×10^{-4}	
						4–6 cm: 1.40×10^{-3}	
						6–8 cm: 4.51×10^{-4}	
				DSE No ponding		0–2 cm: 1.73×10^{-4}	negligible change
						2–4 cm: 2.30×10^{-4}	
						4–6 cm: 8.14×10^{-4}	
						6–8 cm: 3.51×10^{-4}	
				DSE Water ponded to 7.5 ft – 17 ft. deep		0–2 cm: 6.03×10^{-5}	≈ 0.5 order of magnitude reduction
						2–4 cm: 6.96×10^{-4}	
						4–6 cm: 2.23×10^{-4}	
						6–8 cm: 5.75×10^{-4}	
			Sweetwater Soil SP-SM (fine sand)	SE N:15–27; P: 2–5; SS: 20–30	1.9×10^{-2} (53.8)	0–2 cm: 2.48×10^{-3}	≈ 1 order of magnitude reduction
						2–4 cm: 6.57×10^{-3}	
				TE N:15–27 TSS: 5–10 TOC: 10–15		0–2 cm: 4.64×10^{-3}	≈ 1.5 order of magnitude reduction
						2–4 cm: 1.63×10^{-2}	
						4–6 cm: 2.09×10^{-2}	
						6–8 cm: 4.40×10^{-2}	
			Agricultural Field CL (low plasticity clay)	DSE N: 2–9; P: 3–6; TSS: 3–7	3.5×10^{-6} (1 x10^{-2})	0–2 cm: 1.20×10^{-6}	negligible change
						2–4 cm: 4.86×10^{-7}	
						4–6 cm: 2.95×10^{-7}	
						6–8 cm: 3.80×10^{-7}	

Author	Study Conditions	Method	Soil Type, USCS/USDA Classification	Influent Quality* (mg/l)	Initial/ potential K_e (cm/sec, (ft/day))	Final Effective Hydraulic Conductivity K_e (cm/sec)	Reduction in K_e of surface soil (cm/sec)
Rinck-Pfeiffer (2000)	Column Study	Continuous injection of recycled water through columns	Soil from sandy limestone aquifer	SE All units mg/L N: 2.5–3.5 BOD: 2.0–3.0 COD: 165–170 TOC: 18–20 TSS: 3–4	9.03×10^{-4} (2.6)	Week 1: 7.18×10^{-5} Week 2: Stable Week 3: 3.12×10^{-4}	Initially ≈1 order of magnitude reduction, Reversed due to calcite dissolution at the inlet end of columns. Final ≈ 0.5 order of magnitude reduction
Beach (2005)	Column Study	Falling Head Test	Sand	STE Load rate: 200 cm/day	9.57×10^{-3} (27.1)	Week 2: 4.85×10^{-4} Week 6: 6.32×10^{-5} Week 20: 2.49×10^{-5}	≈ 1.5 order of magnitude reduction
				STE Load rate: 100 cm/day	9.86×10^{-3} (27.9)	Week 6: 7.70×10^{-5} Week 20: 3.53×10^{-5}	≈ 1.5 order of magnitude reduction
Taylor and Jaffe (1990)	Column Study	Not Reported	Sand 0.59–0.84mm diameter	Diluted primary and activated sludge	2.5×10^{-1} (709)	Max reduction after 40 weeks: 1.27×10^{-4}	≈ 3 order of magnitude reduction
Magesan (2000)	Column Study	Conductivity after 14 weeks	Sandy loam	C:N ratio 2.5:1	Not Reported	2.44×10^{-3}	≈ 1+ order of magnitude reduction
				C:N ratio 27:1		1.33×10^{-3}	
				C:N ratio 66:1		5.00×10^{-4}	
Rodgers et al. (2004)	Column Study, Synthetic wastewater	Constant-head method	Sand	N: 175.7 P: 23.0 SS: 352.9 BOD: 2208	1.9×10^{-1} (586) $\pm$ 1.7×10^{-4} (0.5)	$3.5 \times 10^{-5} \pm 7.5 \times 10^{-6}$	≈ 5 order of magnitude reduction
Jnad et al. (2001)	Field Study, Treated wastewater	Darcy's Law	Silty clay loam	N: 37 P: 0.9 TSS: 5 BOD: 15	4.6×10^{-4} (1.3)	After 1.5 yrs: 1.97×10^{-7}	≈ 3 order of magnitude reduction
			Fine sandy loam	N: 29 P: 0.7 TSS: 5 BOD: 23	4.6×10^{-4} (1.3)	After 3 yrs: 3.70×10^{-7}	≈ 3 order of magnitude reduction

N: Total Nitrogen; P: Orthophosphate; TSS: Total Suspended Solids; TOC: total organic carbon; DSE: Denitrified Secondary Effluent; SE: Secondary Effluent; STE: Septic Tank Effluent; TE: Tertiary Effluent

Table 2: Effects of Soil Clogging due to Bacteria, Ponding Depth, and Vegetation

Author	Study Conditions	Soil Type, USCS/USDA Classification	Notes	Parameter investigated	Treatment	Magnitude Reduction in K_e of surface soil
Gupta and Swartzendruber (1962)	Column Study	Sand	Cultural techniques used to obtain counts, so underestimated bacterial density	Bacterial density	Density < 0.4 x 10^6 CFU/g	No change
					Density < 1.3 x 10^6 CFU/g	≈ 2 orders of magnitude
Vandevivere and Baveye (1992a)	Column Study	Sand	Sand columns inoculated with *Arthrobacter spp.*	Bacterial density	< 4 mg (wet weight)/ cm^3	No change
					10 mg (wet weight)/ cm^3	≈ 1 order of magnitude
					20 mg (wet weight)/ cm^3	≈ 2 orders of magnitude
					35 mg (wet weight)/ cm^3	≈ 3 orders of magnitude
Vandevivere and Baveye (1992b)	Column Study	Sand	Demonstrates the impact of microbial component	Effect of environmental conditions on microbial community	No treatment	Up to 4 orders of magnitude
					Oxygen-limited conditions	≈ 1–2 orders of magnitude
					Glucose-limiting conditions	≈ 1–2 orders of magnitude
Vandevivere and Baveye (1992c)	Column Study	Sand		Bacterial density	3.8–6.3% pore space occupied by bacteria	≈ 1–2 orders of magnitude
Duryea (1996)	Field Study	Sand		Ponding depth	Ponding depth 16 ft. vs 7 ft.	Up to 1.4 orders of magnitude
		Fine or loamy sand			Ponding depth 17.5 ft. vs 7 ft.	<1 order of magnitude
McIntyre and Riha (1991)	Control and Vegetated Boxes	Sand		Vegetation	Unvegetated vs. Vegetated simulated artificial wetlands	≈ 50% reduction in vegetated boxes

CFU: Colony Forming Units

Table 3: Research Showing Conditions with Limited or No Clogging

Author	Study Information	Influent Quality	Notes
Pavelic (2007)	Aquifer storage and recovery wells in Southern Australia Total amount of reclaimed water: 483 x 10^3 m^3 Mean injection rates: 8–15 L/s Sandy limestone aquifer	Turbidity < 3NTU N_{TOT} < 10mg/L pH < 7.2	Short-term cause of clogging: turbidity/TSS Long-term: biomass production
Masunaga (2007)	Lab-scale multi-soil layering (MSL) system MSL: soil mixture and zeolite layers Soil mixture: volcanic ash soil rich in OM, sawdust, and granular iron metal at a volume ratio of 75%, 12.5% and 12.5%, respectively	Domestic wastewater pH: 7.4 ± 0.25 TSS: 78.3 ± 75.3 mg/L BOD: 69.5 ± 52.7 mg/L COD: 121.6 ±96.7 mg/L TN: 9.6 ± 2.7 mg/L	No clogging at loading rate < 5.6 x 10^{-4} cm/s (1.6 ft./day) Higher loading rates caused clogging
Fischer (2005)	Riverbank filtration in Dresden, Germany along Elbe River Aquifer 15 m thick overlain by 2–4 m of meadow loam Range flow of river: 100–4,500 m^3/s Mean flow of river: 300 m^3/s Range of $K_e \approx 2 \times 10^{-1}$ to 60 cm/s (280 to 170,000 ft/day)	DOC: 5.6 mg/L–6.9 mg/ L Clogging occurs but functioning of Riverbank Filtration system is not compromised	Severe clogging occurred in the 80's due to river water pollution of organics from pulp and paper mills. Mean DOC was 24.2 mg/L
Hollander (2005)	Reports on Dillon, P., (2002) and Dillon, P., and Pavelic, P., (1996)	TSS loads in the infiltrated water of not more than 150 mg/L do not cause considerable clogging	
Winter (2003)	Comparison of clogging of vertical flow constructed wetlands in Germany. All beds were made of coarse sand or gravel filter with $d_{60}/d_{10} \leq 5$ and $K_e \approx 10^{-2}$ to 10^{-1} cm/s (28 to 280 ft/day)	Recommend: TSS < 100 mg/L, esp. particles > 50µm TSS load: < 5 g/m^2/day COD load: < 20 g/m^2/day	
Magesan (2000)	Sandy loam soil cores treated with secondary wastewater with different C:N ratios (2.5:1, 27:1, 66:1) for 28 weeks. Soil cores received weekly irrigation of 23 mm at a rate of 7 mm/h	Secondary treated wastewater pH: 8.6 TOC: 75 mg/L TN: 30 mg/L NH_4-N: 13 mg/L NO_3-N: <0.1 mg/L	Final K_e of soil treated with different C:N ratios 2.5:1 $K_h = 2.4 \times 10^{-3}$ cm/s (6.9 ft/day) 27:1 $K_e = 1.3 \times 10^{-3}$ cm/ (3.8 ft/day) 66:1 $K_e = 5.0 \times 10^{-4}$ cm/s (1.4 ft/day)
Okubo (1983)	Column experiment 10 cm gravel and 40 cm sand Bulk density: 1.4 to 1.5 g/ cm^3 K_e: 5.0 x 10^{-2} cm/s (142 ft/day)	Synthetic wastewater C:N: 1.44 TSS ranging from 1.4–14.6 mg/L TOC ranging from 7.2–21.6 mg/L	TSS < 2 mg/L and TOC < 10 mg/L for no clogging

NTU: Nepholemetric Turbidity Units; NTOT: Total Nitrogen; TSS: Total Suspended Solids; BOD: Biological Oxygen Demand; COD: Chemical Oxygen Demand; DOC: Dissolved Organic Carbon; TOC: Total Organic Carbon; C:N: Carbon to Nitrogen Ratio; NO3-N: Nitrate as N; NH4-N: Ammonia as N

4 Conclusions

The hydraulic properties of infiltration basins used to recharge surface water and wastewater effluent typically become dominated by a low conductivity clogging layer which forms at the water-soil interface. The clogging layer is often thin (millimeters to 4 centimeters) and may consist of suspended solids, algae, microbes, dust, and salts. Clogging layer formation has been observed to reduce the hydraulic conductivity of soil materials by as much as five orders of magnitude.

There are physical, chemical, and biological causes of clogging. Factors that influence the development and extent of a clogging layer include water quality, basin soil texture, ponding depth, hydraulic loading rate and cycle, and vegetation. Research has found that biological oxygen demand and total suspended solids are the most important components of water quality that influence the formation of a clogging layer. In addition, extended ponding periods enhance soil clogging, whereas wetting and drying cycles tend to destroy the clogging layer.

5 References

Aaltomaa, T. and Joy, D.J., (2002) Field testing of absorption bed clogging. CSCE/ EWRI of ASCE Environmental Engineering Conference, Niagara Falls.

Allison, L.E., (1947) Effect of microorganisms on permeability of soil under prolonged submergence. Soil Science. 63:439–450.

Alvarez, J.A., Ruiz, I. Soto, M., (2008) Anaerobic digesters as a pretreatment for constructed wetlands. Ecological Engineering. 33: 54–67.

Batchelor, A. and Loots, P., (1997) A critical evaluation of a pilot scale subsurface flow wetland: 10 years after commissioning. Water Science and Technology 35: 337–343.

Baveye, P., Vandevivere, P. Hoyle, B.L., DeLeo, P.C., and de Lozada, D.S., (1998) Environmental impact and mechanisms of the biological clogging of saturated soils and aquifer materials. Critical Reviews in Environmental Science and Technology. 28:123–191.

Beach, D. N.H., McCray, J., Lowe, K. S., and Siegrist, R. L., (2005) Temporal changes in hydraulic conductivity of sand porous media biofilters during wastewater infiltration due to biomat formation. Journal of Hydrology. (article in press, online)

Becker, M.W., Bauer, B. and Hutchinson, A.S., (2012) Measuring Percolation from an Artificial Recharge Basin using Fiber Optic Distributed Temperature Sensing. Ground Water (In press).

Behnke, J.J., (1969) Clogging in surface spreading operations for artificial groundwater recharge. Water Resources Research. 5(4): 870–876

Berend, J.E., An analytical approach to the clogging effect of suspended matter, Tahal, Water Planning for Israel Ltd. (Tel Aviv).

Blazejewski, R. and Murat-Blazejewski, S., (1997) Soil clogging phenomena in constructed wetlands with subsurface flow. Water Science and Technology. 35: 183–188.

Bouwer, H., (1988) Design and management of infiltration basin for artificial recharge of groundwater. In Proceedings of the 32nd annual New Mexico conference on groundwater management, Albuquerque, New Mexico, November 5-6, 1987, pp. 111–123.

Bouwer, H. and Rice, R.C., (1989) Effect of water depth in groundwater recharge basins on infiltration. Journal of Irrigation and Drainage Engineering, ASCE, 115: 556–567.

Bouwer, H., Ludke, J., and Rice, R.C., (2001) Sealing pond bottoms with muddy water. Ecological Engineering. 18:233–238.

Bouwer, H. and Rice, R.C., (2001) Capturing flood waters for artificial recharge of groundwater. Proceedings of 10th Biennial Symp. Artificial Recharge of Groundwater, Tucson, AZ, AZ Hydroglogical Society, pp 99–106.

Bouwer, H., (2002) Artificial recharge of groundwater: hydrogeology and engineering. Hydrogeology Journal. 10:121–142.

Brix, H., (1994) Functions of macrophytes in constructed wetlands. Water Science and Technology 29: 71–78.

Brix, H., (1997) Do macrophytes play a role in constructed treatment wetlands? Water Science and Technology. 35: 11–17.

Cooper, D., Griffin, P., and Cooper, P., (2005) Factors affecting the longevity of sub-surface horizontal flow systems operating as tertiary treatment for sewage effluent. Water Science and Technology 51: 127–135.

Dahab, M.F., and Surampalli, R.Y., (2001) Subsurface-flow constructed wetlands treatment in the plains: five years of experience. Water Science and Technology 44: 375–380.

Daniel, T.C., and Bouma, J., (1974) Column studies of soil clogging in a slowly permeable soil as a function of effluent quality. Journal of Environmental Quality. 3 (4): 321–326.

Dillon, P., and Pavelic, P., (1996) Guidelines on the quality of stormwater and treated wastewater for injection into aquifers for storage and reuse, Urban Water Research Association of Australian Research, Report No. 109.

Dillon, P., (2002) Banking of stormwater, reclaimed water and potable water in aquifers, Proceedings of IGWC, Dindigul, India.

Duryea, P.D., (1996) Clogging Layer Development and Behavior in Infiltration Basins used for Soil Aquifer Treatment of Wastewater. Doctoral Dissertation. Arizona State University, Tempe, Arizona.

EPA (U.S. Environmental Protection Agency), (1999) Guidance Manual Turbidity Provisions. Accessed on-line: http://www.epa.gov/OGWDW/mdbp/pdf/turbidity/chap_07.pdf. June 29, 2008.

EWRI/ASCE. (2001) Standard guidelines for artificial recharge of groundwater, Environmental and Water Resources Institute, American Society of Civil Engineers EWRI/ASCE 34-01.

Frankenberger, W.T. ,Troeh, F.R., and Dumenil, L.C., (1979) Bacterial effects on hydraulic conductivity of soils. Soil Science Society of America Journal. 43:333–338.

Grischek, T., Schubert, J., Jasperse, J.L., Stowe, S.M., Collins, M.R., (2007) What is the appropriate site for RBF? In Proceedings of the 6th International Symposium on Managed Aquifer Recharge. ISMAR 6, Phoenix, Arizona, October 29– November 2, 2007.

Gupta, R.P., and Swartzendruber, D., (1962) Entrapped air content and hydraulic conductivity of quartz sand. Soil Science Society of America Proceedings. 26:6–10.

Harpaz, Y., (1971) Artificial groundwater recharge by means of wells in Israel. Proceedings of the Journal of the Hydraulic Division. 1947–1964.

Hauser, V.L., and Lotspeich, F.B., (1967) Artificial ground water recharge through wells. Journal of Soil and Water Conservation, 11–15.

Holländer, H.M., Hinz, I., Boochs, P.W., and Billib, M., (2005) Experiments to determine clogging and redevelopment effects of ASR-wells at laboratory scale. In: Proceedings of the 5th International Symposium on Managed Aquifer Recharge ISMAR 5, Berlin, Germany, June 10–16, 2005.

Houston, S.L., Duryea, P.D., and Hong, R., (1999) Infiltration considerations for ground-water recharge with waste effluent. Journal of Irrigation and Drainage Engineering. 125(5): 264–272.

Hutchinson, A.S., (2007) Challenges in optimizing a large-scale managed aquifer recharge operation in an urbanized area. In Proceedings of the 6th International Symposium on Managed Aquifer Recharge. ISMAR 6, Phoenix, Arizona, October 29– November 2, 2007.

Jiang, Y., and Matsumoto, S., (1995) Change in microstructure of clogged soil in soil waste-water treatment under prolonged submergence. Soil Science and Plant Nutrition. 41: 20–213.

Jnad, I., Lesikar, B., Kenimer, A., and Sabbagh, G., (2001) Subsurface drip dispersal of residential effluent. II. Soil hydraulic characteristics. Transactions of the American Society of Agricultural Engineers. 44(5): 1159–1165.

Lacher, L.J., (1996) Recharge Characteristics of an Effluent Dominated Stream near Tucson, Arizona. Doctoral Dissertation. University of Arizona, Tucson, Arizona.

Langergraber, G., Haberl, R., Laber, J., and Pressl, A., (2003) Evaluation of substrate clogging processes in vertical flow constructed wetlands. Water Science and Technology. 48:25–34.

Magesan, G. N., Williamson, J.C., Yeates, G. W., and Lloyd-Jones, A. Rh., (2000) Wastewater C:N ratio effects on solid hydraulic conductivity and potential mechanisms for recovery. Bioresource Technology. 71: 21–27.

Magesan, G.N., Williamson, J.C., Sparling, G.P., Schipper, L.A., and Lloyd-Jones, A. 1999. Hydraulic conductivity in soils irrigated with wastewaters of differing strengths: Field and laboratory studies. Australian Journal of Soil Research. 37:391–402.

Masunaga, T., Sato, K., Mori, J., Shirahama, M., Kudo, H., and Wakatsuki, T. 2007. Characteristics of wastewater treatment using a multi-soil-layering system in relation to wastewater contamination levels and hydraulic loading rates. Soil Science and Plant Nutrition. 53: 215–223.

McDowell-Boyer, L.M., Hunt, J.L., and Sitar, N. 1986. Particle transport through porous media. Water Resources Research. 22:1901–1921.

McIntyre, B.D. and Riha, S.J. 1991. Hydraulic conductivity and nitrogen removal in an artificial wetland system. Journal of Environmental Quality. 20:259–263.

Milczarek, M., Woodside, G., Hutchinson, A., Keller, J., Rice, R., and Canfield, A. 2009. The Orange County Water District Riverbed Filtration Pilot Project: Water Quality and Recharge Improvements Using Induced Riverbed Filtration. In Proceedings of the 7th International Symposium on Managed Aquifer Recharge. ISMAR 7, Abu Dhabi (UAE), October 9 – 13, 2009.

Mohanty, B.P., T.H. Skaggs, and M.Th. van Genuchten. 1998. Impact of saturated hydraulic conductivity on the prediction of tile flow. Soil Science Society of America Journal. 62:1522–1529.

Natural Resources Conservation Service, United States Department of Agriculture, 2005. Saturated Hydraulic Conductivity: Water Movement Concepts and Class History. http://soils.usda.gov/technical/technotes/note6.html.

Natural Resources Conservation Service, United States Department of Agriculture, 1977. Soil Survey of Maricopa County, Central Part. NRCS: see Natural Resources Conservation Service.

Okubo, T. and Matsumoto, J. 1983. Biological clogging of sand and changes of organic constituents during artificial recharge. Water Research. 17: 813–821.

Pavelic, P., Dillon, P.J., Barrya, K.,E., Vanderzalma, J.L.,. Corrella, R.L., and Rinck-Pfeiffer, S.M. 2007. Water quality effects on clogging rates during reclaimed water ASR in a carbonate aquifer. Journal of Hydrology. 334:1–16.

Pavelic, P., Dillon, P.J., Barry, K.W., Herczeg, A.L., Rattray, K.J., Hekmeijer, P., and Gerges, N.Z., (1998) Well clogging effects determined from mass balances and hydraulic response at a stormwater ASR site. TISAR'98 In the Proceedings of the Third Symposium on Artificial Recharge of Groundwater, September 21–25, 1998, Amsterdam, pp 61–66.

Phipps, D., Lyon, S., Hutchinson, A. 2007. Development of a percolation decay model to guide future optimization of surface water recharge basins. In Proceedings of the 6th International Symposium on Managed Aquifer Recharge. ISMAR 6, Phoenix, Arizona, October 29 – November 2, 2007.

Platzer, C. and Mauch, K. 1997. Soil clogging in vertical flow reed beds – mechanisms, parameters, consequences, and solutions? Water Science and Technology. 35: 175–181.

Racz, A.J., Fisher, A.T., Schmidt, C.M., Lockwood, B.S., and Los Huertos, M. 2012. Spatial and Temporal Infiltration Dynamics During Managed Aquifer Recharge. Ground Water 50, No. 4, pp 562–570.

Rehg, K.J., Packman, A.I. and Ren, J. 2005. Effects of suspended sediment characteristics and bed sediment transport on streambed clogging. Hydrological Processes. 19:413–427.

Rinck-Pfeiffer, S, Ragusa, S., Sztajnbok, P., and Vandevelde, T. 2000. Interrelationships between biological, chemical, and physical processes as an analog to clogging in aquifer storage and recovery (ASR) wells. Water Research. 34:2110–2118.

Rodgers, M., Mulqueen, J., and Healy, M.G. 2004. Surface clogging in an intermittent stratified sand filter. Soil Science Society of America. 68: 1827–1832.

Sakthivadivel, R. 1966. Theory and mechanism of filtration of non-colloidal fines through a porous medium. Tech. Rep. HEL 15–5, Hydr. Engerg. Lab., University of California, Berkeley, CA.

Schubert, J 2004. Significance of hydrologic aspects on RBF performance. NATO Advanced Research Workshop, Samorin, Slovakia. September 7–10, 2004. http://www.soulstatic.com/NATORBF/papers/schubert/hydrology.pdf (accessed 6.16.2008).

Siegrist, R.L., (1987) Soil clogging during subsurface wastewater infiltration as affected by effluent composition and loading rate. Journal of Environmental Quality. 16(2): 181–187.

Siegrist, R.L., and Boyle, W.C., (1987) Wastewater-induced soil clogging development. Journal of Environmental Engineering. 113(3): 550–566

Siegrist, R.L., Smed-Hildmann, R., Filip, Z.K., and Jenssen, P.D., 1991. Humic substance formation during wastewater infiltration. In: Conference Proceedings, On-site wastewater treatment. ASAE Publication 10-91, Chicago, IL, USA, pp. 223–232.

Taylor, S., and Jaffe, P.R., (1990) Substrate and Biomass Transport in a Porous Medium. Water Resources Research. 26(9): 2181–2194.

Taylor, S., and Jaffe, P.R., (1990a) Biofilm growth and the related changes in the physical properties of a porous medium. 1. Experimental investigation. Water Resources Research. 26(9): 2153–2159.

Vandevivere, P., and Baveye, P., (1992a) Saturated hydraulic conductivity reduction caused by aerobic bacteria in sand columns. Soil Science Society of America Journal. 56: 1–13.

Vandevivere, P., and Baveye, P., (1992b) Effect of bacterial extracellular polymers on the saturated hydraulic conductivity of sand columns. Applied and Environmental Microbiology. 58: 1690–1698.

Vandevivere, P., and Baveye, P., (1992c) Relationship between transport of bacteria and their clogging efficiency in sand columns. Soil Science Society of America Journal. 58: 2523–2530.

Vecchioli, J., (1972) Experimental injection of tertiary treated sewage in a deep well at Bay Park, Long Island, NY. New England Water Works Association. 86:87–103.

Vyzamal, J., Brix, H., Cooper, P.F., Green, M.B., and Haberl R. (eds.) (1998) Constructed wetlands for wastewater treatment in Europe. Bachhuys Publishers, Leiden, The Netherlands.

Winter, K.J., and Goetz, D., (2003) The impact of sewage composition on the soil clogging phenomena of vertical flow constructed wetlands. Water Science and Technology 48: 9–14.

Surface Spreading Recharge Facility Clogging – The Orange County Water District Experience

A. Hutchinson[1] with assistance from D. Phipps[2], G. Rodriguez[3], G. Woodside[4], and M. Milczarek[5]

[1] *Recharge Planning Manager;* [2] *Research Director, Research and Development;* [3] *Senior Scientist*; [4] *Executive Director of Planning and Natural Resources*; [5] *GeoSystems Analysis, Inc.*

1 Introduction

The Orange County Water District (OCWD or District), located in Orange County, California, has been recharging water from various sources since 1936 in a variety of facilities, including injection wells, surface water infiltration basins, and river/stream channels. Clogging has been and remains a constant constraint in maximizing the performance of these facilities. OCWD and others have conducted extensive research into clogging mechanisms, clogging rates, the nature of the clogging material, how to reduce clogging, and how to clean clogged facilities. The purpose of Part II of the Clogging Monograph is to provide data on the OCWD experience in clogging of surface water recharge facilities to serve as a useful reference for both researchers and practitioners.

2 Hydrogeologic Setting

The Orange County Groundwater Basin (Basin) underlies the northern half of Orange County and covers approximately 900 km^2. Figure 1 shows the District boundaries, which are largely coincident with the Basin boundaries. Basin aquifers form a complex series of interconnected alluvial sand and gravel deposits that extend over 600 m deep (DWR, 1967). In coastal and central portions of the Basin, known as the "Pressure Area", these deposits tend to be separated by extensive lower-permeability clay and silt deposits, which act as aquitards. In the inland area of the Basin, known as the "Forebay", the clay and silt deposits become thinner and more discontinuous, allowing groundwater to flow more easily between shallow and deeper aquifers. Most of the sediments in the Forebay were deposited by the ancestral Santa Ana River (SAR). As a result they are comprised predominately of sands and gravels with occasional silt and clay layers. The depth to groundwater in the Forebay ranges from 5 m adjacent to the SAR and recharge basins (during recharge) to approximately 40 m.

Sediment permeability in the Forebay is high. Average horizontal groundwater velocities near the SAR measured by tracer testing range from 0.3 to 2.9 km/year, or 0.8 to 7.9 m/day (Clark et al., 2004). Given a hydraulic gradient range of 0.01 to 0.005 and an average horizontal velocity of 1 km/year (2.7 m/day), the hydraulic conductivity of sediments is in the range of 100 m/day (Clark et al., 2004). Vertical groundwater velocities near the SAR average 0.13 km/year (0.36 m/day), which is an order of magnitude less than observed horizontal velocities (Clark et al., 2004).

This is not surprising given that vertical hydraulic conductivities are generally much less than horizontal hydraulic conductivities in layered sedimentary deposits (Freeze and Cherry, 1979).

3 Surface Water Spreading Development

Shortly after the District was formed in 1933, the District, along with the Orange County Flood Control District (OCFCD), began experimenting with ways to increase the percolation capacity of the SAR channel. These experiments included removing vegetation and re-sculpting the river bank and river bottom (OCWD, 2003a). Based on the success of these experiments, the District began purchasing portions of the SAR channel as they became available. Today, the District owns approximately 10 km of the SAR channel.

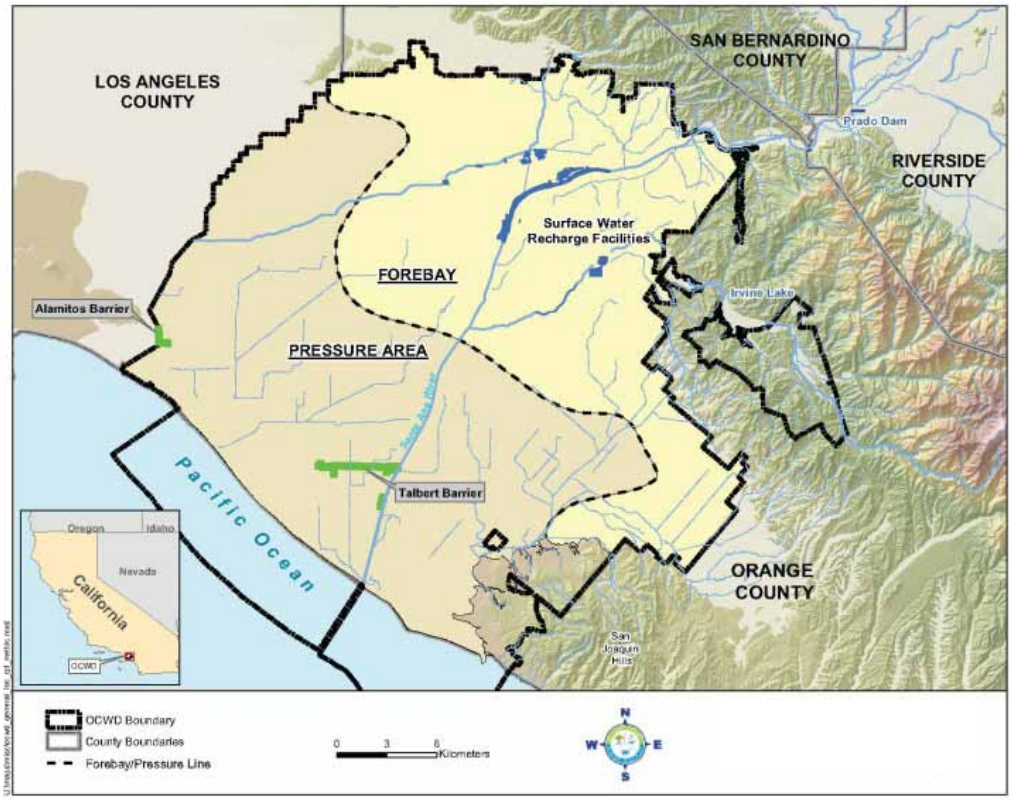

Figure 1: OCWD Location Map

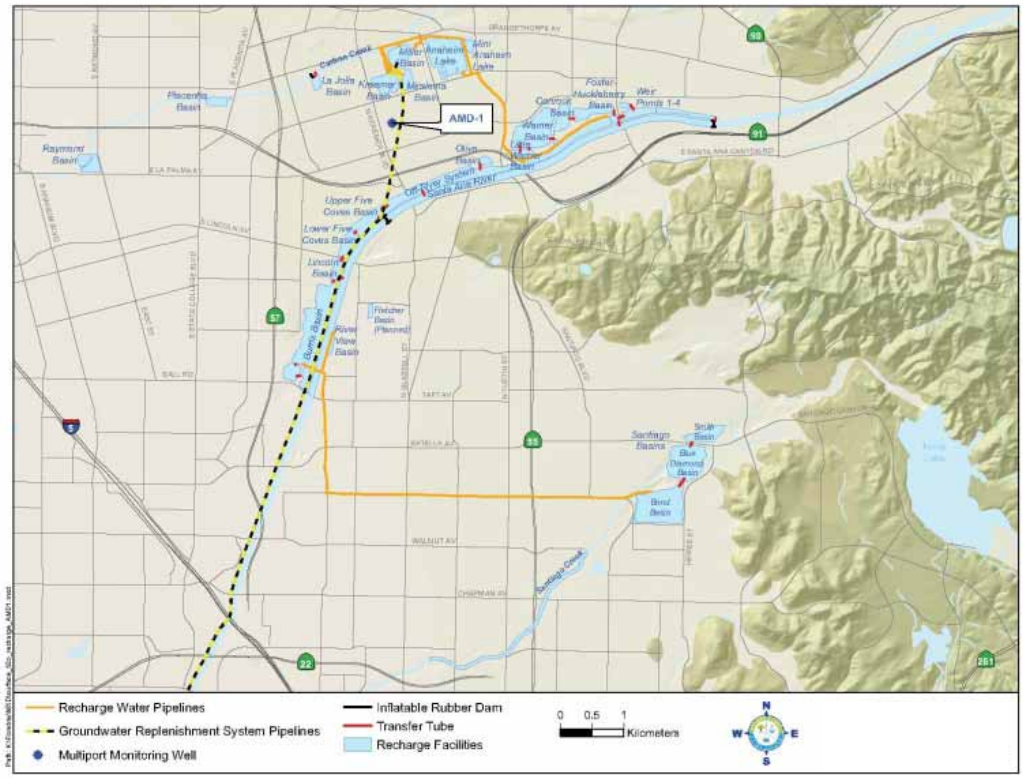

Figure 2: Surface Water Recharge Facilities

Currently, the District owns over 600 hectares of land in the Forebay on which it has constructed or operates over two dozen recharge facilities that cover nearly 440 wetted hectares (OCWD, 2003a; OCWD, 2003b) (see Figure 2). Several types of recharge facilities are used to spread surface water, including:

- River/stream channel (e.g., Santa Ana River, Santiago Creek)
- Deep recharge basins (e.g., Anaheim Lake, Kraemer Basin)
- Former gravel pits (e.g., Santiago Basins, Burris Basin)
- Shallow recharge basins (e.g., River View, La Jolla, and Miraloma Basins)
- Flood-control basins (e.g., Miller, Placentia, and Raymond Basins)

The total storage volume of the surface water spreading system is approximately 32 million m^3. Table 1 summarizes the main characteristics of the surface water spreading facilities. Maximum percolation rates range from 0.1 m/day to 3 m/day. Percolation rates, prior to clogging, are primarily controlled by underlying sediment permeability, but are also influenced in some areas by groundwater mounding.

Over the 10 year period from 2002–2012, total recharge to the groundwater basin averaged 430 million m^3 per year (Table 2). An estimated 19 percent of the recharge is incidental (unmeasured) recharge. The remaining recharge is due to managed aquifer recharge (MAR) by OCWD. MAR is accomplished by surface spreading, in-lieu recharge and seawater barrier recharge. The main source of supply is base and storm flows from the SAR (Table 2). Table 3 shows that the surface spreading facilities are responsible for 80 percent of total MAR to the basin.

Table 1: Characteristics of OCWD Surface Water Spreading Facilities

Facility	Maximum Wetted Area (hectares)	Maximum Depth (m)	Maximum Storage Capacity [(1)] (1,000 m^3)	Maximum Percolation Rate (m/day)
Anaheim Lake	29	15	2,788	0.84
Burris Basin	49	19	3,293	0.15
Conrock Basin (Warner System)	10	16	1,320	(Note 4)
Five Coves Basin: Lower	6	5	224	0.75
Five Coves Basin: Upper	6	5	202	0.40
Foster-Huckleberry Basin (Warner System)	8	11	777	(Note 4)
Kraemer Basin	13	17	1,443	2.34
La Jolla Basin	3	2	32	2.79
Lincoln Basin	4	2	74	0.06
Little Warner Basin (Warner System)	4	10	278	(Note 4)
Miller Basin (2)	10	7	370	1.09
Mini-Anaheim Lake	2	1	16	2.41
Miraloma Basin	4	3	77	3.02
Off-River Channel	36	N/A	N/A	0.17
Olive Basin	2	12	150	1.56
Placentia Basin (2)	4	12	432	0.67
Raymond Basin (2)	8	8	456	0.32
River View Basin	1	1	14	1.68
Santa Ana River: Imperial Hwy to Orangewood Ave.	118	N/A	N/A	0.21
Santiago Basins	76	41	16,923	0.39
Santiago Creek: Santiago Basins to Hart Park (3)	4	N/A	N/A	0.91

Facility	Maximum Wetted Area (hectares)	Maximum Depth (m)	Maximum Storage Capacity [1] (1,000 m^3)	Maximum Percolation Rate (m/day)
Warner Basin	28	16	3,232	0.60
Weir Pond 1	2	2	35	(Note 4)
Weir Pond 2	4	2	52	(Note 4)
Weir Pond 3	6	4	197	(Note 4)
Weir Pond 4	2	3	27	(Note 4)
Totals	**439**		**32,413**	

(1) Maximum storage capacity is typically not achieved for most facilities due to need to reserve buffer space for system flow and level fluctuations. Depths and storage volumes are not applicable (N/A) to stream/river channels.

(2) Owned by Orange County Flood Control District (OCFCD). Maximum storage capacity shown is maximum flood control storage.

(3) Various owners, including OCFCD, City of Orange, and Metropolitan Water District.

(4) Desilting Basins do not contribute to measurable recharge.

Table 2: 10-Year Average Recharge to Orange County Groundwater Basin: By Source 2002–12

Source	(1,000 m^3/yr)	Percent of Total
SAR* (Base and storm flow)	227,141	53%
Imported Water (CRA/SWP)	83,653	20%
Recycled Water (GWRS)	36,128	8%
Total OCWD Recharge	**346,921**	**81%**
Incidental Recharge	82,639	19%
Grand Total	**429,560**	**100%**

*Includes other local drainages, such as Santiago Creek.

Table 3: 10-Year Average Recharge to Orange County Groundwater Basin: By Facility 2002–12

Facility	(1,000 m^3/yr)	Percent of Total
Surface Spreading	276,238	80%
In-lieu*	46,168	13%
Seawater Barrier	24,515	7%
Total OCWD Recharge	**346,921**	**100%**

*In-lieu recharge occurs when groundwater producers turn off their wells and use an alternative source of water, such as imported water, to meet their demands.

4 Groundwater and Recharge Water Quality

Because surface spreading has been taking place in the Forebay since the mid-1930s, the chemical composition of groundwater in the vicinity of the surface recharge facilities is similar to SAR water. Groundwater in the Forebay, as represented by the centrally located multi-depth monitoring well (AMD-1, see Figure 2), and SAR water are both NaCaClHCO3 type waters.

Other sources used for recharge include recycled water produced by the District's Groundwater Replenishment System (GWRS) and imported water from the Colorado River Aqueduct (CRA) and State Water Project (SWP). The CRA coveys water from the Colorado River to the southern California region. The SWP conveys water from northern California to users in other parts of the state, including Orange County. Table 4 (see next page) summarizes the chemical quality of Forebay groundwater and recharge source waters.

4.1 Total Suspended Solids

Based on OCWD's historic operations, the most important water quality constituent is the total suspended solids (TSS) concentration because higher TSS concentrations cause clogging and reduced recharge facility performance.

At the Imperial Rubber Dam, where SAR water enters the recharge system, average TSS concentrations are fairly uniform throughout the year, as indicated in Table 5. Even average TSS concentrations during the storm season, which runs from November to March, are not much different than TSS concentrations during the normally dry months.

The TSS concentration of imported water is generally less than 1 mg/L and the TSS concentration of GWRS water is barely measurable at 0.1 mg/L.

Particle size analyses show that the suspended solids in SAR water range from 0.6– 60 microns in size, with the majority in the 5 to 10 micron range. The size distribution is generally similar for base flow and storm flow seasons as shown on Figure 3. The generally small size of the suspended solids means that even with long retention times, a fraction of the suspended solids will not settle out by gravity and continue to downstream facilities.

Table 5: Historical TSS Concentrations in SAR Water at Imperial Rubber Dam, 1970–2012

Month	Average (mg/L)	Minimum (mg/L)	Maximum (mg/L)	No. of Samples
January	98	3	1,230	101
February	120	<1	1,600	84
March	50	2	620	116
April	34	1	203	109
May	97	<1	2,363	78
June	86	2	1,736	87
July	109	18	1,296	80
August	113	8	3,000	197
September	72	<1	347	79
October	126	3	2,129	73
November	63	4	503	68
December	150	2	4,252	100
Total	**94**			**1,172**

Analyses of the clogging layers found in Anaheim, Kraemer and Miller Basins show that the clogging material consisted of approximately 92 percent mineral materials and approximately 8 percent volatile organics as determined by ashing samples in a 500 ° C muffle furnace. Mineralogical analysis (x-ray diffraction) indicates the mineral materials are comprised of montmorillonite (34–50%), quartz (17–19%), plagioclase feldspar (16–33%), illite/mica (6–9%), and calcite (4–7%). Montmorillonite percentages in Anaheim and Kraemer Basins ranged from 34 to 35 percent.

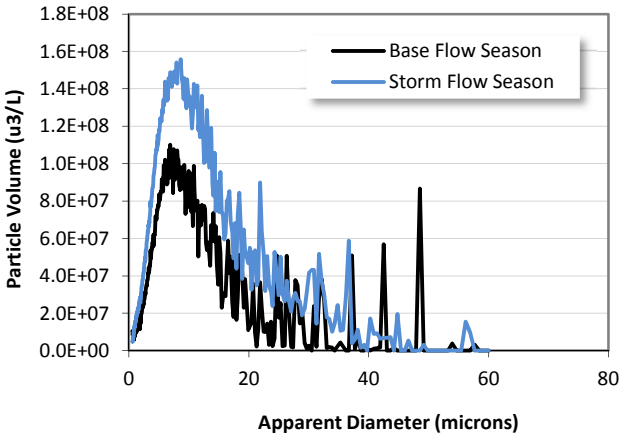

Figure 3: Average Particle Size Distribution in SAR Water at Imperial Dam, 2011–2012

Table 4: Groundwater and Recharge Water Quality

Parameter or Constituent	Acronym	Units	Groundwater (1)			Santa Ana River (2)			GWRS (3)			Imported CRA(4)			Imported SWP (5)		
			Min	Max	Avg	Min	Max	Avg	Min	Max	Avg	Min	Max	Avg	Min	Max	Avg
Total Alkalinity	TOTALK	mg/L	80	214	**159**	81	274	**202**	13	49	**31**	106	138	**127**	50	85	**73**
Total Dissolved Solids	TDS	mg/L	266	628	**484**	268	776	**622**	14	86	**43**	454	712	**624**	132	340	**249**
Turbidity	TURB	NTU				1	360	**30**	0.01	5.90	**1.14**	0.60	1.40	**0.90**	1.20	1.20	**1.20**
Specific Conductance	EC	um/cm	522	1,060	**853**	388	1,280	**1,022**	37	128	**87**	925	1,050	**986**	237	584	**436**
pH (field)	F-pH	UNITS	6.5	9.4	**7.9**	7.7	9.1	**8.4**	7.2	9.1	**8.4**	7.2	9.3	**8.3**	7.4	9.0	**8.2**
Temperature (field)	F-TEMP	C	17.7	24.7	**20.3**	9.2	29.9	**20.6**	23.3	29.3	**26.0**	13.4	26.7	**21.5**	16.5	24.5	**19.1**
Eh (field)	F-ORP	mV				-40	309	**162**	93	371	**229**	-79	583	**227**	118	193	**156**
Chloride	Cl	mg/L	57.5	139.0	**98.3**	32.3	155.0	**119.1**	2.4	7.0	**4.6**	84.0	97.1	**91.4**	23.6	68.7	**57.1**
Sulfate	SO4	mg/L	0.1	158.0	**108.9**	42.3	190.0	**128.7**	0.1	2.4	**0.3**	204.0	294.0	**243.7**	24.7	86.2	**50.0**
Carbonate Alkalinity	CO_3Ca	mg/L	0.1	42.7	**3.8**	0.1	62.3	**18.5**	0.1	18.6	**1.2**	0.1	9.8	**2.4**	0.1	0.1	**0.1**
Bicarbonate Alkalinity	HCO_3Ca	mg/L	80.2	214.0	**155.8**	81.4	257.0	**183.8**	12.5	47.0	**29.9**	98.8	138.0	**124.9**	50.0	85.1	**73.0**
Total Silica	SIO2	mg/L				9.7	24.8	**18.5**	0.1	1.3	**0.2**						
Calcium	Ca	mg/L	8.0	92.5	**56.9**	33.8	103.0	**82.1**	0.5	15.4	**9.2**	65.5	85.6	**75.5**	14.0	29.9	**23.3**
Calcium (dissolved)	Ca-DIS	mg/L				46.9	101.0	**79.3**									
Magnesium	Mg	mg/L	11.2	31.3	**19.6**	7.7	28.9	**21.5**	0.0	0.0	**0.0**	24.8	31.5	**28.4**	6.8	14.5	**11.9**
Magnesium (dissolved)	Mg-DIS	mg/L				11.4	27.3	**21.2**									
Sodium	Na	mg/L	68.1	107.0	**89.0**	26.9	127.0	**99.6**	4.4	8.9	**6.5**	79.9	104.0	**94.0**	22.6	62.3	**49.0**
Sodium (dissolved)	Na-DIS	mg/L				47.9	120.0	**93.7**									
Potassium	K	mg/L	4.2	7.5	**5.9**	5.7	15.8	**10.7**	0.0	0.7	**0.4**	3.9	5.6	**4.7**	1.7	3.0	**2.6**
Potassium (dissolved)	K-DIS	mg/L				5.5	13.1	**9.7**									
Iron	Fe	ug/L							0.1	33.1	**3.6**	8.4	22.6	**16.8**			
Iron (dissolved)	Fe-DIS	ug/L	0.1	1,810	**166.5**	6.8	111.0	**27.1**									
Aluminum	Al	ug/L							0.1	14.1	**4.6**	6.5	24.2	**16.5**			

Parameter or Constituent	Acronym	Units	Groundwater (1)			Santa Ana River (2)			GWRS (3)			Imported CRA(4)			Imported SWP (5)		
			Min	Max	Avg	Min	Max	Avg	Min	Max	Avg	Min	Max	Avg	Min	Max	Avg
Aluminum (dissolved)	Al-DIS	ug/L	0.1	5.4	**1.7**	4.8	64.1	**17.0**									
Arsenic	As	ug/L				4.00	4.00	**4.00**	<1	<1	**<1**	1.90	2.60	**2.17**			
Arsenic (dissolved)	As-DIS	ug/L	<1	1.10	**0.18**	1.60	4.80	**3.16**	<1	<1	**<1**						
Copper	Cu	ug/L							0.1	0.1	**0.1**	2.0	2.3	**2.1**			
Copper (dissolved)	Cu-DIS	ug/L	0.1	1.8	**0.8**	0.1	3.2	**2.1**									
Manganese	Mn	ug/L							0.1	1.4	**0.2**	1.4	4.8	**2.5**			
Manganese (dissolved)	Mn-DIS	ug/L	11.7	400.0	**131.4**	15.2	95.6	**34.1**	0.1	1.5	**0.2**	0.1	0.1	**0.1**			
Zinc	Zn	ug/L							0.1	4.2	**0.7**	0.1	1.2	**0.8**			
Zinc (dissolved)	Zn-DIS	ug/L	0.1	22.0	**4.7**	0.1	17.9	**7.8**									
Total Hardness	TOTHRD	mg/L	67.8	331.0	**223.8**	116.0	369.0	**293.4**	12.8	38.4	**23.2**	271.0	334.0	**303.4**	63.0	134.0	**106.8**
Nitrate	NO_3	mg/L	0.04	16.30	**5.86**	2.60	27.80	**13.57**	0.04	6.90	**2.99**	0.50	1.70	**1.05**	1.30	4.60	**2.85**
Phosphate	PO4-P	mg/L	0.001	0.170	**0.046**	0.270	1.210	**0.791**	0.001	0.001	**0.001**	0.001	0.010	**0.002**	0.050	0.070	**0.060**
Ammonia Nitrogen	NH_3-N	mg/L				0.01	0.30	**0.03**	0.01	1.90	**0.76**	0.01	0.01	**0.01**	0.01	0.01	**0.01**
Total Organic Carbon	TOC	mg/L	0.9	12.2	**3.8**	3.9	17.3	**5.7**	0.0	2.4	**0.2**	2.6	3.2	**2.9**	3.1	4.4	**3.9**

(1) Groundwater based on OCWD AMD-1: MP-1 to MP-7, 2007–2012 – data based on the average of all 7 MP zones
(2) Santa Ana River water based on 2007–2012 – samples collected at SAR and Imperial Highway
(3) Groundwater Replenishment System (GWRS) based on 2008–2012
(4) Imported Colorado River Water (CRA) based on 2009–2012 – samples collected at OC-28
(5) Imported State Water Project (SWP) based on 2007–2012 – data based on 4 grab samples delivered to OC-28A: 4/11/2007, 4/25/2007, 5/10/2011 and 7/23/2012

A higher concentration of montmorillonite (50%) was found in Miller Basin and is likely due to the fact that this facility also serves as a flood control basin and periodically receives sediment-laden flood flows from a different watershed (Carbon Creek). Based on microscopic examination, the organic portion of the clogging layer contains biological organisms, including bacteria, diatoms, blue-green algae, and green algae.

Due to the high volume of water diverted from the SAR into the recharge system, the loading of suspended solids is significant and exceeds 10,000 metric tons per year as summarized in Table 6.

Table 6: Average Solids Loading of Surface Water Recharge Facilities, 2002–12

Source	Average TSS (mg/L)	Average Water Recharged (1,000 m^3/yr)	Avg. Annual Load (metric tons/yr)
SAR* (Base and storm flow)	94	149,576	14,060
Imported Water (CRA/SWP)	1	83,651	84
Recycled Water (GWRS)	0.1	36,128	3.6
Total Avg. Annual Load			**14,147**

*Based on long-term average from 1970–2012. Excludes recharge in the SAR channel (62,880 afy) because solids are eventually conveyed to the ocean.

The loading of solids into the recharge system not only reduces recharge facility performance, it produces a significant maintenance effort to clean the facilities and restore percolation rates. Cleaning usually entails draining and drying the facilities and removing the clogging layer with heavy equipment. While effective in restoring recharge rates, this process removes some of the underlying native sediment which deepens the basins over time. Eventually the deepened portions of the basins have to be re-filled to ensure proper draining.

For the deeper basins, a key issue is the inability to clean the banks, which have a 3:1 slope. Typically, the banks are disturbed by bulldozers with some minor removal of sediment. Over time, this results in an accumulation of clogging material on the basin sidewalls. Proof of this is that the native sediments in some of deep basins have less than 5 percent fines (as defined by particles passing the 200 sieve – 74 microns and smaller) but the surficial bank sediments have up to 20 percent fines. Even with 20 percent fines, the permeability of the basin sidewall sediments is still high, however, the accumulated fines can be re-suspended when the basin is filled and by wave action. Once re-suspended, these fines settle out and contribute to clogging.

The District has been able to dedicate selected basins to specific sources of water for extended periods, which allows for comparisons of facility performance with different source waters. Figure 4 shows how the percolation rate of Kraemer Basin differs when recharging SAR water and imported/GWRS water. The percolation rate decay seen with imported and GWRS water are very similar and thus are combined for simplicity. The TSS of SAR water entering Kraemer Basin is generally less than 10 mg/L while the TSS of imported water is generally 1 mg/L and 0.1 mg/L for GWRS water.

Figure 4 shows that the rate of percolation decay with SAR water is rapid, which requires the basin be cleaned approximately three times per year. By way of comparison, the total recharge achieved in 60 days with SAR water is 4.8 million m^3, but with imported/GWRS water the total recharge for the same time period is 14.1 million m^3. This shows the negative impact of clogging caused by TSS loading on recharge facility performance.

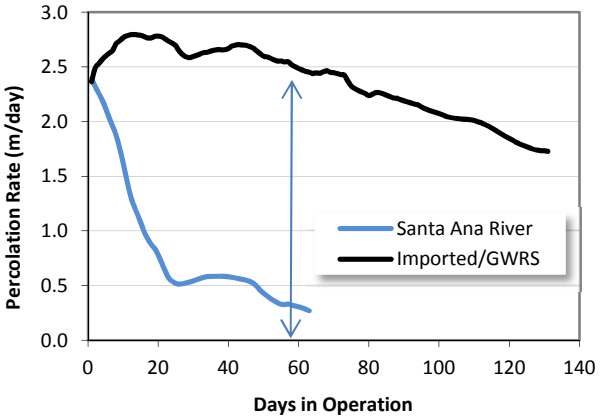

Figure 4: Percolation Rate Decay in Kraemer Basin with Different Water Sources

To better understand the impact of clogging on recharge facility performance, OCWD developed a model to predict percolation rate decay due to clogging by suspended

solids loading (Phipps et al., 2007). The model is able to replicate percolation decay trends seen in facilities using source waters that have different TSS concentrations (e.g., SAR, imported water). This model allows OCWD to evaluate the economic viability of projects to reduce TSS concentrations in SAR water using different pre-treatment methods. The model is based on the following simple log-decay expression:

$Q = Qoe^{-rL}$,

Where Qo= the initial percolation rate, L = the total foulant deposited at the sediment/water interface and Q = percolation observed at L solids loading. The value of r represents a sediment/foulant interaction coefficient and it is presumed to be unique to the nature of the sediment and foulants. The model could be applied to other areas where the accumulation of TSS is the dominant form of clogging; however, site specific testing would have to be done to establish the appropriate sediment/foulant interaction coefficient (r).

5 Clogging Mitigation Strategies

Mitigation strategies to address clogging of surface water recharge facilities fall into several categories:

1. Design strategies
2. Proactive removal strategies
3. Reactive removal strategies

5.1 Design Strategies

It is important to consider ways to minimize the impact of clogging when designing a surface spreading facility, particularly if fine-grained sediments are present (Bouwer, 2002). Key things to consider include:

1. Inflow designed to minimize erosion as basin fills
2. Basin banks protected from erosion/wave action
3. Shallow ponding depths to reduce pressure on the clogging layer
4. Ability to rapidly drain and dry the basin once clogged
5. Ability to operate multiple basins independently to provide maintenance flexibility

Originally, OCWD constructed recharge basins ranging in depth from 15 to 17 meters. The deep basins provided both storage and percolation capacity. In recent years, OCWD has constructed all of its basins to be less than 2 meters deep because storage is not as important as percolation capacity. The shallow basins can be quickly drained, dried and cleaned and thus have a greater on-line efficiency compared to the deep basins.

Many of the above design considerations are not applicable when spreading water in river or creek channels because the constantly moving water and periodic storm events tends to reduce the impact of clogging on the channel bottom. In wide channels, it may be necessary to construct small dikes to force the water to spread and cover the entire channel bottom, which maximizes the percolation potential of the channel. The OCWD constructs "T" and "L" dikes in the SAR in the winter months because they can be constructed quickly and do not require the river channel to be level. The "T" and "L" name refers to the shapes of the dikes when looking at them from above. The disadvantage to "T" and "L" dikes is that they form localized areas of slow moving water where clogging takes place. At the end of the storm season when there is no risk of storm flows washing out the sand dikes, the "T" and "L" dikes are replaced with "runners" which are small dikes that parallel the river channel. When the runners are installed, additional work is required to level the channel bottom to ensure it is completely submerged. The runners allow the water to run continuously downstream and thus do not cause as much clogging as the "T" and "L" dikes. Typically two runners are installed so that sections of the river can be periodically dried up to minimize insect breeding.

5.2 Proactive Removal Strategies

Proactive removal strategies to reduce clogging fall into two categories:

1. Removing suspended solids
2. Removing nutrients

Suspended solids can be removed naturally using desilting basins or they can be removed artificially. The District has several desilting basins that are capable of reducing TSS concentrations by 75 to 80 percent, but there is a fraction of TSS that will always remain in suspension and resist gravity settling. Moreover, desilting

systems are land-intensive and may not be feasible in urbanized areas.

To assess whether water treatment technologies could be used to reduce suspended solids loading and thus reduce the impact of clogging, OCWD embarked on a multi-phase Sediment Removal Feasibility Study in 2008. In the first part of the study, potential water treatment technologies that could be used to remove sediment were evaluated. After preliminary screening of the treatment technologies, the technologies identified for testing were Flocculation-Sedimentation, Ballasted Sedimentation, Dissolved Air Flotation (DAF), Cloth Filtration, and River Bed Filtration.

Flocculation-Sedimentation was achieved by adding ferric chloride to the raw water and then conveying the water to a small clarifier to allow the solids to settle out. Ballasted Sedimentation uses similar principles with the addition of fine-sand which causes the coagulated particles to settle out faster. The fine sand is then recovered and used repeatedly. Dissolved Air Flotation (DAF) removes solids by dissolving air in the water under pressure and then releasing the air at atmospheric pressure in a flotation tank or basin. The released air forms tiny bubbles which adhere to the suspended matter causing the suspended matter to float to the surface of the water where it is removed by a skimming device. Cloth Filtration removes suspended solids by running the water through cloth filter media with a nominal pore size of 5 microns. The cloth filter media is backwashed periodically to maintain a set flow-through rate. River Bed Filtration is similar to River Bank Filtration except the collection laterals are placed 2 to 3 meters below the riverbed with the main objective of removing suspended solids.

Pilot testing of these technologies commenced in January 2009 with the goal of collecting water quality data for each technology, as well as determining the percolation rate decay through bench-top column testing and larger percolation cells. The bench-top columns and percolation cells were filled with clean, native sediment from a recharge basin. Ballasted Sedimentation, Dissolved Air Flotation and Cloth Filtration each achieved significant sediment removal, with River Bed Filtration achieving almost 100 percent removal. Although technologies that employed chemicals as part of the treatment process achieved significant sediment removal, they were not effective in sustaining elevated percolation rates in the columns and percolation cells. This is attributed to the interaction of residual treatment chemicals in the water with native sediments in the columns and percolation cells, which caused rapid decays in percolation rates. In terms of sediment removal and increased percolation rates, River Bed Filtration was the most effective, followed by Cloth Filtration (Milczarek et al., 2009; Woodside et al., 2011).

OCWD is currently conducting field-scale, multi-year demonstration testing of Cloth Filtration and River Bed Filtration to assess their long-term performance and potential cost-effectiveness at the field scale. Testing conducted thus far on Cloth Filtration shows that it is effective in removing suspended solids when the TSS concentration ranges from 10 to 30 mg/L, but is less effective at concentrations lower or higher than this range. Figure 5 shows how TSS removal efficiency varies with loading rate. The River Bed Filtration Demonstration system will be constructed in 2013. Data from the pilot study indicates that the TSS concentration of water produced by River Bed Filtration will be in the order of 0.1 mg/L. One objective of the Demonstration Project is to monitor the clogging of the river bed surface and test various methods to sustain River Bed Filtration performance.

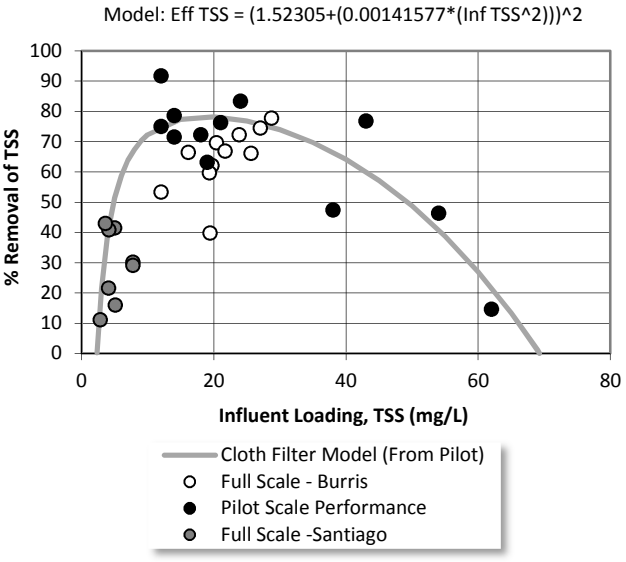

Figure 5: Cloth Filter TSS Removal Efficiency

It has been OCWD's experience that clogging due to suspended solids is the primary cause of clogging but

biological oxygen demand and nitrates and phosphates in recharge water may also serve to facilitate the growth of algae and microrganisms within the recharge facilities, potentially causing clogging. To minimize the potential impact of biological clogging and to improve the quality of the recharge water, the District constructed a 188 hectare wetlands treatment system that is comprised of 50 shallow ponds. The wetland system removes approximately 18 metric tons of nitrate a month from SAR water, and during the summer months reduces nitrate concentrations from 10 mg/L to less than 1 mg/L. This system has successfully improved the overall quality of water being recharged to the basin, however, it is unclear if the wetlands treatment process has reduced biological clogging and positively impacted recharge facility performance.

5.3 Reactive Removal Strategies

Reactive removal strategies, which refers to removing the clogging layer after it has formed, falls into two categories:

1. On-line removal
2. Off-line removal

On-line removal refers to removing the clogging layer after it has formed and while the recharge facility remains in service. The advantage to this approach is that the facility remains on-line during cleaning. The District tested this approach using a Basin Cleaning Vehicle (BCV) (OCWD, 2010). Several generations of BCVs were manufactured, including a fully submersible device as well as a floating device. The concept behind the BCV is to vacuum up the clogging layer and leave the underlying clean sand behind. The fourth generation BCV (BCV-4), which was a floating version, was placed in four recharge facilities and tested over an 8 year period. Test results showed that the BCV was able to sustain elevated recharge rates in a basin that received relatively clean water with TSS concentrations less than 10 mg/L. The BCVs placed in the other three facilities were not as successful due to a number of factors, including high TSS loading rates, poor contact of the BCV with the basin bottom, and slow BCV coverage rate. Although the concept of in-situ removal was found to be a valid approach, the BCVs as designed were not found to be cost-effective. Pending the outcome of the proactive treatment method tests (Cloth/River Bed Filtration), this approach may be revisited in the future.

Off-line removal refers to taking a recharge facility off-line and removing the clogging layer with no water present. This is the most common method of basin cleaning. Depending on the facility it may take from 2 to 45 days to drain, and then another 5 to 25 days to allow drying. Basins are then either refilled after the clogging layer has dried and cracked, or equipment is used to scarify or remove the clogging layer before it is placed back into service. This method is very effective in restoring percolation rates; however, it can be expensive and reduces the overall recharge capacity of the facility.

OCWD has refrained from ripping or scarifying the basin bottoms because this approach can create a deep layer of native sediment mixed with clogging material. One recharge facility in southern California used to provide tertiary treatment of wastewater routinely scarifies the basin bottoms. As performance declines, the near-surface sediments must be overexcavated and then washed in an on-site sand washing operation before being placed back into the basin. Without this process, the recharge capacity of the facility would degrade to unacceptable levels. (Personal Communication, San Bernardino Operations Staff, http://www.ci.san-bernardino.ca.us/sbmwd_divisions/water_reclamation/default.asp.).

Currently, OCWD uses a motor-grader to push the clogging layer into long windrows so it can be picked up by a paddle-wheel scraper. This process is analogous to sweeping the dirt on a floor to a corner and then using a broom to sweep the dirt into a dustpan. This process minimizes, but does not prevent, the removal of the underlying clean sediment. As a result, OCWD has to import clean sand to fill in low spots every two to five cleaning cycles.

Generally, a recharge facility is taken off-line for cleaning when the percolation rate has declined to approximately 30 percent of the initial rate. Sometimes system constraints prevent this from happening and the facility is taken off-line later. Depending on the cost and time it takes to clean a facility, it is possible to clean a facility too frequently. Figure 6 shows, for Anaheim Lake, that the maximum net water value is obtained when the basin is cleaned no more than three times per year. While additional cleanings would increase the overall amount of

water recharged, the cost of the cleanings would reduce the net value of water recharged.

The optimum cleaning frequency is unique for each facility and must be determined on a case-by-case basis.

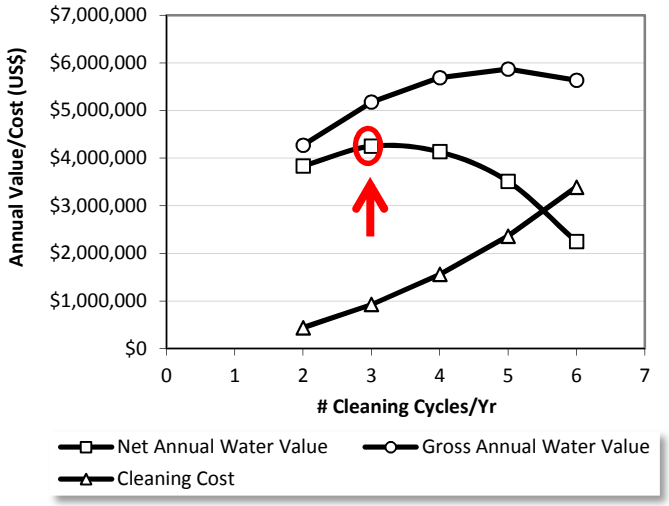

Figure 6: Cleaning Cycles per Year, Gross Water Value and Net Water Value for Anaheim Lake

6 Conclusions

MAR and clogging are inextricably linked. Since OCWD started recharging water in the SAR channel in the mid-1930s, clogging has been taking place. Even though OCWD has been able to construct a system that is capable of recharging large volumes of water, clogging still constrains system yield.

Clogging in the OCWD recharge system is primarily due to suspended solids with biological clogging appearing to have a minor role. Recharge rates achieved with water sources with low suspended solids concentrations, such as imported water or GWRS water, are high and remain high for long periods of time, showing that the potential benefit of reducing suspended solids concentrations in the source water is significant. As a result, OCWD is actively looking for ways to pre-treat SAR water to reduce clogging by reducing TSS concentrations.

Based on the OCWD experience, addressing the clogging menace must be at the forefront of every phase of MAR, from site investigations all the way to every-day operations. A failure to keep clogging front and center will lead to a system that under-performs.

7 References

Bouwer, H., (2002) Artificial recharge of groundwater: hydrogeology and engineering. Hydrogeology Journal. 10:121–142.

California Department of Water Resources (DWR), (1967) Progress Report on the Groundwater Geology of the Coastal Plain of Orange County.

Clark, J.F., Hudson, G.B., Davisson, M.L., Woodside, G., and Herndon, R., (2004) Geochemical Imaging of Flow Near an Artificial Recharge Facility, Orange County, California. Ground Water 42, 167–174.

DWR: see California Department of Water Resources

Freeze, R.A. and Cherry, J.A., (1979) Groundwater. Prentice-Hall, Inc. Englewood Cliffs, New Jersey.

Orange County Water District, (2003a) A History of Orange County Water District.

Orange County Water District, (2003b) Orange County Water District Recharge Study. December 2003.

Orange County Water District, (2010) Basin Cleaning Vehicle Program Review. June 1, 2010. Prepared by Recharge Operations Staff. Internal OCWD Report.

OCWD: See Orange County Water District

Milczarek, M., Woodside, G., Hutchinson, A., Keller, J., Rice, R., and Canfield, A., (2009) The Orange County Water District Riverbed Filtration Pilot Project: Water Quality and Recharge Improvements Using Induced Riverbed Filtration. In Proceedings of the 7th International Symposium on Managed Aquifer Recharge. ISMAR 7, Abu Dhabi (UAE), October 9–13, 2009.

Phipps, D., Lyon, S., and Hutchinson, A., (2007) Development of a percolation decay model to guide future optimization of surface water recharge basins. In Proceedings of the 6th International Symposium on Managed Aquifer Recharge. ISMAR 6, Phoenix, Arizona, October 29–November 2, 2007.

Woodside, G., Hutchinson, A., Canfield, A., Miller, C., Toland, S., and Bradshaw, G., (2011) Recharge Performance Enhancement through Sediment Removal: Orange County Water District Sediment Removal Feasibility Study.In Proceedings of Managed Aquifer Symposium, January 25–26, 2011, Irvine, California. Organized by the National Water Research Institute (www.nwri-usa.org).

Practical Criteria in the Design and Maintenance of MAR Facilities in Order to Minimise Clogging Impacts Obtained from Two Different Operative Sites in Spain

FERNÁNDEZ ESCALANTE, A. Enrique. TRAGSA I+D+i

Edited by R. Martin

1 Abstract

According to the experiments carried out under a research and development framework to address the objectives of the DINA-MAR Project (*Depth Investigation of New Areas for Managed Aquifer Recharge*) which focuses on the management of aquifer recharge in the context of sustainable development, we have conducted investigations of clogging in managed aquifer recharge facilities, specifically focusing on detection and distribution of physical (including air), chemical and biological clogging processes. Synergistic combinations have been studied by means of core sampling, analysis, and field photographs at different scales, from aerial to microscopic, and the use of serial radiometric images.

These studies have been carried out at three experimental sites where other investigations are being carried out including chemical analysis, interaction models, sequential gauging tests, infiltration tests, etc.

Results from three distributed pilot sites have been used to design and implement a practical specific methodology for cleaning and maintenance of infiltration ponds, canals and wells; as well as design recommendations prior to construction work designed to be extrapolated to other analogous scenarios.

This chapter summarises most of the practical rules reached during the project's development.

2 Introduction

The DINA-MAR project has been financed by the Tragsa Group and the Spanish Government. Following ten years of trials and analyses to improve the design of Managed Aquifer Recharge (MAR) facilities, operative techniques have been developed in order to avoid or minimise the clogging processes affecting these schemes.

These operational rules have resulted from three test sites; two are from the Arenales aquifer (Santiuste Basin, Carracillo region) and the third study is in the Guadiana Channel, in the Guadiana Basin (Central Spain). All schemes divert water from rivers in the wet period to recharge the aquifers primarily through a combination of infiltration and recharge bores. The stored water is recovered in the summer mainly for irrigation and environmental purposes.

Studies have focussed on permanent design improvements and implementation of Soil and Aquifer Treatment Techniques (SATs) applied to source water (in both quantity and quality), to the receiving medium and to a combination of both. The practical measures to be taken into account have been classified according to which part of the annual MAR cycle that they occur within: winter recharge, summer recovery, and non-operational periods.

This paper presents the study areas, the main clogging types detected and the actions designed to remediate clogging in all its various forms. This paper is a summary of several years of research, and due to space limitations,

interested readers are advised to consult the specific references for more detailed descriptions.

3 Objectives

The main objective of the studies undertaken was to propose various "problem-solution" binomials in order to improve the effectiveness of the studied MAR facilities (based on SATs, engineering criteria, risk assessment and environmental impact). In this way the generation of a continuous 'detect – improve' loop was intended: detect new deficiencies – develop new improvements; thus the understanding of the clogging processes and remediation actions was improved.

The techniques commonly employed at the research sites were:

- Identification of the dominant clogging mechanism affecting the MAR facility through characterisation of physical, chemical and biological factors. Technologies including underwater video-camera and thermographic imaging were used to this end.
- Design improvements applied to the site-specific MAR recharge infrastructure (ASR wells, channels and infiltration ponds).
- Source water pre-treatment.
- Observation of the influence of the active MAR operational period; wet/dry periods and the activities performed during each.
- Determination of optimal site-specific MAR flow rates for channels, wells and infiltration ponds.
- Practical interventions ad hoc in order to reduce the clogging genesis and to increase the effectiveness of the facilities.
- Reduction of air entrainment into the aquifer during MAR operations.
- Cleaning and maintenance operations.

The investigation of these common techniques and their efficacy is ongoing.

The investigated activities were grouped according to which part of the annual MAR cycle that they occur within: winter recharge, summer recovery and non-operational periods.

4 Methods

Data collection has focussed on permeability and infiltration rate determined in situ. These data have been generated using a range of methodologies including double-ring infiltrometers, Lugeon tests, Lambe tests, and laboratory tri-axial permeameter testing. Sequential flow gauges were also monitored along channels. Site-specific clogging remediation activities were driven by changes in these collected data over the observation periods at the various sites (10 years for Arenales aquifer schemes and four years at the Guadiana canal scheme).

The variation in storage within each studied aquifer was established using the Water Table Fluctuation (WTF) method (Schict and Walton, 1961, in Healy and Cook, 2002), with input data from control networks comprised of more than 50 observation points at each MAR site. This input data was treated with algebraic mapping functions within a Geographic Information Systems (GIS) environment.

Assessment of the proportion of aquifer recharge volume attributed to managed recharge and that attributed to rainfall seepage was achieved by means of the Hydrological Evaluation Landfill Performance (HELP) model (Gogolev and Ostrander, 2000) and by water balances conducted in isolated zones.

Additionally, thermographic camera imagery has been implemented since 2010 for the detection and characterisation of clogging processes. The Therma-Cam E2, developed by Flir systems, has been employed in order to study the distribution of clogging through temperature differences between clogged and non-clogged zones. These zones show different thermal profiles when visualised; background information is presented in Fernández and Prieto (2013).

Gas clogging was investigated using various indirect methods, allowing estimations rather than direct determinations. Air held in ground pores was estimated through dissolved oxygen changes between MAR water and groundwater in sealed observation wells; with seepage capacity evolution monitored throughout a full MAR cycle. The evolution of air trapped in the aquifer was also estimated using the techniques of Blaxejewski (1979), with sequential infiltration testing during a complete MAR cycle utilising a specifically designed bench-ditch.

Unsaturated zone processes were monitored by means of remote sensing DINA-MAR ZNS stations; a combination of sensors installed near MAR channels, wells and ponds recording changes in unsaturated zone parameters (water table, humidity, temperature and capillary tension – connected to data-loggers), built into telemonitoring stations. These stations provide accurate natural infiltration data to assist with water balance calculations. Sensors are placed crosswise to the artificial recharge channel, so as to identify and quantify the speed and shape of the humidification bulb as artificially recharged water migrates through the phreatic zone towards the water table. Some sensors became saturated during winter due to the increase of the water table levels associated with recharge (Figure 4-1, detailed description in DINA-MAR (2010)). The comparison of capillary tension values and changes of infiltration rate have led to valuable insights.

Total Dissolved Oxygen (TDO) data were determined by means of a pH meter (Hanna Instruments HI 9018) and a multiparametric meter with PH/ORP/EC/DO sensors (HI 9828) and through field titration.

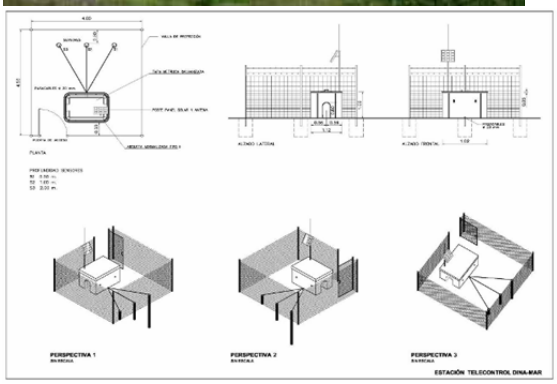

Figure 4-1a) and b): Aspects of the 1st DINA-MAR ZNS station in Santiuste Basin (Segovia, Spain) and composition scheme

Scientifically based trial and error was also regularly employed throughout the study. Device design modifications were conducted, with the associated results recorded; a technique that remains in use.

5 MAR Study Sites and Characterisation of Clogging Processes

Three MAR study sites were established by the Spanish Government's Agriculture, Food and Environment Ministry (MAGRAMA), and are employed as "experimental laboratories" to study relevant processes by the DINA-MAR research and development project.

Two of these sites which are reported on in detail herein access the Arenales aquifer, in the Santiuste Basin and Carracillo Region respectively. These two sites have very similar characteristics, achieving recharge through infiltration ponds and channels, and large diameter wells. The two Arenales aquifer MAR sites have been operational for substantial periods of time (10 years for the Santiuste Basin scheme, and eight years for the Carracillo region scheme).

The third study MAR site is located in the Guadiana Channel, in the Guadiana Basin, which captures surplus water storage from the Peñarroya dam to recharge the 23rd aquifer via a well-field of 25 wells, along the channel sides. This scheme has been operational for approximately four years but due to space limitations within the monograph is not reported on in detail here but will be included in subsequent updates.

The following section describes the studied MAR sites, highlighting the following aspects:

- General hydrogeological setting of the target aquifer.
- Geochemical composition of the MAR target aquifer.
- Groundwater and recharge water quality.
- General overview of operative aspects.
- Recharge volumes and associated water table infiltration times.
- Description of pre-treatment of source waters prior to recharge.
- Characterisation of site specific clogging mechanisms (remediation of clogging is described in the discussion and conclusion sections).

Figure 5-1a) to d): a) Position of MAR facilities where pilot tests are accomplished; b) Santiuste Basin; c) Carracillo district (Segovia and Valladolid provinces)' and d) Guadiana channel (Ciudad Real province). All photos do not explicitly correspond to authorship Tragsa Group and/or the author.

5.1 The Arenales Aquifer

The Arenales aquifer or Hydrogeologic Unit 02-17 covers an area of 1,504 km^2 located in Castille and Leon Regions of Spain. The aquifer has polygenic origins, with a predominance of Quaternary dune sands (Arevalo facies) of variable thickness (up to 50 m), in-filling an irregular contact boundary of complex Miocence epoch small palaeo-basins within argillaceous (Cuestas facies) or sandy/clayey (Runnel Bridge facies) lithology.

Exploitation of the surficial Quaternary aquifer has intensified in recent decades, causing the phreatic level to recede by over 10 m; also instigating salinisation and contamination processes. To address these observed negative trends within the Arenales aquifer, four managed aquifer recharge schemes are being trialled, with the recovered water used for irrigation. These MAR schemes are located in Morana, Santiuste Carracillo and the fourth scheme is currently under construction in the Alcazarén region.

5.1.1 Santiuste Basin

General hydrogeological setting of the target aquifer

Located in the west of Segovia province and south-west of Valladolid province, the Santuiste Basin lies on the left shore of Voltoya and Eresma Rivers, covering a surface area of about 48 km^2, including 600 ha of irrigation area. It is perhaps one of the best studied aquifers in Spain due to the investigations conducted by MAPA and subsequent R&D activities.

The Arenales aquifer targeted for MAR operations is characterised by sandy Quaternary deposits, up to 55 meters thick (Arevalo facies), which in-fill a series of small, semi-interconnected Tertiary palaeo-basins in clay (Slopes facies) or sandy-clay (Runel Bridge facies) substrata. These Quaternary sands give rise to the surface morphology of Coca-Arévalo, consisting of sandy fluvial deposits, partially covered by aeolian deposits and endorreic areas, with several fossilized and lagoon systems.

A north-south cross-section is presented as Figure 5-3 and illustrates the series of small paleo-basins, partially interconnected, that constitute the target MAR aquifer. Thickness of these palaeo-basins ranges from less than one meter to over 50 metres for two basins in the northern region. A detailed description of the relevant hydrogeological facies of appears in MAP (2005) and Fernández (2005).

Figure 5-2a) to c): Examples for some Santiuste basin' MAR activities

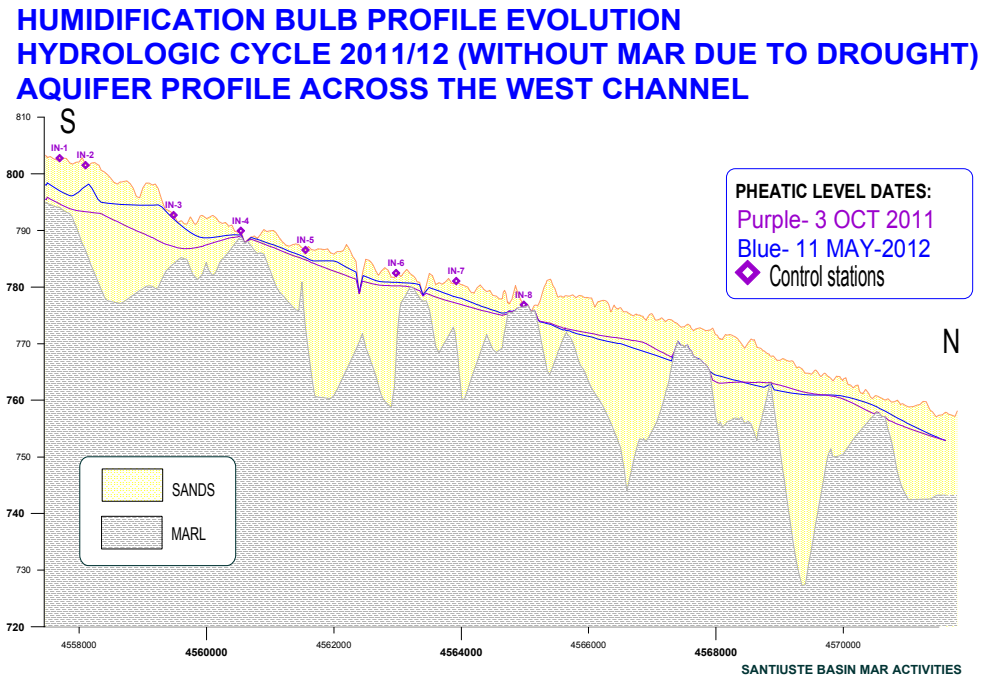

Figure 5-3: Lithostratigraphic profile of the aquifer and base along the East Channel, confirming the aquifer functioning as a system of little Tertiary basins "in relay" filled of detritic sediments over a marl base. Infiltration and clogging stations position (IV).

Results from monitoring employing the remote sensing DINA-MAR stations has enabled the determinination of horizontal aquifer properties at various locations throughout the Santiuste Basin study site, revealing hydraulic gradient values of 1 to 6%, permeability values of 4 to 5 m^2/day (station ZNS-1) and 1 to 4 m^2/day (station ZNS-2), and transmissivity values between 1.2 and 1.4 m^2/day. Observed water table depth in the wells ranges from 2 to 10 m, depending on the location. Specific Yield ranges from 14 to 25%.

Estimates of vertical hydraulic conductivity for the target MAR aquifer from published sources range from estimated at 1,095 mm/year (IRYDA, 1990; MAP, 1999) to between 2,200 and 3,600 mm/year (MOPTMA, 1994: MAP, 2005). Specific Yield estimates are around 18%.

Geochemical composition of MAR target aquifer

The soils of the study area are generally sandy therefore have poor structure, good ventilation, high permeability and low water retention. From a chemical perspective, the soils are very poor, with limited nutrients and colloidal properties.

In addition to the generally sandy soils, some clay dominant soils occur within the Santiuste Basin study area. These clay dominant soils are by definition well structured, poorly aerated, have lower permeability and high water retention. Chemically, these clay dominant soils are more active, with greater ion exchange and adsorption capacity, flocculation and dispersal, and are very nutrient rich.

Silty lenticular soil bodies occur in parts throughout the target aquifer. In comparison to the clay dominant soils, these silty lenses have poor structure, reduced colloidal properties; have low permeability and poor ventilation.

The shallow Quaternary aquifer contains some stratigraphic complexity despite its apparent homogeneity and isotropy. A 'type' lithologic profile is presented as Figure 5-4, illustrating the changes in strata texture and composition with depth within the target MAR aquifer.

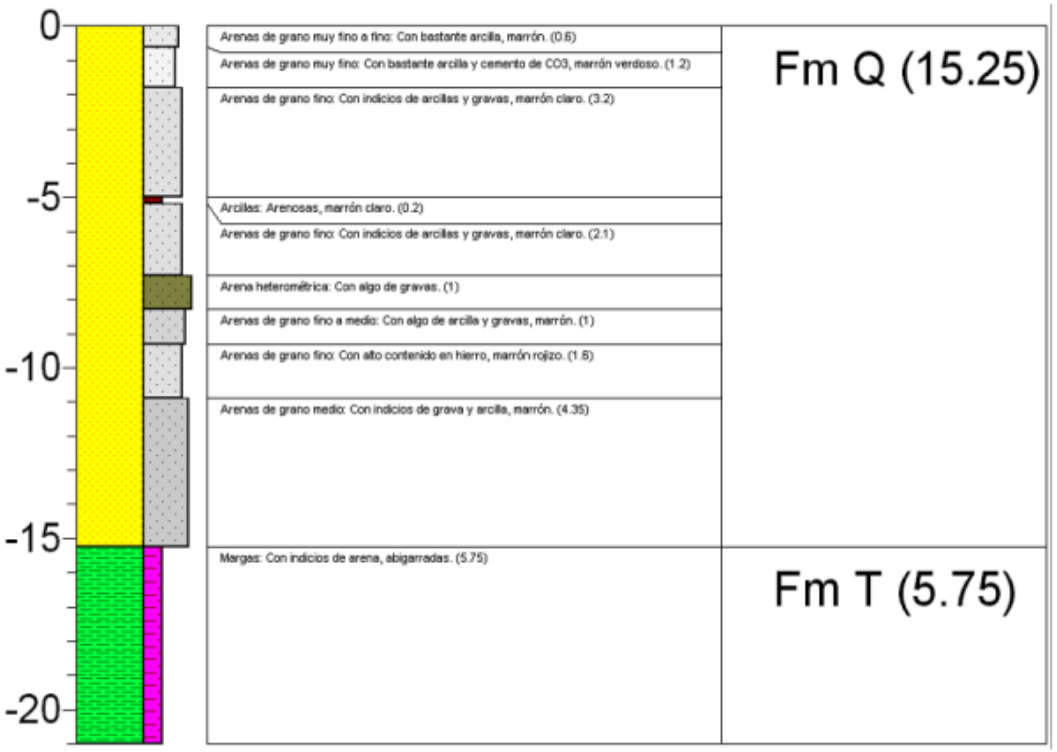

Figure 5-4: Characteristic lithostratigraphic column for Santiuste Basin. Central Area. Borehole 84, coordinates UTM 369377 / 4562450, huse 30. Q: Quaternary sands. T: Tertiary marl and clay

Details and results from textural and compositional samples taken to define the lithology involved in geochemical interaction processes within the target MAR aquifer are presented in Table 5-1 (a – c). Three textural and compositional samples were taken for strata representing compositional units of the Arenales aquifer and compared to the Tertiary marl and clay basement (sample 1, Table 5-1).

Tables 5-1 a) to c): Soils and drilling cores analysis. a) samples position, including the marl basement of impermeable behaviour (sample 1); b) soils geochemical analysis; and c) granulometric determinations

N	NAME	X (UTM)	Y (UTM)	Z	Date
1	Facies Coca Slopes	371615	4563282	769.7	6/28/02
IN-11	Spot Cañadilla	367939	4569405	768.0	6/28/02
IV-3	Sanchón	369695	4560322	792.0	6/28/02
IV-5	Sand dunes	370061	4562904	786.0	6/28/02

N	C (mhos/cm)	pH	HCO_3 (mg/l)	Cl (mg/l)	SO_4 (mg/l)	N t %	P (ppm)	OM %
1	0.60	7.8	194	62	45	0.021	8	0.12
IV-3	0.50	8.6	194	44	162	0.015	4	0.10
IV-5	0.40	7.2	155	53	41	0.070	4	0.01
IN-11	0.70	8.1	181	98	39	0.022	24	0.18

N	Sand %	Silt %	Clay %	Clasif.
1	11.85	33.8	54.35	AC
IV-3	90.53	2.87	6.6	AR
IV-5	94.81	1.94	3.25	AR
IN-11	92.78	3.72	3.5	AR

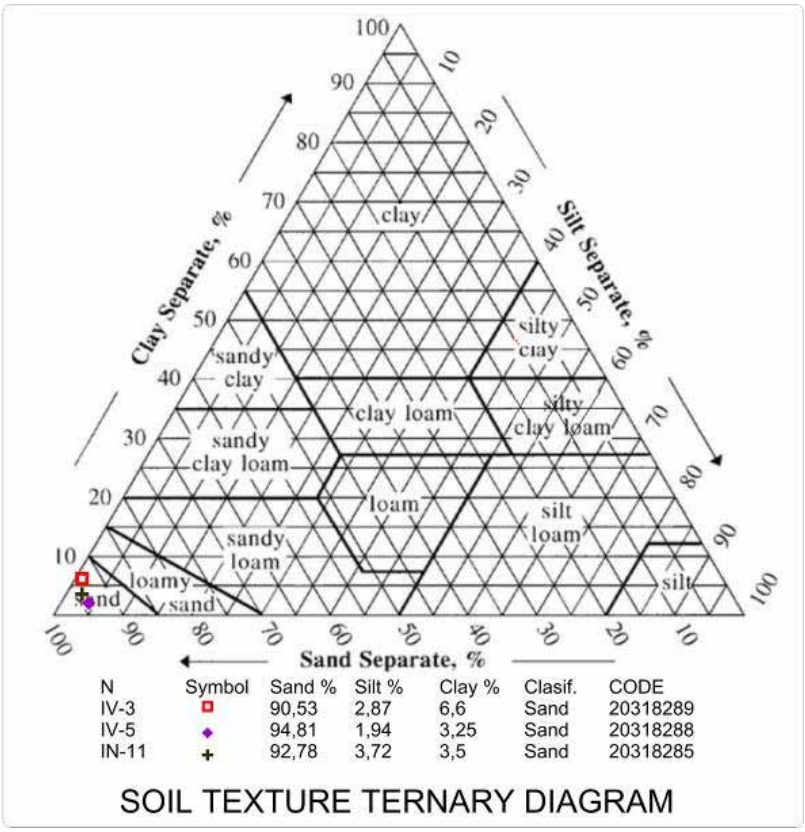

Figure 5-5: Textural representation in a Ternary diagram of soil and core samples

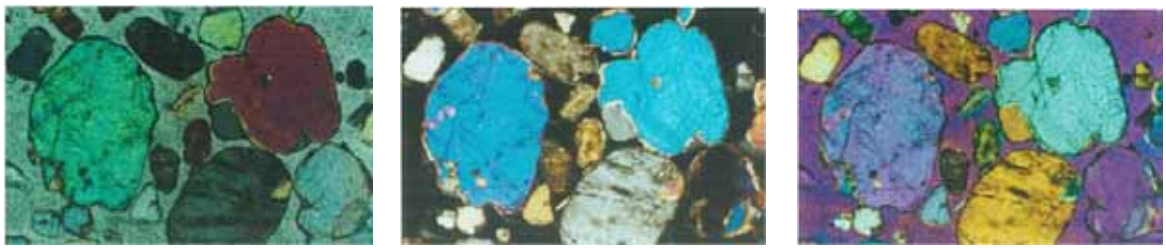

Figure 5-6: Polarising micrographs of different aspects of the sample IV-5. Depth: 1.3 m

Soils were found to be generally clay loam (Figures 5-5 and 5-6) with small lenticular marl and carbonate levels interspersed. Frequently there are variations in the colour depending on the composition and cation exchange processes. There are also abundant fossilised levels alluvial gravels and floodplain clays. The organic material is generally limited.

Interaction processes were modelled in PHREEQC (in Fernandez, 2005), demonstrating a high complexity hydrochemical environments despite the apparently homogenous medium.

Groundwater and recharge water quality

Groundwater in the Quaternary aquifer is generally calcium bicarbonate type, with regions where groundwater facies appear sulphated, with calcium bicarbonate and magnesium. Complex reducing processes occur in the eastern-central regions of the Quaternary aquifer system, attributable to the presence of pyrite. The western sector of the Quaternary aquifer system generally displays more saline groundwater with elevated gypsum content due to infiltration through the loam hills that surround the western aquifer. Carbonate equilibrium concentration distribution throughout the Quaternary aquifer was found to be complex.

Nitrates are elevated within the Quaternary aquifer, often occurring at approximately 50 ppm. Nitrate values are even higher in the north-east, where groundwater flow lines converge and the aquifer receives substantial recharge from the Eresma River though high permeability zones. Nitrate concentrations exceeding 300 ppm have been observed in the north-east, but a gradual decline in concentration has also been observed over subsequent managed recharge cycles.

Multi-variate statistics for macro-constituent hydrochemical analysis of groundwater sampled at control points along the MAR system network are presented as Table 5-2 below, and represent groundwater chemistry at depth less than 50 metres below ground level.

Hydrochemical analyses of recharge waters are presented as Table 5-3; with samples taken from the Voltoya River (from which recharge flows are derived), rainwater, and recharge water at the artificial recharge facilities themselves. The samples taken at the AR facilities enable water quality changes to be captured due to hydrochemical interactions along the MAR system channels. Rainwater samples were taken from above artificial recharge facilities, being decanted and filtered prior to analysis. These chemical analyses establish the 'recharge end members' for hydrochemistry within the Santiuste MAR study groundwater site.

Table 5-2: Statistical analysis of the hydrochemical results. Operational phase, 2003. Collected from wells less than 50 m depth. Detailed characterisation of groundwater in Fernández, 2005

mg/l⇒	Na	K	Ca	Mg	Cl	SO_4	CO_3	HCO_3	NO_3
Min.⇒ (n.º well)	12 (19)	2 (19)	31 (27)	7 (19)	20 (19)	11 (27)	17 (9 y 12)	112 (19)	3 (25)
Max.⇒ (n.º well)	106 (8)	116 (8)	182 (4)	166 (8)	174 (8)	443 (8)	0 –	568 (8)	378 (26)
Mean	59.4	15.4	88.5	63.9	75.9	123.25	–	323.8	133

Table 5-3: Chemical analysis of 'recharge end members' of the Satiuste Basin MAR groundwater chemistry system. These comprise the Voltoya River, rainwater collected in Santiuste and recharge water collected at the MAR facilities in 2003, 2007 and 2009

STATION	X	Y	Na	K	Ca	Mg	Cl	HCO_3	CO_3	SO_4	Fe	SiO_2	NO_3
29 Voltoya	371013	4556560	31.54	2.23	70.54	1.95	39	247.74	0	2.19			
30 Rain	368195	4557313	1.61	1.19	7.21	1.95	8.51	26.85	0	3.31			
REC 2003	371038	4558192	5.0	1	15	6	2	78	0	5			
REC 2007	371038	4558192	24.3	2.15	38.55	4.82	34.7	125.73	0	16.26	0.06	5.01	1.5
REC 2009	371038	4558192	14.67	1.75	26.30	<2	25.16	67.81	0	9.74	0.11	8.55	1.32

Piper-Hill-Langelier plots were used to identify the dominant water chemistry facies in the Santiuste MAR system and are presented as Figure 5-7 for recharge waters and groundwater sampled along the Santiuste MAR groundwater quality control network. The location of the observation points within the groundwater quality network are presented in Figure 5-8.

Laboratory analyses of the recharge waters were supplemented with unstable parameter determinations in situ, with an example of results presented as Figure 5-9.

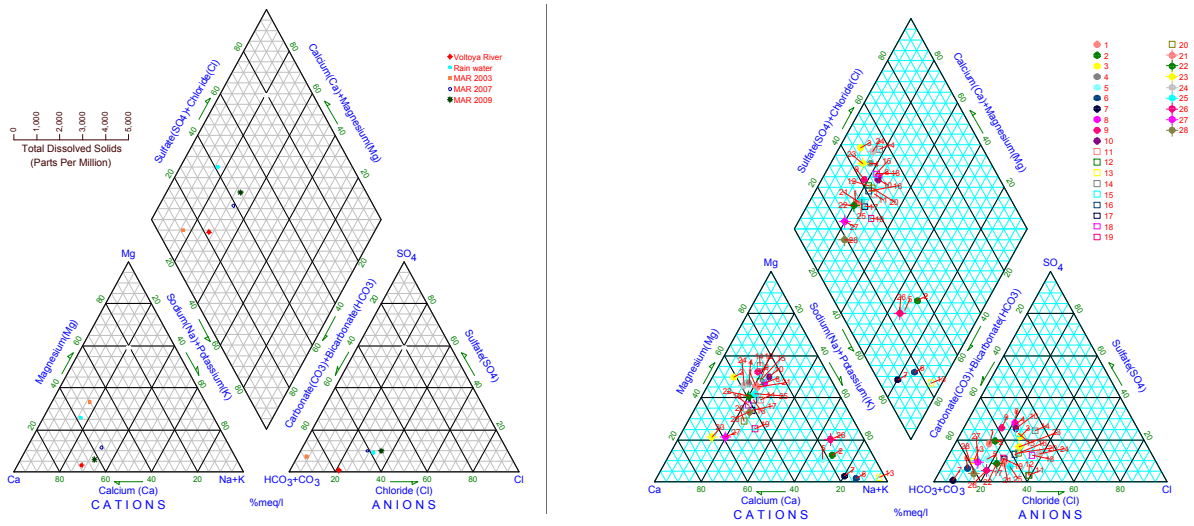

Figures 5-7 a) and b): Piper-Hill-Langelier hydrograms for water representing MAR water and "cold poles" in the interaction system (a); and for groundwater quality Control Net (RCH), upper hemisphere for wells with a deep minor than 75 m, as lower is for deep boreholes

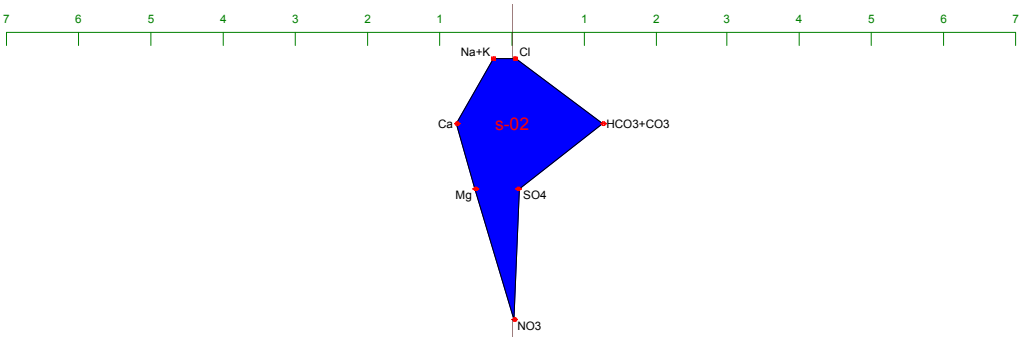

Figure 5-8: Stiff hydrograms for a Santiuste MAR recharge water sample

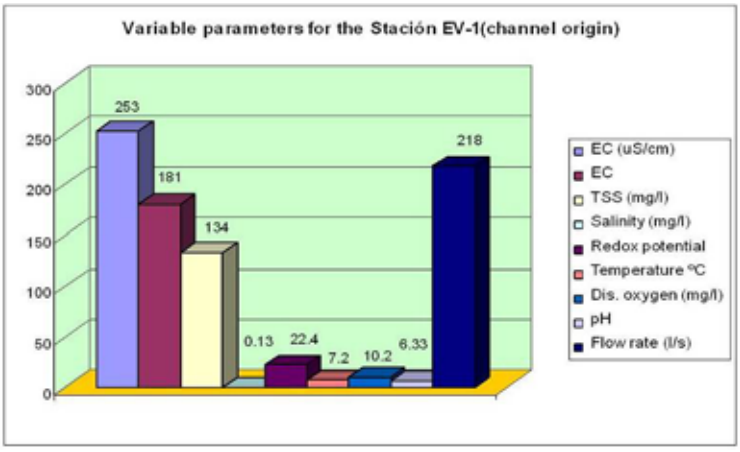

Figure 5-9: Variable parameters in the head of MAR facilities, Santiuste basin. January 22, 2009

Chemistry results for recharge waters revealed strong variability, despite their common origin. This is interpreted as due to environmental factors, particularly the influence of weather variability on the Voltoya River. The composition of the recharge waters is considered important in the genesis of clogging processes, especially dissolved oxygen in recharge water, and pH and its relations with flow, expanded upon in the discussion (below).

General operational overview

The Santiuste Basin MAR scheme was initially comprised of a small dam on the Voltoya River, from where a buried 9.7 km long pipeline delivered diverted water to 36 m^3 tank (header device) equipped with a flow meter. The captured water was then dispersed into a settling and infiltration pond covering 14,322 m^2, located at the hub of the subsequently constructed two main MAR channels.

Operation of the Santiuste Basin scheme's first MAR channel (East Channel) began in 2002. The East Channel closely follows the ancient river bed of the now dry Hermitage River, descending 30 metres over its 10.7 km length; with an average gradient of 0.28%. The channel contains 54 artificial recharge devices covering an approximate area of 33,300 m^2, allowing infiltration through the channel bed and walls.

The second MAR channel (Western Channel) has been operational since 2005 and runs semi-parallel to the East Channel. The West Channel was constructed in three stages, with a total length of 17.3 km and an infiltration surface of 27,960m^2.

The Santiuste Basin MAR scheme has been successively expanded throughout its operational life and currently consists of 27 km of MAR channel, five infiltration ponds, three MAR wells, a River Bank Filtration (RBF) system and three artificial wetlands plus incidental recharge through irrigation return.

The flow from the Voltoya River into the Santiuste Basin MAR scheme is approximately 500 L/s, with an annual harvest period granted by the Douro River Basin Authority extending from the 1st of November to the final day of April. This harvest period is dependent on annual river flows, being void if the circulating flow in the Voltoya River is less than 1,100 L/s.

The aerial layout of the Santiuste Basin MAR scheme is presented as Figure 5-18, showing the layout and locations of the channels, major basins, piezometric grid control points (SPC), gauging stations and figures for infiltration rate in different regions of the scheme.

Small concrete weirs regulate the maximum depth of water overlying the bed of the artificial recharge channels and ponds. The height of these weirs ranges between 60 – 100 cm in the channels and 60–140 cm in the ponds. Recharge wells are located in the vicinity of the channels and the water level reaches a similar point to that in the channel, resulting in a standing water column of up to 4 m during operation.

The water inlet at the Voltoya River is permanent and the height of the water surface is manually controlled via an inlet valve to suit changes in environmental conditions. Water depth at the inlet remains constant throughout the concession period, aside from appropriate manual adjustments. There are also two weirs on the river in case of heavy rains or floods.

Recharge volumes and associated water table infiltration times

Results from infiltration testing conducted along the East Channel during 2003 and 2004 gave the average infiltration rate per MAR cycle of between 314 and 1,100 mm/year (Fernandez, 2005). These values almost tripled for the MAR scheme as a whole once the second (West) MAR channel was added. According to HELP model results, the natural infiltration rate of the basin is between 25.09–25.11% of the total precipitation for the three years 1999–2002. Model predictions for 15 and 35 years were 24.78% and 24.56% respectively, showing a slight decrease over time.

A summary of operational volume calculations for 10 years' MAR operation at the Santiuste Basin scheme is presented as Table 5-4. The length of MAR activity in each year was variable, and it follows that the annual infiltration volume was also variable (Table 4-4). Total annual MAR operational days were considered as excluding incidents and instances where the inlet valve was manually closed. The total annual volume entering the Santiuste Basin MAR scheme was derived at the inlet valve on the Voltoya River (Q deriv.), the average flow rate along the along the MAR channels was established through data logger observations (Channel Qm), infiltration volume was calculated using fluctuations in the water table corresponding to recharge (modified WTF

Table 5-4: Summary of 10 cycles of artificial recharge in Santiuste bucket. Data and calculations of R & D project-SEA DINA (measurements until 01/05/2012). In http://www.dina-mar.es. Meteorological data taken from http://www.inforiego.es.

MAR cycle	Prec. (mm)	Cycle Start date	Cycle Final date	Total MAR days	Q derive. (hm^3)	Channel Q_m (l/s)	Tot inf. Vol. (hm^3)	% vol inf/Q derivated	P.L mean oscillation (m)
2002/03	291.4	05/12/2002	01/05/2003	148	3.5	278	1.30	37.14	2.3
2003/04	n/a	10/10/2003	01/04/2004	175	2.25	149	1.80	80.00	2.1
2004/05	n/a	01/10/2004	01/05/2005	212	1.26	68	0.97	76.98	1.17
2005/06	305.4	15/11/2005	01/04/2006	137	5.11	372	3.56	69.67	3.36
2006/07	331	01/10/2006	01/05/2007	212	12.68	692	12.19	96.13	3.57
2007/08	203.4	30/05/2008	06/06/2008	8	0.526	902	0.46	87.41	0.31
2008/09	85	01/11/2008	30/04/2009	181	3.88	248	2.50	64.50	0.62
2009/10	89.2	17/02/2010	31/03/2010	43	0.71	191	1.62	100	0.41
2010/11	92.4	22/02/2011	30/04/2011	68	3.13	493	2.13	68.03	1.28
2011/12	180.8	01/11/2011	01/05/2012	0	0	0	–	–	1.03

method as in Fernández (2005)), the ratio of annual infiltration volume to total annual volume taken at the River inlet was assessed, and finally, the oscillation mean increase in water table surface from initial conditions due to each annual artificial recharge cycle was calculated (Table 5-4). Calculations involving groundwater levels were conducted using data from 44 data points within the Santiuste Basin MAR scheme's piezometric control grid (RCP); the locations of these points are presented as Figure 4-19. The results presented in Table 4-4 are the work of both the MAGRAMA (formerly MAP), RDi, and the DINA-MAR research groups.

Remote observations of unsaturated zone processes revealed that the humidification bulb (recharge front extending from MAR infrastructure) took between 1 – 15 days to reach the phreatic surface within the target aquifer. Lateral expansion of the humidification bulb was much slower, observed at the ZNS-MAR DINA station as taking 55 days to saturate sensors installed 2.1 metres below ground level at a distance of 38 metres from the MAR channel.

Pre-treatment of source water prior to managed recharge

The water treatment prior to refilling is performed in three steps and locations:

- The storage dam and diversion of river water is located to one side of the Voltoya and functions as a settling square. The design features three metal filters starting halfway up the structure each decreasing in grid size, the first for roughing, the third for filtration.
- Filter intercalated gravels and a conduction pipe is located near the meter. The concrete pit was initially sealed with a metal filter, which was redesigned with subsequent improvements improving accessibility by an airtight lid and substituting one metal filter gravel.
- Great settling basin/infiltration at the top of the channels (14,322 m^2), which performs a second settling of fine particles. The beginning of the channels is above the level of the bottom. At first they were for landfill, currently below the stop device, regulating the opening to regulate the flow.

Clogging characterisation

Clogging affects the study area differentially in both type and degree of development.

Processes must have an initial characterisation of clogging to adequately monitor its evolution and therefore design the most effective remedial actions.

Generically, the infiltration rate depends on the texture, structure and heterogeneity of the soil; its humidity and the depth of water table. Some factors that also affect the infiltration capacity of the soil are compaction, washing of fine particles into the surface pores and macropores (cracks and fissures). Other factors to consider include the

surface vegetation or crop type and the amount of air trapped in the unsaturated zone above the aquifer, which enters the same from the atmosphere directly or transported by water (rain or artificial recharge) in solution or suspension.

Clogging process was detected in both substance and in the walls of the device surface (rafts and channels). The most abundant type of clogging processes are physical, biological, chemical [generally motivated by the precipitation of calcite under ponds and canals (in Fernandez et al., 2009)] and their combinations (Figures 5-10 to 5-15). The coexistence of different types brings synergistic processes. To these must be added the silting generated gas and compaction due to the weight of excessive water depths, while decreasing the infiltration rate of the bottom of the infiltration basin or canal, and even, to a lesser extent, on the canal walls.

Regarding physical clogging, note the presence of a crust or cake, clay and silt coverage area originated either by retention effect of suspended particles (fines) which are blocked in the aquifer and undergo subsequent compression, or "self mulching effect."

In the soil profile coarser particles are deposited on the soil surface or at shallow depths, while the finest are more penetrative and can be "trapped" in the pores, filling them and thus hindering the flow of water. Once the movement of the larger particles is blocked, the particles themselves serve as filters to trap particles successively smaller entering a progressive clogging the hydraulic conductivity was reduced to a fraction compared to the original value. Failure to implement remedial measures, it may be necessary to abandon the work.

Self mulching effect manifests as a surface crust as a result of different degree of wetting of the soil as a function of depth (Ryan and Elimelech, 1996). Its thickness is greater in the hollows of the corrugations of the bottom of the pond and the "talveg" or deepest area of the channels (Figure 5-10).

Added to these phenomena is the eluviation-illuviation processes of clay, which is a very complex process caused by the mobilisation of clays from the recharge water (rain and artificial). From the surface horizons, the finer particles pass into the soil solution suspension. By infiltrating the pores of larger size, form thin films, first aqueous clay then arranged parallel to each other, forming cutans or argillans or clay-skins. These surrounding walls of the macropores, being strongly retained (Figures 5-11 and 5-16) and associates silicate gels, humic acids and other colloidal substances which complicate the process. With the following rainfall or recharge cycles, the process is repeated, stressing the ability to maintain consistent infiltration rates within the basin or canals.

Generally seen a level of cake and illuviation horizons in the area S of the device, up to 20 cm deep on average (Figure 5-12).

Figure 5-10 a) to c): Clogging deposited in microtopographical depressions at the bottom of the infiltration pond due to self-mulching effect

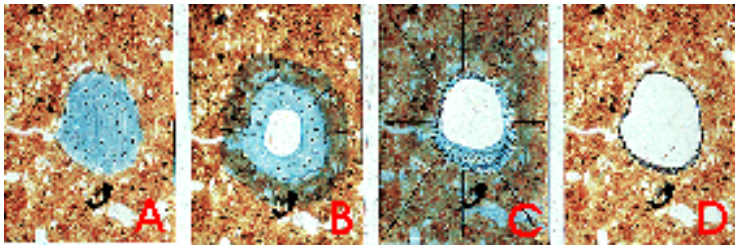

Figure 5-11: Evolution of the formation of clay-skins or clay coatings (from http://edafologia.ugr.es/introeda/)

Figure 5-12 a) to c): Examples of clogging processes detected in the rafts and channels "artificial recharge" predominant physical processes

Chemical processes that initiate clogging are usually of two types. For one site calcite was detected as either carbonated superficial crusts (Figure 5-13) or as a strip calcareous precipitates located between 40 and 60 cm deep under the bottom of the channels and basins (detected by the curves infiltration tests with double ring (in DINA-MAR, 2010, Figures 5-9 and 5-13).

The former are generated by the precipitation of minerals present in the recharge water to decrease the concentration of dissolved CO_2, a process often motivated by the photosynthetic activity of the water. In the 2nd case, its origin is attributed to changes in temperature of the recharge water as infiltrate the aquifer, for your warm under very cold conditions at the surface.

Another type detected corresponding to sulphurised processes associated dark hue reducing environments, associated with abundant diagenetic pyrite (east central sector of the Basin, monitoring points IV-5 and 6, Figure 5-18).

Figure 5-13 a) to c): Carbonate precipitation in the bottom of the artificial recharge West channel (IN-11 Station)

In IN-11 point (near Villeguillo) the formation of a hard crust on the bottom of the channel while performing field work in October 2008 was noted. This whitish carbonate crust reacted strongly to acid. It is not unprecedented and is considered to result from direct precipitation from the recharge water under specific environmental conditions.

Biological processes that cause clogging manifest mainly by increasing soil organic matter, generally from water recharge and especially wastewater discharges and input from the sewage by impoundment (Figure 5-14). The bioburden and organic carbon modify the physical and chemical properties, giving the floor a dark colour, which varies according to the degree of humification and the

percentage of organic matter in the soil profile. Simultaneously provide the genesis of aggregates, the capacity to retain water promotes the settling of vegetation.

Figure 5-14 a) and b): Biological clogging processes associated to spills areas and waste water treatment plant inputs, with development of lemnáceas. Santiuste basin, SE zone

Clogging biochemical processes are manifested in areas with an abundance of algae, filamentous blue overall. These catalyse the precipitation of minerals to remove dissolved CO_2 in photosynthetic activity (Figure 5-15).

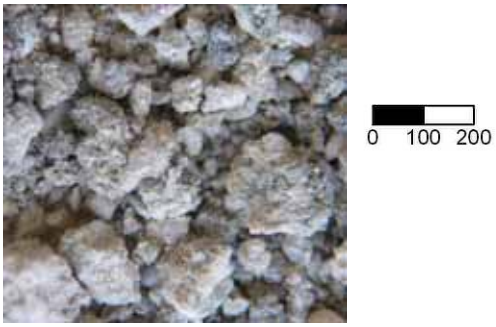

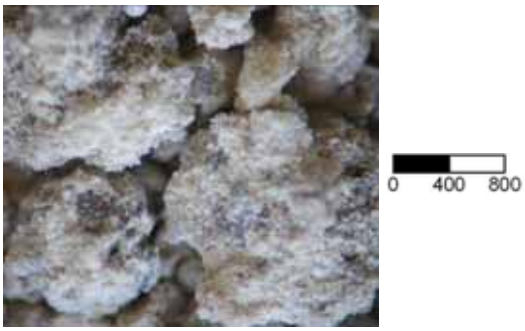

Figure 5-15 a) to c): Photographs with binocular loupe of the receiving medium and clogging processes as bio-clogging aggregates, spores, grains of pollen, clay skins and a clay film covering the sand grains

Some sectors have associations of different types, complicating the clogging process. Consequently, the study area has a wide variety of clogging processes, many in coexistence, which interact virtually all vectors with greatest influence on sedimentation as defined by Van Beek (1986) in a wheel diagram. Each "radio" is scaled within the ranges of magnitude (lower limit in the wheel spindle and the upper end) measured in nature (Figure 5-16).

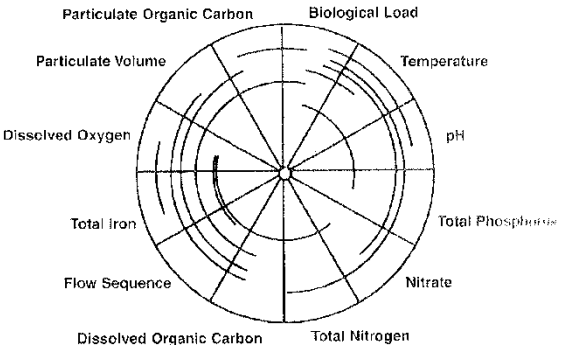

Figure 5-16: Factors affecting the growing of microorganisms and clogging processes in an infiltration well (Van Beek, 1986)

According to the field study of the materials obtained from the bottom and walls of the infiltration (Figure 5-17), a characterisation of clogging in the study area from the predominance of certain processes, has distinguished five types of clogging physical, chemical, biological, biochemical and mixed. The predominant clogging mechanism in each sector is presented in Table 5-5.

The process indentified is the most common physical clogging reaction, since the filtering and decanting operations have sometimes been ineffective. In particular at the beginning of both channels and in the central sector of the Western Channel.

Carbonated chemical clogging appears in the northern sector of the channel in the Central West and North-East sector. The processes associated with reducing environments were detected in the infiltration devices Central East, where the sands contain abundant diagenetic pyrite placer (pepitas).

It has been detected in areas across the basin with scarce biological aquifer thickness and proximity of loamy substrate (base of the aquifer to less than five feet deep) and high water tables (south-central section of the channel west).

In the west central sector of the infiltration channel the discharge of sewage waters by Santiuste impoundment generated a layer of organic sludge up to 15 cm thick. These are coated with Lemnaceae, due to its high nutrient load. Also detected were grids or mats of algae. Its genesis is attributed to biochemical processes. Downstream of station IV-5 is considered as a "mixed" area where all types of clogging processes coexist.

According to the spatial distribution of key processes and combinations thereof, an initial mapping for characterisation of clogging types across the scheme commenced in February 2010 situation (Figure 5-18). This mapping presents significant variations over time. Further characterisation of clogging processes can be found in Fernandez and Prieto, 2013.

Figure 5-17 a) and b): Soil and clogging processes profiles collected in the stations for the study of clogging and infiltration capacity evolution for the stations IN (West channel) and IV (East channel). Their position is presented in Figure 5-18 cartography

Table 5-5: Properties pit profiles and determination of major clogging processes detected in the study stations clogging. Modified from Fernández et al., 2009

EST	Date	Main clogging process	Observations
IN-0 Are	01/08/07	Physical	Banded profile
IN-0 Arc	01/08/07	Cake+physical	Surface crust in depressions
IN-1	28/08/07	Cake+physical	*Cake* determined by the microtopography
IN-2	28/08/07	Physical	Sand pasted by microtopography
IN-3		Cake+physical	
IN-4		Physical	Sand pasted by microtopography
IN-5	28/08/07	Physical-biologic	Clay and abundant organic matter
IN-6		Physical-biologic	Tangle of weed, clay and organic matter

IN-7	28/08/07	Cake+ biologic	Cake and organic matter differs to A horizon
IN-8	01/08/07	Physical-biologic	Cake and banded profile
IN-9		Physical-biologic	Cake and organic matter
IN-10	01/08/07	Physical-biologic	Cake and organic matter
IN-11	01/08/07	Chemical	Cake, carbonates and organic matter
IV-1	01/08/07	Physical	Banded profile
IV-2	28/08/07	Biologic-physical	Organic matter and lemnaceas
IV-3	28/08/07	Biologic-physical	Organic matter and lemnaceas
IV-4	28/08/07	Physical-biologic	Organic matter
IV-5	01/08/07	Mixed	Cake, clay, biologic vectors and carbonates
IV-6	28/08/07	Physical-biologic	Cake , organic matter and carbonates
IV-7	28/08/07	Biologic-physical	Horizon A with organic matter and clay

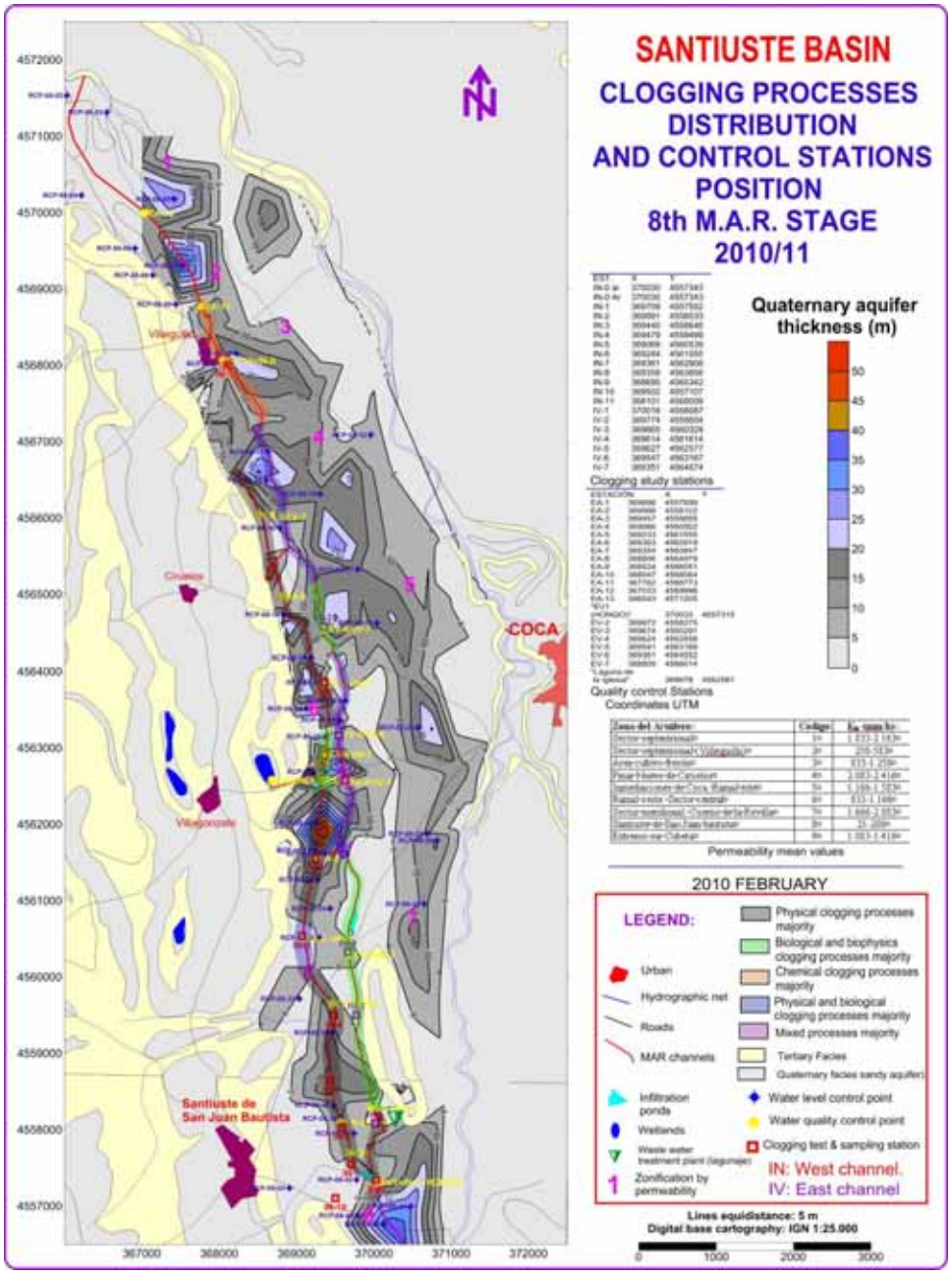

Figure 5-18: Cartography for Santiuste basin MAR devices and clogging processes distribution according to their nature. The map also exposes geological facies, the position of clogging, infiltration evolution and variable parameters stations, piezometric control water points and other singular elements. Graphic scale (Modified from Fernández and Prieto, 2013)

6 Discussion

The selected working method consists of a series of problem-solution pairs (once clogging has occurred what are the methods employed for unclogging) for subsequent comprehensive treatment.

The solutions proposed for the environmental impacts and dysfunctions mentioned have involved several years of research and progressive improvements. Generally speaking, the initiatives have been a reiterative process, up to the point that there are still several problems that are not adequately resolved and designs are pending construction. However, the current devices present notable quantitative and qualitative improvements over the initial design built ten years ago.

The main activities undertaken and proposed solutions, presented in chronological order, include:

6.1 Preoperational Stage

6.1.1 MAR Water Pretreatment

In agreement with Bouwer (1999 and 2002) we consider that pretreatment of the water to be recharged is the most important factor in producing optimal and sustainable MAR operations. Four main pre-treatment methods were applied:

1. River bank filtration (RBF),
2. Dam filtration,
3. Pre-treatment *In Itinere*, and
4. The use of run-off traps and stagnation/decantation structures.

These methods are individually discussed below.

1. River Bank Filtration (RBF)

A Ranney well is installed in the Voltoya River bed itself in the northern region of the Santiuste Basin MAR scheme. This process leads to natural filtration (river bank filtration) as the river water is filtered through the alluvium on its way to the lateral screens within the river bed that extend from the central well structure (Figure 6-1). After the water is filtered through the river bank, it is pumped and used for urban supply (after ozone treatment). Any surplus is sent to the MAR scheme.

After 10 years of operation, the system is providing good results, indicating that the RBF technique is a suitable method for pre-treatment of water recharge when the conditions are conducive. This being said, RBF is not generally employed throughout the Santiuste Basin MAR scheme because it usually requires pumping. The majority of filtration devices throughout this MAR scheme are gravity driven so as to remove the energy costs.

Figure 6-1 a) and b): Ranney well using a River Bank Filtration (RBF) system for water supply from which surpluses are applied for MAR in Santiuste Basin

2. Dam Filtration

Dam filtration is a source water pre-treatment method employed throughout the Santiuste Basin MAR scheme. Interleaving reservoirs are placed in the same channel, with filtering devices in the dam wall and settling on the downstream side. Filters are also installed prior to the bypass valve for the dam. This option has been applied in the intake of all the Arenales Aquifer devices (Figure 6-2).

Figure 6-2 a) to c): Dams specially designed for water filtration and pretreatment in one side's specific facilities (filters and a decantation system). Santiuste Basin catchment dam (a-c. Some of the designs applied are inspired from the works of Bouwer (1999 and 2002) and Olsthoorn (1982)

3. Pre-treatment in Itinere

Source water is treated in transport from the Voltoya River inlet by passing through filters constructed from a range of materials including stainless metal, plastic and gravel. These filters are interspersed throughout the piping work of the MAR scheme and substantially reduce source water suspended load, while also influencing pH according to the rock type of the selected gravel.

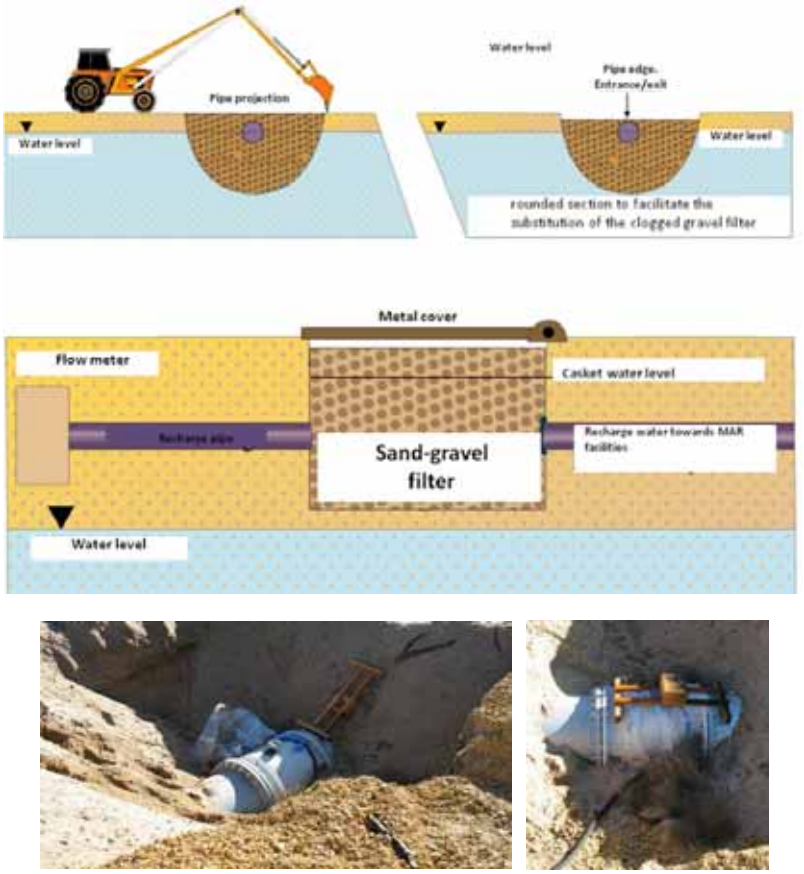

Figure 6-3 a) to c): Sandy filter scheme (a) equipped with a flowmeter after the filter (b-c)

4. Run-off Traps, Stagnation and Decantation Structures

Water drained from impermeable surfaces, such as high speed railway and some roads, is captured in run-off traps and introduced to the MAR channels after treatment via stagnation and decantation structures, designed to expose the captured water to sunlight (Figure 6-4). The discharge points from these structures are above the structure floor, avoiding fine sediments. Sometimes these structures are also equipped with flow control devices (Figure 6-4 c). Re-circulation of water back through stagnation and decantation structures is avoided by the system design in which all drainage is gravity driven, towards the MAR channel.

Evaluation of other pretreatment methods e.g. modifications to the original artificial recharge dams to facilitate river bank filtration, use of chemical treatments such as chlorine and denitrification byproducts and nitrofilic plant barriers to reduce nitrate concentrations are planned.

Figure 6-4 a) to c): Run-off traps, stagnation and decantation structures to pre-treat runoff water prior reaching MAR facilities

6.1.2 Design Improvements Applied on the Morphology of the Receiving Medium

Soil and Aquifer Treatment (SAT) that improve the performance of the MAR receiving environment are highly relevant, and, proper execution of appropriate designs will result in reduced clogging.

Treatments applied to MAR receiving media in the Santiuste Basin have included variations in the walls and bottom of artificial recharge channels and ponds, and the specific design improvements applied to large diameter recharge wells. These individual treatments are discussed in detail:

A. Actions in the pond and pool walls to minimise clogging

The formation of clogging processes within infiltration ponds and their vertical and horizontal distribution were studied. In order to improve their effectiveness, the surface areas of the infiltration ponds were increased by ploughing furrows (Figure 6-5). These furrows also allow silt to be deposited in the furrow bottom due to gravity, while remaining relatively clean along the furrow crest.

Figure 6-5 a) to c): Infiltration pond bench to test infiltration rate in order to different furrows wavelengths. The 80 cm distance has proved to be the most efficient for these environmental conditions

The design of furrows in the infiltration pond bed was investigated in detail, with various furrow spacings being trialled in the Santiuste Basin MAR scheme decantation and MAR pond, undertaken over three annual MAR cycles. Observations were conducted in September 2007, June 2008 and June 2009; with pond bed infiltration rate being measured with a double-ring infiltrometer (Figure 6-6).

Figure 6-6 a) to c): Furrows plugged with different width at the bottom of a decantation and infiltration pond, infiltration test by double ring infiltrometer in the convex (sandy) and concave (clay) surface of them and the clogging profile. Headwater of the Santiuste's MAR device

The first infiltration tests were conducted with a flat pond bed (September 2007), with the subsequent years' tests being conducted with furrow spacing ranging between 60 and 100 cm. The range in furrow spacing was used to quantify the difference in infiltration rate with increasing furrow spacing, while also allowing comparison with the infiltration rate recorded through the non-ploughed pond bed. The furrows were installed using a Roman plough, after the initial infiltrometer tests in 2007. Double-ring infiltrometer observations were taken at the end of the following MAR cycle, taken both on the 'ridge' and in the 'valley' of the furrows. Further details of this infiltrometer investigation are presented in Fernández et al. (2009).

Physical and biological clogging processes were found to be relatively evenly distributed along the bottom of the flooded ponds, with clogging observed both on the crest and in the valley of the ploughed furrows. This being said the thickness of the fine silts (clogging material) was reduced on the furrow crest compared to the valleys.

Calculated infiltration rates from test observations are presented in Table 6-1, with infiltration curve analysis plots presented as Figure 6-7. Infiltration results generally demonstrated an increase infiltration rate following the installation the furrows in the pond bed (measured in June 2008), with a subsequent decrease in rate measured in 2009 due to clogging (Table 6-1). The exception to this was the 60 cm furrow spacing, which had decreasing observed infiltration rate over all years. Infiltration rates were generally higher on the furrow crests compared to the valleys. Infiltration rates recorded for furrows spaced at 80 cm were greater than those for 60 or 100 cm furrow spacing, for both the furrow crest and valley, during both the 2008 and 2009 observation events (Table 6-1).

Table 6-1: Results of infiltration tests in the headwaters infiltration pond. Values for 2007 September (pre-operational), 2008 June and 2009 June (post operational) respectively

	Coordinates UTM		Campaigns: t and inf. rate Sept 2007/Jun 08/Jun 09		Characteristics	
STATION	X	Y	Test (min)	Infiltration rate (mm/h)	Site	Soil type
POND 1	369832	4557443	100/255/101	2500/95/38	ridge 0.6 m	sand
POND 2	369839	4557436	100/248/100	100/90/65	valley 0.6 m	silty sand
POND 3	369821	4557448	148/120/68	90/**420**/100	ridge 0.8 m	sand
POND 4	369803	4557426	180/120/81	220/**232**/108	valley 0.8 m	silty sand
POND 5			150/150/nd	200/350/nd	ridge 1.0 m	sand
POND 6			nd	250/220/44	valley 1.0 m	silty sand

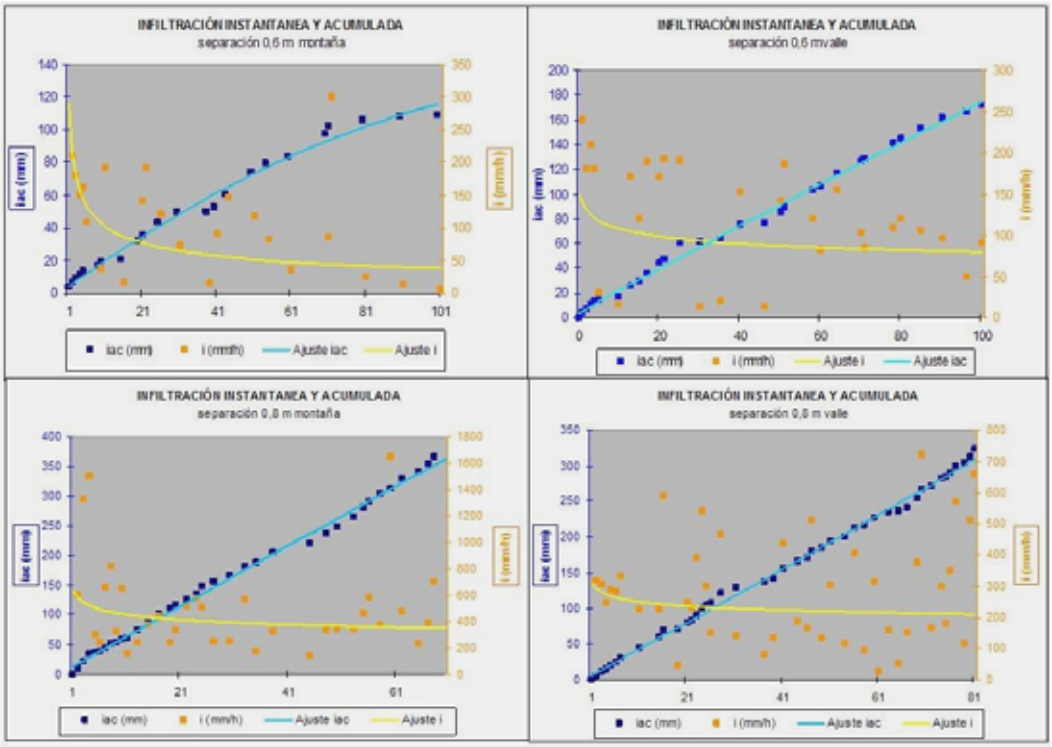

Figures 6-7 a) to d): Test interpretation graphs with double ring infiltrometer in basin 3, with 0.6 and 0.8 m, made in June 2007 to 2010. Graphs made with 2008 data sets, confirming clogging problems in infiltration ponds at different depths, as well as the generation of carbonated crusts in sectors of the aquifer that could be due to recharge during frost cycles

Interpretation of the infiltration curves (Figure 5-9) suggests there is a horizon between 40–50 and 60 cm deep where a reduction in the vertical permeability ratio (Kv) is observed and is inferred to be broadly attributable to physical and chemical clogging processes derived from a decrease in temperatures and calcareous precipitation. Therefore, mechanical treatment in remediation tasks should go far deeper in (increasing the horizon removed up to 60 cm deep).

According to the analysis of results, the observed rate of clogging is usually higher in short-term tests, and lower in longer-term tests. It is believed that there is a higher silt concentration at a certain depth beneath the pond. These results are based on a limited number of tests and it would be useful to increase the number of tests to confirm these preliminary findings and support the development of maintenance options.

The results confirm that, according to the test place and conditions, furrows increase the infiltration rate when compared with flat-bottom basins, with higher infiltration rates achieved through the crest of the mounds than in the furrows. Although it is not possible to set a defined trend, given the few number of tests, furrows with 80 cm spacing perform better in general terms. However, these results are not final.

It is a good practice to open furrows with disc ploughs, which proves to be less harmful than the mouldboard plough.

The depth of the water in the recharge ponds and channels during each charging cycle has been another factor taken into consideration as the hydraulic loading applied by the depth of the water itself can cause compaction of the bottom sediments.

In general the water level in the ponds and channels is maintained between 80 and 140 cm. The higher infiltration rates in the conditions under which the tests have been performed, have occurred with water depths near 80 cm, and this has been adopted as standard practice.

B. Actions on channel morphology to minimize clogging

The actions taken have mainly been by trial and error and have included variations of the morphology of the channel, by incorporating a centre ridge or modifications to the slope of the channel sides.

For detecting the spatial distribution of the different clogging processes thermography techniques have been used based on the differential absorption of heat between the natural soil or clogging processes. This technique is extensively described in Fernández and Prieto, 2013 (Figure 6-8).

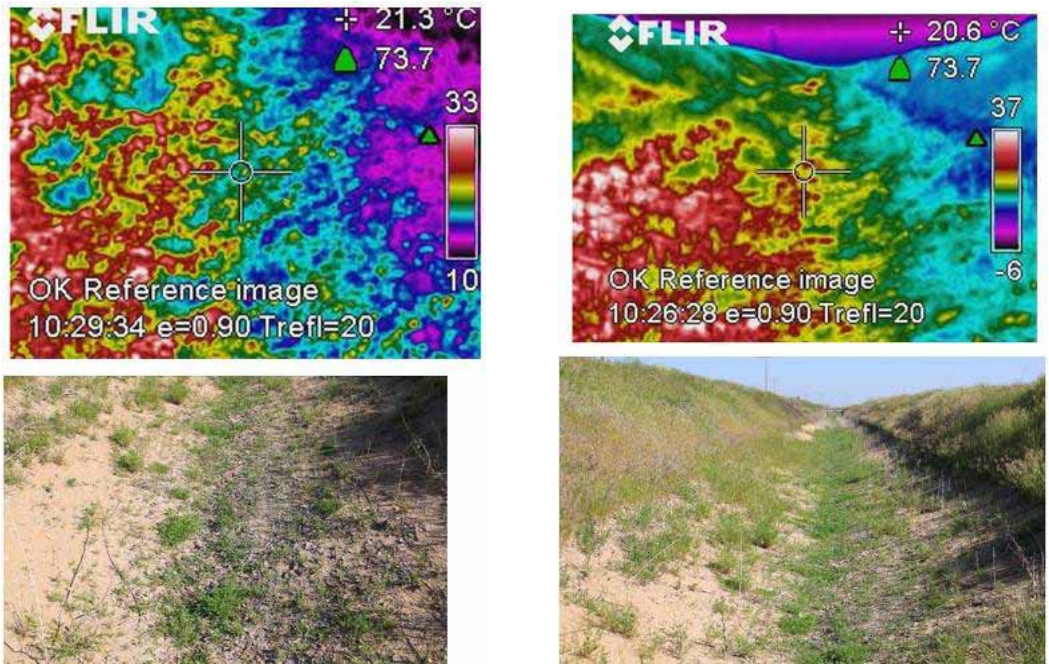

Figure 56-8 a) and b): Employ of thermographic images to detect the differential clogging distribution in MAR facilities. West Canal Fund in an area with geotextiles buried for the study of processes (bottom) and the transition to the natural terrain (top half of the figure to and end of the b). Southern Sector of the device

The concentration of fines in the channels appears to be largely controlled by microtopography. It also often accompanied by further development of herbaceous vegetation, which is kept cool by the effects of moisture on the bottom of the channel and, hopefully, for the nutrients provided by clogging physical and biological processes.

At the bottom of the channel infiltration tests (Figure 6-9) have identified the presence of clay and carbonate accumulate at a depth of around 40 cm.

The carbonate precipitate has been detected especially in the west channel. Calcite precipitates present a whitish hue and the thermal response is opposite to the usual physical and biological processes. These precipitates appear at the bottom of the channels, in depth and in a "stain" on the slopes, usually in the area submerged and the oscillation of the water surface circulation. Its heat absorption rate is high, despite its clear tone and high reflection, in contrast with the surrounding soil and was thus easily identifiable.

The uneven distribution of clogging processes along the channel slopes made it necessary to modify the morphology of the canals and ponds, as well as designing specific cleaning techniques.

Initially 1:1 slopes were selected in fine sands for greater durability and presumed smaller clogging concentration, due to their steeper angle. After some slumps in the channel walls and several trials (Figure 6-10 a-b); channel slopes were modified to 2V:3H (c) and after 3H:2V. The gentler slopes have increased the infiltration rate across the walls but also their clogging development, with even carbonates lenses.

A more detailed description of the factors for making decisions on the slope of the slope is in Dyne-Mar 2009.

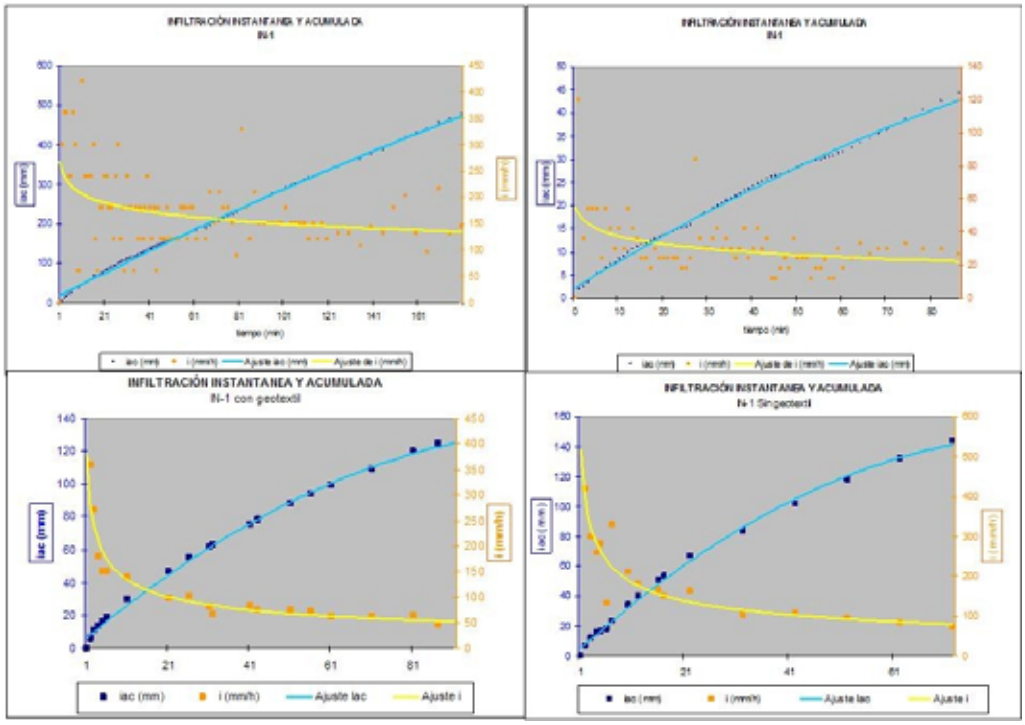

Figure 6-9 a) to d): Infiltration tests in IN-1 station (canal) since September 2007, June 2008 and 2009. Double ring infiltrometer tests graphics and interpretation

Figure 6-10 a) to e): 1:1 slope with potential slices due to desiccation processes (a, b); 2H:3V initial design (c); 3H:2V as the most common slope in the channels and ponds walls (d); and eventual gabions protections (e)

Installation of replaceable geotextiles along the central furrow to facilitate the harvesting of fines has been trialled (Figure 6-11a) and b). This approach has been previously tested in the dune fields of Amsterdam and consists of a gravel drainage layer covered by a nylon geotextile, on which is distributed fine sand.

Figure 6-11 a) and b): Geotextile installed in the bottom of the channels to facilitate the cleaning of clogging processes with minor changes in the infiltration rates

C. Use of mulches

Most of the vegetation in the infiltration canals and basin is preserved during the summer season as roots prepare the soil for a higher infiltration rate, at the same time that plants consume a fraction of the organic matter and nutrients which form part of the clogging process.

The vegetation is typically removed before the new MAR cycle starts; however, some specific species are planted along the spring season as a soil treatment measure.

6.2 Sinoperational Stage

Some practical interventions *c*in order to reduce the clogging genesis and to increase the effectiveness of the facilities whilst managed aquifer recharge activities are being accomplished.

6.2.1 Interventions to Modify MAR Water pH

Actions have been taken in the receiving environment where pH in the recharge water is considerably different from the native water. The chemical imbalance contributes to the clogging processes.

The technique used for pH balancing has been the inclusion into the design of calcareous gravel beds and acid stone breakwater (Figure 6-12). This construction technique allows small corrections of pH on predefined sectors while giving durability and ruggedness to the infiltration channels.

Figure 6-12 a) to c): Gravel filter to result in pH corrections as well as provide stability to some MAR facilities

6.2.2 Management Parameters adopted to control turbidity

A recharge programme designed with manual valve control and operated by the irrigators with the advice of DINA MAR has been implemented. Operation is controlled depending on climatic circumstances where in general, artificial recharge is minimised on frosty days to prevent the formation of carbonated crusts and also when there are storms which greatly increases the turbidity of the river water intake.

6.2.3 Strategies Adopted to Prevent Gas Clogging

Gas entrainment caused through cascading and turbulence (Figure 6-14) can cause severe clogging through generating hyperoxidised conditions, and a significant blockage of the pores of the aquifer, triggering the "Lisse effect" (Krul and Liefrinck, 1946, Bouwer, 1999 and 2002) . This effect is produced by the pressure of air entering the pores of the aquifer, so that "bubbles" trapped reach hydrostatic pressure exerting a centrifugal force contrary to recharging circuit.

The monitoring of the air inflow into the aquifer around the MAR infiltration channels and basins is accomplished with humidimeters, termometers y tensiometers at DINA-MAR ZNS stations (Figure 4-1).

The study of gas clogging is being carried out by three different indirect methods:

- Study of dissolved oxygen concentration versus channel flow rate
- Dissolved oxygen concentration changes between MAR water and groundwater in closed observation wells
- Seepage capacity evolution along a full MAR cycle

Study of Dissolved Oxygen Concentration versus Channel Flow Rate

There have been periodic determinations of dissolved oxygen in the water recharged in the headwaters of the channel, comparing the data with flowmeter (Table 6-2).

Table 6-2: Total Dissolved Oxygen versus MAR cannel flow rate

Q deriv (hm^3)	Qm canal (l/s)	Tol. Inf. Vol.	TOD ppm
3.5	278	1.30	7.2
2.25	149	1.80	7.0
1.26	68	0.97	6.9
5.11	372	3.56	7.5
12.68	692	12.19	8.9

Figure 6-13 a) and b): Manual control of the inlet valve by farmers advised. Close on flood, storms, frost, etc.

Figure 6-14 a) to c): Recharge water with 7.5 ppm of total dissolved oxygen, in situ determinations and sample collection

In general a direct proportional relationship is observed between exponential input flow and dissolved oxygen (consider for this the total air is proportional to dissolved oxygen, by Henry's Law).

From these data points were prepared corresponding Scatter graph of calculated and the equation of the regression curve interpolated (Figure 6-15):

Y= 4.3413 x 0.0993

The curve is concave upward and from this we deduce that there is an optimum dissolved oxygen for a given flow rate corresponding to the minimum of the graph, which is located around the flow of 300 L/s (again for the specific circumstances of the trials). These deductions could be extrapolated to similar scenarios, but should not be applied as a general rule.

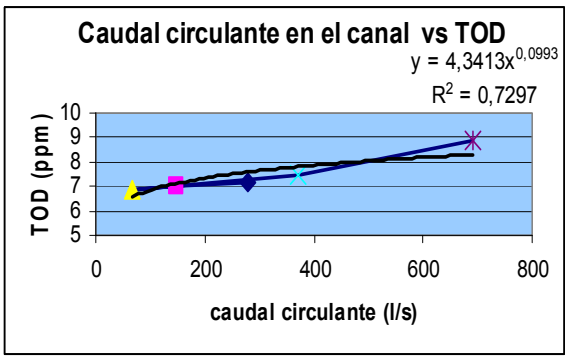

Figure 6-15: Relationship between dissolved oxygen and flow circulating through the MAR channel

Dissolved Oxygen Concentration Changes between MAR Water and Groundwater in Closed Observation Wells

We have conducted measurements of the evolution of variable parameters along the infiltration channels. The parameters are controlled conductivity, Total Dissolved Solids, salinity, redox potential, water and air temperature, total dissolved oxygen and pH. Data can be viewed in the annual project reports (DINA MAR, 2009 b). Determinations for selected target (conductivity (EC), Total Dissolved Oxygen (TDO) and pH) are shown in Tables 6-3 and 6-4. Sampling points are projected on Figure 6-18.

Figure 6-16 (a-f) show the evolution of these parameters along the various infiltration channels.

Table 6-3: Selected unstable parameters determined in six stations along MAR canals

EStation	X	Y	TDO (ppm)	EC (µs/cm)	TSS (ppm)	SAL (ppm)	pH	Date
EA-0b	369833	4557404	10.7	171	138	0.13	7.5	22/01/2009
EA-2	369563	4558102	11	142	113	0.11		22/01/2009
EA-3b	369152	4560188	7.6	274	205	0.2	6.98	22/01/2009
EA-4b	369095	4560809	8.6	288	215	0.21	7.06	22/01/2009
EV-3b	369698	4560204	6.5	179	137	0.13	6.01	22/01/2009
EV-7b	368838	4565954	4.8	293	223	0.22	7.01	22/01/2009

Table 6-4: Selected unstable parameters determined in observation wells close to canal stations and hydraulically connected. Last column for distance (m)

RCH WELL	X	Y	Z	TOD (ppm)	EC (µs/cm)	TSD (ppm)	pH	date	Est. Well Dist.
RCH 08-42	369776	4557346	801.5	5.5	N/A	N/A	N/A	01/03/2009	81
RCH 03-17	369370	4558001	806.0	3.60	932	400.0	8.10	01/03/2009	218
RCH 03-21	369113	4560186	794.0	3.69	1119	450	7.80	01/03/2009	39
RCH 03-13	368889	4560820	790.4	4.20	1437	580.0	7.90	01/03/2009	206
RCH 03-22	369855	4560210	793.6	4.35	513	210.0	9.00	01/03/2009	157
RCH 03-5	368902	4565953	776.6	3.31	1486	550	7.40	01/03/2009	64

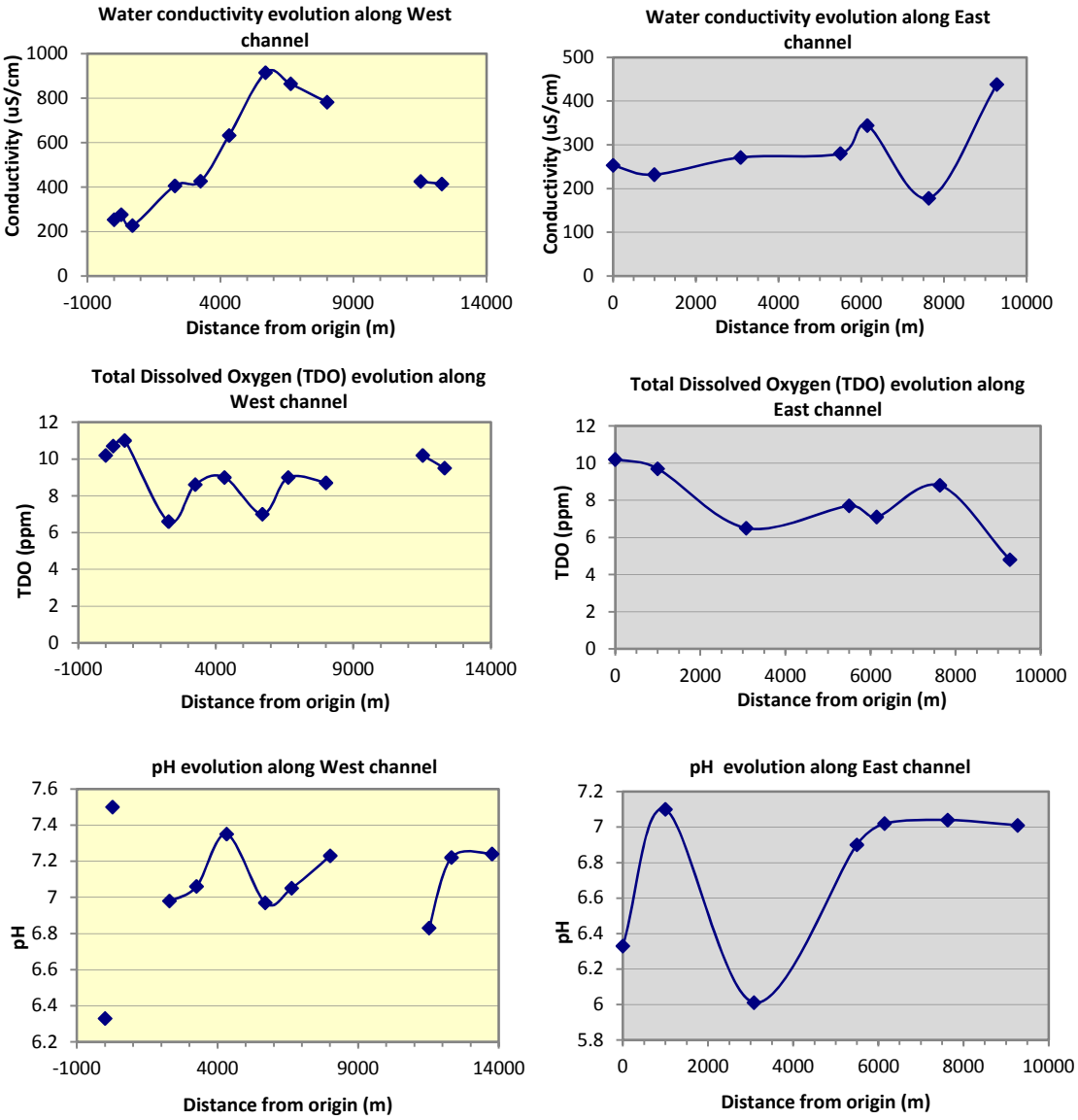

Figures 6-16 a) to f): Representation of the evolution of three selected parameters along the channels: Conductivity in the West channel (a) and East (b); TDO West (c) and East (d), and pH West (e) and East (f)

In the West Channel, the conductivity increases very rapidly during the first few miles until reaching its maximum at a distance of approximately 6 km from the head. From that point the conductivity begins to decrease. This increase in conductivity can be interpreted to the influence of aquifer depth, salinity, incorporation of reclaimed water and agricultural activities, while the decrease is attributed to additional inputs from runoff.

Suspended solids followed a similar trend as the suspended particles remain dispersed in the water by virtue of its colloidal and similar electrical charge, which causes particulates to be kept in suspension by electrokinetic repulsion.

The dissolved oxygen content fluctuates between values of 6 to 11 ppm along the channel path. The oscillations accurately record changes in environmental conditions and external inputs. pH values fluctuate in the range of 6.8 to 7.5 (nearly neutral values).

In the East channel conductivity exhibits a very slow increase along the channel to station EV-5, where the water enters a reducing hydrochemical environment sector attributed to the abundance of pyrite (FeO_2) diagenetic. As the water progresses along the channel, the influence of pyrite and conductivity decreases. However, at the last stations (EA-12 and EA-13) the channel bisects saline land and a saline wetland which strongly influences

conductivities.

The TDO decreases from 10.2 to 6.5 ppm at a distance of about 3 km from the inlet and then begins to rise 7.7 at station EV-4. From station EV-4 to EV-5 there is a marked reducing environment and thus, a reduction in TDO occurs. In EV-6 station TDO increases again (7.6) associated with runoff entering the channel, and at distance of about 9 km from the inlet oxygen concentration decreases to a value of 4.8.

At the inlet the measured pH is 6.33, indicating an acidic environment, but as the water moves through the channel towards the EV-2 station (1 km distant) the recorded pH is 7.1 (neutral). At EV-3 station (3 km from the inlet) there is a decrease in pH to 6.01 (acid), and from there increases to values close to 7, coinciding with reducing chemical section along this channel reach that contain pyrite (FeO_2).

The increase in these parameters between the measurement stations and the control piezometers with respect to the distance is presented in Table 6-5.

Using the data in Table 6-5 we have generated Figure 6-17 to calculate average variation curves of these parameters with the distance between the channel recharge and observation wells recharged from it.

Table 6-5: Distance from canal observation stations to related wells and differences measured in TOD, EC and pH parameters, as well as the ratios: increment (Δ)/ distance

Date	Est. Well Distance (m)	ΔO_2	O_2 Δ/dist (ppm/m)	O_2 Δ/Dist (µg/m)	ΔEC (µs/cm)	EC Δ/dist (µS/cm/m)	pH Δ	ΔpH /dist
01/03/2009	39	3.91	0.100	100	845	22	0.82	0.021
01/03/2009	64	1.49	0.023	23	1,193	19	0.39	0.006
01/03/2009	81	5.2	0.064	64	n/a	n/a	n/a	n/a
01/03/2009	157	2.15	0.014	14	334	2	n/a	n/a
01/03/2009	206	4.4	0.021	21	1,149	6	0.84	0.004
01/03/2009	218	7.4	0.034	34	790	4	n/a	n/a

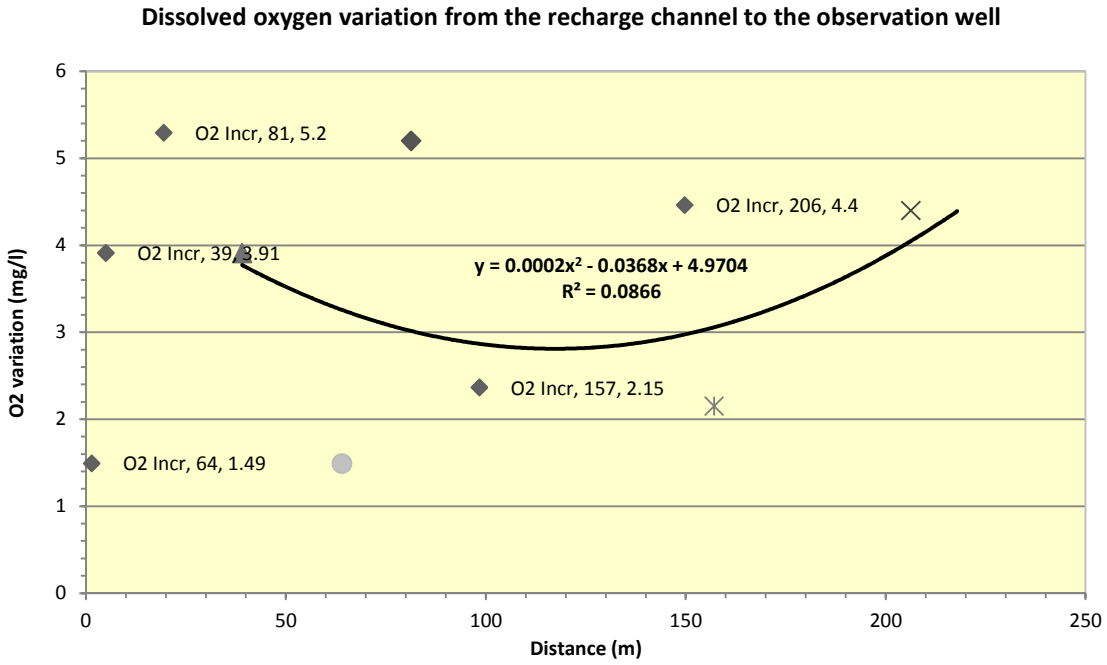

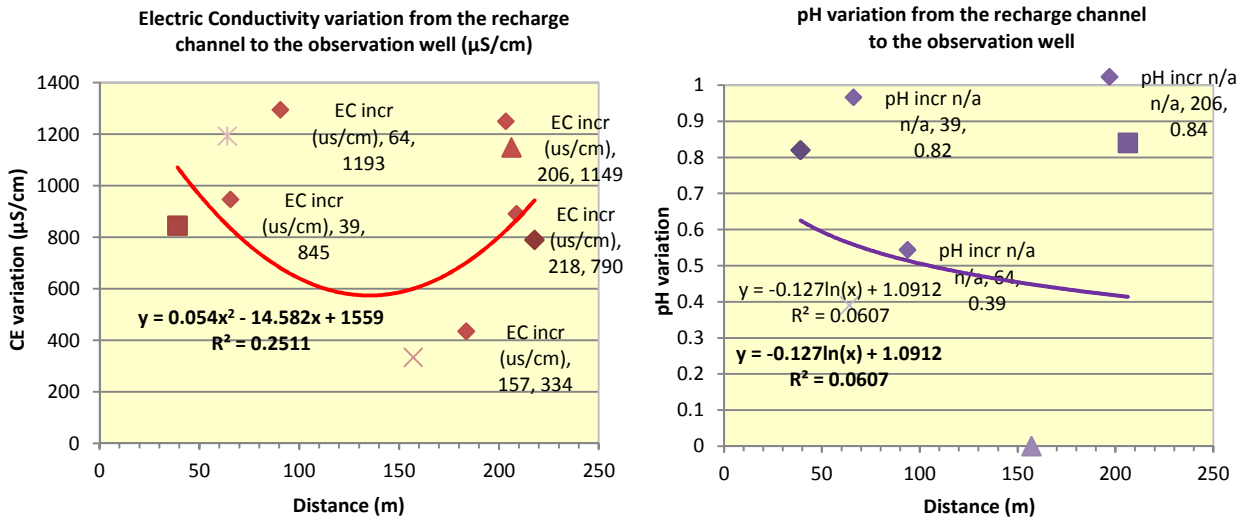

Figures 6-17 a) to c): Graphs representing the variation of the parameters from the channel observation well recharge with respect to the distance between the points

The equations of interpolated polynomial curves for CD and ODD, and logarithmic for pH as well as the values of R^2 and means obtained are:

Table 6-6: Distance from canal observation stations to related wells and differences measured in TOD, EC and pH parameters, as well as the ratios: increment (Δ) / distance

	Equation of the interpolated curve	R^2 value	Δ / D mean
EC	$y = 0.1168\ x^2 - 33.97\ x + 2{,}876.5$	0.6716	9 µS/cm /m
O_2	$y = 0.0002\ x^2 - 0.0368\ x + 4.9704$	0.0866	42 µgr/l /m
pH	$y = 0.3931\ \ln(x) - 1.7719$	0.1792	0.01 /m

With these values and the parameter estimates dissolved oxygen decreases as water flows through the aquifer recharge managed in the order of 1 ppm each 23.8 m. A fraction returns to the atmosphere, while the other is retained in the aquifer generating dynamic mechanical barriers that slow down the infiltration process.

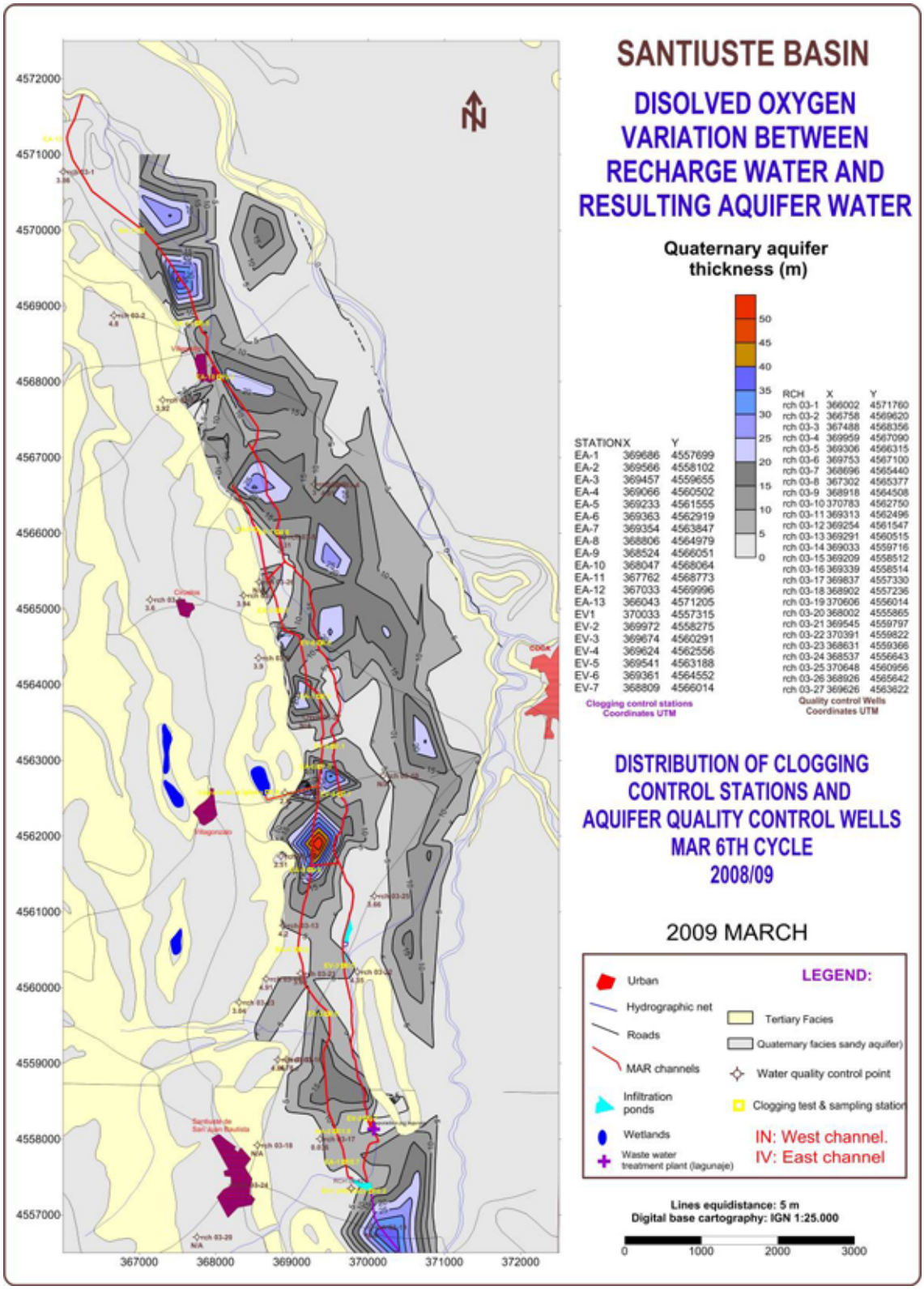

Figure 6-18: Santiuste Basin map showing MAR facilities and the position of clogging test stations and water quality control points plus associated elements used to estimate TDO changes

Seepage Capacity Evolution along a Full MAR Cycle

Another indirect technique to evaluate the TDO parameter was to study the evolution of air trapped in the aquifer during an entire MAR cycle. Sequential infiltration tests were carried out over the artificial recharge cycle (2004/05) in a specific bench ditch in the central site off the Santiuste Basin East channel. Eight infiltration tests were completed in a small bypass channel specially confined and conditioned (Figure 6-19). The results are graphically presented in Figure 6-19b).

DAY Nº AR CYCLE (2004/05)	INFILTRATION RATE(mm/year)
1 (01/10/2004)	35
7	159
14	140
19	315
39	301
108	300
126	291
149 (26/02/2005)	289

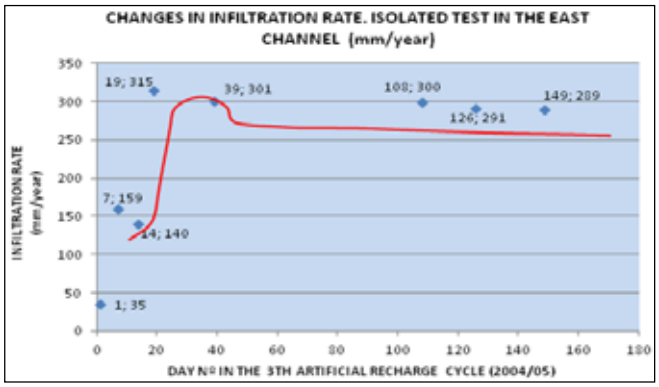

Figure 6-19 a) and b): Infiltration rate evolution along the MAR cycle 2004/05 for a bypass conditioned in Santiuste Basin East channel. Data, aspect and resulting graphic

Figure 6-19 (b) illustrates that the infiltration rate has been increasing continuously from November 1st when the concession started, reaching its peak around the month when the "artificial" recharge began and continuing until the temperature drop occurred in early December. It is considered that saturation plus air trapped in the aquifer pores combined with the low temperatures triggered the decrease in infiltration over the 15 day period.

As regards the rest of the artificial recharge cycle, it shows a slightly decreasing tendency during the winter (frost cycles seem to cause a delay in the infiltration rate increase). At some point slightly after half of the period (February–March), the aquifer has already trapped significant amounts of air (up to 35% according to estimations and references, as Stuyfzand, 2002), which may also be accompanied by the Lisse effect.

The volume of trapped air has not been quantified in the experimental laboratory, even though its presence has been noted, as well as its negative effect on managed recharge.

Communicating Vessels Designs in Order to Reduce Lisse and Cascading Effects

To prevent clogging by air entrainment TDO r should be as low as possible and engineering incorporated to prevent any increase along the channels. In general water in contact with the atmosphere causes a slight rise in TDO, but is significantly increased by cascading.

The initial damming devices placed at the head of the channels and in the connections with the supply pipes, produced a rise in the dissolved oxygen concentration of MAR water and a corresponding reduction in infiltration rates due to the Lisse effect (Krul & Liefrinck, 1946) (Figure 6-20 a and b).

According to estimations, the infiltration volume decreased by 25% from the fist to the second MAR cycle (2003–2004), attributable to the air entrainment.

The measures implemented were aimed at reducing the dissolution and gaseous particles incorporated in the recharge water through changes in the design of the devices at the head of the channel and their operation. Tests carried out so far are based on the placement of communicating vessels below the weirs, precast concrete in the channel interleaved mode dams, (Figure 6-20 c to e).

Figure 6-20 a) to e): Stopping and damming devices MAR evolution in Arenales experiences. Original design (a, b), the stops are flown and passed the water below these above rather than turn are drilled halfway up to combine both methods (c), the central steps are equipped with a gate to regulate the flow along the channel, tending to occur below the contact area with the air, leaving the hands of farmers management properly advised (d, e)

Figure 6-21 illustrates a system of communicating vessels to reduce the "cascading" effect and churning water free fall over the weirs to reduce air entrainment.

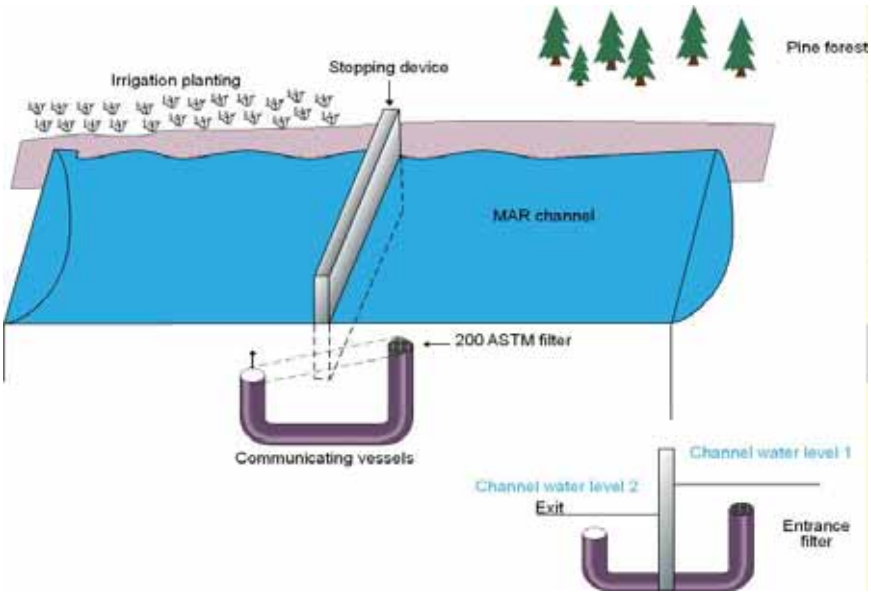

Figure 6-21: Scheme of the communicating vessel systems tested in all detention devices and chutes to minimise aeration as well as emergence under the water level. Modified from Fernández, 2005

Improvements in the design must be accompanied by improvements in the operation, hence the floodgates management has remained in the hands of farmers who have been duly advised, of these impacts and how to reduce them.

6.3 Postoperational Stage

6.3.1 Cleaning and Maintenance Operations in Channels and Infiltrations Ponds

One of the measures taken in channels to maintain infiltration capacity is to carry out "transfer mining" which involves the replacement of the silted sand surface with clean sand. Consideration must be given to where the silted sand can be dumped and where the replacement material is sourced.

Removal of material to depths of 60 cm will incur high maintenance costs, thus, combating carbonated crusts caused by precipitation is best managed through preventive measures rather than extractive measures.

In infiltration basins replacement of material is more complex, so constructing a tapestry by "scratching" with the surface with a blade, then styling ridges separated by 80 cm, distance between crests produces the best infiltration rates.

In the pilot areas clogging processes occurred from the first recharge cycle, making it necessary to perform cleaning operations of the bed, either simultaneously with AR operations but in general, the basins and channels are not operational (Figure 6-22). Under certain specific conditions within each area, the morphology of the basin or canal, governs the frequency of how often the system is taken off-line for cleaning or scraping. Installation of service road parallel to the canal, has allowed cleaning operations to be carried out with bulldozers and tractors.

Figure 6-22: Cleaning and maintenance operations in ponds and canal by means of excavators and tractors with adapted accessories

Where conditions allow the access of vehicles investigations are underway to design and build a prototype cleaning "pilot", which allows comprehensive desilting. This Basin Cleaning Vehicle (BCV) will be designed to be installed on a machine travelling on the service road. The design features should include: a knife to extract the bottom cake, long swing arm which allows operating in the channel from the service road and folded to reach steps, stops, etc. Figure 6-23 presents a schematic for such a generic device.

The material must be roughing sucked and filtered, with the option to carry out a chemical treatment in the same vehicle before reimplantation, recommended option in Van Duijvenbode & Olsthoorn, 1998. It is also possible to remove the material to agricultural or landfill and replace clean sands (option used today).

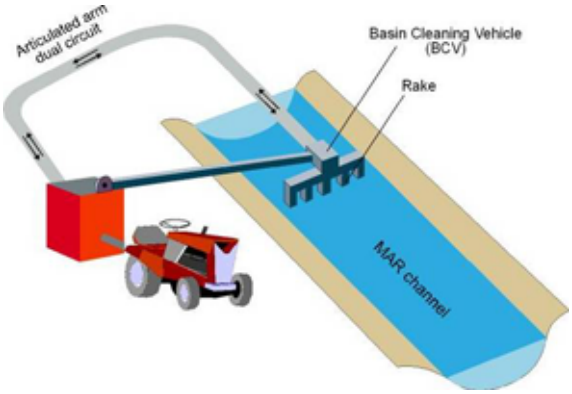

Figure 6-23: Schematic design for a Basin Cleaning Vehicle (BCV) (Hutchinson terminology) adapted to the morphology of the canal and based on the use of traditional machinery with easy assembly and disassembly structural modifications. Modified from Fernández, 2005

7 Conclusions

- Clogging treatment must be considered an integral action rather than in response to a system failure, as there is a complex relationship between all clogging types.
- Modifications to the design of the infiltration canals and basins have been made by trial and error using the best scientific judgement, due to the limited information in the literature on clogging remediation. After each modification testing and monitoring is carried out to gauge the success or otherwise of the modification.
- After 10 years of operations at the Santiuste Basin for managed aquifer recharge, deficiencies have been detected relating to clogging issues and significant effort has been done to ameliorate them. As a general rule, "it seems well done" in the sense that the greater

the MAR canal or basin efficiency, the smaller is the clogging development. Many of these are being resolved by adopting SAT techniques, new structural designs, management parameters or governance changes The preferred working method consists of a series of problem-solution pairs.

- The majority of impacts detected correspond to clogging processes (greater scale and intensity), excessive fine particles, insufficient pre-treatment and intake of air into the aquifer from the recharge water.
- The design changes and management parameters must be created “a la carte”, depending on the intricacies, climate and characteristics of each system.
- A vast list of actions has been proposed with the primary objective of presenting a series of options to be considered when implementing a solution for a problem that affects the superficial type of recharge management mechanisms or injection wells (corollary), as an instrument for decision making.
- Pre-treatment is consolidated as the most effective alternative for the correct operation of the canals and basins to prolong their efficiency and average service life, as long as cleaning and maintenance operations are continued at appropriate intervals.
- To minimize clogging, pretreatment and maintenance of the canals and basins, combinations of filter gravel, pebbles and sand combined with metal and plastic filters have been employed and have yielded good results.
- The downward trend in channel infiltration rates has been reduced by applying flow control techniques (at flow rates below 300 L/s), fine filtering and air reduction in the recharge water.
- The pH of the recharge water is neutralized by interaction with rocks opposite areas along the channels where reactive soils have been identified to provide pH buffering. Although changes are modest, the results are good in general.
- The gas binding is a large-scale impact and intensity. The recharged water from canals is losing about 1 ppm of dissolved oxygen circulate through the aquifer after 25 m in the horizontal. Much of this increase is trapped in the pores of the aquifer. It is advisable to recharge t at slow rates, since air entering the aquifer occupies about 25% of the temporarily effective porosity (estimated by indirect methods)..
- Communicating vessels have been incorporated into designs to minimise water cascading, sand filters and buried channel sections with pipe filters are delivering good outcomes.
- Manual control valve placed on the inlet to the channels that are operated by farmers, supported by continuous technical advice from DINA MAR, is giving progressively better infiltration results. It is minimising the volume of artificial recharge cycles during frosts and prevents high turbidity water from entering the scheme.
- The gradients of the slopes of the channel walls, after trialling with 1:1 and 2:3, we have opted for the stability of the 3:2, provided that there is sufficient space. Where slopes cannot be installed at 3:2 gradients riprap walls are installed to prevent bank erosion of the canal walls.
- Furrowing ridges on the bottom of the basins and canals doubled the infiltration rate. After trial and error it was found that the optimum distance between ridge crests to maximise infiltration rates was 80 cm with an equal depth (80 cm) of water above the base of the channel or basin bed.
- A design aspect must be added to operational costs for cleaning and maintenance "on demand" for each canal or basin case.
- The proposed generic prototypes for basin and canal design require further development to meet the criteria, which basically are: minimize losses (evapotranspiration, clogging, etc.). The designs should provide ease of access for desilting, and reduced transportation costs to dispose of spoil removed.
- The initiated looping process (trial and error) is open. Each improvement becomes a new element to improve upon. That is why any modifications must be complemented with ongoing monitoring to evaluate the success or otherwise of the modification and allow adoption of the best methods.
- It should be noted that one drawback of this approach is that the outcomes are slow since the reaction to any immediate action sometimes takes years to assess its effectiveness. The effectiveness of any action may also potentially be masked by other factors that come

into play as a consequence of the change. Consequently, sedimentation studies require large doses of "patience" and high "hydroimagination" as solutions can often be outside the traditional realms of thinking.

- Consideration of climate change and possible adverse effects, has added a 'new' variable into the mix which also requires management.

8 Acknowledgements

The mentioned tasks and the article itself have been carried out and written within the framework of R&D DINA-MAR project, www.dina-mar.es, code 30/13.053, financed by Tragsa Group and the help of Santiuste and Carracillo Irrigation communities as well as Guadiana water basin authorities (CHG).

9 References

Blaxejewski, M,. (1979) Gases in the ground and their effect during artificial recharge of groundwater Int. Symp. On Artificial Groundwater Recharge. Dortmund. Vol IV, paper VI. 4. DVWK, Bull. 14. Verlag Paul Parey. Hamburg-Berlín, pg. 59-70.

Bouwer, H., (1999) Artificial recharge of groundwater: Systems, design, and management. In: Mays LW (ed.) Hydraulic design handbook. McGraw-Hill, New York, pg 24.1–24.44

Bouwer, H., (2002) Artificial recharge of groundwater: hydrogeology and engineering. Hidrogeology Journal, Volume 10, nº 2, April 2002.

Custodio Gimena, E., (1986) Recarga artificial de acuíferos. Boletín de Informaciones y Estudios, nº 45. Servicio Geológico, Ministerio de Obras Públicas y Urbanismo (MOPU). Madrid. 148 pg.

Custodio Gimena, E., (2013) Groundwater governance. Synthesis of thematic papers/case studies. Preparing the ground for Regional Consultations and Global Diagnosis Report. GEF-FAO Groundwater Governance. Thematic Paper 1.

Denudt, H., and Ricour, J., (1990) Vieillissement du parc de forages et conditions d'abandon des ouvrages de production d'eau dans la Region Nord Pas de Calais. Ann. Soc. Géol. Nord. CIX. B.R.G.M. France.

Dillon, P., Fernández, E., and Twinhof, A., (2012) Management of recharge/discharge processes and aquifer equilibrium states. GEF-FAO Groundwater Governance. T.P. 4. In http://www.groundwatergovernance.org/resources/thematic-papers/en/.

DINA-MAR (2010) Gestión de la recarga artificial de acuíferos en el marco del desarrollo sostenible. November 2010. ISBN 978-84-614-5123-4, 496 pg.

Driscoll, (1987) Groundwater & Wells. Johnson div. Publ. S. Paul, Minnesota. USA.

Fernández Escalante, E., (2005) Recarga artificial de acuíferos en cuencas fluviales. Aspectos cualitativos y medioambientales. Criterios técnicos derivados de la experiencia en la Cubeta de Santiuste, Segovia. Thesys. Universidad Complutense de Madrid. ISBN 13: 978-84-669-2800-7.

Fernández Escalante, E., (2006) Técnicas de tratamiento de suelo y acuífero (S.A.T.) aplicadas a la gestión de la recarga artificial. Serie Hidrogeología Hoy. Grafinat, Noviembre de 2006. http://www.metodografico.com/publicaciones.htm

Fernández Escalante, E., García Asensio, J.M. y Minaya Ovejero, M.J., (2009) Propuestas para la detección y corrección de impactos producidos por procesos colmatantes en el dispositivo de recarga artificial de la cubeta de Santiuste (Segovia). Boletín Geológico y Minero, vol 120, nº 2, 2009. Pg. 215–234.

Fernández Escalante, E., and García Merino, A., (2009) Estudio sobre la evolución de la zona no saturada en las inmediaciones de dispositivos de tipo superficial de gestión de la recarga de acuíferos. Las estaciones DINA-MAR ZNS. Estudios de la ZNS del suelo. Vol. IX, ZNS ´ 09. Barcelona 2009. pg. 271–280. ISBN: 978-84-96736-83-2.

Fernández Escalante, E., and Senent Del Álamo, M.W., (2009) Implementation of Techniques for Soil and Aquifer Treatment (SAT) in Spain. Contributions to the state of the art. Achieving groundwater supply sustainability & reliability through managed aquifer recharge. Proceedings book of the symposium ISMAR 7. Abu Dhabi, 2009 October 9-13th. IAH. Edited by DINA-MAR. pg 624–631.

Fernández Escalante E., and San Sebastián Sauto, J., (2012) Rechargeable sustainability. The key is the Storage. Book written in Spanish and English. Ed. Tragsa. May 2012. ISBN: 13:978-84-615-8704-9. 126 pg.

Fernández Escalante E., and Prieto Leache, I., (2013) Los procesos colmatantes en dispositivos de gestión de la recarga de acuíferos y empleo de la termografía para su detección y estudio. Un ensayo metodológico en el acuífero Los Arenales, España. Número especial Geología Ambiental del Boletín de la Sociedad Geológica Mexicana. Volume 65, nº 1. SCI. Pg. 51–69. 2013 April. ISSN 1405-3322.

Galán, R., López, F., Martínez, J., Macías, C., Galán, G., y Fdez. Escalante, E., (2001) Recarga artificial del acuífero de los Arenales en la comarca de El Carracillo (Segovia). Soporte físico. VII Simposio de hidrogeología, AEH, Murcia.

García Rodríguez, M., y Llamas Madurga, R., (1992) Aspectos hidrogeológicos en relación con la génesis y combustión espontánea de las turbas de los Ojos del Guadiana. Actas del III Congreso geológico de España. 1992 June. T-2. 285–289 pp.

Gogolev, M., and Ostrander, M., (2000) Estimating groundwater recharge with Visual HELP model Proceedings of the IAH 2000 Congress in South Africa, Nov. 2000.

Healy, R., and Cook, P., (2002) Using groundwater levels to estimate recharge. Hydrogeology Journal Vol 10, nº 1. Feb 2002. AIH-Springer.

Woodside, G., and Hutchinson, A., (2001) Use of shallow probes to understand water level, temperature and water quality changes directly beneath a large recharge facility. Proceedings of the 10th Biennial Symposium on the Artificial Recharge of Groundwater, Tucson, Arizona, June 7–9, 2001.

Ingebritsen, S., and Sanford, W., (1998) Groundwater in Geologic Processes. Cambridge University Press.

Krul, W., and Liefrinck, F., (1946) Recent groundwater investigations in the Netherlands. Monograph on the progress of research in Holland. Elsevier, New York, 78 pp.

Langmuir, D., (1997) Aqueous environmental geochemistry. Prentice Hall, 1997.

MAPA (2005) Asistencia técnica para el seguimiento y modelización de la recarga artificial en la cubeta de Santiuste de S. Juan Bautista (Segovia). DGDR-Tragsatec.

Martin, R., and Dillon, P.J., (2002) Aquifer Storage and Recovery. Future directions for South Australia. Department of water, Land and Biodiversity conservation. CSIRO Land and Water. Report 2002/04. August 2002. Australia.

Olsthoorn, T.N., (1982) The clogging of recharge wells, main subjects. KIWA-communications 72, WG on recharge wells (Rijswijk, The Netherlands), 136 pp.

Pyne, D., (1995) Groundwater recharge and wells. A Guide to Aquifer Storage Recovery. Lewis Publishers. CRC Press. Boca Ratón, Florida, USA. 376 pp.

Ryan, J.N., y Elimelech, M., (1996) Colloid mobilization and transport in groundwater. Colloids and Surfaces. A: Physicochemical and Engineering Aspects, 107: 1–56.

Schicht, R.J., and Walton, W.C., (1961) Hydrologic budgets for three small watersheds in Illinois. Illinois State Water Survey Rep Invest 40, 40 p.

Stuyfzand, P.J., (2002) Quantifying the hydrogeochemical impact and sustainability of artificial recharge systems. Management of Aquifer Recharge for Sustainability, Dillon, P.J. (ed). Proceedings of ISAR 4, Adelaide, SA, Sept. 2002. Balkema Publishers-AIH, The Netherlands.

Tragsatec (2010) Informe del registro óptico de vídeo-tv realizado en sondeos de recarga en el Canal del Guadiana (Ciudad Real). CHG-Tragsatec, 2010 February.

Van Beek, C., (1986) Clogging of discharge wells in the Netherlands II: Causes and prevention. International Symposium of biofouled aquifers: prevention and restoration. American Water Works Association. Denver. P. 42–56.

Van Duijvenbode, S.W., and Olsthoorn, T.N., (2002) A pilot study of deep-well recharge by Amsterdam Water Supply. Management of Aquifer Recharge for Sustainability, Dillon, P.J. (ed). Proceedings of ISAR 4, Adelaide, SA, 22–26 September 2002. Balkema Publishers-AIH, The Netherlands.

http://edafologia.ugr.es/introeda

http://www.inforiego.es

http://www.dina-mar.es DINA-MAR, Depth Investigation of New Areas for Managed Aquifer Recharge. Grupo Tragsa, Madrid, 05/2010.

Contact Details

Conde Peñalver 84. 28006 Madrid.

Email: efernan6@tragsa.es

CLOGGING ASSOCIATED WITH WELL INJECTION

Application of Large Scale Managed Aquifer Recharge in Mine Water Management, Cloudbreak Mine, Western Australia

B. Willis-Jones and I. Brandes de Roos

Fortescue Metals Group Limited

Introduction

The Cloudbreak iron ore mine is located in the Pilbara region of Western Australia. The iron ore resource is substantially below the water table and located within a regional groundwater system with contrasting brackish and saline aquifers.

Groundwater management is an integral part of the mining operation. Abstraction is required to meet mine dewatering and water supply requirements and Managed Aquifer Recharge (MAR) is employed to both conserve brackish water and mitigate environmental impacts associated with discharge of saline water and groundwater level drawdown (Figure 1).

In operation since 2008, the Cloudbreak water management system has steadily increased its capacity. In 2012 the total abstraction and injection volumes were around 30 GL and 20 GL respectively. In this period injection comprised approximately 13 GL of saline groundwater and 7 GL of brackish groundwater. Abstraction and injection volumes for 2013 are forecast to be around 70 GL and 60 GL respectively.

A major challenge for both design and operation of large-scale MAR projects is aquifer clogging and the Cloudbreak MAR scheme is an example of the application of pragmatic clogging-control measures.

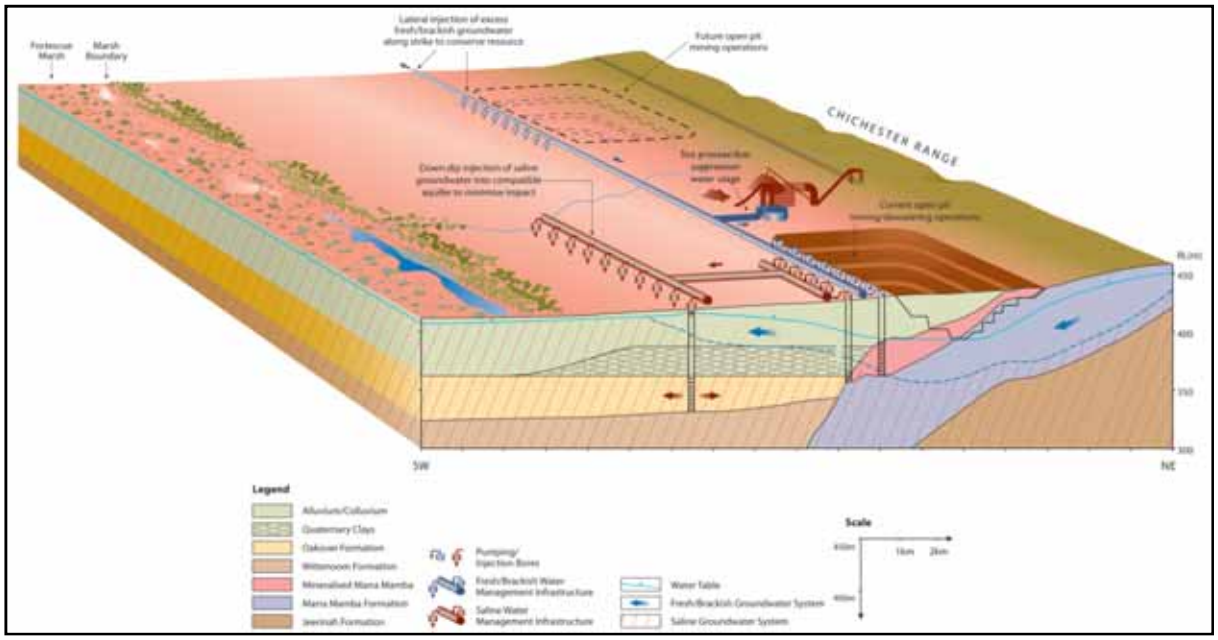

Figure 1: A simplified schematic of the Cloudbreak MAR scheme

Hydrological Setting

The physical setting is dominated by the expansive Upper Fortescue Valley. The Upper Fortescue Valley is bounded to the south by the Hamersley Range; north by The Chichester Range; and to the west by a small series of silicified hills known as the Goodiadarrie Hills (Figure 2). The Fortescue River drains into the valley from the east. The catchment physiography has created an internally draining basin subject to periodic flooding. A key feature of the valley is the ephemeral Fortescue Marsh wetland, which is formed in the lower margins of the valley. The Fortescue Marsh is approximately 100 km long and 3 to 12 km wide, occupies an area of approximately 1,000 km^2, and lies at an elevation of about 400 m to 405 m AHD.

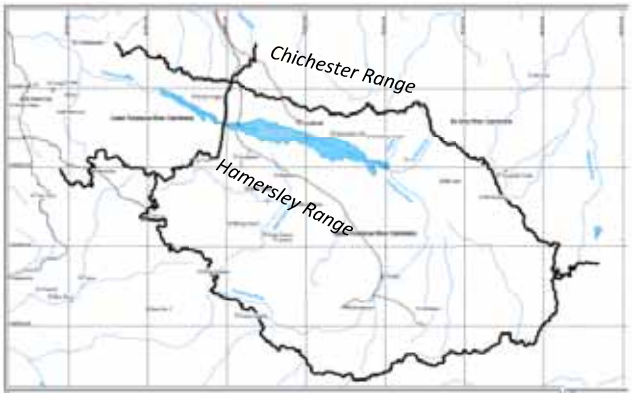

Figure 2: Upper Fortescue Valley

The Upper Fortescue Valley contains a Tertiary depositional sequence up to 60 meters thick in parts. Deposition by fluvial processes (alluvial fans and braided channels) dominated on the margins of the valley and lacustrine processes in the central part of the valley. The sediments are generally low permeability with the exception of the Oakover Formation, a secondary carbonate and silcrete aquifer with very high permeability, occurring in the central part of the valley.

Cycles of flooding and evaporation within the Fortescue Marsh have resulted in formation of highly evolved hypersaline groundwater within the Upper Fortescue Valley aquifer system.

The early Proterozoic Marra Mamba Formation (of the Hamersley Group) outcrops in the Chichester Ranges and dips to the south beneath the Tertiary sequence. The geochemical evolution of the Marra Mamba Formation, which formed the iron ore resource has also created an aquifer with high permeability. Water quality within the orebody aquifer is typically brackish. Rainfall recharges the Marra mamba Formation aquifer on upper slopes and flows through the orebody towards the Fortescue Marsh.

The density driven (saline) groundwater regime adjoins the topographic (brackish) groundwater regime immediately south of (and to some extent, below) the iron ore mineralisation in a heterogeneous saline interface zone (Figure 3).

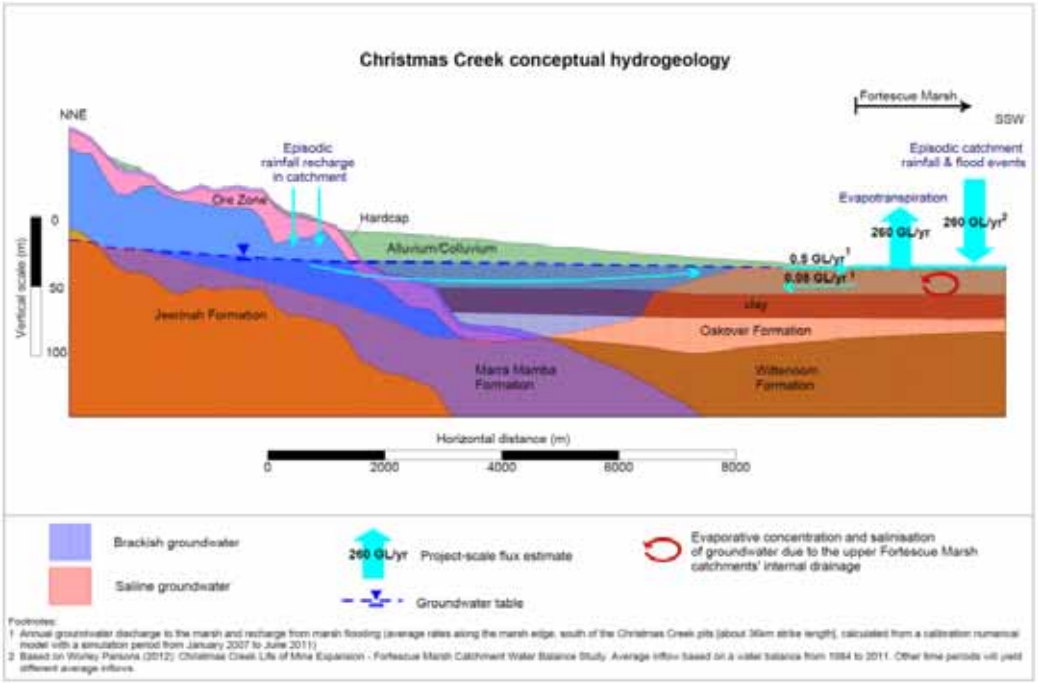

Figure 3: Hydrogeological Cross Section

Injection aquifer

Stratigraphy and hydraulic characteristics (Oakover Formation)

The vast majority of injection is undertaken in the Oakover Formation aquifer that lies between the mine dewatering region and the Fortescue Marsh. The Oakover Formation aquifer is a calcretised, micritic, former-limestone unit that has undergone significant silicification. The aquifer is typically 5 to 30 metres thick, and is encountered from about 50 metres depth. It extends from the iron ore- bearing Marra Mamba Formation (where it onlaps with various levels of aquifer connection) to underneath the Fortescue Marsh. An example of the Oakover Formation stratigraphy is shown in Figure 4 (showing Chichester Range injection bore SAI01).

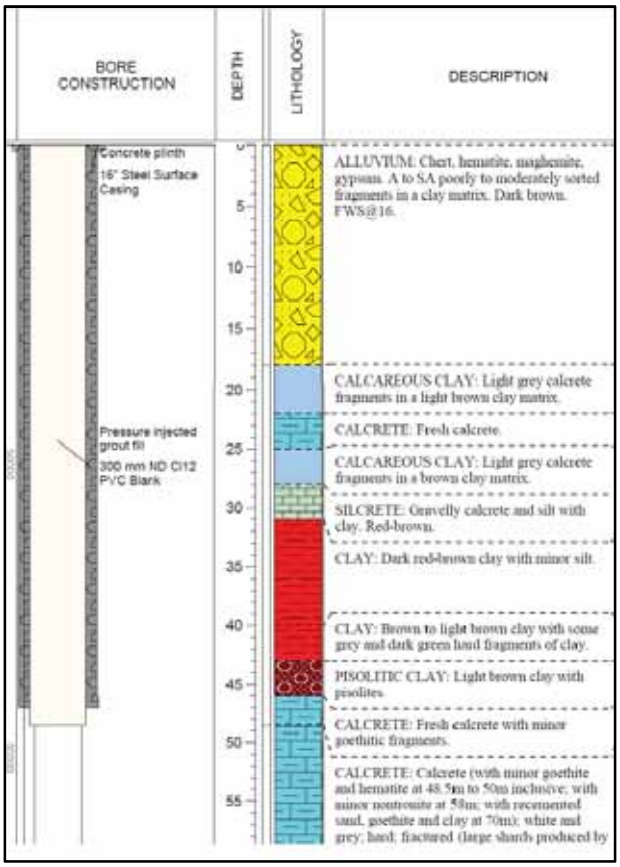

Figure 4: Typical bore log and bore construction

In the injection region, standing water levels in the Oakover formation aquifer are generally between 5 to 15 metres below ground level. A clay aquitard layer of variable thickness (typically 5 to 20 metres) overlies the Oakover Formation aquifer and results in confined aquifer conditions. Hydraulic conductivities are extremely variable and may be extremely high; the current model-calibrated average hydraulic conductivity for this aquifer unit is 200 m/day, which gives transmissivities in the order of 2,000 m^2/day. These high hydraulic conductivities are the result of significant secondary porosity development (note the porosity evident in the field sample shown in Figure 5) in calcrete and silcrete samples.

Reflected light microscopy assessments of the Oakover Formation aquifer (see Figure 6, from Chichester Range bore SAM08_D) reveal it to be heterogeneous, ultrafine (micritic) calcrete with about equal amounts of silicate replacement. Figure 6 shows massive ultrafine crystalline carbonate (calcite), which is microfractured and disassociated. A very irregular network of fractures/partings has extensively permeated and cemented the rock mass with crypocrystalline silica (chalcedony).

Marra Mamba Formation

Whilst the majority of injection occurs in the Oakover Formation aquifer, the Marra Mamba Formation aquifer is also used for brackish injection. The Marra Mamba Formation aquifer is a semi-confined mineralised Banded Iron Formation unit with significant secondary porosity and hydraulic conductivities in the order of 10 to 100 m/day. Injection into this aquifer region occurs along strike from active mining regions, as shown schematically in Figure 1.

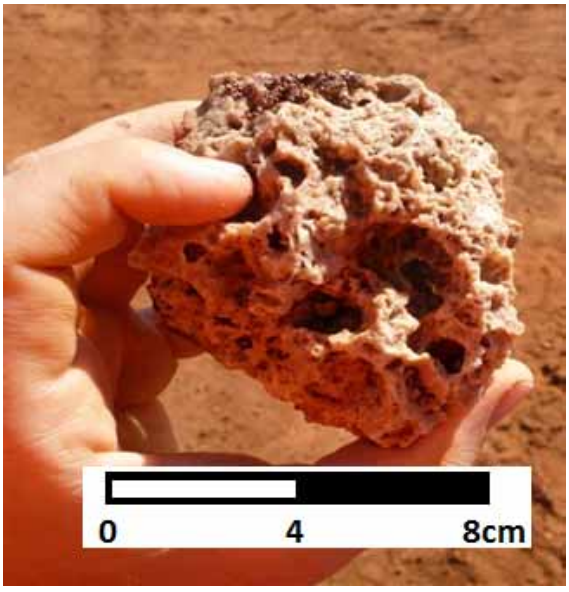

Figure 5: A large drill cutting from a particularly-transmissive section of the Oakover Formation

(a). Cut field sample

(b). polished polarised section
(20x magnification)

Figure 6: Oakover Formation aquifer field sample (cut field sample and polished section view)

Injection aquifer water quality

Target aquifer ambient groundwater quality (for the majority-used Oakover Formation aquifer) is saline to hypersaline. A geochemical modelling study (MWH, 2009) shows that the abstraction and injection groundwater compositions are dominated by Na-Cl with lesser amounts of SO4 (see Piper plot in Figure 7 and tabulated results in Table 1). The sum of Na+K and Cl typically comprises from 79 to 85% of the TDS in the abstraction and injection groundwater. The brackish groundwater (Marra Mamba Formation) shows a spread in compositions from Na-Ca-Mg-SO4-Cl dominated composition to a predominantly Na-Cl composition similar to the abstraction and injection compositions.

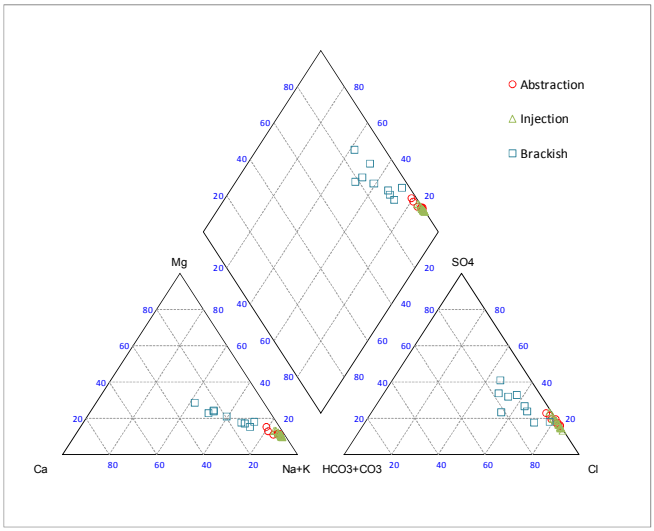

Figure 7: Piper plot of saline abstraction and injection water (plus brackish abstraction water)

Geochemical modelling (MWH, 2009) to assess the potential for mineral precipitates to form and clog injection boreholes and aquifers during saline injection suggested that mineral precipitation is unlikely. Water chemistry and groundwater hydrogeological data were used to define a series of solution mixtures that would result from injection of abstraction water into the subsurface aquifer. The potential for mineral precipitation (e.g., calcite, silica, gypsum, etc.) for the solution mixtures was assessed with the PHREEQC geochemical model. The assessment found the chemical compositions of groundwater from abstraction bores was very similar to the receiving waters in the injection bores. The degrees of saturation with respect to potential mineral precipitates are approximately the same for both the abstraction and injection zone groundwater.

Geochemical model calculations predict that mixing of abstraction water with injection zone water generally reduces the potential for precipitation of most carbonate, sulfate, and silica minerals. There are two exceptions to this conclusion 1) Mn and Fe oxyhydroxides which are predicted to be more likely to be precipitated as a result of mixing of waters around injection zones but precipitation amounts are very low; 2) Mixing of brackish water with abstraction water prior to injection increases the potential for chalcedony precipitation.

Table 1: South Transfer Pond chemical composition (sampling date Sept 4, 2009)

Analyte	Result
pH, s.u.	7.28
Na, mg/L	17,300
Ca, mg/L	360
Mg, mg/L	1,300
Ba, mg/L	0.25
Sr, mg/L	4
Fe, mg/L	0.3
Cl, mg/L	27,520
SO_4, mg/L	7,288
HCO_3, mg/L	257
PO_4-P, mg/L	0.02
NO_3-N, mg/L	0.26

Injection operations

Overview

Cloudbreak has over 40 active injection bores, with the vast majority of injection effort directed at saline water injection down dip of the dewatering zone and towards the Fortescue Marsh. Injection capacity is a critical requirement to the water management operation; loss of capacity through clogging would require that dewatering operations and ore mining be curtailed. However, Cloudbreak currently employs a relatively low level of clogging-prevention, and relatively high levels of sediment enter injection bores.

Saline injection bores operate at injection rates from 20 L/s to up to 150 L/s. Pre-injection groundwater levels are typically within the range of 5 to 10 metres from ground level. Bores are injected with varying pressures (up to about 30 metres head). Bores are typically installed in a line parallel to strike and about 500 metres apart. Regional-aquifer responses are such that the regional mounding cone of impression is extensive and ultimately limits injection capacity. Brackish injection bores do not employ pressure injection, and operate at generally lower injection rates (generally in the order of 20 L/s).

Injection bores and headworks

Saline injection bores are constructed as open-hole bores (that is, no screens are installed over the aquifer interval) to a typical depth of about 70 metres (see Figure 4). Bores are constructed using Dual Rotary (DR) drilling methodologies whereby conductor casing is advanced during drilling progression. A 400 mm ND hole is drilled to the top of the aquifer whilst 400 mm ND steel casing is advanced, then 300 mm ND Class 12 blank PVC casing (with a 'float shoe' attached at the base) is installed to the top of the aquifer whilst the steel casing is removed. Grout is then installed in the annulus between the PVC and hole via drill rods fitted with a 'jab shoe' that connects to the 'float shoe'. The aquifer interval is then drilled out at 250 mm ND through the PVC casing. Previous-generation bore designs (and all brackish injection bores) at Cloudbreak did not incorporate this grouting methodology, and upward-leakage of injected water was observed in some instances.

Injection unit designs have evolved considerably over the life of the project; the following description is focussed on current-generation injection units that dominate the injection system (manufactured by Project Engineering (WA) Pty Ltd).

Injection rates are controlled via the regulation of the down-hole back-pressure unit, a retractable plug which seals the annulus of the down-hole device via a linear actuator. The linear actuator is controlled via a Pressure Reducing Valve (PRV) located on the headworks. The PRV can be adjusted to maintain a specified injection pressure and thus flow rate. If the pressure of the pipeline declines below the specified injection pressure, flows into the well will also decline until the annulus of the down-hole device eventually closes. A Programmable Logic Controller (PLC) is linked to a pressure level probe in the monitoring bore proximal to the injection bore. The PLC operates at several monitoring-bore water level triggers; if the trigger level is reached then an actuator closes or opens a pilot line that links to the hydraulically-driven retractable plug. The system operates on an auto-tune setting whereby, should the injection flow rate be set at a rate that is too high such that the PLC trigger levels are 'tripped' three times in ten minutes the injection flow rate is reduced by 0.5 L/s. This process continues until an appropriate injection rate is reached.

The back-pressure created by the down-hole device, together with the installation of air-bleed valves at the headworks (see Figure 8) and at various locations along the pipeline system successfully prevents air entrainment in the injection bore.

Figure 8: Typical saline injection headworks

Pre-injection water treatment

Water treatment prior to injection currently employs only sediment-settlement (as water is transferring via large ponds) as a particulate-minimisation strategy. Abstraction-bore water is directed via large (about 200 ML capacity) transfer ponds that serve to reduce particles in the injected water. The out-take pipeline in transfer ponds is positioned in a less-optimal location (with respect to removing injection particles) and other designs are being explored. Whilst abstraction bores are employed as the primary means of dewatering, in-pit sump-abstraction can also be employed, which introduces higher sediment loads. Sump abstraction water is directed to a settlement pond (a pond of about 80 ML capacity with a channel design to promote the deposition of sediments).

Injection units only have coarse filters to intercept particles larger than 6 mm.

Clogging

Air entrainment

The injection units have been successful in eliminating air entrainment clogging. Early generation injection units (and incorrectly-commissioned units) have led to air entrainment; simple reconfiguration/upgrades have eliminated this issue.

Particulate

Saline injection bores receive a high load of suspended solids. Injected water has a general background turbidity of about 20 NTU (after settlement in transfer ponds). Changes to the system (for example, the introduction of sump-abstraction water) can result in large spikes in turbidity (regularly in the order of 100 to 200 NTU). One of the most important sources of particulate clogging is the conveyance pipelines themselves. During pipeline construction process the pipeline lengths are dragged around and capture soil before being poly-welded together. The captured soil (together with poly-pipe fragments and construction equipment) then slowly make their way to the injection bores. The highest particulate-load period is therefore often after the construction of a new pipeline section. Figure 9 shows and example of particulates coating a retrieved injection unit.

Figure 9: Sediment (introduced from the pipeline system) coating the injection unit

Biofouling

No biofouling has been observed to date in saline injection bores. The potential for biofouling in the Water Management system is high, and iron-consuming bacteria

has been observed in abstraction bores in the project area. Abstraction bore treatments have included traditional disinfection methodologies and bore-decommissioning. Retrieved injection bore equipment is visually inspected for iron bacteria growth on an ad-hoc basis; potential biofouling is assessed via laboratory analysis.

Other

As the 'saline' aquifer can have salinities of over 120,000 mg/L and as the injected water into the saline aquifer system can at times be a lower salinity, there is the potential that the act of injecting lower-salinity water can promote clay swelling. This can occur as the electrical double layer of clay particles swells as ions are exchanged with the injected water. An assessment of this potential (Fortescue, 2012) was undertaken on injection aquifer (and proximal strata) samples via the Emerson Crumb test. This test is a simple qualitative method for assessing the tendency for a soil sample to disperse in fresh water. Samples (from drill cuttings) are immersed in water of a range of salinities to determine the degree of clay dispersion at a range of potential operational water qualities. The test used samples of calcrete from the Oakover Formation calcrete, calcareous (aquitard) clay, and silty clay from the Tertiary alluvial sequence. Based on this assessment, the clogging of bores from clay swelling is deemed to be highly unlikely. To mitigate any risk of clay swell, the salinity of injection water to the saline system should be maintained above 39,000us/cm.

Injection of less-saline water into a hyper-saline aquifer also has the potential to reduce injection yields due to water density differences. Though not strictly a clogging mechanism, this was found to be an important factor in Cloudbreak saline injection yields, as less-saline water is less dense and therefore results in a higher actual head in the injection aquifer when compared to hypersaline water. As injection is limited by the injection head, this effect can limit injection yields, though increased pressure injection can overcome this limitation.

Injection bore maintenance and cleaning

In contrast to most other major injection systems, the Cloudbeak injection units to date have no dedicated backflushing, bore cleaning equipment or disinfection schedules. Instead, injection bores are cleaned on an ad-hoc basis by removing the injection headworks and down-hole equipment and airlift-agitation and pumping of the injection bore. This is done with a drilling rig set up over the bore site. Airlifted water and sediment is directed to a containment bund on the drill site. Significant volumes of sediment (and pipeline-construction debris) are observed during the airlifting process.

The trigger for airlifting is a regular hydrogeological assessment of bore yield when compared against aquifer water levels in the adjacent monitoring bore. Where injection yields increase at a rate faster than the increase in monitoring-bore groundwater levels (due to regional aquifer yield limitations) airlift development is undertaken. Airlifting is typically undertaken about every 12 months.

References

MWH, (2009) Predicted geochemical interactions for re-injection of Fortescue abstraction water, unpublished technical memo.

Fortescue, (2012) Christmas Creek – Saline injection testing, commissioning and operation, unpublished Fortescue document, 14 September 2012.

Pontifex, (2011) Mineralogical report No. 9998, Unpublished report, Pontifex and Associates Pty Ltd, Rose Park South Australia, 25 October 2011.

Clogging of Deep Well Infiltration Recharge Systems in the Netherlands

B. de la Loma González
KWR Watercycle Research Institute, Nieuwegein, Netherlands

Overview

In this chapter we review data of three deep well artificial recharge systems in the Netherlands to describe their clogging behaviour over a 23 year period. The overall conclusion from this assessment is that managed aquifer recharge using deep well injection (aquifer storage transfer and recovery) can provide a sustainable method to store and treat water. Key aspects to successful operation of deep well MAR systems are: i) pre-treatment of the feed water, ii) monitoring injecting well pressure and iii) tailored back flushing and/or rehabilitation. Special emphasis is given to the effectiveness of the different rehabilitation techniques and suggestions are given to improve the future use of these types of systems. To our knowledge, these systems provide a unique dataset and the comparison of the different systems (well field operation and pre-treatment) is useful for engineers designing future MAR systems that use deep well injection. Some of the results from this comparison are that periodic abstractions with high flows and adequate pre-treatment diminish the clogging rate. In addition, from the chemical regeneration methods the use of hydrogen peroxide and chlorine bleach proved to be the most effective. Finally, the observed tendency to expand the pre-treatment due to quality guidelines with the use of UV/H2O2 could result in an increase of biological clogging.

1 Introduction

Managed aquifer recharge (MAR) is widely applied in the Netherlands to produce drinking water, making up 20% of the total Dutch water supply of 1250 Mm3/year (Stuyfzand, 2010). The various MAR techniques employed in the Netherlands offer the prospect of treating unreliable, polluted surface water into good quality safe raw water by infiltrating it into an aquifer and recovering it after a certain residence time in the subsurface. This aquifer passage not only enhances the water quality and decreases the input quality fluctuations, but also protects the water from evaporation losses, algae blooms, atmospheric fallouts of pollutants (Stuyfzand, 2010). There are however some disadvantages to this method as well, such as a cumbersome clogging phenomena, which is the subject of this chapter, water losses due to mixing with brackish groundwater and natural reactions with the porous medium which can result in unwanted water quality changes such as increasing arsenic levels.

The three MAR systems presented in this chapter are Aquifer Storage Transfer Recovery (ASTR) systems where separate injection and recovery wells are used. The advantage of deep infiltration systems compared to open artificial recharge (infiltration) ponds, which are more frequently used in the Netherlands, is their footprint, lower impact on the terrestrial ecosystems and greater protection against contaminants. On the other hand, the open infiltration systems are easier to build, easier to maintain and have lower operational costs. Moreover, infiltration wells are more susceptible to clogging by a combination of particles, biomass and chemical precipitates than open infiltration systems. Clogging is the most important factor in the degeneration, abandonment and replacement of wells often associated with additional and unexpected costs (Houben and Treskatis, 2007).

Clogging of deep wells systems results in less efficient systems resulting in higher energy and maintenance costs. Here, the experiences with clogging at three different water companies (see Figure 1 1) that use ASTR systems are described. The companies, Dunea, PWN and Waternet are located in the coastal dune systems of Waalsdorp, Watervlak (Castricum) and Amsterdam water supply dunes, respectively. Two of them: Dunea –formerly called DZH- and

PWN have been operating these systems since 1990, Waternet's system was in operation from 1994 until 2003.

The comparison of the three different deep well infiltration systems in terms of clogging can solve important questions relating to the source of clogging, the different types of clogging, the effect of different types of rehabilitation (and construction) of infiltrating wells and the most optimal operational design of deep well infiltration systems.

Figure 1-1: Location of the three deep well infiltration systems in the Netherlands.

2 Methods: monitoring of well resistance, clogging potential and rehabilitation methods

The degree of clogging of a well can be directly related to the infiltration resistance. Clogging is monitored at the three well fields by measuring the well resistance or clogging rate over time. The clogging resistanceate (cm/m^3/hour) is defined as the difference between the water level in the infiltration well and the level in the filter pack or a close by monitoring well (Olsthoorn, 1982):

$$\text{Clogging resistance}_{well} = \frac{H_{well} - H_{observation}}{Q} * \frac{T + 20}{30}$$

Where H_{well} is the water level measured in the well, $H_{observation}$ the water level in the piezometer, Q the flow rate and T the temperature. The clogging rate is corrected for temperature induced viscosity effects with the second term on the right hand side. When multiple piezometers are located in the annulus close to the screen then it is possible to determine if clogging is occurring on the screen or on the borehole wall see Figure 2-2.

Figure 2-1: Location of observation points in an infiltration well and different types of clogging deduced from the measured water levels. Figure after Zwart (2007)

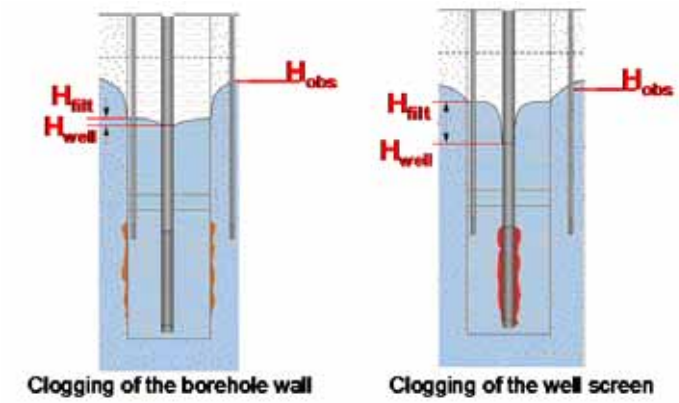

The clogging potential of the infiltrated water is monitored through the membrane filtration index (MFI), this index can be used to forecast the clogging rate (Olsthoorn, 1982) and it is assumed that values below 3 s/L^2 are deemed not to produce clogging due to suspended solids. An additional clogging indicator is the assimilable organic carbon (AOC) concentration of the infiltrating water, which is an indicator of the growth potential r for microorganisms, related to the nutrients present in the water. The concentration of Assimilable Organic Carbon should be < 10 ug acetate-C/L in order to strongly reduce the chance on injection well clogging by bacterial growth (Van der Kooij et al., 1982). The clogging resistance is measured in all the three cases, and to determine the cause of that clogging the MFI was measured in Waalsdorp and Watervlak and the AOC was measured in Waalsdorp.

Since it is unlikely to completely prevent clogging of the infiltration wells, eventually it is necessary to undertake rehabilitation of the well. Following rehabilitation, the infiltration capacity should return close to or, equivalent to, the initial capacity. Rehabilitation is part of two of the infiltration systems presented in this chapter (PWN and Waternet) and it is usually the alternative to an extra pretreatment regarding the one that would be done to water for open infiltration systems. An overview of the preferred rehabilitation techniques in the Netherlands can be found in Table 2-1 (from Bonte et al., 2009).

Table 2-1: Overview rehabilitation methods (Bonte et al., 2009)

METHOD	DESCRIPTION	TARGET
Mechanical		
Brushing	Well screen is brushed and simultaneously the well is drained.	Filter
HD-Cleaning	Filter is cleaned with high pressure. Pressure 20–200 bar.	Filter, somewhat discharge
Cleaning of the Pumps	Pumping out well with increased flow. Wells of the deep infiltration system of PWN and Waternet are frequently pumped clean.	Filter & gravel pack
Section cleaning or pumping	Water is withdrawn from a section (1–2 m) of the filter.	Gravel pack
Jutteren	The water is pushed down with pressure. When the pressure is released, the water level rises quickly. The pressure depends on depth filter and condition of the well.	Gravel pack
Chemical	Chemical resources are always used in combination with a mechanical method.	
Acids	Administrating acid causes a lowering of the pH, with which precipitates can be dissolved. Using inorganic acid such as HCl is preferred over organic acids because of regrowth of bacteria.	Calcite, (iron) hydroxides
Oxidicers	Ensuring oxidation of organic matter in particular. Commonly used area hydrogen peroxide (H2O2) and sodium hypochlorite (CBL). The application of an acidic oxidant as HNO3, combines the advantages of an acid and an oxidizer.	Organic matter
Reducers	Reduction, for example of Fe(III) to Fe (II) dissolving the deposits. The use of an inorganic reducing agent is preferable. Often, a complexator is added (for example, Aixtractor) to ensure that Fe in complexed form remains in solution	Hydroxides

3 Case 1, Dunea: Waalsdorp

Dunea Water Company supplies drinking water to 1.2 million inhabitants of The Hague and surroundings. Dunea has been infiltrating pre-treated river water in the coastal dunes of South Holland since 1955 using infiltration basins (Basin Artificial recharge system, BAR) and since 1990 using deep injection wells (ASTR). The deep infiltration system here described, Waalsdorp, is part of the Meijendel dunes and it has been in operation for the last 23 years. The lengthy experience that Dunea has at Waalsdorp makes it a good example of the sustainability of deep infiltration systems.

3.1 Deep infiltration system in Waalsdorp

The deep infiltration system Waalsdorp was originally designed as a pilot that would eventually be extended with a second deep infiltration system (Waalsdorp 2). Due to a deceasing water demand, the second phase was not required but the deep infiltration system Waalsdorp continues to be a very important production asset for Dunea with a capacity of 4 million m^3 per year.

The intake is located in Brakel, in the Afgedamde Maas, a closed off tributary of the Meuse. Iron sulphate is added upstream of the intake as a coagulant to reduce the level of phosphates. Subsequently it is filtered and transported to Bergambacht (a backup intake point at river Lek) where it is filtered by dual media filters before transporting it to the the Meijendel dunes. The water undergoes additional pretreatment in the production plant of Scheveningen through flotation, coagulation, rapid sand filtration and active carbon (the latter only since 1999).

The pre-treated water is subsequently injected with 24 wells in a NE-SW oriented transect. After a residence time in the aquifer of 100 to 200 days the water is extracted by a double well field of 11 abstraction wells each (Figure 3-1). The extracted water is mixed with the water coming from the open system, softened, dosed with activated carbon, aerated and run through a fast and slow sand filter and distributed.

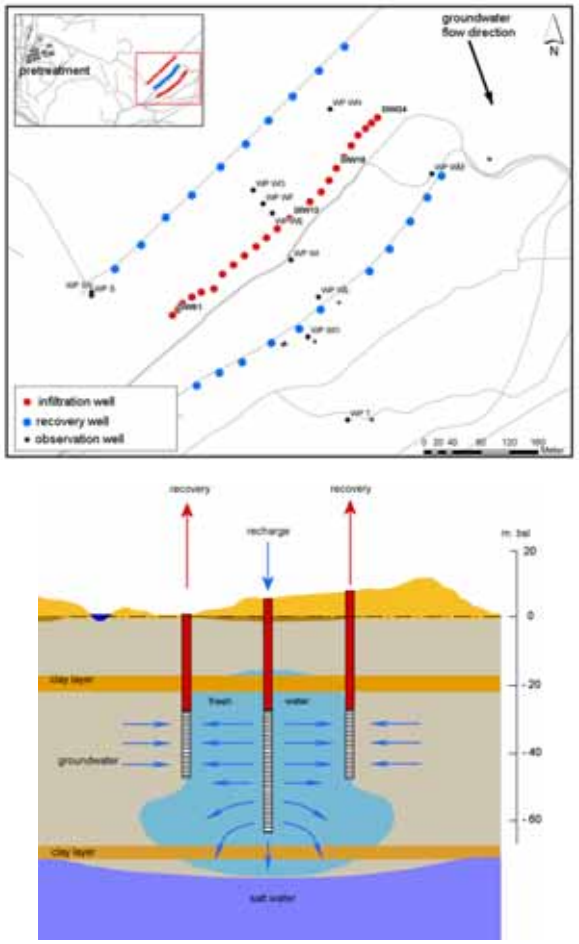

Figure 3-1: Location of the recharge and recovery wells in Waalsdorp and cross section of infiltration system Waalsdorp (de Jonge et al., 2010)

The injection wells are installed using a method called clean drilling. The drilling is done until reaching the aquifer with a mixture of drilling mud with Antisol. Before reaching the aquifer the drilling fluid is replaced with water and during the drilling into the aquifer the drilling cuttings are separated from the drilling water by cyclones and then removed. The drilling technique is important since the drilling mud and the mud cake usually leave some material behind in the borehole, which can affect the clogging processes.

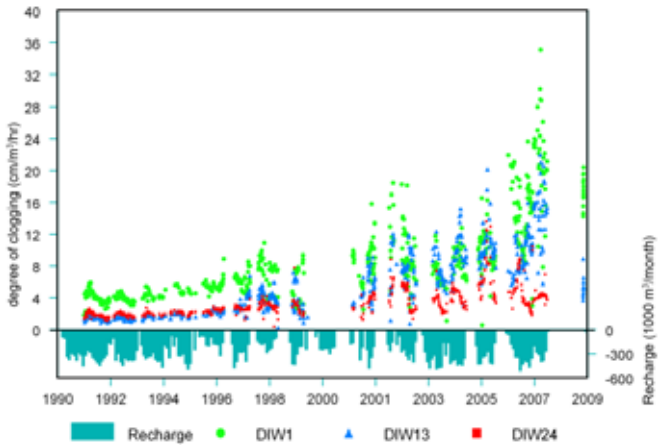

3.2 Clogging experiences in Waalsdorp

The clogging rate has been monitored since 1990 in three of the deep infiltration (Figure 3-2) wells. The clogging rate remained low the first years with values below 6cm/m^3/hour slowly increasing until around the mid-nineties. During those first years and thanks to the frequent monitoring, it is possible to discern a seasonal pattern in the clogging, with higher rates in autumn. The increase from 2001 could be related to the halt in Cl supply for transport of water in 1996. From 1998 onwards, the clogging rates grow exponentially, especially after long periods of inactivity, probably due to biological clogging. The increase in the clogging rate can also be related to the use of carbon filters in the pre-treatment, which began in January of 1999 and to the use of $FeCl_3$ as a coagulant factor since 2003.

Figure 3-2: Clogging rate of infiltration wells and the monthly water abstraction.

In wells DIW13 and DIW24 the water levels were measured in the well and in the gravel pack and compared with the water levels in the aquifer. From these data it was deduced that most of the clogging occurred in the borehole wall, especially in well DIW24 where more than 90% of clogging occurred. In well DIW13 40% of the clogging appeared to be in the filter screen. This was confirmed by camera inspections done after almost 20 years of operation and no rehabilitation (Figure 3-3).

Monitoring of the MFI index of the infiltrating water yielded the results exposed in Figure 3-4. During the first years values well below 3 s/L^2 can be seen and from 2003 somewhat higher MFI values are observed in the injected water. These values would generally imply no danger of recharge well clogging due to suspended solids which is also confirmed by the clogging rate data shown in Figure 3 which does not show a clear increase in the years 2003 and 2004 when the high MFI is measured.

The suspended material in the infiltration well was analyzed which showed that iron, manganese and organic carbon are the main constituents of the clogging. Within the organic carbon, the high content in carbohydrates suggests an important role of the microorganisms in the formation of the clogging. The microorganisms could be promoted by the interrupted infiltration and standstill periods but also by the nutrients present in the pre-treated river water. The AOC monitored indeed increased from 2001 onwards, probably related to the installation of carbon filters.

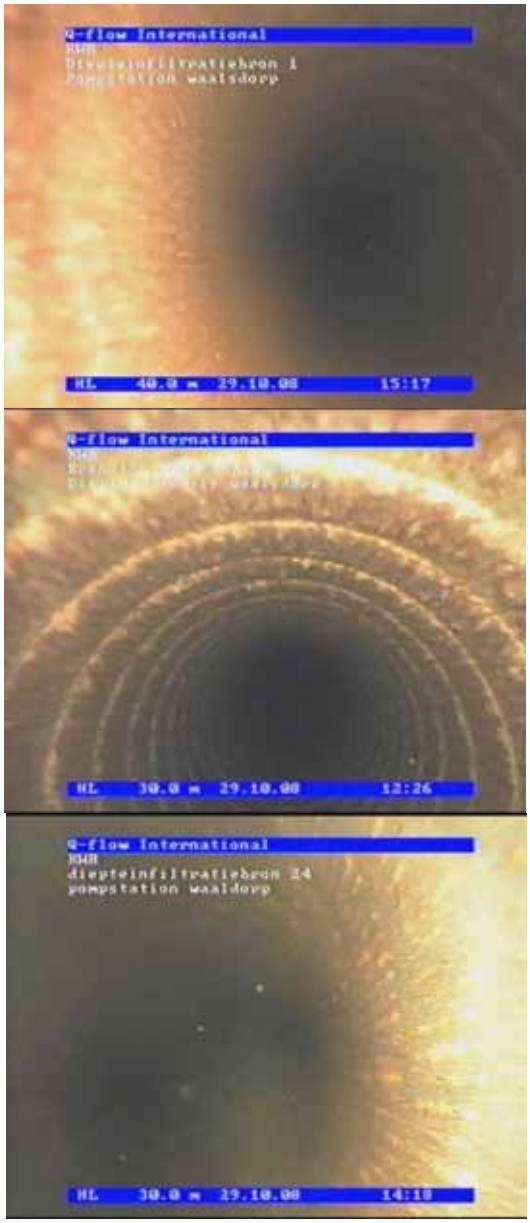

Figure 3-3: Snapshots from the camera inspections in three infiltration wells in Waalsdorp, at 40 (DIW1) and 30 m below the surface (DIW 18 & 24), the 29th of October 2008.

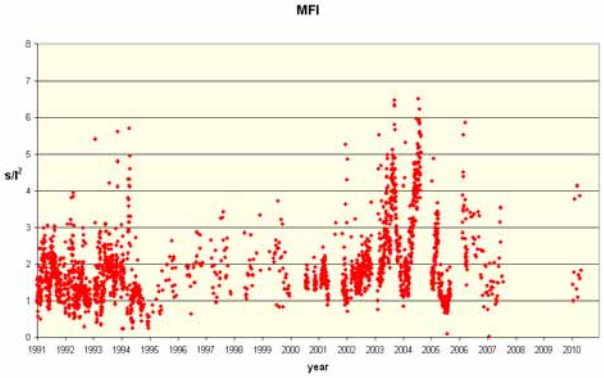

Figure 3-4: MFI during infiltration period (de Jonge et al., 2010)

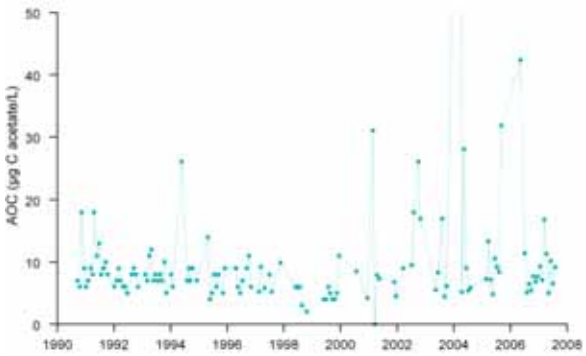

Figure 3-5: AOC in the infiltrated water (de Jonge et al., 2010)

3.3 Rehabilitation experiences in Waalsdorp

No rehabilitation was done since the beginning of the operation plant until 2011. From the clogging data collected where three different types of clogging are observed: mechanical, biological and bio-chemical it was deduced that a rehabilitation plan was suggested for 2011. The following techniques were proposed (Bonte et al., 2009): high pressure cleaning, pumping at high flows, surge and purge with H_2O_2 and surge and purge with a redactor or acid. The aim of using different approaches would be to determine which method is more effective.

The first approach was to perform a regeneration consisting only of high pressure cleaning with accelerated pumping, to check whether that was enough. The results of this clogging campaign were quite positive. The results of the regeneration were monitored through camera inspections, specific flow measurements and entry resistance measurements. The camera inspections showed two different types of clogging; the predominant with a dark color (maybe organic) that was completely removed through the regeneration, the secondary with an orange color (maybe iron precipitates) was not removed completely. The specific flow showed increments from 57 to 73 %. The entry resistance was mainly found in the borehole wall, which after regeneration decreased 43 to 79 %. Whereas the entrance resistance located on the filters decreased 80 to 98.5%. The total resistance measured then decreased 64% to 80%, with the exception of one well where the resistance only decreased 12%. These results proved that the regeneration through high pressure cleaning and accelerated flows is efficient enough, especially for the clogging located on the filters. Nevertheless, the average capacity of the wells is 54 % of what it was when they were built.

4 Case 2 PWN Water Supply Company for North Holland: Watervlak (DWAT)

PWN has been supplying water to the province of North Holland since 1920 and has had its deep infiltration system active since 1990.

4.1 Deep infiltration system DWAT

The deep well infiltration system Watervlak is an indispensable part of the production of PWN, with an infiltration capacity of 5 million m^3/year. The deep infiltration takes place at a depth of about 60 to 80 meters below the surface in the third aquifer of the coastal dune system, confined by clay layers (see Figure 4-1).

Currently the raw water is obtained at two different intake points: Andijk, where water is collected from the IJsselmeer, and in Nieuwegein, where water is obtained from the Lekkanaal, a tributary from the river Rhine. The deep infiltrated water is a mixture of these two waters even though they have had different treatments. The water in Andijk undergoes coagulation with $FeCl_2$, rapid sand filtration and active carbon filtration.

The pretreatment in Nieuwegein does not include activated carbon. Until the year 2000, only the IJsselmeer was used as a raw water source. Since 2008 the water is also disinfected and its organic micropollutants are removed with UV-H_2O_2 before infiltration.

The water is infiltrated through 20 deep wells with screens between 55 and 90 m deep (see Figure 4-1) in a 35 m thick aquifer. The infiltration wells are distributed in space forming a diamond shape to optimize the travel times towards the abstraction wells. The infiltration wells are backflushed daily with a high flow (120 m^3/h) for around 20 minutes to prevent excess infiltration pressure.

Ninety percent of the infiltrated water is recovered through 12 abstraction wells with screens 12.5 m long. Not 100% of the infiltrated water is recovered in order to prevent salt groundwater up-coning.

In DWAT the wells were drilled with conventional drilling techniques.

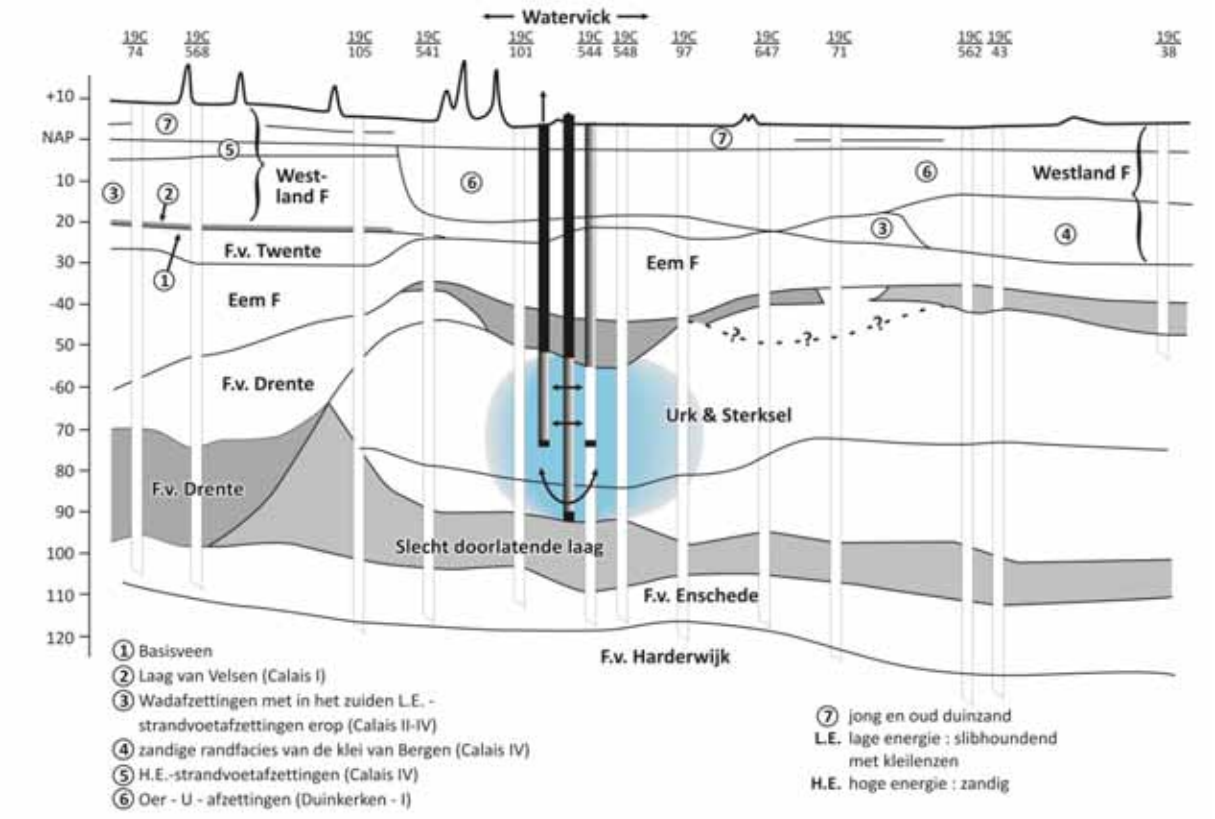

Figure 4-1: Hydrogeological profile of the deep infiltration system DWAT (after Bonte et al., 2009)

4.2 Well clogging experiences in DWAT

Monitoring of the clogging rate was performed in every well of DWAT although from 1998 the frequency of this monitoring was greatly reduced. The results of this monitoring are shown in Figure 4-2. There is an increasing trend in time where also season influence in the clogging can be discerned. Values of 40 cm/m^3/h are reached (similar to Waalsdorp) but recent values of clogging rate are missing.

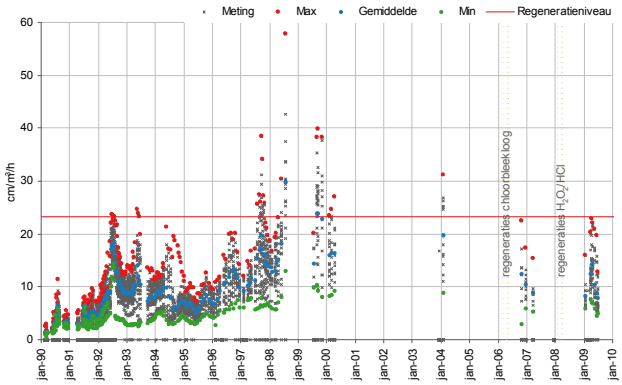

Figure 4-2: Clogging resistance in deep infiltration system DWAT, where in 2006 the rehabilitation was done with chlorine bleach and since 2008 with UV/H_2O_2

The camera inspections done in three of the infiltration wells carried out in 2006 (Figure 4-3) show coloring of the filter screen, especially in the wells that show higher resistance. This suggests iron precipitates that could come from the coagulation methods or from the input infiltrated water.

The MFI index of the infiltrated water is indeed higher than the one reported in Waalsdorp with values between 5 and 10 s/L. The difference is probably due to the extra flotation step that Dunea incorporated. The AOC index of the infiltrating water was 25 ug/L (6-month average in 2009) after expansion of pretreatment while before those treatments it was 6 ug/L which means that the biological growth potential increased(Bonte, 2009).

4.3 Well rehabilitation experiences in DWAT

Several rehabilitation campaigns have taken place in DWAT. The first one in 2006, when rehabilitation by intermittent abstraction with compressed air with hypochlorite and with hydrochloric acid were tested. This test yielded better results for the rehabilitation with hypochlorite, reaching recoveries of the infiltration capacity of 80% in some cases. Subsequently in 2006 ten wells were regenerated with hypochlorite and from this rehabilitation campaign it was

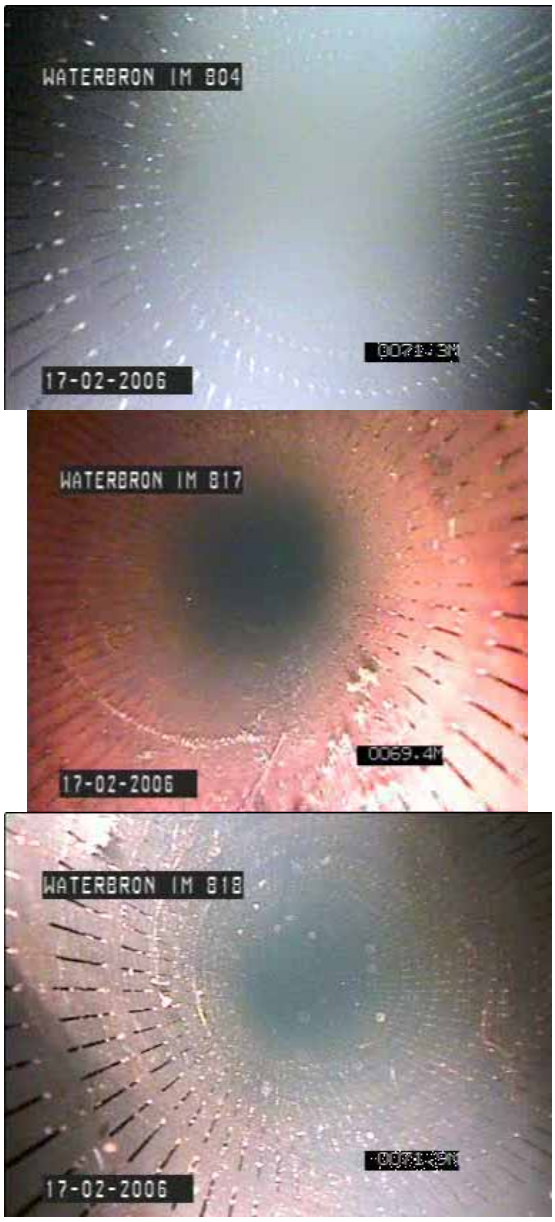

Figure 4-3: Snapshots from the camera inspections from three infiltration wells in Watervlak at 70 m below surface the 17th of February of 2006. The average resistance from the wells from 1995 to 2006 was the following: 6.5 cm/m^3/h in IM804, 13.7 cm/m^3/h in IM817 and 11.8 cm/m^3/h in IM818

learnt that it was more effective to add hypochloride in a section-wise fashion rather than bulk-wise fashion. However, after four months the effects of this rehabilitation decreased considerably. Finally, in 2008, 13 wells were treated with intermittent abstraction with compressed air and with H_20_2 (10%) and chlorine bleach (1%) with very good results, in terms of specific capacity and long term effect. This could be explained by the reducing effect that the H_2O_2 has over the Fe^{3+} compared to the hypochlorite, which only acts over the organic accretions and results in a hardening of the iron precipitates due to the formation of

the goethite that it induces (Stuyfzand, 2007).

5 Case 3, Waternet: Amsterdam water supply dunes (AWD)

Waternet supplies water to Amsterdam and the surroundings, providing water to 1.3 million inhabitants. Their drinking water supply system is an open infiltration system (BAR) located in the Amsterdam Water Supply dunes. This system has been in operation with success since 1957. With the idea of decreasing the ecological impacts of the system, a deep infiltration pilot study was carried out between 1994 and 2003. The intention was to build a deep infiltration well field with a capacity of 13 million m^3/year.

5.1 Deep infiltration system in the AWD

The deep infiltration pilot well field had a capacity of 0.7 million m^3/year and was located between infiltration canals that belonged to the BAR system. Figure 5-1gives an overview of the deep infiltration system.

The intake of the water is shared with that of PWN and located in Nieuwegein (and also the pre-treatment is shared). Once there, the water is transported to the infiltration wells through a channel that has a drain underneath. This drain collects the water after it goes through the sands that form the bottom of the channel that act as slow sand filtration pre-treatment step.

The infiltration is done through four wells with screens between 30 and 60 m deep. The injection flow is kept below 0.2 m/hour to avoid bacterial growth. The pressure in the injection wells is continuously monitored, so that when it is high automatically a back washing method is activated. The abstraction of the system is designed with the already existing abstraction wells. After the water is abstracted it is aerated, rapid-sand filtered, ozonated, softened and it passes through an activated carbon filter and a slow sand filter.

The technique used to install this deep infiltration system was developed specifically for this application and involves removing the drilling mud using a custom built well reamer tool.

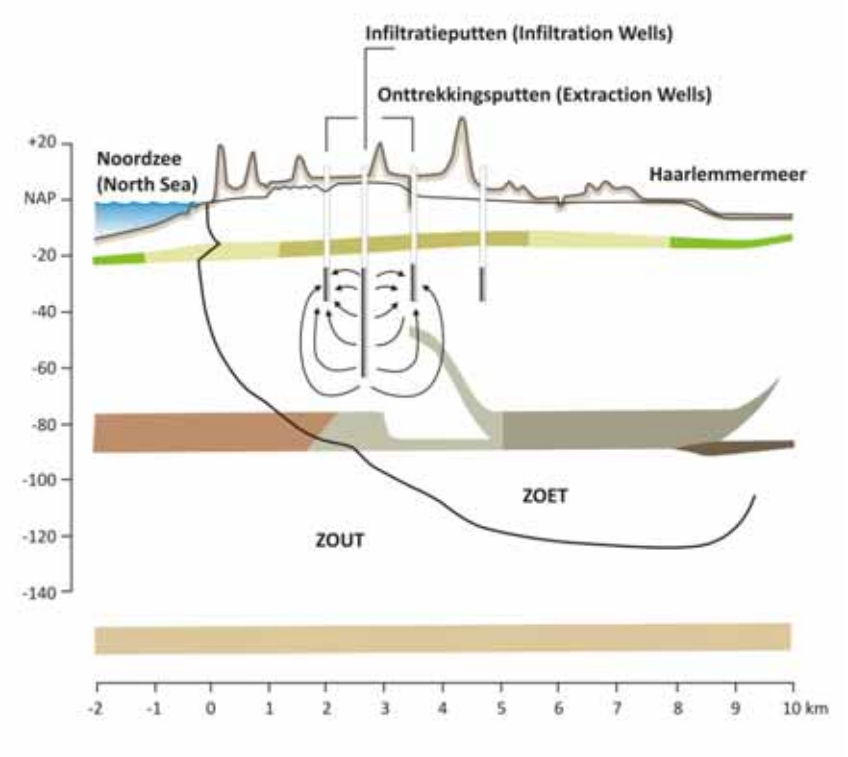

Figure 5-1: Geohydrological profile of the deep infiltration system in the water supply dunes of Amsterdam

5.2 Well clogging experiences in AWD

Well clogging was measured in the injection wells from 1994 to 2002. Figure 5-2 shows the results of this monitoring in one of the deep infiltration wells. This figure shows that the clogging occurs mainly in the gravel pack and that it presents a seasonal pattern with again higher values in autumn. There is however no clear increasing clogging trend.

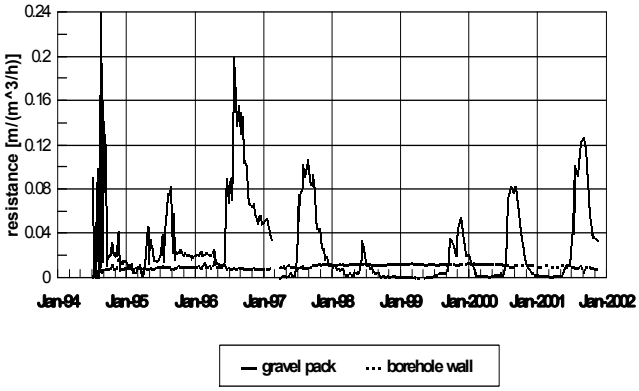

Figure5-2: Clogging of the borehole wall (red) and the gravel pack (black) in the deep infiltration pilot in the Amsterdam Water supply dunes

The degree of clogging of the sand filters located on the bottom of the distribution canal was monitored as well. Figure 5-3 shows the increasing resistance measured over time in the same period mentioned above. It is clear from this graph the magnitude of the clogging in the sand filter and the necessity of its frequent conditioning and cleaning. Van Duijvenbode & Olsthoorn (2002) observed that under the thicker parts of the clogging mud in the canal reduced anaerobic conditions were created where Fe^{3+} is reduced and mobilized. This anaerobic waster gets mixed inside of the well with aerobic water that infiltrated through the sides of the canals where the mud layer is thinner. The iron precipitates that form because of this mixing are the feeding source of iron reducing bacteria that clog the filters of the well.

6 Comparison of the three cases

In all the cases clogging was observed in the infiltration systems. Waternet well field however showed the least clogging of all due to the sand filter located in the distribution canal, prior to injection, and due to the periodic backwashing of the wells, triggered by high pressures in the wells. The clogging in DWAT and in Waalsdorp are comparable. PWN chose less pretreatment in combination with a daily rehabilitation in the form of short pumping,

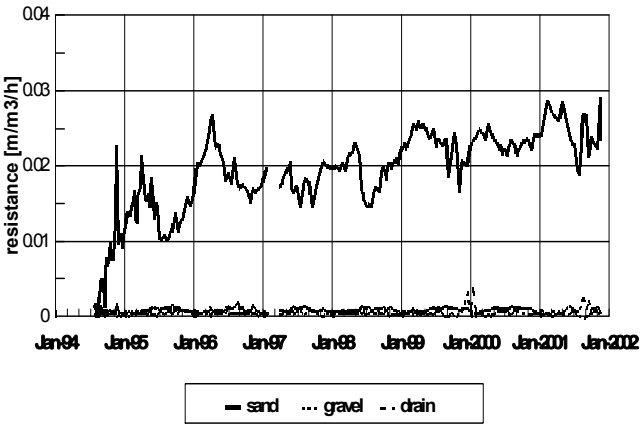

Figure 5-3: Hydraulic resistance monitored in the sand filter located in the feeding canal.

while Dunea used an additional pre-treatment step with flotation that is not done to the water that is being infiltrated through open channels. The well filters in DWAT are cleaner than the ones in Waalsdorp due to its periodic pumping, which cleans the filters but not the gravel pack or the borehole wall, therefore it is the location of the clogging that varies more than the magnitude. See Table 2 for a complete comparison of the three systems.

The clogging is in all cases composed by iron precipitates and iron-reducing bacteria. Dunea and Waternet analyzed the composition of the clogging and from PWN there is only information available from camera inspections. From the research done in Waalsdorp (Bonte et al., 2009) and the results observed in the other deep well infiltration systems, it is concluded that there are different sources of iron:

- Colloidal Fe and Mn present in the infiltrating water, that even in small concentrations, due to the big infiltrated volumes, can be relevant..
- Fe and Fe(OH)3 derived from coagulation, which is either not completely filtered by the rapid sand filters or which is remobilized following backflushing of the filters
- Fe and Mn present in ambient groundwater and transported to wells during the stand still of the systems.
- Fe and Mn dissolved by reductive dissolution of iron and manganese hydroxides in the surroundings of the well during periods of stand still

Table 2: Comparison between the three deep infiltration systems

	DUNEA	PWN	WATERNET
GENERAL			
Permit	4 Mm^3/year	5 Mm^3/year	0.7 Mm^3year
Resisdence time	100 to 200 days	1 to 12 months	No direct abstraction
VOORZUIVERING[1]			
Bron[1]	Afgedamde Maas	Lekkanaal 50% Ijsselmeer 50%	Lekkanaal
Microsieves	Yes	Yes (Ijseelmeer)	No
Coagulation	Yes (FeCl)	Yes (FeCl + wispro)	Yes
Flotation	Yes	No	No
Rapid sand filter	Yes	Yes (upflow)	Yes
Slow sand filter	No	no	Yes
Actieve carbon	Yes (since 1999)	Yes (since end 2008)	no
Target MFI injection water (s/l^2)	3	5	unknown
MANAGEMENT			
Infiltration	1 central pump 1 pipe	20 pumps with 20 pipes	
Maintenance	none	Juttering with CBL and HCl Juttering with CBL Juttering with H_20_2 & Cl	Rinse
Pressure monitoring	handmeting	Until 1998 weekly manual measurement then very occasional + continuous pressure measurement in the injection pipe	Pressure sensors
INFILTRATION WELLS			
Number	24	20	4
Diameter	1 m	1 m	unknown
Drilling technique	Not circulating drilling mud of drinking water & hulp casing to aquifer	Conventional rinse of the well	Scraping of the drilling mud from the borehall after drilling with a special drilling head.
Filters	22 to 38 m filter between NAP - 24 to -64	25 m between NAP -50 to -90	NAP -30 to -50
Disposition	1 transect infiltration 2 parallel transects abstraction	Diamond pattern	1 transect infiltration 2 transects abstraction
Development	0.2 to 0.3 m/h	0.4 m/h	0.2 m/h
Expected time until rehabilitation	5 to 7 years	15 to 20 years	
CLOGGING			
Clogging rate	Increasing trend Low values until 1995 with seasonal pattern High rates after stand still	Increasing trend Seasonal pattern Recent values missing	No increasing trend Seasonal pattern
Location clogging	Borehole wall mainly Filter screen (less)	Filter screen	Sand filter Gravel pack (seasonal) Filter screen (little and constant)
MFI	<3s/L^2 first years towards 5–6 s/L^2	5–50 s/L^2	Not measured
Nature clogging well filter	Fe, Mn, OM	Not analyzed	Fe-reducing bacteria
AOC	Increasing from 2001	around 25	Not measured

Conclusions

Clogging in deep infiltration systems under investigation here is mainly caused by iron precipitates and iron reducing bacteria. There should be more attention paid to the input of iron in the system, while as clogging indicators MFI and AOC indexes proved to be useful. The deep well infiltration systems here reviewed have worked for the last 20 years successfully. The conclusion is that with the appropriate optimization of the pre-treatment and periodic rehabilitation it can last an indefinite time.

Clogging can be prevented through a combination of periodic maintenance abstractions with high flows and good pretreatment with MFI vales below 5s/L^2 and AOC <10ug/L^2, but these case studies have shown that systems function without significant clogging for years with greater MFI and AOC values Also, management of drilling fluids during well construction helps to prevent formation damage and clogging. Using help-casing, removing the drilling mud from the borehole wall with a reaming drilling head, and using degradable additives in the drilling mud are ways to manage formation damage during the drilling process to reduce the impact of future clogging.

The most successful rehabilitations were the ones using mechanical and chemical methods, and as for chemical, the use of hydrogen peroxide with chlorine bleach turned out to be very successful. An early rehabilitation, before the clogging has become too severe gives better results. It is important therefore to perform an accurate and continuous monitoring.

An aspect that is not sufficiently clear currently is the source of the iron forming the precipitates in the infiltration wells. Key to controlling the clogging by the observed combination of biological and chemical (iron(III) rich) clogging layers is understanding the source of iron.

An aspect that is expected to become more important for future maintenance of MAR systems, is that infiltration water quality guidelines will become more stringent and more focus will be put on removing organic micro-pollutants. This could lead to expansion of pretreatment facilities with UV/ H_2O_2, which could result in a higher fraction of AOC in infiltration water and a subsequent increased biological clogging. Combining MAR with UV/ H_2O_2 treatment may be desirable when aiming for a multiple barrier approach against contaminants. However, the formation of AOC and the role of this in well clogging show stacking different treatment steps can lead to unwanted side effects negatively impacting on the overall efficiency.

Bibliography

Bonte, M., Raat, K.J., and Dammers, P., (2009a) Analyse putverstopping en voorstel voor regeneratie diepinfiltratie Waalsdorp. KWR Rapport, kenmerk KWR 09.001

Bonte, M., (2009 b) Regeneratie en verstoping van infiltratieputten. KWR Rapport, kenmerk KWR09.028

Duijvenbode, S.W., and Olsthoorn, T.N., (2002) A pilot study of deep-well recharge by Amsterdam Water Supply. Proc. Management of Aquifer Recharge for Sustainability – Dillon (ed) 2002, 447–451.

Jonge, H.G., Dammers, P.H., and Bonte, M., (2010) Managed deep well aquifer recharge in the Coastal dunes of South Holland: 20 years of experience. ISMAR-7, Abu Dhabi.

Olsthoorn, T.N., (1982) Verstopping van persputten, Kiwa mededelingen #72

Stuyfzand, P.J., (2007) Naar een effectievere diagnose, therapie en preventie van chemische put- en drainverstopping. H2O 2007 #8.

Stuyfzand, P. J., (2010) Hydrogeochemical Processes during river Bank filtration and artificial recharge of polluted surface waters: zonation, identification and quantification. Riverbank Filtration for Water Security in Desert Countries, Nato Science for Peace and Security Series C: Environmental Secuity, 91–128

Stuyfzand, P. J., (2011) Monitoring van effecten van uitbreiding van de voorzuivering met H2O2/UV/AKF op waterkwaliteitsveranderingen tijdens duininfiltratie door PWN. KWR Rapport, kenmerk KWR 2011.003

Zwart, B-R., (2007) Investigation of Clogging processes in Unconsolidated Aquifers near Water Supply Wells. Proefschrift Technische Universiteit Delft. The Netherlands.

Case Study: Recharge of Potable and Tertiary-treated Wastewater into a Deep, Confined Sandstone Aquifer in Perth, Western Australia

K. Johnston[1], M. Martin[2] and S. Higginson[2]

[1] *Rockwater Pty Ltd*

[2] *Water Corporation, Western Australia*

Abstract

The Water Corporation of Western Australia started investigating the feasibility of recharging potable water into the deep, confined aquifers beneath the Perth Metropolitan area, Western Australia, in 2000. Managed aquifer recharge (MAR) was identified as a potentially significant operating strategy for the Integrated Water Supply Scheme with possible benefits to the environment and providing drought security, improved groundwater quality, groundwater banking and maintenance of groundwater levels.

Perth is largely dependent on groundwater for its municipal water supply, with up to 50% of the total supply sourced from the vast groundwater system that underlies the region. The Perth groundwater system is part of the Perth Basin, and is bounded in the east by crystalline rocks of the Yilgarn Craton and extends many kilometres off shore to the west. The onshore portion of the aquifer stretches 250 km along the coast in a narrow strip of clastic sediments that are more than 2,000 m deep. The sediments have been laid down under varying depositional environments over millions of years. The groundwater system can be broadly divided into three main aquifers: the shallow, unconfined superficial aquifer, and the deep, confined Leederville and Yarragadee aquifers. The Leederville aquifer has been the target aquifer for MAR to date, and there are plans to incorporate the deeper Yarragadee aquifer into future groundwater replenishment operations.

The Leederville aquifer is a major confined aquifer that is typically between 150 and 400 m thick. It is subdivided into three members:

- The Pinjar Member comprises mainly thin sandstone beds interlayered with siltstone and shale. It generally acts as an aquitard and conformably overlies the Wanneroo Member;
- Individual sandstone beds of the Wanneroo Member are about 10 to 20 m thick, with interlayered siltstone and shale beds of varying thickness. The sandstone beds are weakly consolidated and composed predominantly of coarse-grained, poorly-sorted quartz. The aquifer transmissivity is in the order of 500 to 2,000 $m^3/d/m$, and groundwater salinity is generally between 250 and 1,000 mg/L TDS. The Wanneroo Member is the target zone for aquifer recharge and conformably overlies the Mariginiup Member;
- The Mariginiup Member consists of thinly interbedded siltstone and shale with few very thin sandstone beds. It acts as a confining layer.

Investigations commenced with the establishment of a small aquifer storage and recovery (ASR) trial at Jandakot, injecting potable surface water into an existing production bore. The preliminary trial was successful, with clogging managed by backwash-pumping techniques. This facility was upgraded to a pilot scale operation with a new recharge bore and associated infrastructure. Having demonstrated the technical feasibility of ASR in the Leederville aquifer, a large scale ASR site was established at Mirrabooka, where potable treated-groundwater was recharged to the aquifer at rates up to 7 ML/d. Clogging was similarly managed using backwash-pumping

techniques. The ASR trials ultimately led to the establishment of a state of the art Groundwater Replenishment Scheme at the Beenyup wastewater treatment plant in Craigie, where ultra-purified wastewater is currently being recharged to the Leederville aquifer for future re-use in the IWSS. This case study presents results from these investigations with particular regard to the degree and type of clogging encountered using different water types at each site and the operational management of clogging.

Introduction

The Water Corporation is the water service provider to the capital city of Perth in Western Australia. Perth is largely dependent on groundwater for its municipal water supply, with up to 50% of the total supply sourced from the extensive groundwater system that underlies the region. While the groundwater resources are vast, there has been significant drawdown in the major aquifers over the last twenty years or more, and the Water Corporation has been investigating the feasibility of recharging potable and reclaimed water into the deep, confined aquifers lying beneath the metropolitan area, since 2000.

Managed aquifer recharge (MAR) was identified as a potentially significant operating strategy for the Integrated Water Supply Scheme (IWSS) with possible benefits to the environment, for example maintaining groundwater levels in areas with groundwater dependent ecosystems and preventing saline water intrusion into the aquifers. It also provides drought security, improves groundwater quality in areas of marginal salinity, facilitates groundwater banking, and, with the use of reclaimed water, increases the amount of water available for drinking-water supplies, as the Water Corporation seeks to identify additional water resources under drying climatic conditions.

This paper briefly reviews the three MAR schemes developed to investigate the feasibility of implementing aquifer recharge technology under local conditions: from a small-scale pilot aquifer storage and recovery (ASR) project at Jandakot, through a large-scale research and development ASR project at Mirrabooka, to a fully operational groundwater replenishment scheme (GWRS) at Beenyup. Figure 1 shows the site locations. The focus of the discussion in this case study will be the degree and type of clogging encountered at each site and how this has been successfully managed.

Hydrogeological Background

The Perth groundwater system lies within the Perth Basin. It has been extensively explored and the results have been detailed and summarised in Davidson (1995) and updated in Davidson and Yu (2008). The Perth groundwater system is bounded to the east by crystalline rocks of the Yilgarn

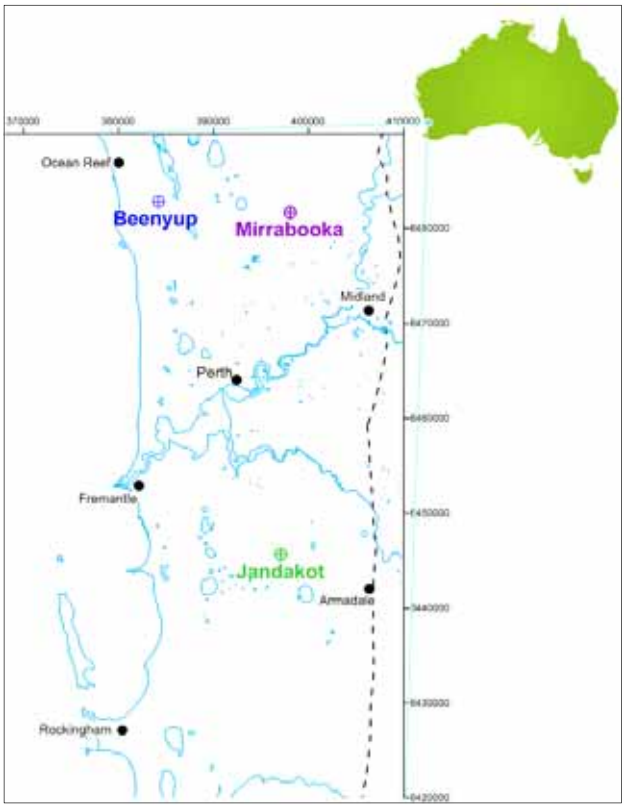

Figure 1: Site Locations

Craton, as marked by the Darling Scarp, and extends many kilometres off shore to the west. The onshore portion of the aquifer system stretches 250 km along the coast in a narrow strip of predominantly siliciclastic sediments that reach more than 2,000 m depth. The sediments have been laid down under various environmental conditions over millions of years. The groundwater system can be broadly divided into three main aquifers: the shallow, unconfined superficial aquifer, and the deep, confined Leederville and Yarragadee aquifers. The Leederville aquifer has been the target aquifer for MAR to date, and will be the focus of the discussion herein, although there are plans to incorporate the deeper Yarragadee aquifer in future groundwater replenishment operations. Figure 2 shows a typical site-scale aquifer profile for these operations.

Information regarding the Leederville aquifer has been taken from the above references and has been supplemented with site-specific data and recent work by Leyland (2011).

The Leederville Formation is typically between 150 and

400 m thick in the Perth region and was deposited during the Early Cretaceous period under marine and non-marine conditions. It is subdivided into three members, the Pinjar Member, the Wanneroo Member and the Mariginiup Member, all of which are present at the sites under consideration.

The Pinjar Member unconformably underlies the Osborne Formation and comprises mainly thin beds (<6 m) of fine- to coarse-grained, poorly sorted and commonly silty sandstone, interlayered with dark grey to black siltstone and shale. It generally acts as an aquitard and conformably overlies the Wanneroo Member.

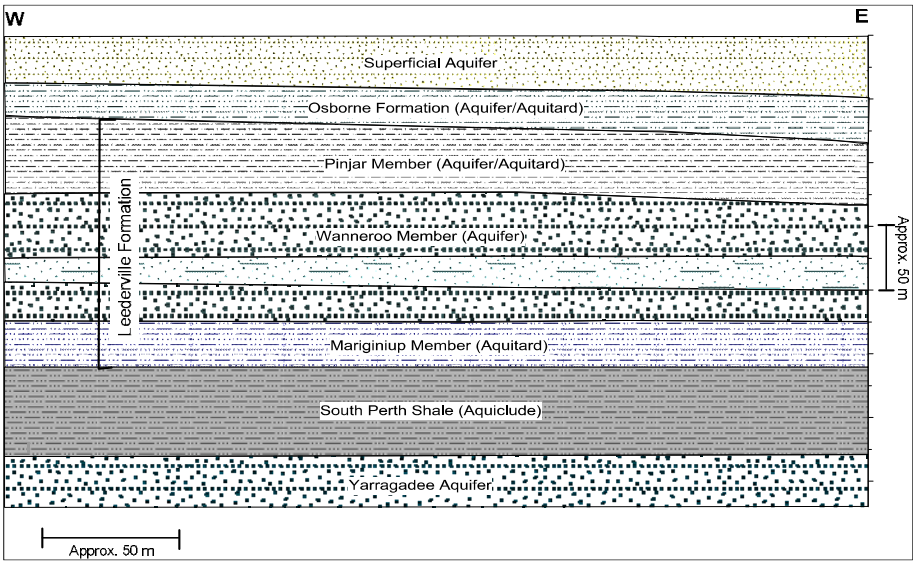

Figure 2: Schematic cross section showing typical aquifer profile for the Perth MAR sites

The Wanneroo Member is the target zone for recharge via injection and comprises weakly consolidated, predominantly coarse-grained but poorly sorted, subarkose sandstone beds, about 4 to 20 m thick with interlayered siltstone and shale beds of varying thickness. The depositional environment has been determined to be predominantly fluvial in the north, with periods of low energy tidal inundation and sedimentation. At the subject sites, the aquifer transmissivity for the screened sandstone beds ranges from about 650 m^3/d/m at Mirrabooka to 2,100 m^3/d/m at Beenyup. Groundwater salinity varies from site to site, with depth in the aquifer, and with aquifer lithology; it is generally between 250 mg/L TDS near recharge areas and in the coarse-sandstone beds with higher permeability, and 1,000 mg/L TDS within the siltstone and shales and in areas of marine deposition or inundation. Table 1 provides a summary of the background hydrogeological data for the receiving aquifer at each site. The Wanneroo Member conformably overlies the Mariginiup Member.

The Mariginiup Member represents a prograding succession of tidal bars and consists of thinly interbedded siltstone and shale with few, very thin sandstone beds. It acts as a confining layer and conformably overlies the South Perth Shale.

Provenance analysis using major and trace elements suggests local granitoids from the Yilgarn Craton have been the principal contributor of sediment to the Leederville Formation in the Perth area (Prommer et. al., 2011). The predominant minerals in the aquifer matrix are quartz and K-feldspar, with kaolinite making up the bulk of the clay fraction. Accessory minerals include Na-feldspar, muscovite, pyrite, siderite, chlorite and crandalite. Groundwater quality and mineralogical data from Jandakot also indicates the presence of calcite at this site, which along with the higher background salinity values, suggests the Wanneroo Member was deposited under marine conditions, or experienced a period of marine inundation at this location.

Background Groundwater and Recharge Water Quality

Groundwater in the Leederville aquifer at the three MAR sites tends to be fresh to slightly brackish, circumneutral to slightly acidic at Mirrabooka and Beenyup to slightly alkaline at Jandakot, and of a sodium-chloride type (Figure 3). In the recharge zone the groundwater is anoxic and reducing conditions prevail.

Table 1: Hydrogeological data for the receiving aquifer at Perth Metropolitan MAR sites

Site	Total Bore Depth	Screened Intervals	Length of Screens	Static Water Level	Static Water Level	Bore Yield	Transmissivity	Hydraulic Conductivity	Groundwater Salinity
	(m bgl)	(m bgl)	(m)	(m bgl)	(m AHD)	(kL/day)	(m^2/day)	(m/day)	(mg/L TDS)
Jandakot	228	178-217	39	30	0	6,030	790	20.3	520-1,550
Mirrabooka	434	320-368 394-427	81	43.5	2.5	7,780	650	8.0	520-1,400
Beenyup	236	122-224	102	27.6	-6.9	8,640	2,100	20.3	450-1,100

Groundwater in the Leederville aquifer at the three MAR sites tends to be fresh to slightly brackish, circumneutral to slightly acidic at Mirrabooka and Beenyup to slightly alkaline at Jandakot, and of a sodium-chloride type (Figure 3). In the recharge zone the groundwater is anoxic and reducing conditions prevail. The groundwater in the Leederville aquifer tends to be naturally high in turbidity, and generally has elevated levels of iron and manganese, which are routinely removed during standard water treatment processes in the IWSS.

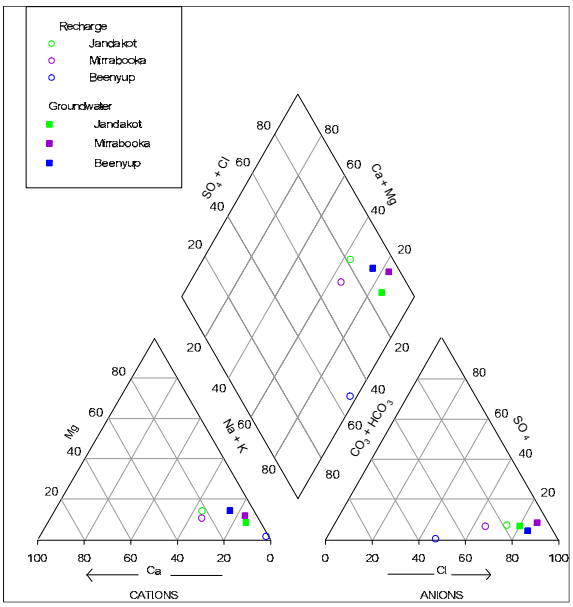

Figure 3: Average water composition for Leederville MAR sites and recharge waters

The recharge water at each site varies, from potable mains water sourced from hills dams at Jandakot and treated groundwater at Mirrabooka, to highly-treated reclaimed wastewater at Beenyup. The geochemical composition of the recharge water for each project is plotted in Figure 3, and average values for key water quality parameters related to clogging are presented in Table 2. The water recharged at all sites is of a very high quality for injection.

Table 2: Recharge water quality parameters related to clogging

At Jandakot, water was diverted from the Serpentine Main, which distributes water from the Serpentine and other dams in the Perth Hills to the southern metropolitan area. The water is fresh (<200 mg/L TDS), slightly acidic and of a sodium-chloride type. The total suspended solids (TSS) are < 5mg/L and turbidity is generally below 1 NTU. Nitrate and dissolved organic carbon (DOC) are very low (<0.2 mg/L and <2.0 mg/L, respectively). Compared to the other sites, total iron and manganese levels are slightly elevated (about 0.1 mg/L and 0.01 mg/L, respectively), and it is believed that this may contribute to the higher modified fouling index (MFI) results (average 70 s/L^2). Particle size distribution (PSD) analysis indicated 100% of all suspended particles were less than 50µm in diameter, 99% were smaller than 10 µm in diameter and about 50% were smaller than 2 µm in diameter.

At Mirrabooka, water was diverted from the Gnangara Rd distribution main, which distributes water from the Wanneroo Reservoir to the northern metropolitan area. The reservoir is supplied from nearby groundwater treatment plants, which source water from the superficial and confined aquifer systems. The water is fresh (<500 mg/L TDS), slightly alkaline and of a sodium-chloride type. Total suspended solids are mostly below 5 mg/L and turbidity is generally very low, <0.3 NTU. Nitrate and DOC are also very low (<0.2 mg/L and <2.0 mg/L, respectively) as are total iron and manganese (about 0.02 mg/L and 0.003 mg/L, respectively). The MFI was measured for a few samples during the first injection cycle, and gave very low values – in the order of 5 s/L^2. The one sample analysed for PSD yielded no results due to insufficient particles.

At Beenyup, highly treated recycled water from the Beenyup Advanced Water Recycling Plant (AWRP) is used to recharge the aquifer. The AWRP further treats secondary-treated wastewater through ultra-filtration, reverse osmosis and ultra-violet disinfection to meet the Australian guidelines for drinking water and water recycling, in addition to other site specific guidelines. The water has a very low ionic strength (<50 mg/L TDS), it is slightly alkaline and of a sodium-bicarbonate type (Figure 3). Total suspended solids and

Site	Total Dissolved Solids		Organic Carbon		Nitrate		Total Iron		Total Manganese		Total Suspended Solids		Turbidity		Particle Size Distribution			Modified Fouling Index	
	Ave.	Max.	Ave.	Max.	Ave.	Max.	Ave.	Max.	Ave.	Max.	Ave.	Max.	Ave.	Max.	50 µm	10 µm	2 µm	Ave.	Max.
	(mg/L)	(mg/L)	(mg/L)	(mg/L)	(mg/L)	(mg/L)	(mg/L)	(mg/L)	(mg/L)	(mg/L)	(mg/L)	(mg/L)	(NTU)	(NTU)	(% <)	(% <)	(% <)	(s/L^2)	(s/L^2)
Jandakot	154 (39)	250	<2 (31)	4.9	<0.2 (22)	2.1	<0.1 (37)	0.24	<0.011 (8)	0.05	<4.2 (39)	5.0	<0.8[1] (26)	11	100 (6)	99 (6)	52 (6)	70 (26)	149.3
Mirrabooka	454 (22)	515	<2.1 (22)	8.4	<0.9 (16)	2.0	<0.02 (24)	0.08	<0.003 (24)	0.008	<5.0 (14)	5.0	<0.3 (24)	1.3	Insufficient particles to measure (1)			8[2] (4)	13.7
Beenyup	31 (33)	50	<1 (29)	<1	2.1 (34)	3.6	<0.01 (34)	0.01	<0.001 (34)	<0.001	<1.1 (34)	4.0	<0.5 (34)	0.5	NA	NA	NA	NA	NA

1. Average calculated without outlier of 11 mg/L

2. Average calculated from available raw data - it has been reported elsewhere as 3 s/L^2 (e.g. Prommer et al)

Numbers in parenthesis indicate number of samples and < indicates values calculated using limit of reporting (LOR) for analysis where values were below LOR

turbidity are very low, generally <1 mg/L and <0.5 NTU, respectively. Nitrate levels are elevated compared to the other sites (generally about 2 mg/L), but DOC is very low, <1.0 mg/L. Total iron and manganese are generally below the limits of reporting (0.01 mg/L and 0.001 mg/L, respectively). No samples have been analysed for MFI or PSD as the treatment process effectively removes all solid particles (Water Corporation, 2012).

Site Set-up

Water is recharged to the Leederville aquifer at each site via an injection bore. At Jandakot and Mirrabooka the bore was also used for production, at Beenyup the bore is used for injection alone.

At each site, the injection bore was drilled using mud-rotary drilling techniques and was constructed using large-diameter, reinforced-fibreglass blank casing to the top of the aquifer, cement-grouted to the surface. Stainless steel riser pipe and screens were telescoped through the aquifer interval and held in place by an inflatable packer. Screen aperture is mainly 0.5 mm. At Jandakot and Beenyup, the aquifer annulus was filled with graded gravel. The annulus was left open at Mirrabooka with the aim of developing a natural gravel pack. This variation in construction was intended to inform future decisions regarding preferred injection bore construction with regard to bore clogging performance and was in response to several studies (e.g. Segalen et al., 2005 and Gerges, 1999) that suggest screens with open hole and/or natural gravel pack may be more efficient for ASR. The bores were developed using standard air-lift and jetting techniques.

A filtration system was installed at Jandakot and Mirrabooka to filter the recharge water to 50 μm prior to injection to minimise the amount of suspended solids introduced to the aquifer, and in particular to minimise the risk of clogging due to a "slug" of poor quality water, should one occur.

A purpose-designed pump was installed in the bores at Jandakot and Mirrabooka to provide automated backwashing capabilities for the management of clogging. The pumps are designed to enable injection at controlled flow rates through an automated down-hole flow valve located above the pump unit. The valve is closed when the pump operates for backwashing or production. The valve is also utilised to implement "surge-backwashing" during the recovery phase, where the down-hole valve is opened during pumping to allow pumped water to recirculate through the valve. The pump is then stopped and the water in the pump column flows back into the bore casing producing a surging action. Finally, the pump is started again and the backwash water removed from the bore.

Monitoring bores were drilled and constructed at each site between 15 and 240 m from the injection bore. There are two monitoring bores at Jandakot (15 m and 60 m), five monitoring bores at Mirrabooka (two at 15 m and three at 40 m) and 22 monitoring bores at Beenyup (seven at 20 m, five at 60 m, four at 120 m, three at 180 m and three at 240 m). At Mirrabooka and Beenyup the multiple bores at each site are screened at various depth intervals to capture information from discreet aquifer zones.

On-line monitoring equipment was installed at the injection bores to monitor flow rates and water quality parameters: salinity, temperature and turbidity. At Beenyup, pH and oxygen reduction potential (ORP) were alos measured online. Down-hole pressure transducers were installed in each of the injection and monitoring bores to provide continuous water-level response data.

Operational Summary for Each Trial

The main operating parameters for each site are summarised in Table 3.

Table 3: Operational summary for the Perth Metropolitan MAR trials

Site	Injection Cycles[1]	Duration of Injection[2]	Volume Injected[2]	Average Injection Rate	Backwash Rate	Backwash Volume[2]	Average Production Rate	Duration of Production
		days	ML	ML/d	ML/d	ML	ML/d	days
Jandakot	5	13 to 162	50 to 640	1.3 to 4.6	2 to 8.4	3.3 to 13.3	2 to 8.4	39 to 325
Mirrabooka	3	59 to 110	190 to 560	2.0 to 7.5	0 to 9.5	0.2 to 1	4 to 9.5	43 to 233
Beenyup[3]	1	814	2,620	2.5 to 4.3	NA	NA	NA	NA

1) An injection cycle represents a continuous period of injection (discounting unplanned or operational shutdowns), followed by a period of residence and/or extraction.
2) During one injection cycle
3) At 1 February 2013

Five injection/extraction cycles were conducted in the purpose-built ASR bore at Jandakot, with injection occurring for periods of between 13 and 162 days at rates of between 1.3 and 4.6 megalitres per day (ML/d). Between 50 and 640 ML of potable water were injected to the aquifer during each of these recharge events. The bore was generally backwashed to remove trapped suspended-sediment from the bore/aquifer interface every two to four days for 15 to 30 minutes during Cycles 1 and 2, and daily for 15 minutes during Cycles 3 to 5. Backwash rates tended to decrease with time during each cycle due to a reduction in bore efficiency.

During Cycles 1 and 2, five per cent of the total water volume recharged was extracted during the backwash events, compared with two to three per cent during Cycles 3 to 5. Following injection and a period of residence in the aquifer the water was recovered by pumping. During extraction the bore was surge backwashed every eight hours for about 15 minutes to further facilitate bore redevelopment. The average production rate ranged from about 2.2 to 8.4 ML/d, depending largely on the bore efficiency, and production continued for between 39 and 325 days.

Three injection/extraction cycles were conducted at Mirrabooka with recharge occurring for periods of 59 to 110 days at rates of between 2.0 and 7.5 ML/d. Between 190 and 560 ML of potable water were recharged to the aquifer during each of these injection events. The bore was only occasionally backwashed during Cycle 1 at a rate of 7 ML/d for 15 to 20 minutes; it was backwashed at a rate of about 7 ML/d, daily for the first two weeks during Cycle 2, then on several occasions thereafter; and at varying intervals and duration and at different rates during Cycle 3. Between 0.2 and 1 ML of recharged water was recovered during these backwash events representing between 0.1 and 1.2 % of the total volume of water recharged. Following injection and a period of residence in the aquifer the water was recovered by pumping. During extraction for Cycle 3 the bore was surge backwashed every four hours for about 15 minutes to further facilitate bore redevelopment. The average production rate ranged from about 4 to 9.5 ML/d, and production continued for between 43 and 233 days. All backwash and recovered water was sent to the Mirrabooka Groundwater Treatment Plant prior to distribution in the IWSS.

There has been injection only at Beenyup, with extraction planned to take place from distant production bores in the future. Recharge commenced in November 2010, and has continued for over 814 days with occasional shut-downs related to the AWRP. More than 2,620 ML of reclaimed water has been recharged to the aquifer at rates of between 2.5 and 4.8 ML/d, depending on the treatment plant output. To date no redevelopment has been required.

Clogging Assessment

Clogging rates were generally assessed by comparing rates of water level rise in the injection bore with those in the nearby monitoring bores; and the degree of clogging and the effectiveness of backwashing and bore redevelopment was assessed using changes to the specific capacity of the injection bore:

$$Sc = \frac{Q}{h_o - h}$$

Where Sc = specific capacity, Q = pumping (or injection) rate, and $h_o - h$ = water level drawdown (or rise).

Jandakot

At Jandakot, a comparison between the water-level rise in the ASR bore and the 15 m observation bore suggested that 80 to 85% of the water-level rise in the ASR bore was attributable to clogging (Rockwater, 2004 and 2008). This was supported by the decline in the specific capacity of the bore from a maximum of almost 350 $m^3/d/m$ at the start of injection to about 50 $m^3/d/m$ by the end of most injection cycles, as shown in the example from Cycle 3 (Figure 4).

Figure 4: Changes to Jandakot injection bore specific capacity during Cycle 3 – injection and extraction

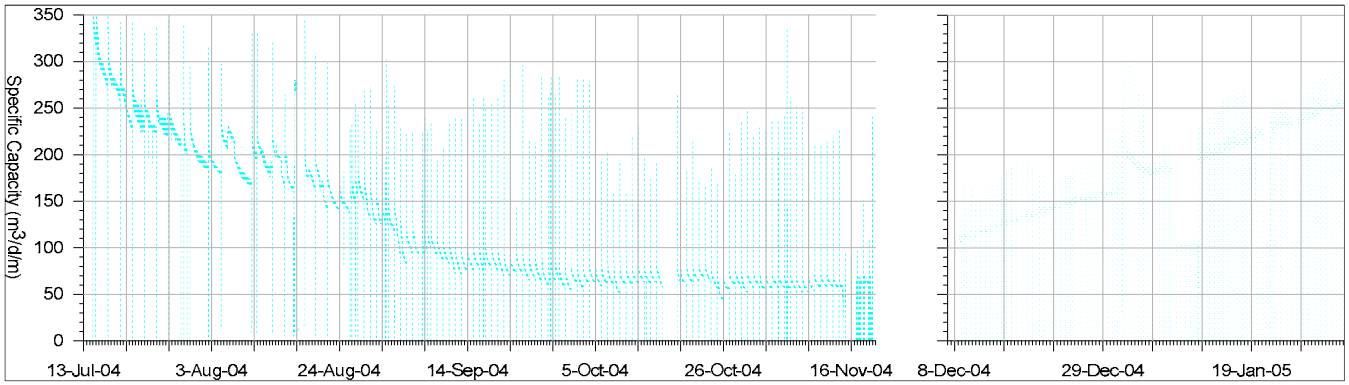

An assessment of clogging rates, based on the difference in ASR bore water-levels measured every 24 hours and normalised to volume of water recharged, showed clogging rates generally increased with time and cumulative recharge volume, and also in response to specific poor water-quality events, particularly periods with elevated iron concentrations, high turbidity and/or high MFI, with clogging rates generally between 0.5 and 1.5 m/ML (Rockwater 2004, 2006 and 2008). It was also found that as the cumulative recharge volume increased, the backwash efficiency was reduced (Rockwater, 2008). Aquifer recharge was effectively prolonged with bore backwashing and by reducing injection flow rates, as required, to maintain injection heads at a predetermined pressure. Clogging was effectively remediated following each injection cycle by implementing surge-backwashing every eight hours during the recovery pumping phase. This technique was effective in redeveloping the ASR bore, returning the specific capacity of the bore to around 250 m^3/d/m (Figure 4).

It was concluded that clogging at Jandakot was due to mainly to suspended solids in the recharge water, and that daily backwashing of the ASR bore decreased the amount of clogging and enabled a greater volume of recharge over a longer period. It did not, however, prevent clogging. It was also noted that the automated backwashing was most effective for reducing clogging close to the bore, and that once clogging occurred further into the aquifer, long-term pumping and surge-backwashing was required to recondition the bore. The operation of the dedicated backwashing system mitigated the need for more-frequent bore redevelopment using alternative methods such as air-lifting.

Mirrabooka

At Mirrabooka, a greater emphasis was placed developing an online tool to monitor clogging during injection, and a system was established monitor the difference in water-levels between the ASR bore and the monitoring bores with time. When plotted, a flat trend represents no clogging and a continual rising trend indicates clogging (after Hutchinson, 1993, as presented by Centre of Groundwater Studies, 2004). The results from the shallower 15 m observation bore over the three injection cycles are shown in Figure 5. It should be noted that because there are only a few manual water-level measurements, and a number of changes were made to transducer levels and pressure range during the trials, it is not possible to be certain as to the absolute difference between the ASR bore and observation bore water-levels. However, the trend in the water level difference is considered reliable. In addition, data representing changes to water levels during water quality sampling events and during periods of no flow and early start up following a shut-down or backwashing event have been deleted for clarity.

Figure 5 shows minor and gradual clogging occurred during Cycle 1, and clogging rates were calculated to be in the order of 0.004 to 0.05 m/ML (Rockwater, 2010). Water levels in the ASR bore remained well below ground level and the specific capacity of the bore decreased from about 550 to 350 m^3/d/m (Rockwater, 2010). There were only three backwash events, which yielded some improvement in specific capacity, but did not noticeably change the rate of clogging. There was no surge backwashing during recovery pumping, and no improvement was observed in the specific capacity of the ASR bore as a result of pumping alone. Clogging rates were an order of magnitude lower than those observed at Jandakot, and this was attributed to a better quality recharge water (lower iron and manganese concentrations and lower MFI) (Rockwater, 2010).

During Cycle 2, there was no notable clogging early in the trial for flow rates of either 3 or 5 ML/d (Figure 5), although the specific capacity of the ASR bore did decrease slightly (Rockwater, 2011). Technical difficulties encountered with the pressure transducers and flow meter resulted in a significant loss of data throughout this Cycle, and there were also problems in maintaining injection flow rates in the desired range. From the data available, however, it can be seen that clogging rates increased significantly following a shut-down event (consistent with a reduction in specific capacity to 250 m^3/d/m (Rockwater, 2011)) and over the last week of the trial (Figure 5). Backwashing occurred during the first week of the trial with only an occasional backwash thereafter. Clogging rates ranged from 0.0 to 0.9 m/ML, with maximum values increasing with depth in the bore (Rockwater, 2011). It was noted that significant clogging might be generated during start-up events and/or following an increase in injection flow rates. At the end of Cycle 2, heads in the ASR bore were well above ground level and the specific capacity had been reduced to less than 200 m^3/d/m. Recovery pumping, which occurred without the surge backwashing, did not significantly improve the bore efficiency (Rockwater, 2011).

At the start of Cycle 3 clogging rates were very low, in the order of 0.01 to 0.04 m/ML for injection rates of 3 and 7 ML/d. They increased significantly, to between 0.07 and 0.11 m/ML, following a shut-down event and a reset of injection flow rates in late July 2011. In response to this increased clogging, a two week period of daily backwashing was initiated; however problems with the down-hole valve

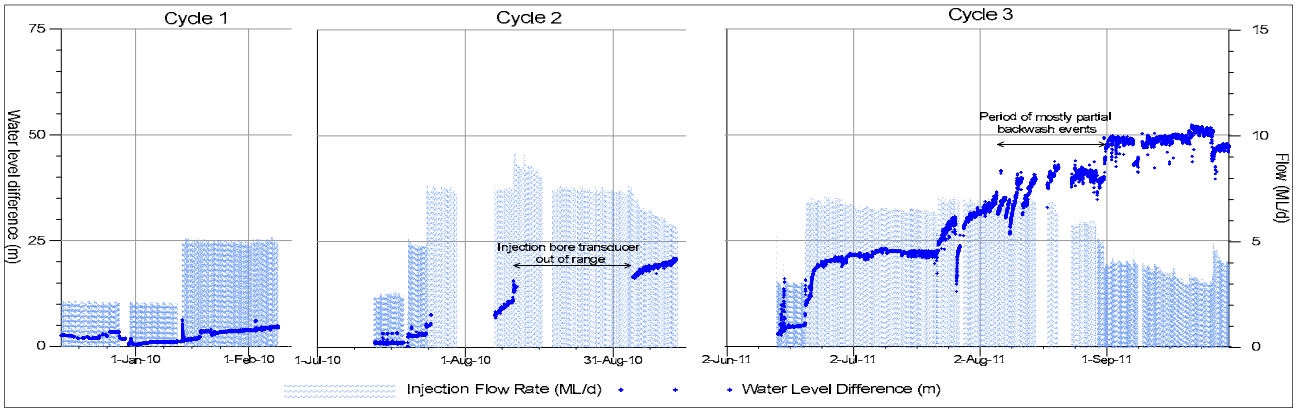

Figure 5: Water level difference between Mirrabooka ASR bore and 15 m observation bore showing clogging trends over the three injection cycles

meant only a few of backwash events were effective, with low pumping rates and frequent recirculation of groundwater in the bore. It was noted that the water pumped from the bore during these backwashing events was highly turbid, and failed to clear even when pumped for an extended period. It is possible that siltstones and shales within the aquifer zone were fretting from an open section of the annulus, where a natural gravel pack had not been developed as anticipated. This is consistent with the steepening trend in start-up water-level difference (Figure 5), which suggests increased clogging with each partial or failed backwash event. From the end of August 2011, there was only one backwash event, and water-levels in the ASR bore were maintained at 20 m above ground level by reducing injection flow rates as required. Clogging rates were in the order of 0.2 m/ML, and were again noted to increase with the depth of the aquifer interval monitored (Rockwater, 2012). The specific capacity of the ASR bore decreased from about 260 to 60 m^3/d/m during this Cycle (Rockwater, 2012). Surge backwashing was implemented every four hours during recovery pumping and the specific capacity of the ASR bore showed some improvement, increasing from 210 to 280 m^3/d/m over the first two weeks of pumping. There was no further improvement over the following two months of pumping, even with continued surge backwash redevelopment (Rockwater, 2012).

It was concluded that the clogging at Mirrabooka was due largely to the remobilisation and compaction of aquifer fines, particularly at the bore/aquifer interface. It is believed that recirculation of aquifer sediments and their incomplete removal from the bore during backwashing contributed significantly to the injection pressure in the ASR bore, particularly on start-up, and this was most likely exacerbated by the absence of gravel pack around the bore screens. Increased clogging with time and injection volume was also evident, which is consistent with the results from Jandakot. It was found that recovery pumping alone was insufficient to recondition the ASR bore, but that surge backwashing was able to improve bore efficiency. The results were not as good as at Jandakot, however, and this could be due to the different bore construction or because clogging extended further into the aquifer by the end of the third cycle of injection.

Beenyup

At Beenyup, clogging in the recharge bore is monitored using a water-level rise differential method, as developed at Mirrabooka and further refined to normalise for potentiometric head difference with depth and changes in recharge flow rates. Figure 6 shows the average change in the water-level rise differential between the recharge bore and the five monitoring bores at the 20 m observation site, normalised to the injection flow rate, using the following equations:

1. $\Delta WL = SWL_{to} - WL_{tn}$

Where ΔWL = change in water level from immediately prior to injection (SWL_{to}) to any given time (WL_{tn});

2. $\Delta WL_{\uparrow} = \Delta WL_R - \Delta WL_{Obs}$

$\Delta WL_{\uparrow}$ = difference in water-level rise between the recharge bore (ΔWL_R) and each observation bore (ΔWL_{Obs});

3. $N\Delta WL_{\uparrow} = \Delta WL_{\uparrow} - (aQ + b)$

Where $N\Delta WL_{\uparrow}$ = difference in water level rise between the recharge bore and each observation bore normalised to a constant flow rate, a = slope of the line for the plot of recharge rate (Q) vs. the difference in water level rise ($\Delta WL_{\uparrow}$), and b = the intercept at zero flow. The average $N\Delta WL_{\uparrow}$ is the average of those normalised values calculated for each of the five individual observation bores.

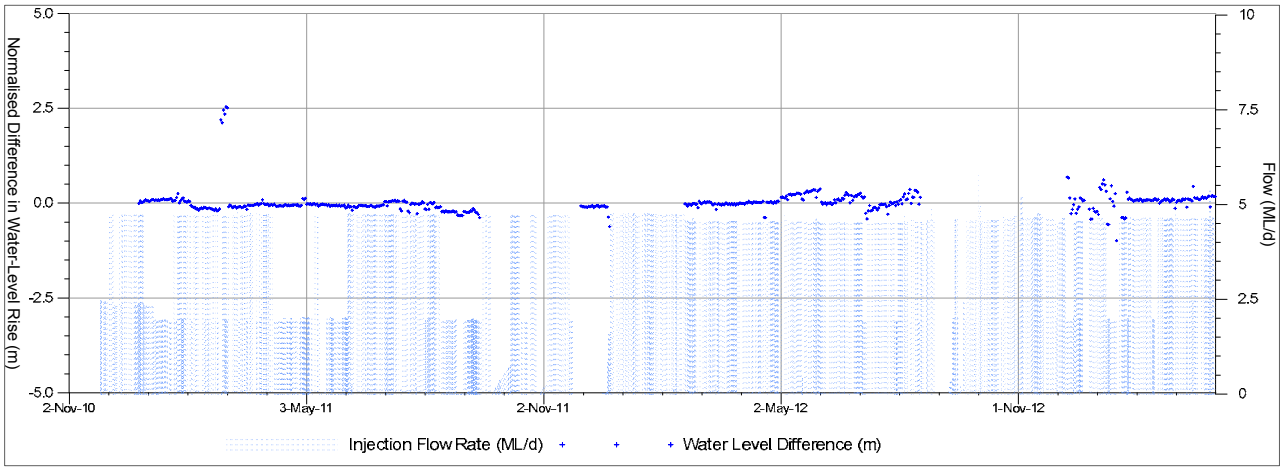

Figure 6: Normalised water-level rise differential averaged over the five monitoring intervals 20 m distant from the recharge bore

It can be seen from the almost completely flat trend in the water-level difference between bores, that very little clogging has occurred at Beenyup in response to recharge of the reclaimed water. In general, the head build up in both the aquifer and the recharge bore has been less than 5 m for recharge rates of up to 5 ML/d. The lack of clogging is likely to be due largely to the absence of suspended solids in the recharge water, and although there is evidence of mobilisation of colloidal fines in the aquifer itself (Water Corporation, 2012), this does not appear to be contributing significantly to clogging at this site. There may have been some low levels of clogging between April and June 2012, which correlates to a period of increased microbial activity, and is consistent with observed de-nitrification at the site, suggesting some minor microbial clogging may have occurred. Water levels have since stabilised, and no further clogging is evident. A clogging alert level is set at the normalised water-level rise differential of 5 m.

Clogging at Beenyup is currently assessed weekly following manual download and manipulation of the monitoring data. In the future it is anticipated that the system will be fully automated and available on-line to operators at the GWR site.

No bore redevelopment has been required to date. Future down-hole investigations, backwashing and pumping tests to assess the bore performance are planned to be conducted during the next period of extended shut-down at the treatment plant.

Conclusions

Managed aquifer recharge to the confined Leederville aquifer has been extensively trialled and assessed in the Perth metropolitan area by the Water Corporation over the last thirteen years. The studies have shown a general consistency between aquifer characteristics and aquifer response, and have confirmed the technical viability of large-scale recharge of potable and reclaimed water to the aquifer as a means of protecting and potentially increasing groundwater supplies.

From the results of the trials, it is clear that the quality of the recharge water is important in determining the degree of clogging from suspended solids, with very small amounts of suspended sediment – particularly when associated with iron and manganese, contributing significantly to the clogging. Comparison of the results from Jandakot and Mirrabooka suggest that the degree of clogging associated the recharge water could be determined prior to injection by measuring MFI: MFI values of up to 14 L/s^2 appear to be readily acceptable in this coarse sandstone aquifer. Particle size analysis has shown that particles <10 μm in diameter are responsible for the clogging seen at Jandakot.

It is likely that the predominant cause of clogging at Mirrabooka was the remobilisation of aquifer fines, particularly at the aquifer/bore interface. It is believed that the absence of gravel pack around the screens contributed significantly to the problem, with fretting and recirculation of aquifer fines occurring, particularly during start-up and backwash events. Contrary to findings at other locations, this method of bore construction does not seem suited to the conditions in the Leederville aquifer (weakly consolidated, interbedded sandstone, siltstone and shale).

While dedicated bore backwashing techniques have been shown to effectively reduce the severity of clogging, increase the recharge volume and extend the duration of injection, it does not prevent clogging and regular periods of redevelopment are required. Utilising the pump system

to facilitate surge backwashing during recovery pumping has also been shown to be an effective method of bore redevelopment, significantly increasing the time between more traditional bore development methods, such as air-lifting. It should be noted, however, that this method has been difficult to implement at an operational level, with common technical difficulties and the additional requirement to dispose of sometimes large amounts of very poor quality backwash water. Neither of the trial schemes has continued to a fully operational site.

The most successful site has been Beenyup, where the recharge water has been of such high quality that significant clogging has not occurred, and recharge operations are set to continue into the foreseeable future.

References

Centre for Groundwater Studies, (2004) 4th ASR national workshop: management of aquifer recharge. Notes and PowerPoint presentations, October 2004.

Segalen, A-S., Pavelic P. and Dillon P., (2005) Review of drilling, completion and remediation methods for ASR wells in unconsolidated aquifers. CSIRO Land and Water Technical Report No. 04/05. March 2005.

Davidson, W. A., (1995) Hydrogeology and groundwater resources of the Perth Region, Western Australia: Western Australian Geological Survey, Bulletin 142.

Davidson, W.A., and Yu, X., (2008) Perth regional aquifer modelling system (PRAMS) model development: Hydrogeology and groundwater modelling, Western Australia Department of Water, Hydrogeological record series HG 20.

Gerges N.Z., (1999) Methods of well completion for ASR wells and injection testing. Centre for Groundwater Studies, 4th ASR national workshop: management of aquifer recharge. Notes and PowerPoint presentations, October 2004.

Leyland, L., (2011) Hydrogeology of the Leederville Aquifer, Central Perth Basin, Western Australia. Thesis presented for the degree of PhD. University of Western Australia, School of Earth and Environment, July 2011.

NHMRC, (2011) Australian drinking water guidelines Paper 6 National water quality management strategy. National Health and Medical Research Council and the Natural Resource Management Ministerial Council, Canberra.

Prommer, H., Descourvieres C.D., Handyside, M., Johnston, K., Harris, B., Li, Q., Costello, P., and Martin, M., (2011) Interim Report – Aquifer storage and recovery of potable water in the Leederville Aquifer. CSIRO: Water for a Healthy Country National Research Flagship

Rockwater, (2004) Jandakot aquifer storage and recovery project. Results of Cycles 1 & 2: operational pilot. Unpublished report to Water Corporation of Western Australia, November 2004.

Rockwater, (2006) Jandakot aquifer storage and recovery project. Results of Cycles 3 & 4: operational pilot. Unpublished report to Water Corporation of Western Australia, July 2006.

Rockwater, (2008) Jandakot aquifer storage and recovery project. Results of Cycle 5: operational pilot. Unpublished report to Water Corporation of Western Australia, November 2008.

Rockwater, (2010) Mirrabooka aquifer storage and recovery trial. Results of Cycle 1: December 2009– April 2010. Unpublished report to Water Corporation of Western Australia, October 2010.

Rockwater, (2011) Mirrabooka aquifer storage and recovery trial. Results and technical review for Cycle 2: July 2010 to January 2011. Unpublished report to Water Corporation of Western Australia, October 2011.

Rockwater, (2012) Mirrabooka aquifer storage and recovery trial. Results and technical review for Cycle 3: June 2011 to January 2012. Unpublished report to Water Corporation of Western Australia, December 2012.

Water Corporation, (2012) Groundwater Report 2012. Groundwater Replenishment Trial. Published by the Water Corporation of Western Australia, ISBN 1 74043 810 8, October 2012.

Domestic Scale Rainwater ASR Observations of Clogging and Effectiveness of its Management

K. Barry[1], P. Dillon[1] and P. Pavelic[2]
[1] *CSIRO Land and Water,*
[2] *International Water Management Institute*

1 Introduction

Rainwater derived from roof surfaces may offer useful quantities of good quality water if it can be successfully harvested and stored. Climate variability in more seasonally arid climates makes surface water storage risky and viable alternatives are sought. Aquifer Storage and Recovery (ASR) is a technology whereby water is collected, stored below ground and later recovered using a single well (Pyne, 2005). This can be effective in urban areas where above ground storage is limited and the hydrogeology is favourable. An evaluation of a shallow Quaternary system of alluvial aquifers of the Adelaide Plains (Pavelic et al., 1992) revealed that much of the metropolitan area has potential for storage of water on a smaller scale in brackish aquifers. For example, by recharging domestic roof runoff for use in garden watering in summer to further reduce demand on a stressed water supply system. This was one of the activities explored in support of improved stormwater management as part of plans by the Patawalonga Catchment Water Management Board (2002) and which also conformed to the 2004 South Australian Government draft strategy 'Water Proofing Adelaide', now incorporated into the 'Water for Good' plan (2009). However, one of the key measures of the success of the project would be whether clogging in the alluvial aquifer could be managed with regular backwash/recovery events. Clogging of wells remains a major operational issue for injection wells and aquifer storage and recovery (ASR) wells and can limit the quantity of water that can be stored within the aquifer and may necessitate regular well redevelopment or even lead to site abandonment in extreme cases (Pérez-Paricio and Carrera, 1999; Rinck-Pfeiffer et al., 2000). There are different causes of clogging in wells, which can be driven by physical, chemical and biological processes that may act individually or collectively in-fill pore spaces at or near the well-aquifer interface and thereby decrease aquifer permeability (Olsthoorn, 1982; Baveye et al., 1998).

The primary objective of this study was to assess the operational performance of domestic-scale ASR with roof-runoff (rainwater), determine causes for departures from predicted performance, and identify solutions to any problems that arise, so that evidence-based advice can be given in the event that regulators wish to license such installations. Various aspects of this project have been reported on previously in Barry et al (2005, 2007), Dillon and Barry (2005) and this paper focuses largely on clogging and its management.

2 Site Description and Operation

In June 2003 a domestic scale ASR demonstration trial commenced in the rear garden of a residential dwelling at Kingswood, South Australia, 6 km south-east of the city of Adelaide. Establishment of the site began in April 2002 when two boreholes were drilled, located 5 m apart with respective diameters of 100 mm for the northern well (#6628-20967), and 125 mm for the southern well (#6628-20968). These were installed to a depth of 24 m in the upper Quaternary alluvial aquifer by rotary drilling with mud. Although this form of drilling has been found to be problematic for ASR in clay-rich alluvial profiles by Segalen et al. (2005) and Pavelic et al. (2005), alternative methods were not available due to constraints on access to the site and limited budget. Each well was cased to the full 24 m depth below ground, with slotted casing over the bottom 12 m interval. Below the surficial clay layer the profile is a mixture of clay, sand and gravel to 21 m depth underlain by

a stiff clay base. The annulus around the slotted casing was backfilled with washed gravel and the upper part of the casing was sealed with a mixture of clay slurry and bentonite. On completion of construction each well was 'air lifted' until the discharging water appeared clear.

Pumping tests were conducted at a constant flow rate on 12th December 2002, and based on steady-state analysis well yields of 95 m^3/d (1.1 L/s) in the 100 mm well and 34 m^3/d (0.4 L/s) in the 125 mm well were calculated. Depth to static groundwater level was 12 m below ground surface and ambient groundwater salinity was 2,500 mg/L. Groundwater flows in a north-westerly direction with an average hydraulic gradient of ~ 0.007. From these initial results it was decided in June 2003 to install the injection pipe in the 100 mm well with the higher hydraulic conductivity (inferred from the well yield) and hence greater capacity to receive injected water. The recovery pipe fitted in the same well was connected to a pump and installed to a depth of 18 m. The roof area of 285 m^2 was connected to a 4 m^3 surface tank (3 m^3 active storage). At the inlet on the top of the tank was a 0.12 m^2, 1 mm strainer. An off-take approximately 0.5 m above the base of the tank was connected to the ASR well via a 100 µm filter, allowing gravity feed when the volume of the water in the tank rose above the outlet level. There was no other pre-treatment of the injected rainwater.

ASR operations commenced 29 June 2003. Initial flow rates were slow until air was expelled from the line, then flow accelerated due to the hydraulic gradient between the tank and the aquifer. Between June 2003 and August 2004 two low-head flow meters monitored inflows and outflows to and from the ASR well. Monitoring of groundwater levels at hourly intervals was carried out using a pressure transducer in the ASR well and a capacitance probe in the observation well, as well as occasional manual measurements. On 30 July 2003 a water quality sonde was installed in the ASR well at 16 m depth and programmed to continuously monitor the electrical conductivity (EC) and temperature at a half hourly rate. Daily rainfall was read manually using a rain gauge. Domestic water consumption within the house from reticulated potable water supplies was determined from monthly water meter readings.

Sampling of ambient water quality for each well was done in December 2002, prior to the start of any injection. Periodic samples of the roof run-off were collected before, during and after the recharge season (winter months), with samples submitted to the CSIRO Analytical Chemistry Unit (ACU) for analyses of majors ions, nutrients and metals. Monthly gutter clearing was carried out (from April 2004) and the collections of leaf and gutter detritus were dried and weighed, with one collection being analysed for nutrient organic content. The 100 µm filter also required regular cleaning out due to the loads introduced by the decomposing leaf litter and fine sediment in runoff. Once recharge commenced, an average 0.6 m^3 was recovered per month to purge the ASR well of any accumulated biofilm or sediments and to assess the quality of the stored water. Samples collected were analysed for electrical conductivity (EC) and turbidity. Recovered sediment material from one of these events, was also submitted for X-ray diffraction (XRD), major and trace X-ray fluorescence (XRF) to the CSIRO XRF laboratory and particle size analysis was carried out by the ACU.

Although 142 m^3 of rainwater was injected during this first year of operation (29th June 2003 to 21st July 2004) the water recovered during purging events showed the salinity of water was still close to background level and hence not suitable for garden irrigation. Following assessment of the recovered water quality data collected to date, a second set of pumping tests was carried out on 21st/22nd July 2004 to assess the transmissivity changes and it was decided to move the injection pipe to the lower yielding 125 mm diameter well, to determine if the lower aquifer transmissivity would retain the fresh injectant closer to the well and thereby produce recovered water of lower salinity.

In September 2004, to further automate the monitoring of the ASR site, a logger unit was connected to pressure transducers, to monitor water levels in the ASR well and the house rainwater tank, a pluviometer was connected to monitor rainfall. The unit also had the capability to monitor the volumes and temperature of inflow and outflow and the electrical conductivity (EC) of recovered water. The sensors for these parameters were installed in August 2005. The logger unit recorded data in three modes; (i) event data collection was triggered at 20 L volume increments during injection and 10 L volume increments during recovery and readings of depth, EC, temperature and volume were recorded, (ii) two hourly readings of all sensors were collected on an ongoing basis and (iii) daily volumes were calculated from the monitored flowmeters. The rainfall catchment was increased partially between August–December 2005 when the runoff from a neighbouring roof (78 m^2) was connected. Figure 1 summarises the final site layout as of September 2005.

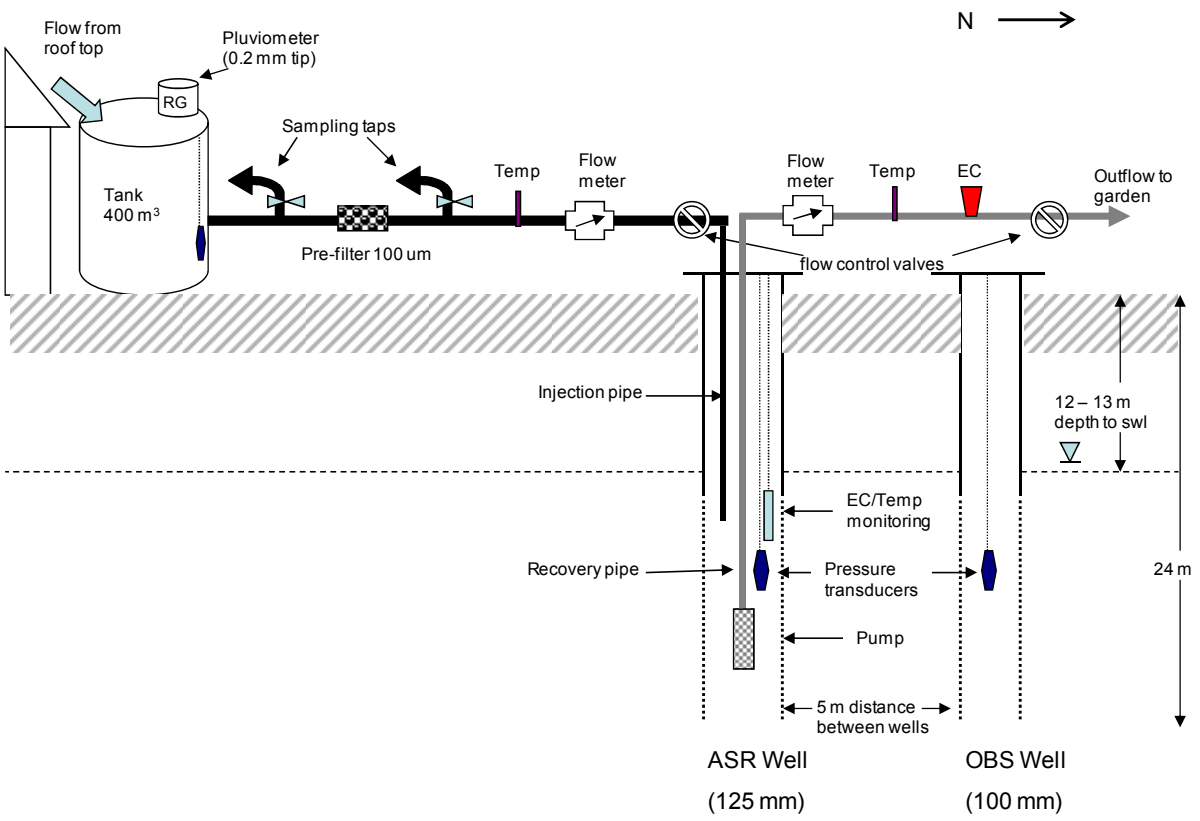

Figure 1: ASR site layout as of September 2005 and monitoring equipment

Downhole electromagnetic flowmeter metering, downhole resistivity, gamma logging and EC profiling were carried out on 31st May 2005 to enable more detailed analysis of the aquifer hydraulic property variations with respect to depth to establish procedures in which the volume of recoverable water could be further improved. That is to increase the recovery efficiency (RE) as described by Pyne (2005), defined as the proportion of injected water that can be pumped at a quality that is suitable for its intended use, in this case irrigation. The flowmeter survey was performed under pumped conditions, where each well was pumped at a constant flow rate of 4.3 m^3/d (0.05 L/s) in the 100 mm well and 1.4 m^3/d (0.016 L/s) in the 125 mm well, and the flow distribution determined after the drawdown had stabilized. Before any pumping had occurred the ambient rate of flow within the well was determined to assess the net differential flow. Details on the test procedure are given by Molz et al., (1994). Changes in flow rate between adjacent depths revealed the rate of flow into or out of the well over that particular interval.

Flow metering defined a zone of preferential flow between the 15 and 16 m depth in the 100 mm well (Figure 2) indicating the reason for the low recovery efficiency observed. In the 125 mm well (the ASR well at the time) flow metering revealed a low hydraulic conductivity section below ~ 20 m, while the EC profiling revealed a layer of more saline groundwater approximately 4 weeks after the last recovery event (Figure 2). This is supported by the initial lithology as described in the drillers well log report. As a consequence the ASR well was partially backfilled to 19.7 m on 2nd September 2005, in an attempt to increase the recovery efficiency, with expected minimal loss in well yield.

Electrical conductivity and temperature profiling using a downhole water quality sonde was carried out on six occasions in the 125 mm well and on five occasions in the 100 mm well during the course of the three year study, with a further series of profiles run at the end of the study in the 125 mm well (then ASR well in September 2006) before, during and after a 24 hour pumping event to determine how quickly the recovery water quality returned to ambient conditions.

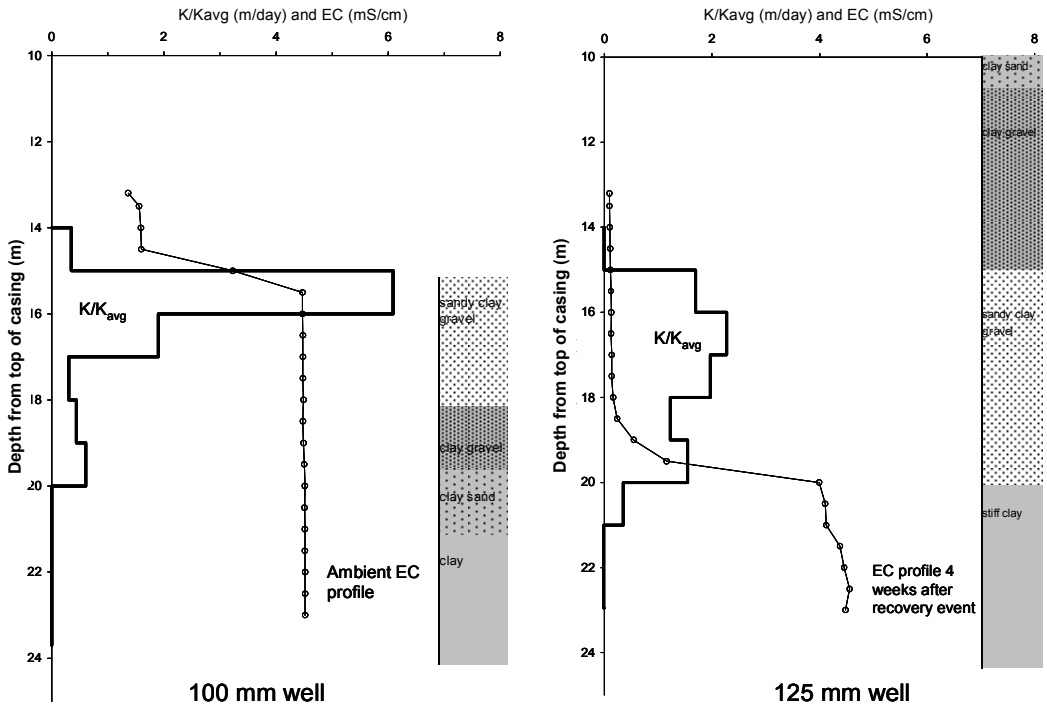

Figure 2: Well profiles of K/K_{avg} and Electrical Conductivity (EC) for the 100 mm (obs) and 125 mm (ASR) wells carried out on 31st May 2005 (K=hydraulic conductivity at a particular depth, K_{avg} is over the entire depth), plus well log from drillers report

3 Results and Discussion

3.1 Water balance

Rainfall data recorded from the on-site rainwater gauge showed total yearly rainfalls of 563 mm (2003/04), 571 mm (2004/05) and 684 mm (2005/06) for each year of the study.

Over the 39 month period of the study a total volume of 487 m^3 was injected and 38 m^3 was recovered (7%), leaving a net increase in storage of 449 m^3. Recovery consisted mostly of intermittently purging the well to remove any accumulated particulate matter on a monthly basis. This water was discharged onto the garden or into a nearby sump and soaked into the ground as additional recharge to shallower alluvium, along with a small amount of runoff from paved areas adjacent the house. Occasionally the 100 µm filter became blocked or air within the injection pipe inhibited injection immediately following the cleaning of the filter. If this happened prior to or during a large storm event, the tank overflowed to the sump, which over the course of the trial accounted for an approximate 2% potential water loss.

3.2 Aquifer characterisation

Aquifer material recovered during a pump out event in August 2005 from the 125 mm well (then ASR well) was made up of 48% sand with the remainder silt and clay (< 53 µm fraction). Figure 3 shows the cumulative and frequency particle size distributions. Quantitative XRD data showed the sample consisted mostly of quartz (40%) and smectite/montmorillonite (33%) with smaller amounts of albite (10%), mica (7%), orthoclase (6%), kaolin (3%), goethite (1%) and calcite (<1%). Of these, montmorillonite would be expected to be the most reactive phase present. It has the greatest capacity for cation exchange (CEC 80–120 meq/100 g; Appelo and Postma, 1999) and may be affected by clay swelling and dispersion thus leading to concerns about aquifer permeability decline. With low calcite (1%) there is little chance of dissolution of the aquifer to offset the potential for clay swelling.

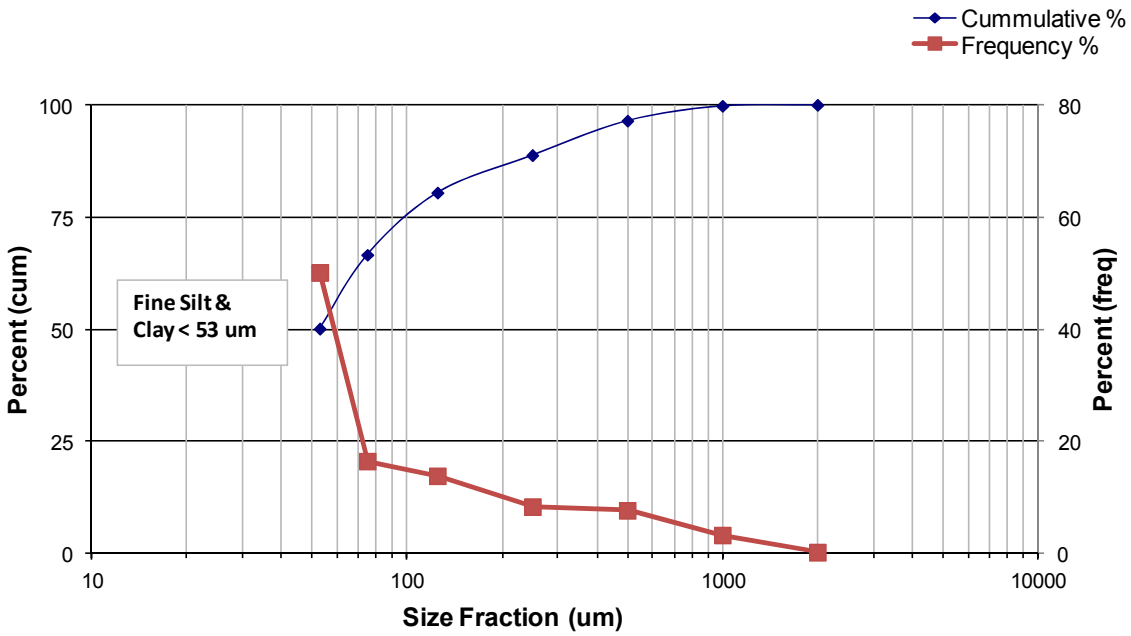

Figure 3: Particle size distribution for aquifer material recovered during a typical pump out event

3.3 Ambient and injectant water quality

The ambient groundwater is brackish (~4,500 µS/cm) with a sodium absorption ratio (SAR) of 6.8, low organic carbon (2.3 mg/L) and phosphorus (<0.025 mg/L) but has significant nitrate-N (5.8 mg/L). The rainwater/injectant is fresh (25 µS/cm) with an SAR of 0.45, low average nutrient levels (Total N = 0.69 mg/L, Total P = 0.03 mg/L) but contained detectable zinc levels (0.14 mg/L), as a result of the galvanized steel roof. There was little difference in pH between the two water types, with the ambient water at pH 6.6 and injectant at an average of pH 6.5. In Table 1 the ambient groundwater and injectant water quality range is presented, with mean values being calculated where two or more samples were collected.

Aquifer clogging due to interaction between low salinity source water and clay minerals, namely montmorillonite, within the storage zone may have contributed to a decrease in injection rate. The injectant was low in SAR (0.45) compared to the groundwater (6.8) which could partially mitigate the effect of the lower salinity on potential for smectic clay swelling. This would be expected to be significant given that the salinity was more than two orders of magnitude lower than in the native groundwater and the abundance of montmorillonite.

In May 2003 a sample of water considered to be a 'worst case scenario' for potential nutrient loading in the injectant was collected from a stagnant pool in the roof gutter as the down-pipe leaf guard had become choked with decaying leaves. It contained coloured water with a musty odour and had a high organic carbon and nutrient load (Total Organic Carbon = 694 mg/L, Total N = 275 mg/L and Total P = 40 mg/L). Thus in 2004/05 operational maintenance began to include monthly gutter clearing, with drying and weighing of leaves and gutter detritus, with a view to developing an approximate mass balance for organic carbon. This material included varying mixtures of leaf matter and silt with occasional debris from insects, feathers, bird droppings etc. As expected, the peak period corresponds with the autumn months, when deciduous trees drop their leaves. In October 2005 samples of leaf and sediment were collected from the gutters, tank strainer and 100 µm filter unit, dried, weighed and analysed for nutrients. Their respective percentage organic carbon contents were 39%, 36% and 32%, indicating there was potential for degradation and dissolution within the injectant and consequently potential for biological well clogging if gutters were not cleaned regularly.

3.4 Hydraulic response to injection and recovery events

Standing water level (piezometric head) was monitored from July 2002 using a combination of data loggers and manual measurements. The annual groundwater level fluctuation was found to average 1 m, with the peak in December and the trough in June. This response lags by 3–4 months from seasonal rainfall fluctuations. Both wells had

a similar piezometric response when there was no recharge or recovery from the ASR well. During the first year of ASR operation in the 100 mm well, piezometric levels only rose by about 1 metre during injection, with injection rates typically at 26 m^3/d (0.3 L/s). Based on experience with severe and irreversible clogging in a nearby ASR trial in a fine-grained sand aquifer (Pavelic et al., 2008), when the first attempts at redeveloping the well occurred too late, it was decided to redevelop the rainwater ASR well on a monthly basis. Monthly purging (recovery) events in the 100 mm well were run at up to 86 m^3/d (1 L/s) for 10 minutes, with the well never running dry. Piezometric response in the second and third years of the trial (when the 125 mm well was the ASR well), was monitored with a dedicated logger unit and monitoring reliability increased. Event triggered monitoring introduced in September 2005, enabled detailed monitoring of piezometric response in the lower yielding well (125 mm), where head rises during injection of up to 8 m were recorded.

When pumping at 86 m^3/d (1 L/s), drawdown rapidly reached the level of the pump at 18 m, which was the maximum drawdown head available for purging the well which is lower than the impressed head during injection. This shows that the efficiency of the particulate recovery is low in comparison with the ability to drive particulates into the near-well profile. Recovery events in the 2nd and 3rd years of operation were subsequently run at a lower average rate of 26 m^3/d (0.3 L/s) for 35 minutes, including intermittent short periods of pumping at 1 L/s. Injection rates in the 125 mm well also began at 0.3 L/s, however rates gradually reduced to 22 m^3/d (0.26 L/s) and piezometric head rises increased though to the end of the study, suggesting reduced well efficiency due to very gradual clogging. Figure 4 shows head levels monitored over a one month period from 15th December 2005 to 12th January 2006, where it is observed there is some connection between the two wells with a 0.1 m (average) response in the 100 mm well whenever an injection of recovery event is carried out in the 125 mm well 5 m away. Considerably larger responses were expected in the observation well, suggesting that a small annulus of reduced hydraulic conductivity may be surrounding the ASR well.

As stated earlier, well yields calculated from pump tests at the start of the study were 95 m^3/d (1.1 L/s) in the 100 mm well and 34 m^3/d (0.4 L/s) in the 125 mm well. Two further pump tests were carried out in the 125 mm well in July 2004 prior to it becoming the ASR well and September 2006 at the end of the study. Figure 5 shows the steady state specific capacity for each of the three tests carried out in the 125 mm well (ASR well for two out of three years of the study). Where it is observed the specific capacity has increased significantly through the duration of the study indicating clogging has occurred. The water specific capacity of the well had stabilized within less than 15 minutes in each case, indicating that steady-state conditions were quickly established.

Using steady-state (Thiem) analysis of the pumping phase of the pump test results, Table 2 summarises the calculated changes in transmissivity and specific capacity of the 125 mm well for each of the three tests. Transmissivity reduced from 5.2 m^2/day to 2.5 m^2/day and specific capacity of the well reduced significantly from 8.3 to 4 m^3/d/m (by >half), which was greater than the proportion expected (~ 30%) based on the partial backfilling of the well from 24 m to 19.7 m depth.

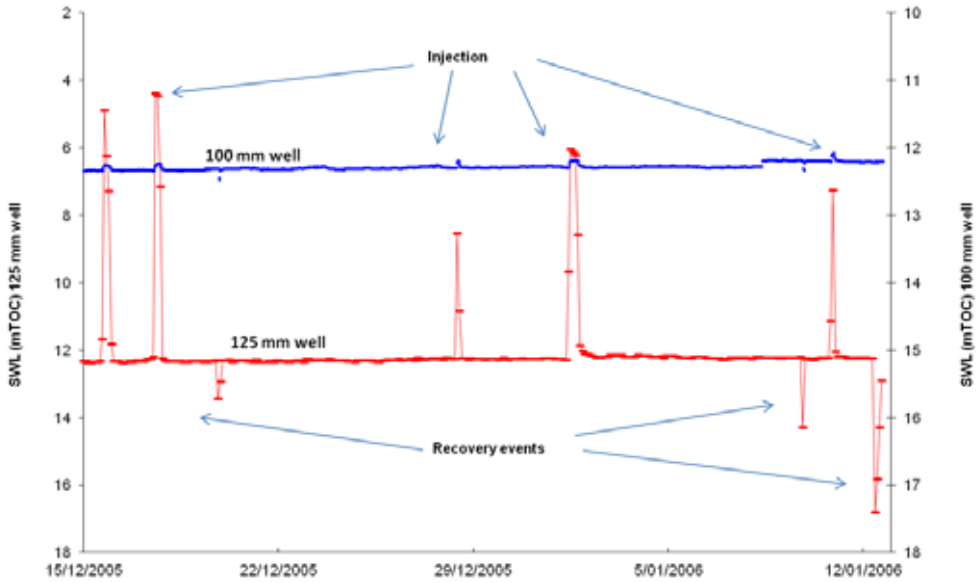

Figure 4: Changes in piezometric heads levels in the 100 mm and 125 mm wells over a 1 month period

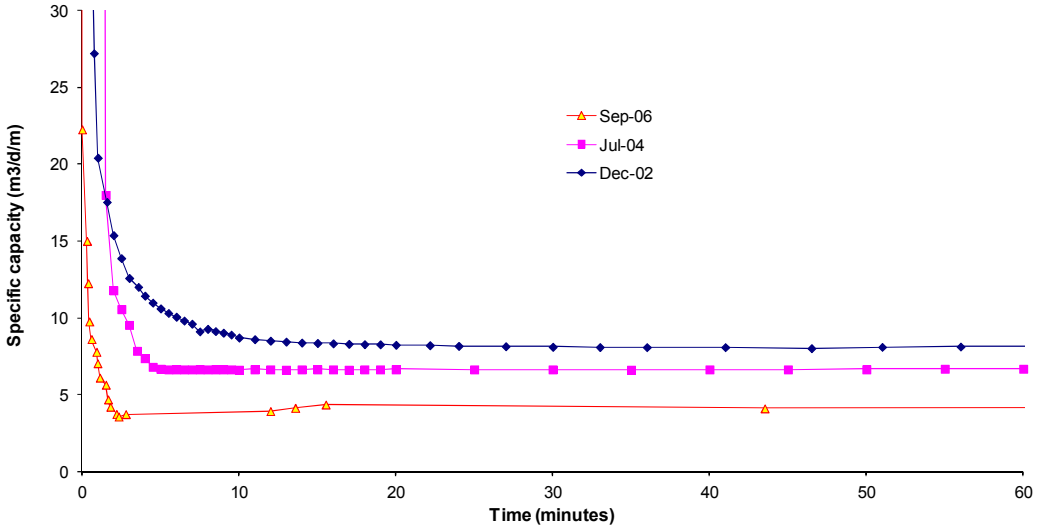

Figure 5: Specific capacity changes in the 125 mm well over three pump test carried out at the beginning (Dec '02), middle (July '04) and end (Sept '06) of the study

Table 2: Summary data from three pump tests carried out in December 2002, July 2004 and September 2006

Test	Q_{avg} (m^3/d)	dH_{avg} (m)	b (m)	k (m/d)	T (m^2/d)	Sp.Cap ($m^3/d/m$)
Dec '02	23.1	2.78	11.9	0.44	5.19	8.30
Jul '04	34.6	5.20	11.9	0.35	4.16	6.67
Sep '06	13.8	3.45	7.70	0.33	2.51	4.01

During each backwash/recovery event samples were collected for EC and turbidity measurement. The turbidity of rainwater injectant ranged from 0.75 to 2.1 NTU and the total organic carbon ranged from 0.8 to 2.6 mg/L. Initial water recovered from the regular recovery/purging events in the 125 mm well were highly turbid (average 620 NTU) but after repeated 'surging' of the pump, particulate matter is removed and the turbidity drops significantly to an average level of 20 NTU. However, this appears not to be enough to eliminate all the accumulated clogging agents from around the well. If this build-up of clogging agents was to continue, thought to be derived from residual particulate matter, dispersion of clay minerals and biofilm growth, then chronic clogging would eventuate, requiring more extensive treatment of the well.

4 Conclusions

In spite of sub-optimal well construction using rotary drilling with mud and the presence of dispersive clays in the aquifer interval, a small scale rainwater ASR well was operated with satisfactory injection rates over a period of 39 months (>3 years). Operation at the site ceased largely due to the low recovery efficiency of the ASR well and lack of ongoing resources (financial and time) as opposed to the decline in specific capacity of the well.

There was considerable potential for clay dispersion and swelling considering the injected rainwater water had a very low EC at 25 µS/cm compared to the ambient groundwater with 4,460 µS/cm EC. However this could be partially mitigated by the low injectant SAR of 0.45 compared to the groundwater SAR of 6.8.

Analysis of flow rates and change in piezometric head has shown that some gradual and persistent clogging of the ASR well has occurred, even with the monthly pumping out of approximately 0.6 m^3 at flow rates up to three to four times higher than the recharge rate. Initially quite turbid water (> 600 NTU) is recovered at the start of each event, with particulate concentrations rapidly decreasing to < 20 NTU with pumping. This suggests that purging does have real value in helping to alleviate clogging. However a decline in specific capacity of 50% from the start to the end of the study was observed suggesting that more vigorous well redevelopment strategies would be needed in the longer term, if the ASR operations were to continue.

Operational maintenance continued to be very intensive with the 100 micron filter requiring flushing every 2 to 10 KL depending on the turbidity and nutrients in the runoff, especially during the autumn months when organic loads were at the peak with deciduous leaves, resulting in higher carbon loads, which could also increase the potential for

clogging of the injection well if not managed by regular gutter cleaning.

Determining which mechanism; (i) well construction, (ii) aquifer lithology, (iii) low injectant salinity, (iv) particulates or (v) organic carbon load, was the primary reason for gradual reduction in specific capacity of the well is difficult. However given that the salinity was more than two orders of magnitude lower than in the native groundwater and with the abundance of montmorillonite (33%) in the profile and with minimal calcite (<1%) available for dissolution, there was a significant risk that clogging would occur in the ASR well. Turbidity and carbon loads in the injectant were kept at a minimum with the regular maintenance regime.

No other water treatments were considered during this field trial. With minimal difference in pH between the ambient and rainwater and low calcite in the aquifer material, pH buffering of the rainwater was not considered, but other options which could have been investigated had the project continued would be; (a) disinfection of the well to kill off any polysaccharide producing bacteria and (b) further decreasing the SAR value of the water by adding a divalent cation solution, though in this case the injectant was already low in SAR.

5 Acknowledgements

The monitoring reported in this paper was made possible through the support of the Patawalonga Catchment Water Management Board now incorporated within the Adelaide and Mt Lofty Ranges Natural Resources Management Board. Flow meters were provided by SA Water Corporation. Downhole flowmetering was performed by Don Freebairn and Vic Freschi from the Geophysics Section of the Department of Water, Land and Biodiversity Conservation, SA. James Ward from Flinders University of South Australia assisted with a level survey of local wells. Water quality and sediment analysis was provided by CSIRO Land and Water Analytical Services and Mineralogical Services.

6 References

Appelo, C.A.J., and Postma, D., (1999) Groundwater, geochemistry and pollution. A. A. Balkema, Netherlands.

Barry, K., and Dillon, P., (2005) Domestic-scale ASR with rainwater at Kingswood, South Australia. Proceedings of the 5th International Symposium on Management of Aquifer Recharge. ISMAR5, Berlin, Germany. 11–16 June 2005.

Barry, K., Dillon, P., and Pavelic, P., Mixing and clogging constraints on domestic-scale ASR at Kingswood, South Australia (2007). Procs ISMAR6, Phoenix 28 Oct–2 Nov 2007.

Baveye, P., Vandevivere, P., Hoyle, B.L., DeLeo, P.C., and Sanchez de Lozada, D., (1998) Environmental impact and mechanisms of the biological clogging of saturated soils and aquifer materials. Critical Reviews in Environmental Science and Technology 28(2):123–191.

Dillon, P., and Barry, K., (2005) Domestic Scale Rainwater ASR Demonstration Project. Progress Status Report July 2003 – June 2005. CSIRO Land and Water Report to Adelaide and Mount Lofty Ranges Natural Resources Management Board.

Molz, F.J., Boman, G.K., Young, S.C., and Waldrop, W.R., (1994) Borehole flowmeters: field application and data analysis. Journal of Hydrology 163:347–371.

Olsthoorn, T.N., (1982) The clogging of recharge wells, main subjects, KIWA-Communications 72, 150p.

Patawalonga Catchment Water Management Board, (2002) Catchment Water Management Plan 2002–2007. http://www.cwmb.sa.gov.au/patawalonga/plans/Pat01_Cover.pdf

Pavelic P., Gerges N.Z., Dillon P.J., and Armstrong D., (1992) The potential for storage and re-use of Adelaide stormwater runoff using the upper Quaternary groundwater system. Centre for Groundwater Studies Report No. 40.

Pavelic, P., Dillon P., and Barry, K., (2005) Results from the Drilling of Two Wells in the Upper Quaternary Aquifer at the Urrbrae Wetland Site. CSIRO Client Report, Dec 2005, 16p.

Pavelic, P., Dillon, P., Barry, K., Armstrong, D., Hodson, A., Callaghan, J., and Gerges, N., (2008) Lessons Drawn from Attempts to Unclog an ASR Well in an Unconsolidated Sand Aquifer. February 2008. CSIRO Water for a Healthy Country Report, Feb 2008. http://www.clw.csiro.au/publications/waterforahealthycountry/2008/wfhc_ASRwell.pdf

Pérez-Paricio, A., and Carrera, J., (1999) Clogging Handbook. EU Project on Artificial Recharge of Groundwater, Research program on Environment and Climate, Contract ENV-CT95-0071.

Pyne, R.D.G., (2005) Aquifer Storage Recovery: A Guide to Groundwater Recharge Through Wells. 2nd edition. ASR Systems.

Rinck-Pfeiffer, S.M., (2000) Physical and biochemical clogging processes arising from Aquifer Storage and Recovery (ASR) with treated wastewater. PhD Thesis, School of Chemistry, Physics and Earth Sciences, Flinders University of SA, September 2000.

Segalen, A-S., Pavelic, P., and Dillon, P., (2005) Review of drilling, completion and remediation methods for ASR wells in unconsolidated aquifers. CSIRO Land and Water Tech Report 04/05, March 2005. http://www.clw.csiro.au/publications/technical2005/tr4-05.pdf

South Australian Government, (2004) Water Proofing Adelaide Draft Strategy: A thirst for change. http://www.waterproofingadelaide.sa.gov.au/pdf/Strategy_full.pdf

South Australian Government, (2009) Water for good: a plan to ensure our water future to 2050 http://www.waterforgood.sa.gov.au/water-planning/the-plan/

Characterisation of Clogging during Urban Stormwater Aquifer Storage and Recovery Operations in a low Permeability Fractured Rock Aquifer

D. Page and P. Dillon
Commonwealth Scientific and Industrial Research Organisation (CSIRO)

1 Introduction

A variety of clogging processes may arise during ASR when fresh, high turbidity and nutrient rich stormwater is injected into a brackish anoxic aquifer. Clogging of injection wells is a commonly reported problem, particularly when waters of low quality are used (Olsthoorn, 1982; Pérez-Paricio and Carrera, 1999; Pavelic et al., 2006). However, there have been few reports of full scale field studies on well clogging (Schubert, 2002; Pavelic et al., 2006; 2008) that have identified processes of clogging or the success of any remedial or preventative measures (Olsthoorn, 1982; Pavelic et al., 2008). The lack of any defined water quality targets for injection in fractured rock aquifers (and subsequent evaluation of pre-treatment options) continues to remain a limitation for the uptake of ASR. Hence the aims of this study were to establish localised water quality targets for injection of urban stormwater into a low transmissivity fractured rock aquifer and to assess the clogging that occurs during treated stormwater ASR as compared to a higher quality potable water.

2 Materials and Methods

2.1 Site description

A full-scale ASR trial was conducted at the Rossdale Golf Course in Aspendale, a southeast suburb of Melbourne, approximately 1.2 km from Port Philip Bay. Rossdale Golf Club was selected as it was located in an area identified as having moderate potential for ASR; had obtained a diversion licence for harvesting stormwater from the Centre Swamp Drain, and had an existing stormwater storage dam. Full details of the site are given in Page et al. (2011)

2.2 Aquifer characterisation

The ASR well targets the Siluro-Devonian formation of the Melbourne Trough (Garrat 1983) which is encountered at a depth of ~75 m below sea level. The formation consists of interbedded and fractured shale, siltstone and sandstone layers. The Siluro-Devonian formation is overlaid by clastic sediments and basalts of Cainozoic (Paleogene, Neogene and Quaternary) age. The aquifer is confined with piezometric surface at an elevation ~4 m above sea level (1 m below ground surface). Regional hydraulic gradients are low due and there is no extraction from the aquifer within several kilometres. All wells were completed as "open hole" and developed until groundwater turbidity dissipated. Further pumping tests prior to ASR operation implied transmissivity values in the range of 1.2–1.85 m^2/d, which corresponds to an average hydraulic conductivity of 0.035–0.054 m/d. Further hydrogeological information is presented in Dillon et al. (2010).

Slumping initially occurred in weathered shale and siltstone of both wells drilled in the fractured bedrock. High particulate concentrations in the extracted waters during pumping tests indicate that the Silurian aquifer is susceptible to erosion, and reveal a risk of mechanical clogging by particle mobilisation and re-deposition.

During drilling of the observation well intact cores of aquifer material were collected between 102.8 and 110.5 m bgs using a 63.5 mm diameter core barrel. The recovered core sample was analysed by quantitative XRD analysis on a ground, 1 g sub-sample using a Philips PW1710 microprocessor-controlled diffractometer and the software package SIROQUANT.

2.3 Groundwater and stormwater characterisation

Water-quality testing of the potable water, stormwater, recovered water and ambient groundwater injected into and withdrawn from the ASR well was performed for a suite of physico-chemical parameters according to APHA (2005). A number of water quality parameters were assessed for each treatment option including: pH, turbidity, total suspended solids (TSS), total nitrogen (TN), total phosphorous (TP), dissolved organic carbon (DOC) and biodegradable dissolved organic carbon (BDOC) using the standard methods described in APHA (2005).

In addition to the water quality analyses, tests were performed to assess the potential for the various types of ASR source water to cause clogging of the pore spaces within the Silurian aquifer due to dispersion of clay minerals using a modified version of the 'Emerson' method (Standards Association of Australia 1980) and more fully described by Page et al. (2010).

The membrane filtration index (MFI) first developed by Schippers and Verdouw (1980) to measure fouling potentials of membranes and documented in the MAR context by Dillon et al. (2001) was also measured to determine the physical clogging potential. The method involves passing water through a 0.45 µm membrane and measuring change in flux.

2.4 Quantification of ASR well clogging

The most significant risk of ASR operational failure over the short-term was considered to be excessive deterioration in the hydraulic performance of the ASR well (BH3) due to near-well clogging or well slumping (Olsthoorn, 1982). Aquifer clogging can be assessed using various methods for evaluation in both steady (Pavelic et al. 2006) and unsteady flow conditions (Hunt, 1999; Mucha et al., 2006). Two methods were used to characterise the change in hydraulic performance of the ASR well. These were:

1. change in well efficiency during recovery after calibrating a Dupuit analytical model on the second potable water cycle, and
2. change in specific capacity during recovery in each cycle.

The coefficient of linear formation loss (A0) derived from Dupuit formula states as follows (Kresic, 2006):

$$A_0 = \frac{1}{2\pi T}\ln\frac{R_D}{r_w} \quad (1)$$

where T is the transmissivity of the aquifer (L2/T), RD is the radius of well influence (L), and rw is the radius of a well (L). The radius of well influence in transient conditions is calculated from the formula:

$$R_D = 1.5\times\sqrt{\frac{T*t}{S}} \quad (2)$$

where t is time of pumping (T) and S is the storage coefficient of the aquifer (-). Consequently the theoretical drawdown (s0) recorded at the end of recovery period for a given pumping rate Q (L2/T) is calculated:

$$s_0 = \frac{Q}{2\pi T}\ln\frac{1.5\times\sqrt{\frac{T*t}{S}}}{r_w} \quad (3)$$

If a clogging layer develops around the ASR well, the difference between s_0 and measured drawdown will increase, as neither the transmissivity or storativity of the aquifer do not change over time.

Finally in assessing ASR well clogging, the efficiency of the ASR system is often characterised using the concept of specific capacity (Pyne, 2005; Pavelic et al., 2006). When steady-state conditions prevail in an aquifer, specific capacity of the well may be given as:

$$SC = \frac{Q}{s} \quad (4)$$

where SC is the specific capacity (m^2/d), Q is the injection or pumping rate (m^3/d) and s is the drawdown in the ASR well (m). SC is used to measure well performance i.e. clogging development since this parameter is particularly sensitive to the well-loss component of piezometric head build-up or drawdown.

3 Results and Discussion

3.1 Aquifer characterisation

XRD analysis of aquifer core indicated that the mineralogical composition of the sandstone is dominated by quartz, SiO2 (48–73%), with lesser amounts of kaolinite, Al2Si2O5(OH)4 (13–23%) and muscovite, KAl2(AlSi3O10)(F,OH)2 (7–18%), and trace amounts of siderite, FeCO3 (0–11%), chlorite, (Fe,Mg,Al)6(Si,Al)4O10(OH)8 (0– 6%) and pyrite, FeS2 (0.3–1.3%). Sandstone samples are associated with higher levels of quartz (>70%) and lower levels of kaolinite (<20%), muscovite (<10%) and siderite (<2%). The organic carbon content of the aquifer matrix is < 0.3%.

The average cation exchange capacity for the storage zone

is 3.2 milliequivalents (meq)/100 g and is comprised of 2.0 meq/100 g as Ca-X2, 0.7 meq/100 g as Mg-X2, 0.3 meq/100 g Na-X and 0.2 meq/100 g as K-X. Some displacement of Ca by Na would be expected.

3.2 ASR well operation

Two phases of ASR were investigated each of which consisted of several cycles of injection, storage and recovery. The first phase consisted of four cycles of potable water (PW) injection of increasing storage duration. The second phase consisted of two cycles of treated stormwater (SW) injection also of increasing storage duration (Table 1).

During the potable water phase, a total of 1,377 m^3 was injected into the aquifer and 1,403 m^3 recovered, with an injection flow rate of 0.46 L/s for the 4th cycle. Each successive cycle of the potable water ASR injection, storage and recovery was scaled up from an hour each, to one day, one week and one month each. This was intended to determine the magnitude and timescale of any clogging observed. During the subsequent treated stormwater phase 3,300 m^3 was injected and 2,410 m^3 recovered over the two cycles with average injection rates of 0.37 L/s during each cycle (~20% reduction from injection rates during the potable water phase).

3.3 Clogging behaviour during ASR injection cycles

Clogging of the ASR system was characterised by changes in well efficiency over the successive potable and treated stormwater ASR phases. The changes in well efficiency obtained by comparison of measured and theoretical drawdown are shown in Table 2. Transmissivity and storage coefficient of the aquifer were assumed to be 1.8 m^2/d and 2×10^{-5} (-), respectively which is within a range of the pumping tests results prior to injection operation. During the 2nd PW cycle the theoretical drawdown converged with that measured indicating full efficiency of the ASR well (100%). However, after the 3rd PW cycle the well efficiency declined to 59%. The implication is that if the pumping rate is constant in all recovery cycles, the larger values of well loss and the lower values of well efficiency indicate development of a clogging layer (Table 2).

Table 1: Volume of recharged water in storage during the four potable water cycles and the two stormwater cycles between December 2006 and March 2010

ASR phase	ASR cycle	Cycle duration (days)	Injection flow (L/s)	Volume injected (m^3)	Volume recovered (m^3)
PW phase	1st PW cycle	0.125	0.51	1.8	1.9
	2nd PW cycle	3	0.49	35	51
	3rd PW cycle	21	0.48	190	290
	4th PW cycle	90	0.46	1,150	1,060
SW phase	1st SW cycle	67	0.35	830	830
	2nd SW cycle	300	0.39	2,470	1,580

PW potable water, SW stormwater

Table 2: Drawdown and efficiency of the ASR well during the four potable water cycles and the two stormwater cycles

ASR phase	ASR cycle	Recovery duration (days)	Recovery rate (L/s)	Measured drawdown s (m)	Theoretical drawdown s* (m)	Relative Well loss (m)	Well efficiency (%)
PW phase	1st	0.042	0.52	15.56	28.28	n/a	–
	2nd	1	0.59	39.04	39.04	0.00	100
	3rd	7	0.49	44.29	35.97	8.32	81
	4th	24.54	0.50	54.43	39.04	15.39	72
SW phase	1st	24.7	0.39	42.14	30.46	11.68	72
	2nd	36.3	0.50	68.16	40.00	28.16	59

n/a not applicable

Additional characterisation of the development of clogging in the ASR well is shown in Figure 1 which presents temporal specific capacity (SC) changes for all ASR test cycles. The decline in SC due to clogging is evidenced by a downward shift in the curves over time during successive ASR test cycles.

SC declines during recovery to ~1 m^2/day for all recovery tests (Figure 1). There is evidence of clogging of the well-face as a result of reduced SCs in the first day of recovery for the 4th PW cycle (Table 1). The SC of the ASR well after 25 days declined from 0.79 m^2/d to 0.63 m^2/d between the 4th PW cycle and the 2nd SW cycle, reflecting the observed 20% decline in injection rate (Table 1).

3.4 Water quality evaluation of groundwater, potable water and stormwater

The untreated stormwater, ambient groundwater and potable water qualities are shown in Table 3.

The Membrane Filtration Index (MFI) values ranged from 38 to 83 s/L^2 for the potable water compared with 99 to 371 s/L^2 for the untreated stormwater (Table 3). Dillon et al. (2001) reported similar MFI ranges of 90–389 s/L^2 for untreated urban stormwater associated with physical clogging in ASR operations in an alluvial aquifer. They indicated that treatment would be required to reduce the potential for physical clogging of ASR injection wells.

While the required water quality parameters for sustainable injection of stormwater are still difficult to define, operationally it was initially assumed in this study that the success of the potable water ASR phase indicated that it was of a suitable quality to minimise risks of clogging. Hence the quality of the injected potable water (Table 3) was used as the treatment water quality targets for the stormwater prior to injection into the aquifer. Notably, these targets included maintaining turbidity to ≤ 0.6 NTU, dissolved organic carbon DOC to ≤ 1.7 mg/L and biodegradable dissolved organic carbon (BDOC) to ≤ 0.2 mg/L. This takes into account the very low yielding nature of the target aquifer (0.5 L/s) in this study and knowledge of the quality of water that has been injected successfully (Pavelic et al., 2006; 2007) and unsuccessfully (Pavelic et al., 2008) into aquifers at other ASR sites. Ultra filtration with Granular Activated Carbon was eventually selected to treat the raw stormwater and meet the above water quality targets.

3.5 Water quality of injectant and ASR well clogging

This full scale ASR study aimed to specify and test specific water quality targets for injection into a low transmissivity, fractured-rock aquifer. Previous work by Pavelic et al. (2007) had identified levels of turbidity < 3 NTU, TN < 10 mg/L and pH < 7.2 as suitable targets for source water to prevent clogging in a limestone aquifer with an initial mean hydraulic conductivity of 3 m/d; two orders of magnitude greater than for this fractured rock aquifer. Pavelic et al. (2007) used turbidity as an indicator of physical clogging, pH as an indicator of calcite dissolution (unclogging) and TN as an indicator of biological clogging. However Pavelic et al. (2007) advised that these targets were not applicable in aquifers with lower permeability or calcite content.

In the present study all three mechanisms could have contributed to the observed clogging to varying degrees. Physical clogging is usually caused by suspended particulates in the injectant. Although the stormwater had a low mean TSS of 6 mg/L, it also had occasionally high levels of algae visible in the detention pond. The maximum concentrations were considerably higher (TSS 24 mg/L) indicating the variability of the raw stormwater quality (also apparent in the variability of MFI). Given this variation, the resulting risk of physical clogging of the injection well could at times also be high.

Risks of clogging were also slightly increased when the fresh stormwater (215 mg/L TDS) was injected into the brackish aquifer (1,600 mg/L TDS) due to potential for dispersion of clays present in the aquifer matrix. Other authors (Goldenberg et al., 1984; Goldenberg, 1985; Konikow et al., 2001; Appelo and Postma, 2005) have reported a decrease in hydraulic conductivity during displacement of saline water by freshwater plumes and attributed it to deflocculation of the colloidal solution and dispersion of fine particles due to clay swelling. Most studies on chemically-induced clogging involve the use of admixtures of clay minerals like kaolinite (a non-swelling clay) and montmorillonite (a swelling clay). Goldenberg (1985) and Konikow et al. (2001) reported that even small proportions of montmorillonite in sand may cause physical clogging. Goldenberg (1985) used dune sand mixed with montmorillonite clay and found that amounts of clay as small as 0.005% caused an irreversible reduction of aquifer transmissivity when seawater was replaced by freshwater. Konikow et al. (2001) found in laboratory studies that the decline in permeability due to dispersion of kaolinite was reversible. On the other hand in the montmorillonite clays the permeability reduction was irreversible due to their complex layered structure.

Although the salinity difference between the injectant and the brackish groundwater is much smaller in this study

compared to both Goldbenberg (1985) and Konikow's et al. (2001) studies the mechanism of transmissivity reduction due to physical clogging are likely to be similar. At Rossdale, the content of kaolinite was in the range from 13–23%, which could contribute to reversible clogging. The large contribution of muscovite (from 7 to 18%) and chlorite (0–6%) indicates that irreversible physical clogging may potentially occur.

Turbidity values for the Emerson tests for the control waters ranged from 0.5–0.7 NTU compared with 0.8– 8.4 NTU for the different sediment-water solutions. This indicated that the presence of aquifer material consistently produced higher turbidity waters. The increase in turbidity for the potable and storm waters was 0.1–3.3 NTU. The net dispersive potential of each water type can be expressed in terms of the increase in turbidity relative to the control. These measured turbidity increases are estimated to have caused between <0.01% and 0.11% of the solid phase to have dispersed into solution which may contribute to the physical clogging and potential for slumping of aquifer material at the well-aquifer interface.

Chemical clogging may also occur through precipitation of iron oxyhydroxides. Aquifer mineralogy indicates the presence of reactive iron bearing-minerals, pyrite (FeS2) and siderite (FeCO3), within the sediments. Injection of an oxygenated source water (mains or treated stormwater) will oxygenate the storage zone and potentially oxidise Fe(II) within these mineral phases to produce Fe(III) oxides.

Clogging may also be biologically-induced. In this study DOC and BDOC were used as indicators with higher values suggesting greater potential for biological clogging. The character of DOC and its relative biodegradability are known drivers of biological clogging (Pavelic et al., 2008); causing increased production of extracellular polysaccharides in the biofilm surrounding the injection well. This was confirmed by Wakelin et al. (2010) in biofiltration studies linked to the current study as well as laboratory column studies with reclaimed water by Rinck-Pfeifer et al. (2000). Biological clogging is potentially also related to the observed specific capacity changes (Figure 1) as it is difficult to differentiate the clogging mechanisms. Furthermore DOC character and concentration have been shown in controlled laboratory studies to influence the rate of microbial production of polysaccharides (Baveye et al., 1998). Generally, DOC from freshly derived leaf litter leachate (as found in stormwater) has a higher lability than DOC derived from more humified material (Page et al., 2002a; 2002b). This indicates that, for stormwater harvesting as used in the current study, there exists the potential for pulses of highly labile DOC to be injected into the aquifer if pre-treatment is insufficient.

4 Conclusions

The ASR potable water phase of the field trial showed that turbidity, DOC and BDOC in the injectant were useful for establishing water quality targets for stormwater injection into a low permeability fractured hard rock aquifer. The water quality targets required for injection of Ultrafiltration-granular activated carbon treated stormwater were based on the potable water ASR phase and used water quality targets of ≤0.6 NTU, ≤1.7 mg/L and ≤0.2 mg/L for turbidity, DOC and BDOC respectively. When selecting ASR sites in low permeability fractured rock aquifers, care must be taken in selecting appropriate water qualities suitable for injection or clogging may reduce the operational performance of the system.

5 Acknowledgements

The authors gratefully acknowledge the Project Advisory Committee comprised of representatives of Smart Water Fund, South East Water Limited, Southern Rural Water, Melbourne Water Corporation, Department of Sustainability and Environment, EPA, Department of Human Services, CSIRO Water for Healthy Country Flagship, CSIRO Land and Water and Sinclair Knight Merz. We thank Adrian Booth, Paul Kortholt (Rossdale Golf Club), David Love (Orica Watercare) Stephen Parsons (Sinclair Knight Merz), Hartmut Holländer, Antoine Chassagne, Sven Laube, Alex Cierpka, Joao Mimosa and Nigel Goodman (CSIRO Land and Water) for their assistance over the course of these investigations.

6 References

ANZECC–ARMCANZ, (Australian and New Zealand Environmental and Conservation Council and Agriculture and Resource Management Council of Australia and New Zealand), (2000) Australian and New Zealand Guidelines for Fresh and Marine Water Quality. National Water Quality Management Strategy Paper no 4. ANZECC–ARMCANZ, Canberra.

APHA (American Public Health Association), (2005) Standard Methods for the Examination of Water and Wastewater. 735 APHA-WEF-AWWA, Washington.

Appelo, C.A.J., and Postma, D., (2005) Geochemistry, groundwater and pollution. 2nd Edition. Balkema Publ.

Baveye, P., Vandevivere, P., Hoyle, B.L., DeLeo, P.C., and Sanchez de Lozada, D., (1998) Environmental impact and mechanisms of the biological clogging of saturated soils

and aquifer materials. Crit. Rev. Env. Sci. Tec. 28, 123–191.

Dillon, P., Pavelic, P., Massmann, G., Barry, K., and Correll, R., (2001) Enhancement of the membrane filtration index (MFI) method for determining the clogging potential of turbid urban stormwater and reclaimed water used for aquifer storage and recovery, Desalination. 140, 153–165.

Dillon, P., Pavelic, P., Page, D., Miotlinski, K., Levett, K., Barry, K., Taylor, R., Wakelin, S., Vanderzalm, J., Chassagne A., Molloy, R., Lennon, L., Parsons, S., Dudding, M., and Goode, A., (2010) Developing Aquifer Storage and Recovery (ASR) Opportunities in Melbourne – Rossdale ASR demonstration project final report, CSIRO Water for a Healthy Country Flagship Report http://www.clw.csiro.au/publications/waterforahealthycountry/2010/wfhc-Rossdale-ASR-demonstration.pdf

Garrat, M.J., (1983) Silurian to Early Devonian facies and biofacies patterns for the Melbourne trough, central Victoria. J. Geol. Soc. Aust. 30, 121–147.

Goldenberg, L.C., Magaritz, M., Amiel, A.J., and Mandel, S., (1984) Changes in hydraulic conductivity of laboratory sand-clay mixtures caused by a seawater-freshwater interface. J. Hydrol. 70, 329–336.

Goldenberg, L.C., (1985) Decrease in hydraulic conductivity in sand at the interface between seawater and dilute clay suspensions. J. Hydrol. 78, 183–199

Harrington, G.A., Love, A.J., Sanford, W.E., (2002) Aquifer Storage and Recovery in a fractured rock aquifer of the Clare Valley, South Australia. In Dillon (ed). Management of Aquifer Recharge for Sustainability, 315-318, A. A. Balkema.

Hunt, B., (1999) Unsteady stream depletion from ground water pumping. Ground Water, 37, 98–102.

Konikow, L.F., August, L.L., and Voss, C.I., (2001) Effects of clay dispersion on aquifer storage and recovery in coastal aquifers. Transport Porous Med. 43, 45–64.

Kresic, N., (2006) Hydrogeology and groundwater modelling. Second edition. CRC Press.

Levett, K. J., Page, D. W., Dillon, P. J., Taylor, R., Booth, A., and Kortholt, P., (2009) Pre-treatment of urban stormwater prior to aquifer storage and recovery (ASR) in a fractured rock aquifer. Proceedings of the 7th IWA World Congress on Water Reclamation and Reuse, Reuse09, 21–25 September 2009, Brisbane, Australia

Lin, E., Page, D., and Pavelic, P., (2008) A new method to evaluate polydisperse kaolinite clay particle removal in roughing filtration using colloid filtration theory, Wat. Res. 42, 669– 676.

Mirecki, J.E., Campbell, B.G., Conlon, K.J., and Petkevich, M.D., (1998) Solute changes during aquifer storage recovery testing in a limestone/clastic aquifer. Ground Water, 36, 394–403.

Mucha, I., Bansky, L., Hlavaty, Z., and Rodak, D., (2006) Impact of riverbed clogging – colmatation – on groundwater. In: Hubbs, S.A. (ed) Riverbank Filtration Hydrology, 43-72. Springer.

Murray, E. C., Tredoux, G., (2002) Borehole injection tests in Windhoek's fractured quartzite aquifer. In Dillon (ed). Management of Aquifer Recharge for Sustainability, 251–256, A. A. Balkema.

NRMMC–EPHC–NHMRC, (Natural Resource Management Ministerial Council, Environment Protection and Heritage Council, National Health and Medical Research Council) (2009) Australian Guidelines for Water Recycling: Managed Aquifer Recharge (Phase 2), Natural Resource Ministerial Management Council, Environment Protection and Heritage Council and National Health and Medical Research Council, Canberra. http://www.ephc.gov.au/sites/default/files/WQ_AGWR_GL__Managed_Aquifer_Recharge_Final_200907.pdf

Olsthoorn, T.N., (1982) The clogging of recharge wells, main subjects. KIWA-Communications 72, p 150

Page, D.W., van Leeuwen, J.A., Spark, K.M., Drikas, M., and Mulcahy, D.E., (2002a) Effect of alum treatment on the trihalomethane formation and bacterial regrowth potentials of natural and synthetic waters. Wat. Res. 36, 4884-4892.

Page, D.W., van Leeuwen, J.A., Spark, K.M., Mulcahy, D.E., (2002b) Pyrolysis characterisation of soil, litter and vegetation extracts from Australian catchments. J. Anal. App. Pyrol. 65, 249–265.

Page, D.W., Miotlinski, K., Dillon, P., Taylor, R.J., Wakelin, S., Levett, K., Barry, K., and Pavelic, P., (2011) Stormwater pre-treatment options for sustaining aquifer storage and recovery in low permeability fractured rock aquifer, Journal of Environmental Management, 92, 2410–2418.

Pavelic, P. and Dillon, P., (1997) Guidelines on the quality of stormwater and treated wastewater for injection into aquifers for storage and reuse. Centre for Groundwater Studies Report No. 74.

Pavelic, P., Dillon, P., Barry, K., and Gerges, N., (2006) Hydraulic evaluation of aquifer storage and recovery (ASR) with urban stormwater in a brackish limestone aquifer, Hydrogeol. J. 14. 1544–1555

Pavelic, P., Dillon, P., Barry, K., Vanderzalm, J., Correll, R., and Rinck-Pfeiffer, S., (2007) Water quality effects on clogging rates during reclaimed water ASR in a carbonate aquifer. J. Hydrol. 334, 1– 16.

Pavelic, P., Dillon, P., Barry, K., Armstrong, D., Hodson, A., Callaghan, J., and Gerges, N., (2008) Lessons drawn from attempts to unclog an ASR well in an unconsolidated sand aquifer, CSIRO Water for a Healthy Country Flagship Report. http://www.clw.csiro.au/publications/waterforahealthycountry/2008/wfhc_ASRwell.pdf

Pérez-Paricio, A., and Carrera, J., (1999) Clogging handbook. EU Project on Artificial Recharge of Groundwater, Research program on Environment and Climate, Contract ENV-CT95-0071, European Commonwealth, Brussels.

Petkewich, M.D., Parkhurst, D.L., Conlon, K.J., Campbell, B.G., and Mirecki, J.E., (2004) Hydrologic and geochemical evaluation of aquifer storage and recovery in the Santee Limestone/Black Mingo aquifer, Charleston, South Carolina, 1998–2002. USGS Scientific Investigation Report 2004-5046.

Pyne, R.D.G., (2005) Aquifer Storage Recovery: A guide to groundwater recharge through wells. ASR Press, USA.

Rinck-Pfeiffer, S.M., Ragusa, S.R., Sztajnbok, P., and Vandevelde, T., (2000) Interrelationships between biological, chemical and physical processes as an analog to clogging in aquifer storage and recovery (ASR) wells. Wat. Res. 34, 2110–2118.

Schippers, J.C., and Verdouw, J., (1980) The modified fouling index, a method of determining the fouling characteristics of water. Desalination, 32, 137–148.

Schubert, J., (2002) Hydraulic aspects of riverbank filtration - field studies. J. Hydrol. 266, 145–161.

Standards Association of Australia, (1980) Determination of Emerson Class Number of a Soil. AS 1289.C8.1.

Vanderzalm, J., Page, D., Barry, K., and Dillon, P., (2010) A comparison of the geochemical response to different managed aquifer recharge operations for injection of urban storm water in a carbonate aquifer. Appl. Geochem. 25, 1350–1360.

Wakelin, S.A., Page, D.W., Pavelic, P., Gregg, A.L., and Dillon, P.J., (2010) Rich microbial communities that inhabit water treatment biofilters are differentially affected by filter type and sampling depth. Wa. Sci. Technol. 10, 145–156.

Identification and Management of Clogging in a Fractured Rock Aquifer during ASR Operations

R. Martin *(General Manager, Australian Groundwater Technologies)*

Abstract

Control of clogging is a key consideration for the long-term sustainable operation of managed aquifer recharge (MAR) schemes. Control of the source water quality is the first and most obvious measure to minimise the potential for clogging. However, over time, loss of injection or infiltration performance due to clogging which can manifest from; the accumulation of suspended solids; biological growth; microbiological activity; geochemical reactions; dissolved or entrained air from turbulence; mobilisation of interstitial clays or a temperature differential between the injected water and ambient groundwater, is not uncommon. Often multiple cause of clogging may be occurring simultaneously, for example, gas entrainment may induce precipitation of iron which can stimulate an increase in iron bacteria. What started out as a simple air entrainment problem has the potential to develop into a significant clogging problem driven by three different processes. Each potential clogging cause may now require individual treatment. This paper discusses some of the clogging mechanisms encountered when the injection to, and recovery from, the aquifer utilises bores, more commonly referred to as aquifer storage and recovery (ASR). Results of a case study and the approach to identification of clogging using the aquifer hydraulic response are presented and the corrective measure adopted are discussed.

The City of Tea Tree Gully has an integrated MAR system comprising four individual aquifer storage and recovery (ASR) sites linked by a common pipeline. Collectively the schemes harvest, treat and recharge, to the underlying fractured rock aquifer, approximately 300 megalitres per year (ML/yr) of urban stormwater runoff. A further two schemes, outside of the linear pipeline, harvest up to 80 ML/yr each. Integration of the schemes through the single pipeline has enabled greater operating flexibility and the servicing of many smaller open spaces that may otherwise have had to continue to be irrigated with potable mains water. During pre-commissioning one of the schemes, Tilley Reserve, experienced significant head build up beyond the pre-selected trigger limits set for safe operation of the scheme. Investigations into the origin of the greater than expected head buildup identified gas entrainment at the onset of injection followed shortly thereafter by colonisation of the drillhole by iron bacteria as the causes of the clogging. Gas entrainment resulted from an oversight in the overall engineering design when the scheme was linked into the common pipeline. The air entrainment encouraged the growth of iron bacteria which have a propensity to colonise areas of highest velocity, that is, pump intakes, or in this case, the fracture zones within the bore.

Introduction

Physical scarcity of water, in terms of limited availability in many of the arid regions across the globe and the availability of clean drinking water, is a significant and growing problem. Today, about one third of the world's population lives in countries with moderate to high water stress; by 2025, largely because of population growth, fully two out of three of the world's people will live under those conditions (Mazur, 2012). Managed Aquifer Recharge (MAR), in its many forms, and related water management practices are evolving rapidly. There is immense potential for MAR, used in conjunction with other water management techniques, to make more efficient use of existing water resources and to reuse more water now that in many cases is discarded after a single use or channelled rapidly away from urban areas to be discharged into rivers or the sea (Martin, 2002).

One of the challenges for the sustainable operation of MAR schemes is the management of clogging. Physical,

biological, and chemical clogging of infiltrating surfaces and injection bores with the resulting reduction in infiltration rates is perhaps the most obvious problem in MAR systems. Invariably an MAR scheme will experience clogging which is a considerably higher risk when the selected MAR method involves and injection and recovery bore (aquifer storage and recovery). In the case where ASR is the selected MAR method there are two fundamental questions that should be asked and answered by the investigator before a bore is constructed. The first question is *"what clogging issues are likely to be experienced at this site?"* and the second question is; *"which clogging issues can be engineered out?"*

Asking these fundamental questions will assist in determining the drilling method for the bore and the completion method. The drilling method is critical as incorrect management of drilling fluids may cause significant formation damage (clogging) immediately the target aquifer is penetrated. The completion method is critical in order to provide as many options as possible to remediate the bore when ultimately clogging occurs.

Tilley Reserve Case Study

Geology

The project area lies at the head of the Golden Grove Embayment, Adelaide, South Australia, where thin but isolated layers of Quaternary and/or Tertiary sands and gravels occur in outcrop; however the dominant geology underlying the surficial sediments is consistent with the major geological rock types of the adjacent Mount Lofty Ranges which are part of the Adelaide Geosyncline.

The regional geology within the study area is presented as Figure 1. Beneath the thin veneer of Quaternary/Tertiary sediments three major geological units; the Woolshed Flat Shale; Montacute Dolomite and Stoneyfell Quartzite of the Burra Group complex occur in the immediate area. Along the western edge of the study area remnant outcrops of the Belair subgroup, Glen Osmond Slate and Mitcham Quartzite crop out (Figure 1). An outcropping splinter of the Saddleworth Formation occurs to the south of the study area. Major folding and faulting during tectonic upheavals have resulted in these geological units occurring along an almost vertical plane with sharp transitions occurring between units.

Within the study area the stratigraphic units (from oldest to youngest) are likely to comprise the Castambul Formation which is described by Preiss (1987) as a pale grey to white, finely crystalline, massive dolomite which occurs as a 50–100 m thick interbed within a dark grey and greenish, silty and phyllitic sequence overlying the Aldgate Sandstone. The dolomite is sandy in the upper sections and grades up into ~30 m of coarse grained quartzite (Preiss, 1987).

The Montacute Dolomite is dominantly blue-grey in colour, fine-grained with interbeds of dolomitic sandstone, quartzite, magnesite conglomerate and minor dolomitic phyllite and can be up to ~130 m thick to the east of Athelstone (Preiss, 1987).

Figure 1: 1:100 k Geology surrounding the study area

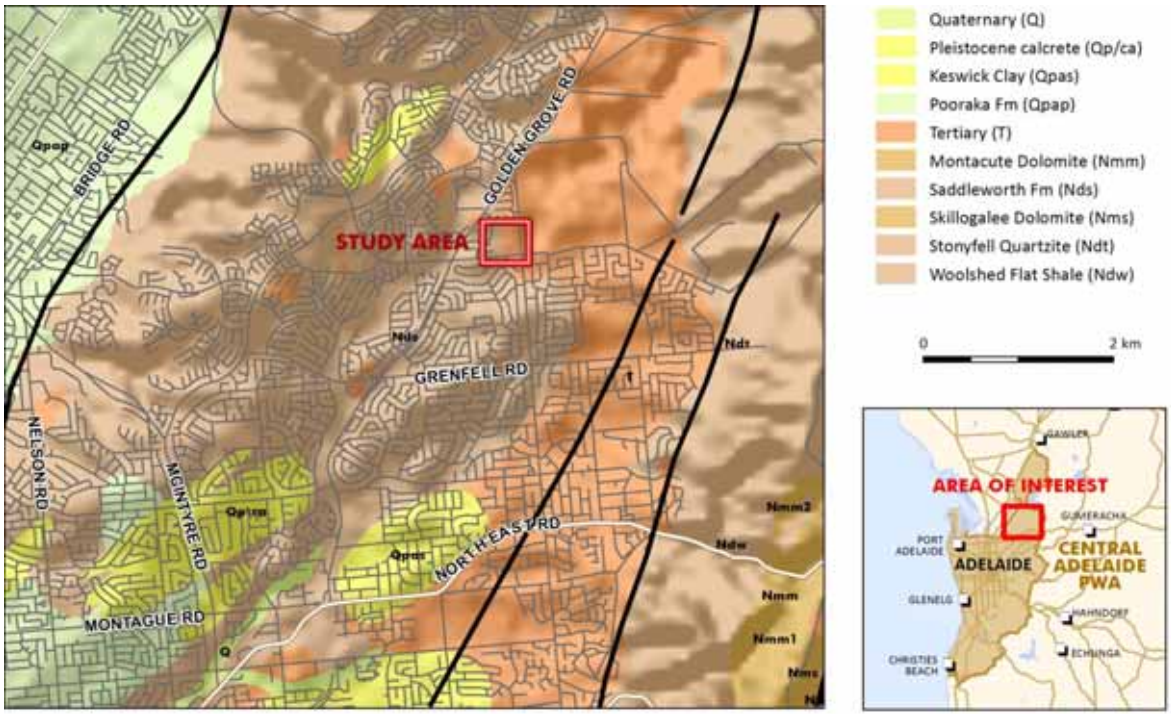

In the Montacute – Tea Tree Gully area, the Woolshed Flat Shale typically comprises an upper unit of laminated sandy or silty shale and phyllite, and a lower unit of dolomitic phyllite with thin dolomite lenses (Preiss, 1987). Where the phyllite is strongly laminated that has resulted in high yielding (>10 L/s) bores in some locations.

The Stonyfell Quartzite occurs predominantly to the east of the Burnside-Eden fault and is responsible for much of the prominent relief of the Adelaide Hills Face Zone (HFZ), especially north of the Black Hill in the Athelstone area. Close to the study area, the Stonyfell Quartzite is ~250 m thick and comprised predominantly of feldspathic quartzite with secondary pyrite crystallisation filling many of the fractures.

Hydrogeological setting

Locally, groundwater occurs within the Quaternary gravels along the drainage lines and in the underlying fractured rock of the Woolshed Flat Shale, Montacute Dolomite and Saddleworth Formations. The fractured rock aquifer system is considered to be part of a regional confined aquifer and is the main focus for aquifer storage and recovery (ASR) schemes in this area. It is inferred that groundwater found within the dolomite, quartzites and shales is hydraulically connected with the Stonyfell Quartzite outcropping to the east of the Eden-Burnside Fault and the Tertiary sediments to the west of the study area.

The local aquifer is recharged by infiltration of rainfall at a rate which depends on rainfall intensity, soil type and land cover. Across the hills face zone the surrounding land cover is mainly native vegetation which means the rainfall recharge rate is expected to be low (~1 mm/yr). Areas without native vegetation will have a higher rainfall recharge rate at an estimated rate of approximately 5% of rainfall (39 mm/yr).

Groundwater discharge occurs through springs and seeps, baseflow to nearby streams (e.g. the tributaries of the Torrens River), and through flow to the Adelaide Plains. There is limited extraction of groundwater as the yields are typically low and groundwater salinity is highly variable ranging from 1,000 mg/L up to > 3,000 mg/L although minor extraction does occur via small domestic bores where groundwater is reported to be between 1,000 mg/L and 1,500 mg/L.

Bore construction and aquifer hydraulic properties

A summary of the bore construction details is presented in Table 1.

Table 1: Summary of bore completion

Parameter (unit)	ASR Production bore	ASR Monitoring bore
Permit Number	141146	141147
Drillhole Unit number	6628-23433	6628-23432
Drilling method	Rotary mud	Rotary mud
Total Depth (m)	103	79
Casing Type	Class 12 uPVC	Class 12 uPVC
Casing Diameter (mm)	203	203
Casing interval (m)	0 to 20	0 to 20
Annulus cementing method	Pressure cement	Pressure cement
Production zone (m)	20 to 103	20 to 79
Production zone completion type	Open Hole	Open Hole
Standing water level (m bgl)	20	19
Airlift yield (L/s)	8.5	2.2
Ambient groundwater salinity (mg/L)[1]	1,800	2,200

Notes: [1] Measured in field at completion of airlift development.

Following completion of the bores an injection and recovery test was undertaken.

From the head build up versus square root of time ($\sqrt{t}$) plot (Figure 3) the following fractured rock bore equation (FRAE) was derived:

$$St = Q (0.33 + 0.3015 \cdot t) \quad (1)$$

Equation 1 accurately describes the head build up in the injection bore and compares favourably with the observed head build-up of 4.25 m during the constant rate injection test. Theoretically this equation is considered to be reliable for calculating head build up at a given time. The head build up was calculated from the fractured rock aquifer (FRA) bore equation for various injection rates and times and result is summarised in Table 2.

Table 2: Calculated head build up for various injection rates and times

Injection rates (L/s)	Head Build up (m)		
	t= 1 day	t= 10 day	t= 30 day
8	5.05	10.27	15.85
10	6.32	12.83	19.81
15	9.47	19.25	29.72
20	12.63	25.67	39.63
30	18.95	38.5	59.44

Note: For this unconfined aquifer, the available safe head build up during injection = depth to water level +60% of the thickness of overburden. Safe head build up = approx. 18 + 10 = 28 m

Scheme commissioning

Final construction and commissioning of the scheme was completed 24 months after the completion of the initial injection and recovery trials and aquifer testing. The pressure transducer in the injection bore was set at 70 m bgl, therefore, the at rest head of water above the pressure transducer is 30 m as the standing water level in the bore at rest is 20 m bgl. With the safe operating head determined to be approximately 28 m above the at rest water level the system is set to shut down if the head above the pressure transducer exceeds 60 m.

Figure 2 presents the results of the head buildup during five successive injection cycles. Immediately on start-up on cycle 1 the head exceeded the set pressure limits. On injection cycles 2, 3 and 4 the set threshold pressure was exceeded within the first 120 minutes of operation. The set threshold pressure was adjusted to over 100 m head and the system reset and allowed to run to ascertain if, as a result of the construction and pump selection, greater bore loss was occurring. A larger diameter pump effectively reduces the annular space in the bore potentially creating greater backpressure and thus greater head buildup. For each cycle the injection rate was maintained constant at 5 L/s.

From the initial rapid buildup in heads a steady increase in injection pressures at the constant injection rate ensued until after seven days of operation the threshold pressure (100 m head) was exceeded. Figure 3 presents the normalised head buildup plotted against the square root of time. In each successive cycle the initial head rise is rapid (within the first 100 minutes of operation) which is indicative of air entrainment. Compared to the original test the initial head buildup on start-up is some 20 to 25 m greater and increasing slightly on each successive cycle. During the fifth injection cycle there was a steady but persistent rise in heads for a constant injection rate which is indicative of other clogging mechanisms occurring.

The Specific Capacity (equation 2) was determined for each cycle and results are presented as Figure 4 and illustrate the significant change in injection performance from the initial trial to full operation.

SC = - [Q/S] (L/s)/m of injection/extraction head (2)

Where: S = injection/extraction head (m)

Q= injection/extraction rate (L/s)

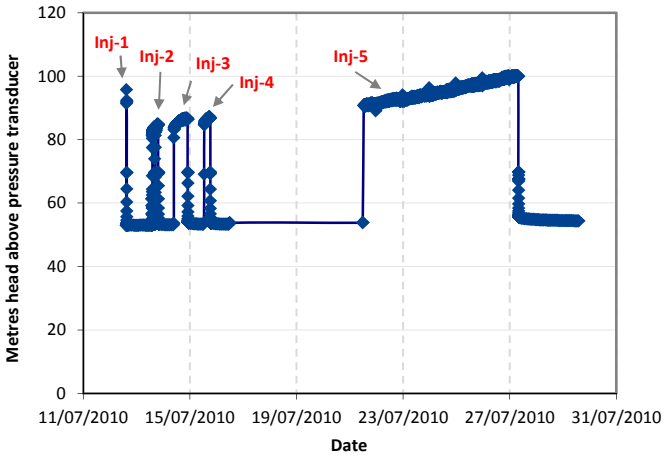

Figure 2: Recorded head build up during successive injection cycles

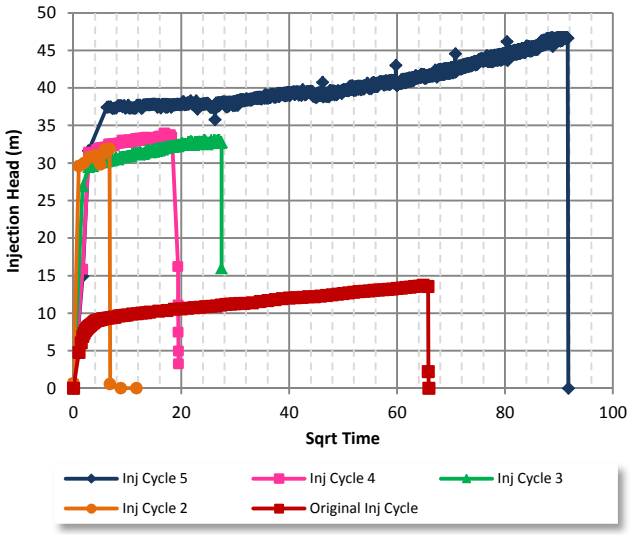

Figure 3: Normalised head build up during successive injection cycles

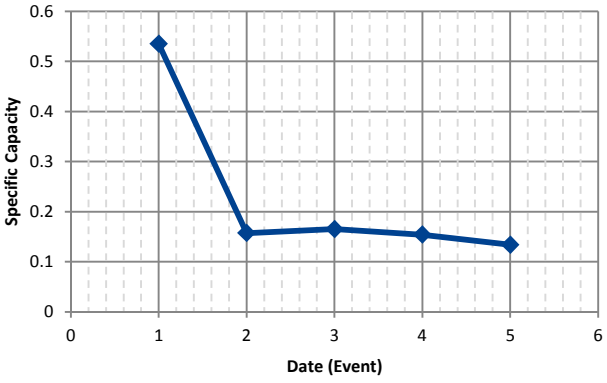

Figure 4: Calculated specific capacity

Further testing

The initial indications were that a clogging mechanism was clearly responsible for the significant head buildup and thought initially to be associated with either the injection of high turbidity water, although the inline instrumentation did not record any significant turbidity exceedance, or from microbiological activity. While the observed hydraulic response appears more typical of air entrainment every effort had been taken during initial design to eliminate this possibility as it was considered that unlike a sedimentary aquifer clogging of one or two of the more highly fractured zones would have a significant impact on injection rates and heads. Further aquifer testing was carried out to rule out the possibility of formation clogging. It was noted that when the pump was removed significant slimes associated with iron bacteria coated the pump and rising main (Figure 5).

Figure 5: Iron bacteria coating pump collar and rising main. Colonisation occurred within 4 weeks of the pump installation

Step discharge test results for adjacent wells (Unit number 6628-21392 and 6628-23433) were reviewed and compared to the results from examined and appear below:

- At Tilley Reserve, the 30th July 2003 (Unit number 6628-21392):

$st = 0.012931Q + 0.001987Q \log t + 2.32*10^{-5}Q^2$, with another calculating method, giving a value of 23.2 m drawdown, at a discharge rate of 9 L/s. The transmissivity calculated was between 92 and 102 m^2/d, from the first step.

- At Tilley Reserve, the 3rd March 2008 (Unit number 6628-23433):

$st = 17.07Q + 3.52Q \log t + 42.06Q^2$, giving a value of 31.5 m drawdown, at a discharge rate of 10L/s.

- At Tilley Reserve, the 16th April 2009 (Unit number 6628-24861):

$st = 2.13Q + 1.07Q \log t + 2.22Q^2$, giving a value of 2.56 m drawdown, at a discharge rate of 8 L/s.

At this time the transmissivity was calculated to be 200 m^2/d from the last step which compares favourably with the transmissivity calculated for the last aquifer discharge test on 18th April 2011. Table 3 presents the observed drawdown in the drill hole at the end of each of the three rates.

Table 3: Recorded drawdown of two step discharge tests

Pumping rate (L/s)	Observed drawdown after 100 mins (m)		Change in drawdown (m)
	Test 1 16 April 2009	Test 2 18 April 2011	
2	0.52	0.68	0.16
4	1.23	1.49	0.26
8	2.86	3.26	0.40

Figure 6 presents the plotted difference in the reported drawdown for each of the selected pump rates. The almost linear plot suggests one of the following:

- a slight loss in pump efficiency; or
- a small error in the flow meter readings.

The results from the two tests indicate that there has been no significant change in well hydraulic properties over the intervening two years. The almost linear response in the reported drawdown and pump rates also confirms that there has been little or no change in the well hydraulic properties. It was however recommended that the well is treated with a biocide for iron bacteria prior to installing any equipment.

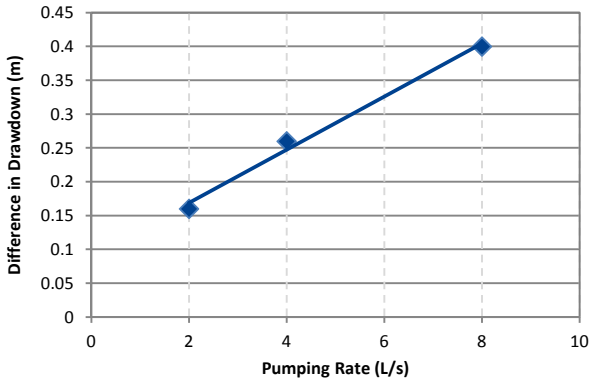

Figure 6: Pumping rate versus observed difference in heads between the two tests

Conclusions

- The results show a significant change in injection performance of the bore between the initial trial injection and scheme start up.
- It was considered that whilst the hydraulic response was more typical of air entrainment that may be observed in a sedimentary aquifer clogging of one or two of the major fractures could lead to significant changes in hydraulic properties in the injection bore. All reasonable measures to prevent air entrainment including submergence of the injection line below the standing water level in the bore had been included in the design.
- On removal of the pump and subsequent testing significant iron bacteria colonisation in the bore and on equipment was noted indicating the possibility of biological clogging.
- The results for the subsequent step drawdown test returned similar aquifer properties as had been determined two years previously indicating little or no loss in bore performance.
- It was concluded that the rapid increase in heads immediately upon start up was indicative of air entrainment and the whole scheme design was reviewed.
- It was found that cascading of water into the balancing storage tank, added later in the design and located remotely from the site, resulted in aeration.
- Where there are limited highly permeable zones within the fractured bedrock across the open bore interval the aeration was sufficient to significantly alter the injection performance of the bore.
- The inlet pipe to the balancing storage tank was lowered to below the water level to eliminate cascading and thus eliminate the aeration problem.
- The bore was also treated with a biocide to remove the iron bacteria and as part of the operational maintenance undergoes regular dosing.

References

Hem, J.D., (1989) Study and interpretation of the chemical characteristics of natural water. US Geological Survey Water Supply Paper 2254 .

Martin, R., (2002) Aquifer storage and recovery, future directions for South Australia. Department of Land, Water and Biodiversity and Conservation, Report No. 2002/04.

Mazur, L., (2012) Water and Population: Limits to Growth? http://www.newsecuritybeat.org/2012/02/water-and-population-limits-to-growth/#.UPCkUqzAqPg

Preiss, W.V., (1987) The Adelaide Geosyncline, late Proterozoic stratigraphy, sedimentation, palaeontology and tectonics. Bulletin 53 Geological Survey of South Australia pp 438.

Pyne, R.G.D., (2005) Aquifer storage and recovery: A guide to groundwater recharge through wells. Second Edition ISBN 0-9774337-090000

CLOGGING REHABILITATION AND REMEDIATION METHODS

Clogging Remediation Methods to Restore Well Injection Capacity

R. Martin
General Manager, Australian Groundwater Technologies

Abstract

A MAR scheme will invariably experience clogging of some type, and to some degree, during its operational life. To recognise the potential for clogging and employ the appropriate mitigation or remediation measures, either through engineering design or through operational management practices, requires specialist knowledge and skills. It should also be noted that remediation methods to address clogging are very site specific and what works in one hydrogeological setting may not always be successful in another location. Indeed remediation approaches may differ between injection bores across the same scheme. This paper presents an overview of some of the approaches that can be adopted to remediate bores once clogging has occurred.

Introduction

Clogging is an ever present issue facing many operators of managed aquifer recharge (MAR) schemes and can result in lost harvesting opportunities where the scheme is shut down for extended periods to carry out remediation activities, often at significant cost.

Frequently, clogging that leads to the failure of a MAR scheme occurs from a lack of proper aquifer characterisation resulting from 1) poor data collection and organization; 2) little or no integrated analysis of existing data by experienced geological and engineering personnel; 3) failure due to inexperience of practitioners to consider remediation methods; 4) engagement of multiple sub-contractors by the proponent during the various stages of investigation, design, construction and operation that typically results in problems at the interface of each work package; and 5) not identifying optimum management techniques to prevent clogging or allow for remediation in the event of it occurring.

This section deals primarily with remediation methods that can be employed to restore and improve injection capability within recharge wells. It should be noted that the well remediation methods presented herein are not exhaustive, for example, there are proprietary techniques developed by experienced ASR practitioners that are not discussed.

To adopt the correct remediation method requires adequate and detailed aquifer characterisation during the initial site investigations followed by reliable monitoring during operation. It is becoming increasingly apparent that inexperienced practitioners are failing to adequately characterise the target aquifer which is leading to poor well design and poor selection of casing materials thereby limiting the options for well remediation when clogging arises. There is a real risk that poor practice increasingly puts at risk the uptake of MAR as a viable and effective water resources management tool.

There are various measures that can be incorporated to minimise clogging and prolong the operational life of the well ranging from engineering through to operational controls. These preventative measures include:

- Selection of appropriate drilling methods and drilling fluids to avoid formation damage.
- Appropriate development of the well on completion of drilling and casing installation.
- Selection of the appropriate well design for the target aquifer.
- Periodic backwashing of the recharge wells at specified times or volumes recharged.
- Removal of air from the recharge water using dissolved oxygen scrubbers or through the addition of carbon dioxide.
- Eliminating as much as reasonably possible the potential for air entrainment in the recharge water within the MAR scheme infrastructure.
- Periodic or constant chemical dosing to treat for algae and microbiological activity.
- Ultra filtration (membrane and Ultra Violet treatment) prior to recharge via the well.
- Reverse osmosis pre-treatment and ultra-filtration if wastewater is the primary recharge water source.

- Chemical treatment to aid in flocculation of suspended sediments followed by ultra-filtration to improve source water quality.
- Management of operating pressures to prevent failure of the target aquifer.
- Periodic dosing to prevent the build-up of scale within the pipe networks and wells.
- Following dosing of pipes and other infrastructure to remove scale or other build-up "pigging" may be required.
- Eliminating the potential for sub-surface geochemical reactions through pH adjustment or salinity adjustment.

The preventative measures selected will largely depend on the source water, the receiving water and the mineralogy of the host aquifer. Despite the incorporation of effective preventative measures it is still highly probable that at some point during its operational life the MAR scheme will experience clogging that will require more extensive remediation.

Identifying the onset of clogging

Practitioners should always consider the potential for serious clogging and the types of remediation methods that are appropriate for the hydrogeological setting as this will influence the well design and the selection of materials used during construction. A well may experience several years of operation before any loss in injection efficiency becomes apparent. Clogging due to microbiological activity, geochemical reactions, air entrainment or mechanical blocking causes an increase in friction losses near the well bore or screen and the specific capacity is reduced.

Recording the aquifer hydraulic response during recharge via a well provides the first indication of the onset of clogging. Figure 1 presents the typical hydraulic responses (Pyne, R.D.G., 1995) that are observed for some of the clogging types that occur in wells used for MAR. The characteristic hydraulic response curves hold in general, but it is not uncommon for the hydraulic response associated with the mobilisation of insitu fines to be similar to the clogging hydraulic response that may be observed where microbiological populations have an abundant food supply. The subtle difference that points to the mobilisation of insitu fines is that as with suspended solids the early response of hydraulic head (resistance) with time is likely to be linear before becoming exponential.

Monitoring of source water quality in-line (turbidity, pH, Electrical conductivity), injection rates and the aquifer hydraulic response, in both the injection well and any associated observation wells, is critical as often multiple clogging processes may be acting in concert. Without identifying and treating the primary cause the associated types of clogging may continue to cause operational issues.

Figure 1: Aquifer hydraulic response associated with the different clogging types (after Pyne, R.D.G., 1995)

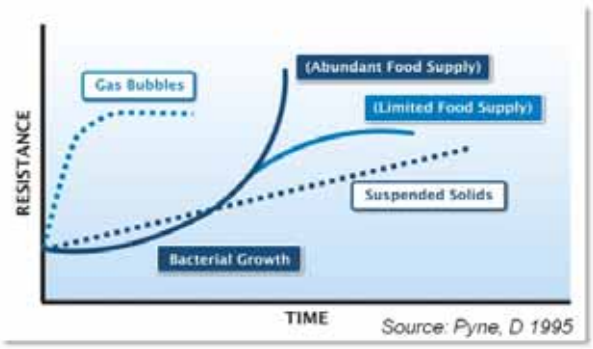

Remediation Methods

Airlift Development

Airlift development procedures are one of the most common methods for remediating wells, both during completion and also to clean out wells following the onset of clogging. Airlift development procedures should begin by determining that groundwater can flow freely into the well. Application of too much air volume in the recharge well when the formation is clogged can result in a collapsed screen (Driscoll, 1986).

Where wells have been completed using a screen, during development, the air line should initially be placed at a relatively shallow submergence and high above the screen to minimise the potential for the screen to collapse. By placing the air line at a shallow submergence, even with large air volumes, only a low collapse pressure can be applied to the screen. Once a steady uninhibited flow into the well is achieved the air line can be steadily lowered to within a metre of the top of the screen. Airlifting should continue until the water discharged from the well is free of any suspended solids.

If clogging of the screen or formation has occurred as a result of fine sediments then it may be advantageous to pre-treat the well prior to using airlifting of jetting with a number of the chemicals (e.g. Kalgon) that can assist the breakdown of the sediment particulates.

It may seem counter intuitive to remediate a well through airlifting as one of the primary causes of clogging is air entrainment. However provided the air line remains above the screen air will invariably be forced up the drillhole rather

than into the formation. Cleaning of the screen is achieved by the sudden inrush of water from the aquifer to replace the water expelled out of the top of the well.

Air lift development should be avoided in aquifers that are prone to "air locking" such as stratified formations consisting of coarse sand or gravel lenses separated by thin, impermeable clay layers. "Air locking", as with air entrainment in general may impede the flow of water into and from the well, while also increasing the potential for iron precipitation within the formation thus creating a secondary clogging issue.

High Velocity Jetting

Jetting involves injection of compressed air or water at the bottom of the well, and the accumulated sediment is forced out the top. The frequency with which recharge wells should be cleaned will vary greatly depending on the sediment load from the site and the depth of the well.

The jetting procedure consists of operating a horizontal water jet inside the well screen so that high velocity streams of water shoot out through the screen openings. Jetting is extremely successful in developing highly stratified, unconsolidated formations. The equipment required for jet development includes a jetting tool with two or more equally spaced nozzles, high pressure pump, high pressure hose and connections, pipe, and water tank or other water supply. Material loosened from the screen or formation accumulates at the bottom of the screen (or in the sump if included in the well completion design) as the jetting tool is raised slowly. This material is removed later by airlift pumping (Driscoll, 1986).

Vacuum Pumping

Vacuum pumping involves a dual pipe system. Air is forced down the inner tube and returns up the annular space between the inner and outer tubing. As the outer tubing extends past the inner tube outlet a vacuum is created and sucks up the fine material that has accumulated on the walls of the formation. It is an extremely effective method if there are concerns about introducing air into the formation.

Vacuum pumping is only suitable for wells where there is no gravel pack or screen. As in some cases the high inflow velocity generated is higher than the average calculated for a screen dimension and slot size, and a concentration of clogging can be induced behind the screen in this high-velocity zone.

Acidisation

Acidising is typically performed to increase formation permeability in undamaged wells; however, it can be applied to improve injection performance in wells that have become clogged by either particulate matter or through microbiological activity. Care needs to be taken when acidising as sometimes additional fines are mobilised through the dissolution process. Furthermore a propping agent may need to be used to maintain the stability of the aquifer matrix and keep the formation open after dissolution.

An ideal acidising fluid is able to penetrate long distances, etch fracture faces, increase the permeability of the matrix where the fluid enters the formation by diffusion, and remove any existing formation damage.

A number of different acids are used in conventional acidising treatments. The most common are:

- Hydrochloric, HCl
- Hydrofluoric, HF
- Acetic, CH_3COOH
- Formic, HCOOH
- Sulfamic, H_2NSO_3H
- Chloroacetic, $ClCH_2COOH$.

These acids differ in their characteristics. Choice of the acid and any additives for a given situation depends on the aquifer matrix characteristics and the specific intention of the treatment, for example, near well damage removal, dissolution of scale in fractures, etc.

Portier et al. (2007) outline a number of factors controlling the reaction rate of acid:

- area of contact per unit volume of acid;
- formation temperature;
- pressure;
- acid concentration;
- acid type;
- physical and chemical properties of formation rock; and
- flow velocity of acid.

Hydrochloric acid and hydrofluoric acid are the two most common acidizing treatments. However, the very fast reaction rate of hydrochloric acid, and other acids listed above, can limit their effectiveness in a number of applications. All conventional acids including HCl and organic acids react very rapidly on contact with acid sensitive material in the well or formation. "Worm-holing" is a common phenomenon. The rapid reaction means the acid does not penetrate very far into the formation before it is spent. Conventional acid systems are therefore of limited effectiveness in treatments where deep acid penetration is

needed.

Portier et al. (2007) discuss acid stimulation in significant detail including the addition of polymers and surfactants to retard acid reaction rates and achieve deeper formation penetration of the acid before it is spent.

Less known and less used than either HCL or sulfamic acid, hydroxyacetic acid is safer to use and has the benefit of being a bactericide and will directly attack and kill iron bacteria. It works the slowest of the HCL, Sulfamic or Hydrofluoric acids, so its contact time in the well will be the longest to achieve the desired effect. Hydroxyacetic acid is relatively non-corrosive and produces no fumes.

Biocides

Where Environmental Protection Agency regulations permit, shock chlorination may be used to limit the growth of iron bacteria and other microorganisms. The shock chlorination approach is widely used in the rehabilitation of wells severely plugged by biofouling bacteria. Concentrations as high as 500 to 2,000 ppm are used. Once injected into the well, water is added to force the chlorine mixture out into the formation. Agitation is always recommended to increase surface contact between the biofouling agents and the high concentration chlorine solution. Mechanical brushing, agitation, surging and jetting are all used to increase the turbulence of the chlorine solution in the well. Shock chlorination may be used as the first step, then acidisation of the well (note- the well must be fully purged of the chlorine solution before acidisation) with agitation to improve removal of encrustation, and thirdly another shock chlorination treatment.

Chlorine based approaches are more effective the longer the contact time between the chlorine solution and the biofouling agents. Disposal of the waste water after both the shock chlorination and the acidisation must be done with awareness of safe disposal procedures.

Under-reaming

Where a well hole has been completed as an open hole construction and under-reamer can be used to enlarge the well beyond bit diameter. Assuming that the clogging has occurred primarily within the first few centimetres of the aquifer matrix the under-reamer can be used to effectively create a fresh well face by removing the clogged section of the aquifer. An under reamer can be opened and closed several times down hole, making it easy to enlarge the well hole over specific sections.

This approach is useful where jetting or airlift development have failed to improve the injection capacity of the well.

Scrubbing

Wire brushing and scraping are effective means for removing encrustations from inside the casing and well screen. The loosened material can be removed by air lifted, bailing, or other means. This approach may be a good first step in rehabilitation as it may allow greater access to the formation for chemicals to be introduced later if the scrubbing fails to improve well injection capacity.

In some cases it may be difficult to find a drilling contractor that has the appropriate tools necessary to scrub the casing and screens. Where such an activity is undertaken it may be necessary to shut down or scale back the injection operations in any nearby wells so that the bore can be effectively worked on.

Heating

Heat can be used to increase the effectiveness of chemical treatments in well rehabilitation. Water is withdrawn from the well, heated and recirculated into the well to increase the action of chemical solutions. Several specialists in rehabilitation routinely employ heated chemical treatments as part a blended of a multi-step approach to well remediation. Heat alone can also be an effective biofouling removal method where chemicals cannot be used.

Summary

A rule of thumb is that if the injection capacity of a well has declined by about 25%, it is time to begin rehabilitation efforts. The earlier the rehabilitation commences the more efficient and cost effective the remediation will be. Down time of the scheme and thus lost harvesting opportunities can also be kept to a minimum. The approach to be adopted for the well remediation will be determined by the clogging type, well construction and target aquifer mineralogy. Not all remediation methods are suitable for every site and indeed different remediation methods may need to be adopted for different wells within the same well field.

A multi-step or blended approach to rehabilitation that involves combinations of mechanical brushing, agitation, surging and/or jetting produces a superior result.

Acidisation and other remediation methods such as shock chlorination should only be carried out by experienced practitioners. In some cases this may present a barrier to the implementation of an ASR scheme as there may be an insufficient number of experienced practitioners available that have the skills or the equipment necessary to carry out

the remediation work. Therefore, this presents a potential risk to the sustainable operation of the schemes when significant capital may have been invested and there are insufficient local skills to effectively rehabilitate the wells when required.

To determine the effectiveness of the adopted remediation action some reference point is needed. Typically this is the aquifer hydraulic properties in particular specific capacity, prior to the commencement of injection. It is recommended as a minimum to undertake a step drawdown aquifer discharge test on all injection wells that can then be used as the performance baseline against which clogging and remediation effectiveness can be assessed.

References

Bennion, D.B., Bennion, D.W., Thomas, F.B. and Bietz, R.F., (1998) *Injection Water quality – a key factor to successful waterflooding.* Journal of Canadian Petroleum Technology Vol 37. No. 26

Driscoll, F.G., (1986) *Groundwater and wells second edition*. Published by Johnson Screens, St Paul, Minnesota 55112 ISBN 0-9616456-0-1 Eighth printing

Portier, S., André, L. and Vuataz, F.D., (2007), *Review on chemical stimulation techniques in oil industry and applications to geothermal systems* by CREGE – Centre for Geothermal Research, Neuchâtel, Switzerland

Pyne, R.D.G., (1995) *Groundwater recharge and wells: A guide to* a*quifer storage and recovery: A*. ISBN 1-56670-097-3

Pyne, R. D.G., (2005) *Aquifer storage and recovery: A guide to groundwater recharge through wells* 2nd Edition. ISBN 0-9774337-090000

Contact Details of Authors

Name	Co-contributors	e-mail
Russell MARTIN		rmartin@agwt.com.au
Peter DILLON		Peter.Dillon@csiro.au
Saeed TORKZABAN		Saeed.Torkzaban@csiro.au
Adam HUTCHINSON		AHutchinson@ocwd.com
	Don PHIPPS	DPhipps@ocwd.com
	Grizel RODRIGUEZ	GRodriguez@ocwd.com
	Greg WOODSIDE	GWoodside@ocwd.com
Michael MARTIN		Michael.Martin@WaterCorporation.com.au
Karen JOHNSTON		KJohnston@rockwater.com.au
David MAYS		David.Mays@ucdenver.edu
Bobak Willis-Jones		bwillisjones@fmgl.com.au
	Ian Brandes de Roos	ibrandesderoos@fmgl.com.au
Sahmed Benamar		ahmed.benamar@univ-lehavre.fr
Ray RUEMENAPP		ray.ruemenapp@googlemail.com
	Claudia HARTWIG	claudia_hartwig@gmx.net
	Makoto NISHIGAKI	n_makoto@cc.okayama-u.ac.jp
Beatriz de la Loma González		Beatriz.Dela.LomaGonzalez@kwrwater.nl
	Pieter Stuyfzand	
Victor HEILWEIL		heilweil@usgs.gov
Declan Page		declan.page@csiro.au
Joanne VANDERZALM	Vanderzalm	joanne.vanderzalm@csiro.au

[THIS PAGE INTENTIONALLY LEFT BLANK]